US Army Corps
of Engineers
Construction Engineering
Research Laboratories

USACERL Technical Report 97/137
September 1997

Advanced Oxidation Treatment of Army Industrial Wastewaters: Propellant Wastewater

by
Stephen W. Maloney
Veera M. Boddu
Gary R. Peyton

Advanced Oxidation Processes (AOPs) are water treatment processes that generate hydroxyl (OH) radicals for destruction of organic contaminants using ozone/UV, hydrogen peroxide/UV, or ozone/hydrogen peroxide. These processes are important methods for Army wastewater treatment and contamination remediation. This project: (1) analyzed information on AOPs for treatment of Army waste streams; (2) developed predictive models for process development, optimization, and cost projection; and (3) demonstrated on a laboratory scale AOP treatability of wastewater-containing DNT and ethanol.

A kinetic model was found most suitable for modeling the contaminant destruction process. For the DNT-containing wastewater, not only OH, but also α-hydroxyethyl radical (HE) produced by the action of hydroxyl radical on ethanol, were important for the destruction of DNT, depending on the oxygen concentration in solution. Techniques of kinetic analysis were used to determine the form of the rate equation for HE radical, and to evaluate the appropriate rate constants to yield the general model for reductive treatment. Combination with the OH-radical model gave a comprehensive model that correctly described systems in which both OH and HE processes occurred simultaneously. Discovery of the reductive reaction using the kinetic techniques led to a factor of 230 improvement in AOP treatment efficiency.

The contents of this report are not to be used for advertising, publication, or promotional purposes. Citation of trade names does not constitute an official endorsement or approval of the use of such commercial products. The findings of this report are not to be construed as an official Department of the Army position, unless so designated by other authorized documents.

DESTROY THIS REPORT WHEN IT IS NO LONGER NEEDED

DO NOT RETURN IT TO THE ORIGINATOR

USER EVALUATION OF REPORT

REFERENCE: USACERL Technical Report 97/137, *Advanced Oxidation Treatment of Army Industrial Wastewaters: Propellant Wastewater*

Please take a few minutes to answer the questions below, tear out this sheet, and return it to USACERL. As user of this report, your customer comments will provide USACERL with information essential for improving future reports.

1. Does this report satisfy a need? (Comment on purpose, related project, or other area of interest for which report will be used.)

_____

_____

_____

2. How, specifically, is the report being used? (Information source, design data or procedure, management procedure, source of ideas, etc.)

_____

_____

3. Has the information in this report led to any quantitative savings as far as manhours/contract dollars saved, operating costs avoided, efficiencies achieved, etc.? If so, please elaborate.

_____

_____

4. What is your evaluation of this report in the following areas?

a. Presentation: _____

b. Completeness: _____

c. Easy to Understand: _____

d. Easy to Implement: _____

e. Adequate Reference Material: _____

f. Relates to Area of Interest: _____

g. Did the report meet your expectations? _____

h. Does the report raise unanswered questions? _____

i. General Comments. (Indicate what you think should be changed to make this report and future reports of this type more responsive to your needs, more usable, improve readability, etc.)

_____

_____

_____

_____

_____

_____

5. If you would like to be contacted by the personnel who prepared this report to raise specific questions or discuss the topic, please fill in the following information.

Name: _____

Telephone Number: _____

Organization Address: _____

_____

_____

6. Please mail the completed form to:

Department of the Army
CONSTRUCTION ENGINEERING RESEARCH LABORATORIES
ATTN: CECER-TR-I
P.O. Box 9005
Champaign, IL 61826-9005

REPORT DOCUMENTATION PAGE

Form Approved
OMB No. 0704-0188

1. AGENCY USE ONLY *(Leave Blank)*	2. REPORT DATE	3. REPORT TYPE AND DATES COVERED
	September 1997	Final

4. TITLE AND SUBTITLE
Advanced Oxidation Treatment of Army Industrial Wastewaters: Propellant Wastewater

5. FUNDING NUMBERS
4A162720
D048
UX6

6. AUTHOR(S)
Stephen W. Maloney

7. PERFORMING ORGANIZATION NAME(S) AND ADDRESS(ES)
U.S. Army Construction Engineering Research Laboratories (USACERL)
P.O. Box 9005
Champaign, IL 61826-9005

8. PERFORMING ORGANIZATION REPORT NUMBER
TR 97/137

9. SPONSORING / MONITORING AGENCY NAME(S) AND ADDRESS(ES)
U.S. Army Environmental Center (USAEC)
ATTN: SFIM-AEC-ET
PO Box 4435
Aberdeen Proving Ground, MD 21020-5401

10. SPONSORING / MONITORING AGENCY REPORT NUMBER

11. SUPPLEMENTARY NOTES
Copies are available from the National Technical Information Service, 5285 Port Royal Road, Springfield, VA 22161.

12a. DISTRIBUTION / AVAILABILITY STATEMENT
Approved for public release; distribution is unlimited.

12b. DISTRIBUTION CODE

13. ABSTRACT (Maximum 200 words)

Advanced Oxidation Processes (AOPs) are water treatment processes that generate hydroxyl (OH) radicals for destruction of organic contaminants using ozone/UV, hydrogen peroxide/UV, or ozone/hydrogen peroxide. These processes are important methods for Army wastewater treatment and contamination remediation. This project: (1) analyzed information on AOPs for treatment of Army waste streams; (2) developed predictive models for process development, optimization, and cost projection; and (3) demonstrated on a laboratory scale AOP treatability of wastewater-containing DNT and ethanol.

A kinetic model was found most suitable for modeling the contaminant destruction process. For the DNT-containing wastewater, not only OH, but also α-hydroxyethyl radical (HE) produced by the action of hydroxyl radical on ethanol, were important for the destruction of DNT, depending on the oxygen concentration in solution. Techniques of kinetic analysis were used to determine the form of the rate equation for HE radical, and to evaluate the appropriate rate constants to yield the general model for reductive treatment. Combination with the OH-radical model gave a comprehensive model that correctly described systems in which both OH and HE processes occurred simultaneously. Discovery of the reductive reaction using the kinetic techniques led to a factor of 230 improvement in AOP treatment efficiency.

14. SUBJECT TERMS
Army facilities
models
wastewater treatment systems
water treatment

15. NUMBER OF PAGES
160

16. PRICE CODE

17. SECURITY CLASSIFICATION OF REPORT	18. SECURITY CLASSIFICATION OF THIS PAGE	19. SECURITY CLASSIFICATION OF ABSTRACT	20. LIMITATION OF ABSTRACT

Executive Summary

Water treatment processes that generate hydroxyl (OH) radicals for destruction of organic contaminants by means of ozone/UV, hydrogen peroxide/UV, or ozone/hydrogen peroxide are termed as Advanced Oxidation Processes (AOPs). These processes represent an important subgroup of the available methods for Army wastewater treatment and contamination remediation. These processes are, in general, effective for the destruction of most organic (carbon-containing) contaminants because the hydroxyl radical can indiscriminately attack most organic compounds. Oxidation by-products (OBPs) are therefore also attacked, which can lead to the complete conversion of most organic contaminants to carbon dioxide and water, with mineralization of heteroatoms such as nitrogen and sulfur to their oxidized forms, nitrate, and sulfate. Although complete mineralization of contaminants is not always necessary, it represents a safe alternative in critical applications where OBPs have not been thoroughly identified.

The objectives of this project were to: (1) analyze information available on AOPs for treatment of Army waste streams; (2) develop predictive models for process development, optimization and cost projection; and (3) demonstrate on a laboratory scale the AOP treatability of wastewater from Radford Army Ammunition Plant (RAAP) containing DNT and ethanol.

A literature survey on the application of AOPs to Army wastewater treatment was done. The data were analyzed in terms of target compound and total organic carbon (TOC) removal, overall treatment efficiency, and cost. A table was prepared that summarizes the analysis of existing experimental data for various groups of Army wastes treated with AOPs and related methods. The factors affecting AOP treatment efficiency such as oxidant dose and mass transfer, UV light intensity, pH, etc. were evaluated. AOP kinetics and by-products formed in the course of treatment by various AOPs were also reviewed. AOP chemistry and mathematical modeling of AOPs were discussed.

The literature survey showed that many of the Army wastewaters can be successfully treated with AOPs. Ozone/UV treatment appears to be the most successful for TOC removal although some target compounds may be eliminated by photolysis or ozonation alone. The analysis of the literature information also indicated; however, that most investigators have not made use in their data analyses of existing knowledge of the fundamental principles underlying AOP processes. The importance of mathematical modeling of AOPs as a means to optimize the treatment and therefore make it more cost-effective, has not been recognized. Frequently conflicting data between investigators indicates that modeling based on the free-radical chemistry of the system must be used to

compare results. Significant data gaps were identified such as the lack of comparative analysis of various AOPs, lack of identification of important types of wastewater components, shortage of TOC and by-product data, lack of oxidant dose and concentration data, and shortage of data on AOP treatment of wastes other than explosive-contaminated wastewaters.

Laboratory studies were conducted in which synthetic wastewaters composed of aqueous solutions of 2,4-dinitrotoluene (DNT), ethanol, and diethyl ether were treated with various AOPs and UV photolysis. In addition to supplying treatability information, the experiments provided data for modeling in an attempt to develop a predictive relationship between wastewater composition and treatment effectiveness. Aqueous solutions of DNT containing high concentrations of ethanol were treated with H_2O_2/UV at various concentrations of dissolved oxygen. The DNT disappearance rate was found to be inversely dependent on the oxygen concentration in the solution, with more than two orders of magnitude of difference between the rates observed in the oxygen- and nitrogen-sparged experiments. This was taken to indicate that DNT removal was due to its reduction by α-hydroxyethyl radical formed in reaction of hydroxyl radical with ethanol, rather than by direct OH radical attack on DNT.

It was determined that a kinetic model was most suitable for modeling the contaminant destruction process. It was found that, for the DNT-containing wastewater, not only hydroxyl radical (OH), but also α-hydroxyethyl radical (HE) produced by the action of hydroxyl radical on ethanol, were important for the destruction of DNT depending on the oxygen concentration in solution. The rate of HE attack was inversely proportional to oxygen concentration. Techniques of kinetic analysis developed during the formulation of the hydroxyl radical model were used to determine the form of the rate equation for HE radical, and to evaluate the appropriate rate constants to yield the general model for reductive treatment. Combination with the OH-radical model gave a comprehensive model that correctly described systems in which both oxidative (OH) and reductive (HE) processes occurred simultaneously. Discovery of the reductive reaction using the kinetic techniques led to a factor of 230 improvement in the AOP treatment efficiency, which should yield a significant economic improvement in treatment. The model has only been verified over a wide range of batch conditions for chemicals typical of water dry wastewater. However, the mechanism discovered may have much broader applications to Army-unique water constituents such as nitrate esters, nitro-aromatics and nitramines because the HE radical attacks the nitro group rather than other locations on these molecules.

Foreword

This study was conducted for U.S. Army Environmental Center (USAEC) under Project 4A162720D048, "Industrial Operations Pollution Control Technology"; Work Unit UX6, "Factors Affecting ADVOX Processes." The technical monitor was Richard Eichholtz, SFIM-AEC-ET.

The work was performed by the Industrial Operations Division (UL-I) of the Utilities and Industrial Operations Laboratory (UL), U.S. Army Construction Engineering Research Laboratories (USACERL). This study was performed in part by the Illinois State Water Survey, Champaign, IL, under contract to the Industrial Operations Division (UL-I), U.S. Army Construction Engineering Research Laboratories (USACERL). The USACERL principal investigator was Dr. Stephen W. Maloney. Walter J. Mikucki is Chief, CECER-UL-I; John T. Bandy is Operations Chief, CECER-UL; and the responsible Technical Director was Gary W. Schanche, CECER-UL. The USACERL technical editor was William J. Wolfe, Technical Resources.

COL James A. Walter is Commander and Dr. Michael J. O'Connor is Director of USACERL.

Contents

SF 298 1

Executive Summary 3

Foreword 5

List of Tables and Figures 8

1 Introduction 11

Background 11

Objectives 11

Approach 12

Scope 13

Mode of Technology Transfer 13

Metric Conversion Factors 13

2 Literature Review: Application of AOPs to Army Wastewater Treatment 14

Army Wastewaters Characterization 14

Treatment Studies 16

TNT and RDX Photolysis 41

3 Experimental Details 50

The Ozonation System and the Reactor 50

High-Power Lamp Reactor 51

Materials 53

Analytical Methods 53

Inorganic Analytes 55

Selection of AOPs To Be Investigated 57

Flow-Through Treatment Studies 57

Flow Reactor 58

Gas Manifold 59

Solutions, Chemicals, and Procedures 61

4 Experimental Results, Analysis, and Discussion 62

Coupling of Mass Transfer and Chemical Reactions 62

Origin of the Model 64
Determination of $k_{OH,DNT}$ 65
Comparison of Ozone/UV and Ozone/H_2O_2 67
Effect of High-Power UV Lamp on DNT Removal 69
Oxidation Byproducts 72
Nitrite and Nitrate 76
Dependence of DNT Removal on Ethanol Concentration 76
Modeling of Ethanol Oxidation 83
Implications of Conclusions From the Pulse Radiolysis Literature 89
Identification and Modeling of the Unknown Active Species 90
Byproduct Study 106
Study System I: RAAP Wastewater—DNT in Aqueous Ethanol 111
Importance of Dissolved Oxygen to AOP Performance for DNT Removal 118
Kinetic Model for Flow Treatment 126
Results of Flow Through Studies 131
Discussion of Results From Flow-Through Experiments 135

5 Conclusions And Recommendations 138
Conclusions 138
Recommendations 143

References 145

Appendix: Details of Superoxide Liberation 153

Distribution

List of Tables and Figures

Tables

2-1 Summary of reported AOP testing on Army wastes. 15
2-2 Typical concentrations of target compounds in Army wastewaters. 16
2-3 Redwater characterization. 17
2-4 Photodegradation products of TNT 26
2-5 Treatability data. 33
2-6 Byproduct yield from RDX photolysis and thermolysis (as % of possible nitrogen or carbon available from RDX). 42
2-7 Photodegradation products from DNT (Burlinson et al. 1979) 49
3-1 Analytical methods. 54
4-1 Typical concentrations of organic constituents of RAAP DNT wastewater 62
4-2 Chemical characterization of RAAP DNT wastewaters. 63
4-3 DNT treatability experiments. 66
4-4 Nitrogen mass balance. 77
4-5 DNT treatability experiments: effect of oxygen concentration. 91
4-6 Comparison of theoretical and "best-fit" values for parameters in kinetic model. 104
4-7 Effect of oxygen concentration on the efficiency of the reductive pathway. 119

Figures

2-1 Scheme I: The initial step of RDX photolysis. 43
3-1 Laboratory-scale UV/peroxide photochemical reactor 51
3-2 Continuously stirred-tank photochemical reactor 58
3-3 Gas manifold from the laboratory ozonation system. 60
4-1 DNT removal by O_3/H_2O_2 treatment (no ethanol present) 68
4-2 Efficiency of DNT removal by O_3/UV and O_3/H_2O_2 (no ethanol present) 68
4-3 DNT removal by UV photolysis using low-pressure lamps. 70
4-4 DNT removal by O_3/UV and O_3/H_2O_2 treatment in the presence of ethanol. 70

4-5 Efficiency of DNT removal by O_3/UV and O_3/H_2O_2 treatment in the presence of ethanol. 71

4-6 DNT removal by UV photolysis and O_3/UV treatment using a high-power lamp: Experiment A01-photolysis with 13-Watt lamps (presented for comparison); Experiment A17-photolysis, ethanol 17.8 mM; Experiment A18-photolysis; Experiment A19-O_3/UV, ethanol 13.3 mM. 71

4-7 DNT byproduct distribution on C18 column: (a) after 360 min of photolysis; (b) after 20 min of O_3/UV treatment; (c) after 120 min of O_3/UV treatment; DNBA elutes as an unretained peak at ~2 mn on this column. 73

4-8 DNT byproduct distribution on C_{18} column after 330 min of O_3/UV treatment at various ethanol concentrations (mM): (a) 4.5; (b) 16.3; (c) 69.5; DNBA elutes as an unretained peak at ~2 min on this column. 75

4-9 Experiment A10: DNT removal by O_3/UV treatment in the presence of 442 mM of ethanol. 78

4-10 Experiment A11: DNT removal by O_3/UV treatment in the presence of 74.4 mM of ethanol and 6.1 mM of ether. 78

4-11 Experiment A14: DNT removal by O_3/UV treatment in the presence of 16.3 mM of ethanol. 79

4-12 Experiment A15: DNT removal by O_3/UV treatment in the presence of 69.5 mM of ethanol and 4.5 mM of ether. 79

4-13 Experiment A16: DNT removal by O_3/UV treatment in the presence of 4.5 mM of ethanol. 80

4-14 Experiment A12: DNT removal by O_3/UV treatment in the presence of 4.2 mM of DEE 80

4-15 Comparison of observed and calculated DNT destruction efficiencies, as a function of initial ethanol concentration (mM). 81

4-16 Efficiency of DNT removal by AOPs at various ethanol concentrations (mM): (a) 4.0; (b) 4.5; (c) 4.8; (d) 16.3; (e) 69.5; (f) 74.4; (g) 442; all experiments were O_3/UV except (a), which was O_3/H_2O_2. 82

4-17 Reaction 1, Scheme I, abstraction of hydrogen atom. 84

4-18 Scheme II: Hydroxyl radical chemistry of acetaldehyde. 88

4-19 DNR removal by H_2O_2/UV treatment in oxygen- and nitrogen-sparged solutions (no ethanol present). 92

4-20 DNR removal by H_2O_2/UV treatment in oxygen- and nitrogen-sparged solutions in the presence of ethanol. 92

4-21 Effect of oxygen concentration on DNT removal by H_2/O_2/UV treatment; oxygen concentration (mg/L) given in parenthesis. 94

4-22 Scheme III: radical anion of the nitro-compound "escapes" the reaction system. 94

4-23 Scheme IV: replacement of generic escape mechanism 95

4-24 Ordnance compound initial rate data in terms of the escape model. 97

4-25 Effect of ethanol addition and nitrogen sparging on the destruction of carbon tetrachloride in water. 99

4-26 Fit of combined escape and radical generation models to data from Experiment A-39. 103

4-27 Comparison of original extrapolation line to that resulting from Experiment A-39 data fit. 104

4-28 Refined competition-kinetic analysis of ozone/UV treatability data. 106

4-29 DNT byproduct distribution on C_{18} column: (a) after 90 min of H_2O_2 /UV treatment in O_2-sparged solution (ξ_{DNT} = 0.29); (b) after 2 min of H_2O_2/UV treatment in N_2-sparged solution (ξ_{DNT} = 0.68) Peaks at 7.03 and 17.32 min in chromatogram (a) are artifacts. 108

4-30 Chromatogram of successive samples from Experiment A24 (N_2-sparge). Peaks with retention times 18.26 min (chromatogram at 15 min) and 19.30 min (chromatogram at 30 min) are artifacts. 108

4-31 DNT byproduct distribution on C_{18} column: (a) after 1 mn of H_2O_2/UV treatment in N_2-sparged solution (ξ_{DNT} = 0.34), (b) after 220 min of H_2O_2/UV treatment in O_2-sparged solution (ξ_{DNT} = 0.16). 109

4-32 Chromatogram of 45-min sample from Experiment A39 (N_2-sparge). 109

4-33 Byproduct accumulation in Experiment A39 (N_2-sparge) 110

4-34 Effect of oxygen on calculated DNT profiles. 114

4-35 Model failure for high-pressure lamp (O_3/UV treatment of DNT using high-intensity lamp) 115

4-36 Numerical modeling of DNT removal (combined oxidative and reductive removal). 116

4-37 Equilibrium oxygen concentration (mg/L) as a function of oxygen consumption rate. 125

4-38 Oxygen concentration (mg/L) as a function of oxygen consumption rate 125

4-39 Effect of oxygen on DNT removal flow system, D_o = 147-172 µM, $EtOH_o$ = 4.9-7.6 mM (Group A) 133

4-40 Effect of oxygen on DNT removal flow system, D_o = 147-172 µM, $EtOH_o$ = 4.9-7.6 mM (Groups A & B). 133

4-41 Effect of oxygen on DNT removal; high DNT concentrations = 402-422 µM (Group D) 136

1 Introduction

Background

Water treatment processes that generate hydroxyl radicals for the destruction of organic contaminants appeared in the early 1970s and immediately appeared quite promising (Glaze et al.) Glaze, Kang, and Chapin (1987) later called these processes Advanced Oxidation Processes (AOPs), a category that includes ozone/UV, hydrogen peroxide/UV, and ozone/hydrogen peroxide treatment. Later this group of processes have been appended with wet air oxidation, supercritical oxidation and oxidation using Fenton's reagent (Glaze, February 1993). AOPs represent an important subgroup of the methods available to the Army for wastewater treatment and contamination remediation. These processes are, in general, effective for the destruction of most organic (carbon-containing) contaminants because the common characteristic of AOPs is the generation of a hydroxyl radical, which can indiscriminately attack most organic compounds. Oxidation byproducts (OBPs) are therefore also attacked, leading to the complete conversion of most organic contaminants to carbon dioxide and water, with mineralization of heteroatoms such as nitrogen and sulfur to their oxidized forms, nitrate, and sulfate. Although complete mineralization of contaminants is not always necessary, it represents a safe alternative in critical applications where OBPs have not been thoroughly identified.

The AOPs have been commercially available for the past two decades. Because of their power to completely mineralize organic pollutants, AOPs have been applied to many Army water contamination problems. However, a general lack of understanding among researchers concerning the chemistry of the processes, and the effect of the composition of the wastestream on the optimal application of these complex processes has resulted in some inconsistency in the reported results of treatability studies. Literature data also indicate that the chemistry is more complex when compounds such as ethanol are present in the wastestream. This may limit the type of modeling that can be applied. In view of the above points, further studies were undertaken to evaluate the possible oxidative and reductive reaction pathways and their contribution in the overall chemistry of AOP treatment, and to determine appropriate means of modeling the treatment processes.

Objectives

The overall objective of this investigation is to develop a rational basis for selection of one AOP over another based on parameters of the wastestream composition and other factors. The data basis is intended to guide engineers to

the process most likely to succeed. Although fundamental understanding of AOPs has been increasing during the last decade, no general mechanistic model has emerged that can be widely applied across the variety of treatment problems that arise. Thus, a predictive tool is needed to aid decisionmakers in their initial consideration of treatment alternatives, and to help engineers and scientists select starting conditions for treatability studies, project treatment cost estimates, and optimize process designs. A specific objective of the project was to use these methods to address the AOP treatability of wastewater from the manufacture of dinitrotoluene (DNT) and pinkwater.

The purpose of this project was to determine if the chemistry of the processes could be understood and kinetically modeled at a fundamental level that explicitly includes the matrix effects of the water being treated. Specifically, in addition to treatment process operational parameters such as ultraviolet (UV) light intensity and oxidant dose rate, the model was meant to consider factors such as the presence of UV light-absorbing solution components, solutes that act as radical scavengers, and other solute effects that may interact with the chemistry of the system to affect the efficiency of AOP treatment.

Approach

A literature search was done to gather and analyze existing data on AOP treatment of Army wastes, and to identify gaps in the existing data that must be filled by further bench scale testing and/or model development. Laboratory treatability experiments were done to model the effect of significant parameters on the efficiency of the treatment process. Factors known to affect AOP efficiency were considered and experiments were designed to elucidate the more important effects such as the presence of known radical scavengers, AOP type, etc. A prototype model was selected as the starting point for modeling of the DNT data.

The model was developed by the following steps:

1. A series of preliminary experiments were done to determine whether the second DNT destruction pathway (in addition to that due to OH radical) was oxidative or reductive.
2. Candidate reaction schemes were considered based on literature information.
3. A prototype model was designed based on as complete a mechanistic description of the system as possible.
4. The model was experimentally verified, parameters of the model were determined, and its limitations were investigated, ultimately to develop a predictive model formulated in terms of treatment process parameters.

A system selected for study was: wastewater from the manufacture of propellant containing 2,4-dinitrotoluene (DNT), ether, and ethanol. The results of many treatability studies have been reported in the literature for both of these systems. For the DNT wastewater, effluent from the water dry process from

Radford Army Ammunition Plant (RAAP) was selected, and ozone/UV treatment was used as the starting point since that treatment was under consideration for use at RAAP. The general approach to model development is described.

Scope

The techniques described and evaluated in this report apply to Army industrial activities. The agencies responsible for development and treatment of Army-specific explosives and other aqueous wastestreams will benefit from the information presented in this report. The goals of developing efficient technologies for munitions-contaminated wastestreams are addressed. The model developed in this study would allow rational selection of treatment conditions for specific Army applications, and would provide a guidance tool for process optimization. The model developed will provide information required for estimation of treatment efficiency and associated costs.

Mode of Technology Transfer

It is anticipated that the findings and recommendations in this report will be used as a foundation for developing and selecting full scale processes for use by the U.S. Army Environmental Center (USAEC) to treat waste streams contaminated with munitions compounds.

Metric Conversion Factors

The following metric conversion factors are provided for standard units of measure used throughout this report:

1 in.	=	25.4 mm
1 ft	=	0.305 m
1 sq ft	=	0.093 m^2
1 cu ft	=	0.028 m^3
1 cu yd	=	0.7645 m^3
1 lb	=	0.453 kg
1 gal	=	3.78 L
F	=	(C × 1.8) +32
1 BTU	=	1.055 kJ

2 Literature Review: Application of AOPs to Army Wastewater Treatment

Army Wastewaters Characterization

Military wastewaters are primarily aqueous effluents generated in maintenance, manufacturing, and "load, assemble, and pack" (LAP) operations of the U.S. Army industrial base. Groundwaters contaminated with Army constituents and industrial wastewaters with military-related compounds may also be included in this category. The contaminants widely range from explosives and propellants to solvents and acids. Table 2-1 presents major groups of wastewaters and compounds of interest and Table 2-2 shows typical concentrations of specific pollutants. The literature information summarized in Table 2-1 shows that Army applications of AOPs primarily treat explosive-contaminated wastewaters. Other areas of application have yet to be fully explored. However, it should be understood that target compounds in military wastewaters are not limited to ordnance constituents but also include many compounds resulting from manufacturing processes and maintenance operations.

One problem in wastewater characterization and treatment is to determine the identity and concentrations of nontarget compounds. Army wastewaters in general are more than simply aqueous solutions of specific compounds. Very often they have large amounts of inorganic anions, suspended solids, etc. It has been shown (Hoigné and Bader 1977; Peyton and Glaze 1988) that species such as carbonate/bicarbonate or even sulfate may affect treatment efficiency by acting as radical scavengers. Nontarget organic material present in solution may also consume radicals. Reliable and sensitive analytical methods should be available and/or developed to characterize matrix components before and after treatment. Standardizing a characterization protocol would provide a common basis for matrix characterization during studies by different investigators.

Overall composition of a wastewater as well as concentration of target compounds and the desired level of treatment may dictate the need for pretreatments and/or the selection of one AOP treatment method over another. In this respect, the content of redwater generated in TNT production (Table 2-3) may be an extreme illustration of the complexity of waters to be treated and, consequently, of treatment problems faced by engineers. Nitrite, sulfite, and nontarget TOC will all consume OH radical, lowering the overall efficiency of target compound destruction.

Table 2-1. Summary of reported AOP testing on Army wastes.

Wastewater	Target compounds	Treatment processes	# of papers evaluated	Treatment scale
Synthetic mixtures of explosives, wastewater from explosive manufacturing plants	TNT, RDX, HMX, TAX, SEX, DNT, TNB, Explosive D, NB, DMN	Ozonation, photolysis, O_3/UV, H_2O_2/UV, H_2O_2/UV/catalyst, H_2O_2/catalyst, O_3/H_2O_2, O_3/H_2O_2/UV, O_3/ultrasound	39	Bench, commercial UV units, pilot plants
Ground- and waste-waters from chemical warfare manufacturing plants, synthetic mix-tures	Chlorinated hydrocarbons, organophosphorous, organosulfur and other heterocom-pounds, i.e., DIMP, DCPD, CPMS, etc.	Ozonation, O_3/UV, H_2O_2/UV	6	Bench, commercial units, pilot plants
Industrial wastewaters with military-related compounds	Pesticides, herbicides	O_3/UV	2	Bench, pilot plants
Wastewaters from electroplating processes	Cyanide, metal cya-nide complexes	O_3/UV, ozonation	1	Pilot plant
Wastewaters from rocket fuel cleanup, synthetic mixtures	Hydrazine, MMH, UDMH	O_3/UV, O_3/ultrasound	2	Bench
Solvent mixtures, wastewaters from propellants production	Alcohols, ethers, chlorinated solvents	Ozonation, photolysis, photocatalytic oxidation	4	Bench, commercial scale

Table 2-2. Typical concentrations of target compounds in Army wastewaters.

	Concentration, mg/L		
Compound	**Low**	**High**	**Average**
TNT	12.3 [3]	221 [4]	100-140
RDX	1.2 [5]	158 [3]	30-80
HMX	0.05 [3]	15 [6]	2-4
TAX	1.2 [5]	3.4 [5]	1-2
SEX	1.3 [5]	2.8 [7]	1-2
PCB's	0.001 [8]	40 [9]	N.A.
DNT*	3	400	160-280**
Cyanide	40 [11]	30,000 [11]	N.A.
DMN	7 [12]	500 [12]	12-14

* Data for RAAP (Heffinger and Jake 1991)

** Concentration in samples, collected at particular sites at RAAP

Another example is the composition of the groundwater collected around Rocky Mountain Arsenal. This water is contaminated with chlorinated hydrocarbons, organophosphates, organosulfates, and other organic compounds (carbonate, sulfate, chloride, and numerous metals such as iron, sodium, calcium, zinc, etc.) at concentrations up to 500 mg/L are also present.

Treatment Studies

The information obtained from the literature indicates that the majority of studies have been done for synthetic or actual pinkwater or for aqueous solutions of basic constituents of pinkwater such as 2,4,6-trinitrotoluene (TNT) and 1,3,5-trinitro-1,3,5-triazine (RDX) (Naval Weapons Support Center, June 1985; Andrews and Osmon 1977; Burrows and Brueggermann 1986; Andrews 1980; Layne et al. 1982; DeBerry, Viehbeck, and Meldrum 1984; Roth and Murphy 1979; Burrows, Jackson, and Lachowski 1984; Smetana and Bulusu 1979; Brabets and Marks 1973; Noss and Chyrek 1984; Fochtman and Huff 1975; Fischer, Jackson, and Lachowski 1982; and Burrows 1983). Photolysis, ozonation, O_3/UV and H_2O_2/UV have been primarily used for Army wastewater treatment. O_3/H_2O_2/UV and H_2O_2/UV/catalyst processes were applied occasionally and O_3/H_2O_2 has not received much study, except the study of DeBerry and co-workers (DeBerry, Viehbeck, and Meldrum 1984). Zappi and co-workers have studied AOPs for treatment of groundwater contaminated with explosive components (Zappi, Hong, and Cerar 1993; Zappi, Fleming and Cullinane 1992; Zappi et al. 1989, Hong, Zappi, and Kuo 1994; and Hong et al. 1996); Fleming et al. 1997; Zappi et al. 1997; and Miller, Toro, and Hernandez 1996.

Table 2-3. Redwater characterization.

Parameter*	Concentration**
pH, units	7.6
Specific Gravity	1.0
Solids	
Total	2840
Volatile	1020
Fixed	1820
% Organics	36
Inorganic Salts	
$NaNO_2$	209
$NaNO_3$	0
Na_2NO_3	55
Na_2SO_4	514
Na_2SO_3-Na_2SO_4	569
Alkalinity (as $CaCO_3$)	43
Organic Content	
COD	685
TOC	544
Nitrobodies	
a-TNT	2.27
2,4-DNT	0.21
2,6-DNT	0.03
1,3,5-TNB	3.10
DNT Sulfonates***	
2,4-DNT-3-SO_3Na	271.7**
2,4-DNT-5-SO_3Na	227.5(2)

* Source: Hao and Phull (1991)
** All results in mg/L (ppm), unless otherwise noted
*** Estimated (calculated) values

A common scenario in these studies was to apply a single AOP method and then to compare the results with those obtained from simple photolysis, ozonation, or H_2O_2 treatment. Only a few studies (DeBerry, Viehbeck, and Meldrum 1984, and Roth and Murphy 1979) did comparative analyses of different AOPs. Several attempts have been made (Burrows 1983; Leitis 1980; Glover and Hoffosommer 1979) to identify oxidation/photolysis byproducts, but only a few have come close to identifying a full suite of products. Even less satisfactory kinetic and mechanistic data were available in literature, although many speculations on AOP mechanisms in Army wastewaters have been made. It should be noted that the purpose of this review is to focus on general implications of AOP chemistry with respect to treatment efficiency rather than to interpret reaction pathways in particular wastewaters treated with AOPs. Still, this review will discuss some mechanistic aspects of AOP studies reflecting the nature of these processes.

Results From Past Treatability Studies

TNT and Nitramines. Ozonation and treatment with H_2O_2 have been found, in general to be ineffective for both TNT (Burrows, Jackson, and Lachowski 1984; Brabets and Marks 1973; Leitis 1980) and nitramines (Burrows, Jackson, and Lachowski 1984; Smetana and Bulusu 1979; Noss and Chyrek 1984). However, ozonation is very sensitive to the conditions of the experiment, such as ozone dose and pH, and efficiency can sometimes be improved by changing the parameters of oxidation.

Photolysis of Army wastewater constituents has been studied in a number of works (Andrews and Osmon 1977; Burrows and Buggermann 1986; Layne et al 1982; Burrows, Jackson, and Lachowski 1984; Smetana and Bulusu 1979; and Burrows 1983). The decomposition of TNT in pinkwater was relatively slow, although quantitative data were contradictory, apparently due to the difference in experimental conditions. Thus, while Andrews and Osmon (1977) found that TNT concentration was reduced to detection limits in 3 hours, Burrows et al. (1984) detected only 10 percent of initial TNT after 30 minutes of treatment and DeBerry et al. (1984) found TNT photodecomposition to be practically negligible. On the other hand, Peyton et al. (1992, Unpublished data) saw 90 percent destruction of TNT in 15 minutes and destruction of RDX to below the detection limit in 5 minutes during the photolysis of contaminated groundwater. A significant amount of 1,3,5-TNB remained as a recalcitrant byproduct. In all cases where it occurred, TNT photolysis resulted in highly colored byproducts and a significant amount of TOC was left behind.

Photolysis of nitramines is very effective. For example, RDX can be destroyed within a few minutes (Smetana and Bulusu 1979; and Glover and Hoffsommer 1979), although that is not always the case for its byproducts. Noss and Chyrek (1984) studied photolysis of TNT and nitroamine mixtures. They found that TNT degradation rate increased when TNT was treated in a mixture with nitramines compared with that in individual treatment. The opposite effect was observed for the nitroamine degradation rate, which implies that the destruction mechanism for these classes of compounds may be different. Apparently, TNT

either reacts with radicals and/or byproducts formed in the decomposition of nitramines, or is photosensitized by the nitramines. These results clearly illustrate the importance of matrix composition and the nature of constituents. Another example is the enhancement of TNT photodecomposition rate in the presence of small amounts of acetone when TNT solutions were prepared from acetone concentrates (Andrews and Osmon 1977).

No significant advantage of adding O_3 or H_2O_2 for photolytic destruction of nitramines has been found (Burrows, Jackson, and Lachowski 1984; Noss and Chyrek 1984). The TNT and TOC degradation rate considerably increased when pinkwater was treated with O_3/UV or H_2O_2/UV compared with photolysis or ozonation (Naval Weapons Support Center June 1985: Andrews 1980; Layne et al 1982; BeBerry, Viehbeck, and Meldrum 1984; Noss and Chyrek 1984). TOC was in many cases almost completely mineralized when treatment involved both photolysis and oxidants (Andrews and Osmon 1977; Roth and Murphy 1979). Unlike photolysis, during O_3/UV treatment both TNT and nitramines decomposed more slowly when they were treated as a mixture, but the destruction rate depression was five- to fifteen-fold for nitramines and only two-fold for TNT (Burrows, Jackson, and Lachowski 1984). These results may indicate a difference in reaction mechanisms, matrix composition, or competition for some limiting agent such as hydroxyl radicals or photons.

DeBerry et al. (1984) studied O_3/UV and H_2O_2/UV treatment of both TNT and TNB solutions. They found TNB to be a major product of TNT decomposition. They applied different AOPs to treat TNB solutions and found that, in all cases, it disappeared more slowly than TNT. The authors reported that although the highest rate of TNB destruction was in O_3/H_2O_2/UV treatment, the efficiency (defined as the number of moles of TNB removed per mole of oxidant consumed) was highest for the O_3/H_2O_2 system. They state that only 4.2 moles of total oxidant (O_3 + H_2O_2) were consumed per mole of TNB destroyed using O_3/H_2O_2 as compared to 20.4 moles for O_3/H_2O_2/UV system. About 200 moles H_2O_2 were consumed per mole TNB removed in H_2O_2/UV treatment. However, our calculations based on the same data indicate a different result. These calculations gave efficiency values identical or similar to those obtained by DeBerry et al., except for the efficiency for O_3/H_2O_2 treatment, which indicated that about 30 moles of oxidant were used per mole TNB removed, instead of 4.2 moles, as the authors stated. These calculations also indicate that O_3/UV was the most efficient in TNB destruction with an efficiency of 0.055, compared to 0.034 for the O_3/H_2O_2 system.

In contrast to the findings of DeBerry and co-workers (1984), Peyton et al. (1992, unpublished data) found that TNT (and RDX) could be effectively removed from contaminated groundwater by UV photolysis, but that the persistent byproduct TNB was most efficiently removed by ozone/UV. Zappi, M. E., Hong, A. and Cerar, R. (1993) have also found the same results that TNT leads to TNB and O_3/UV is effective in treating the byproduct TNB.

O_3/UV has been found to be, in general, more effective for pinkwater treatment than H_2O_2/UV (DeBerry, Viehbeck, and Meldrum 1984; Roth and Murphy 1979)

although this statement should be qualified, since the majority of data was obtained under widely varying experimental conditions.

Fenton's reagent (a combination of H_2O_2 and ferrous ion) is known to generate hydroxyl radicals, so the processes using this reagent may be included in the category of AOPs. The system is quite complicated due to side reactions of ferrous ions; there is also a possibility of OH• scavenging by hydrogen peroxide. Not much is known about treatment of military constituents with Fenton's reagent. DeBerry et al. (1984) studied TNB removal at various composition of Fenton's reagent and found that the rate constant of TNB destruction was about an order of magnitude higher than that estimated from H_2O_2/UV experiments. However, the best Fenton's reagent composition was only half as fast in TNT removal in comparison with O_3/UV treatment.

The same authors (DeBerry and Payne 1985) treated dimethyl methyl phosphonate with various AOPs and found the oxidation by Fenton's reagent the least effective (the treatment with H_2O_2/UV was the fastest).

DNT. Much less is known about AOP application to the treatment of 2,4-DNT, which is used in the production of propellants. It is also one of the byproducts in the TNT manufacturing process. Ho (1986) identified DNT degradation byproducts in aqueous solutions treated with H_2O_2/UV. The data indicated that DNT was eventually converted to HNO_3, CO_2, and H_2O. Organic products are discussed later in this section.

Andrews and Osmon [1977] treated 2,4-DNT and 2,6-DNT aqueous solutions with UV light in a continuous flow system and with H_2O_2/UV in a batch system. Photolysis alone was successful in eliminating DNT, but it may, in part, be attributed to the presence of acetone, since DNT solutions were prepared from its acetone concentrates. Acetone is a known photosensitizer. The authors did not investigate the effect of acetone concentration on the DNT destruction rate in detail, but they found that, for TNT, the rate of photolysis increased with an increase in the acetone concentration from 0.01 to 1 percent. After 6 hours of irradiation, 2,4- and 2,6-DNT were practically gone, but in the case of 2,4-DNT, a fluorescent product was detected. When DNT was treated with H_2O_2/UV the target compound and TOC were eliminated after 1 and 2 hours of the treatment, respectively.

The Ordnance Group from Hercules Aerospace Co. (Heffinger and Jake 1991) studied feasibility of AOPs for 2,4-DNT treatment. They found that ozonation, photolysis, and H_2O_2 treatment were individually ineffective for DNT solutions. The application of H_2O_2/UV showed a significant improvement in DNT degradation and O_3/UV treatment resulted in nearly complete destruction after 5 minutes. When O_3/UV was applied to actual wastewater, the DNT degradation proceeded at a lower rate, as expected. TOC changes were not monitored.

Miscellaneous Energetic Compounds. Both ozonation and O_3/UV were effective in nitrobenzene (NB) destruction, but TOC removal was achieved only when O_3/UV was applied (Leitis 1980). Similar results were obtained for selected

compounds such as di-isopropylmethyl phosphonate (DIMP) and dicyclopentadiene (DCPD) in groundwater collected around Rocky Mountain Arsenal (Buhts, Malone, and Thompson 1978). O_3/UV proved effective in treatment of pesticides (Buhts, Malone, and Thompson 1978; Arisman et al 1980; Mauk, Prengle, and Payne 1976). H_2O_2/UV was successfully applied for destruction of organophosphorus wastes, containing isopropylmethyl-phosphonate (IMP) and methyl phosphonic acid (MPA) (Mill, Epstein and Schiff 1976). In a number of cases (Mauk, Prengle, and Payne 1976; Mill, Epstein and Schiff 1976) TOC was reported to be converted to CO_2 and H_2O. Ozonation alone did not cause any destruction of 1,1-dimethylnitrosoamine (DMN) in a wastewater from RDX production (Kobylinski and Peterman 1979). Although the authors claim that photolysis was more effective than O_3/UV treatment, the experimental data indicate that both methods were almost equally effective in reduction of the DMN concentration.

H_2O_2/UV proved effective (Andrews and Osmon 1977) in destroying high concentrations (up to 500 mg/L) of Explosive D (ammonium picrate). TOC was also eliminated after 3 to 5 hours of treatment.

Sierka and Cowen (1980) studied O_3/UV application to treat monomethyl hydrazine (MMH) and unsymmetrical dimethyl hydrazine (UDMH) rocket fuels along with hydrazine, which are contaminants of washwater from cleanup of tank cars. They found that O_3/UV was more effective than ozonation alone in removing the compounds of interest and even more beneficial for the destruction of some of the byproducts. Since the treatment was stopped at the point of complete elimination of the hydrazines, and considerable TOC still remained, the advantage of O_3/UV system (over ozonation alone) for TOC removal is difficult to evaluate.

Solvents. Little data are available for the application of AOPs to solvent-contaminated Army wastewaters. The available data (Patterson et al 1976, Pacheco, Prairie, and Yellowhorse 1991) are limited and inconclusive. However, numerous other (non-Army) bench scale studies on ozonation of various nonchlorinated and chlorinated hydrocarbons have been carried out since the late 1960s and O_3/UV was first applied to treat these systems in the mid 1970s. The results of these studies Judeikis and Hill 1991; Takahahsi 1190; Kuo, Chian, and Chang 1977; Mallevialle 1982; Masten and Butler 1986) show that the compounds of interest and majority of their byproducts can be completely destroyed during O_3/UV treatment. (Judeikis and Hill (1991) successfully treated methanol, isopropyl alcohol, trichloroethylene and trichlorethane (these compounds were found in space launch-generated wastewaters) with O_3/UV, but they found that the ozone concentration in the gas effluent was virtually the same as the influent concentration, although target compounds and TOC were removed to detection limits. Since, even in the absence of organics, partial consumption of ozone occurs due to the decomposition by UV light, these findings may be attributed to the huge excess of ozone that was put through the reactor during these experiments. On the other hand, these results indicate that the amount of ozone required for complete destruction of TOC may indeed be very small. Extensive data are also available from the drinking water and groundwater remediation literature. These data indicate that nonchlorinated

solvents that are not photolyzed, can be expected to react by the usual pathways of OH radical reactions, and can be modeled as such. Chlorinated solvents are subject to UV photolysis, which must be included in the modeling effort for H_2O_2/UV treatment in dilute solution (and perhaps for O_3/UV as well). Degradation pathways and byproducts are less well understood for chlorinated solvents.

Peyton and Law (1990) first applied the combined concepts of efficiency and competition calculations for process optimization during their study of the AOP remediation of groundwater that had been contaminated with partially-oxidized hydrocarbons from previous fire training activities at Lakehurst Naval Air Engineering Center. They found that H_2O_2/UV was the most efficient process in the early stages, but was too slow. O_3/H_2O_2 at slightly alkaline pH was rapid and efficient initially, but became slow and inefficient by the 50 percent TOC removal point, due to accumulation of carbonate that then acted as a radical scavenger. The carbonate accumulated due to carbon dioxide dissolution in the alkaline water as TOC was mineralized. Treatment with O_3/UV at pH 3 to 4 was rapid but less efficient initially, but the efficiency was seen to increase dramatically in the latter stages of TOC removal. Competition calculations verified that radical scavenging was responsible for the loss in efficiency for the O_3/H_2O_2 process, while efficiency calculations suggested that sequential application of O_3/H_2O_2 followed by O_3/UV at lower pH (to allow CO_2 sparging) might be justified on the basis of the potential efficiency increase. Peyton and Law (1990) experimentally confirmed this hypothesis.

Effect of pH. As seen above, and as will be shown in the later discussion on the AOP mechanistic model, pH is an important factor that affects the way AOP and related processes work. The pH effect has been studied in a number of works (Naval Weapons Support Center June 1985; Andrews 1980; Layne et al 1982; DeBerry, Viehbeck, and Meldrum 1984; Brabets and Marks 1973; Sierka and Cowen 1980) and some general trends can be revealed based on the data obtained in these studies.

Brabets and Marks (1973) ozonated actual pinkwater at pH 7.0 until all visible color was removed. The resulting solution had a pH of 4.0 to 5.0; neutralization to a pH 6.5 to 7.0 reintroduced some noticeable color. When the initial pH of pinkwater was raised to 8 to 10.5, ozonation permanently removed all the color and the treated water had a neutral pH. The ozone consumption in the latter case was much higher. The results can be explained in terms of the base-catalyzed decomposition of ozone, resulting in the production of hydroxyl radicals, which remove the products responsible for color. However, since TOC data are not available, the difference in treatment efficiency between the two processes cannot be evaluated.

Layne et al. (1982) found that the addition of base (in which the pH was raised from 7.0 to 9.7) enhanced TNT decomposition in its solutions treated with O_3/UV. Increasing the pH increases the rate of ozone reaction with OH^-, as well as with the HO_2^- anion of the hydrogen peroxide that is formed in ozone photolysis. Both reactions may, at different points of treatment, contribute to the initiation process. Similarly, low pH was found to inhibit the destruction

rate for TNT, TNB, and NB treated with O_3 and O_3/UV (Leitis 1980). The oxidation of TNB, for instance, did not occur at all in the presence of 0.04 N HCl, but was fast at ambient pH.

Alkaline pH considerably accelerated the degradation rate of hydrazine fuels and their oxidation byproducts, such as methanol, in O_3/UV treatment (Sierka and Cowen 1980). The ozone consumption at pH 9.1 was about four times higher than at pH 3.1. As in the pinkwater ozonation study cited above (Brabets and Marks 1973), TOC measurements were not performed, which makes it impossible to evaluate benefits of high pH for the TOC removal efficiency.

The pH effect on H_2O_2/UV treatment has been primarily studied for TNT solutions (Naval Weapons Support Center 1985; Andrews 1980; DeBerry, Viehbeck and Meldrum 1984). It was determined (Andrews 1980) that extremely acidic pH (1 or 2) negatively affected the TNT and TOC destruction rates compared with those at ambient pH. This fact was attributed to the stabilization of H_2O_2 in acidic condition. Similar results were obtained by DeBerry, Viehbeck and Meldrum (1984). The pH adjustment in the range 7.0 to 10.0 did not have any significant effect on the treatment (Andrews 1980).

The pH effect, in general, is not limited to the oxidant behavior since many organic compounds, such as phenols, amines, etc., can exist in various protonated and deprotonated forms depending on the pH of the solution. One very important pH effect is on the equilibrium between carbonate and bicarbonate, since the former is a better OH-radical scavenger by a factor of 46. Relatively minor changes in pH in the region of the pK_a for bicarbonate (10.25) can have a significant effect on treatment efficiency of carbonate-containing solutions.

Effect of UV Intensity. Photolysis of ozone and hydrogen peroxide are important processes in AOP treatment. The rate of photolysis is proportional to the amount of UV light delivered into the solution and depends, among other factors, on UV intensity, solution absorbance, and on the location and design of UV lamp sites. The effect of UV intensity has been studied as a dependence of the contaminant destruction rate on number or power output of UV lamps. The experimental data obtained from the literature are inconclusive and sometimes appear contradictory; however, they indicate, for example, that in the O_3/UV system, a variation in UV intensity usually has less of an effect on contaminant removal rate than does ozone mass flow, while the H_2O_2/UV system is very sensitive to UV input.

The rate of TNT destruction in O_3/UV treatment of TNT aqueous solutions was markedly higher at UV intensity 4.5 Watt/L (W/L) than at 1.5 W/L (Leitis 1981). Fisher, Jackson, and Lachowski (1982) found that 26 lamps provided slightly faster removal of RDX, than did 30 lamps, when pinkwater was treated with O_3/UV. The TNB decomposition rate was found to be independent of UV intensity in the range of 0.8 to 6.5 W/L, but the rate strongly depended on the ozone dose rate (DeBerry, Viehbeck, and Meldrum 1984).

The percent of DIMP removal in O_3/UV treatment of the groundwater collected around Rocky Mountain Arsenal was found to be dependent on the reactor

design (Buhts, Malone, and Thompson 1978). When the Westgate research unit with one lamp and two spargers for ozone introduction was used, the increase in UV power from 28 to 43 W did not have any significant effect on DIMP removal. The greatest DIMP removal was associated with the highest ozone mass flow rate. The same effect was found for TOC. If the groundwater was treated in a Holston (stirred tank) reactor with two lamps, a sparger, and an impeller (which allowed for greater UV input and ozone concentrations), the most effective removal of DIMP was achieved at much shorter contact times when both UV intensity and ozone mass flow rate were the highest. However, with a long contact time and the highest ozone input, low levels of DIMP could be achieved even without UV light. The same group (Thompson et al. 1979) showed that in the Westgate (ULTROX) commercial unit used in a field scale treatability study the percent of DIMP removal increased quickly with ozone dose rate and UV input until the ozone mass flow rate reached its highest value allowed in that reactor (300 mg/min) and the number of operating UV lamps reached 10 (out of 30 possible in that reactor). The data above show that the optimization of O_3/UV system in terms of both ozone and UV input should be considered. In general, the optimum ozone/UV ratio may be expected to vary with wastewater and contaminants to be treated.

DeBerry, Viehbeck, and Meldrum (1984) have found that the decrease in UV input to the H_2O_2/UV treatment decreased both the apparent quantum yield of H_2O_2 decomposition and the TNB destruction rate. Both the H_2O_2 concentration and UV intensity affected TNT removal in pinkwater treated with H_2O_2/UV (Naval Weapons Support Center 1985), but changes in UV input caused the most dramatic effect on TNT degradation rate.

The effect of UV wavelength on the rate of contaminant removal has also been studied. The data obtained from studies on DNT treatment with H_2O_2/UV (Ho 1986) and O_3/UV (Heffinger and Jake 1991) indicated that the shorter the UV wavelength, the higher the extent of DNT removal. Similar results were obtained by Smetana and Bulusu (1979) for RDX photolysis in a wavelength range from ~250 to 350 nm.

Effect of Oxidant Dose and Dose Rate. Only a few investigators have reported the results of studies in which the oxidant dose rate was varied. Fochtman and Huff (1975) studied O_3/UV treatment of TNT in synthetic pinkwater. They showed that the amount of ozone needed to remove the same quantity of TOC decreased when ozone mass flow was reduced. They also found that this amount might be further reduced when mechanical mixing in the reactor (additional to that from simple gas bubbling) was used. These observations are most likely related more closely to ozone mass transfer efficiency than to differences in chemical efficiency. Layne et al. (1982) found that in O_3/UV treatment of TNT solutions, the ozone uptake/ozone input ratio increased when the ozone concentration in gas flow decreased. There are several possible offsetting complications that could explain these observations, and the probable cause(s) cannot be identified without careful data analysis. A peroxide concentration effect was found in H_2O_2/UV treatment of TNT (Naval Weapons Support Center 1985, Andrews and Osmon 1977), where the peroxide concentration larger than 0.1 to 0.5 percent inhibited TNT decomposition. In other studies (Andrews

1980; Noss and Chyrek 1984) this threshold value was even less than 0.1 percent. These findings may indicate a simple competition effect. It should be pointed out, however, that in the studies of Andrews (1980) and Andrews and Osmon (1977), the experimental section states that the 254-nm lamp was enclosed in a Pyrex tube. Pyrex cuts off wavelengths shorter than 300 nm, so it is not clear exactly what effect was being measured in this work.

The data discussed above agree with the mechanistic model for AOPs, which predicts that at high concentrations, ozone or H_2O_2 can compete with organics for OH•, which contributes to reduction in treatment efficiency. Recent studies (Peyton 1992) have shown that it is possible to improve the efficiency of AOPs by reducing the rate of oxidant addition. Experimental methods for accurate delivery and measurement of gaseous ozone have been developed (Peyton et al. 1995). Once again it should be emphasized that careful measurement and accounting of oxidant doses and concentrations is one of the key requirements for optimization of treatment efficiency and, therefore, process economics, in conjunction with a workable mathematical model of the processes.

AOP Byproducts. As already mentioned in this review, the knowledge of the composition of the wastewater to be treated including target compounds, other products resulting from the manufacturing process, and other matrix components is important for the successful selection of appropriate AOPs or their combinations. The knowledge of byproducts formed in the treatment process is also of great importance, since they may be more (or less) resistant to treatment, more toxic than original target compounds, and may vary for different AOPs as well. For instance, Glover and Hoffsommer (1979) found that O_3/UV treatment of RDX aqueous solutions produced ammonia, nitrate, CO_2, and several organic nitrocompounds. Photolysis alone resulted in production of ammonia, nitrite, formaldehyde, and a few organic nitro- and nitrosocompounds. When a solution of RDX was first exposed to UV radiation and then allowed to react with ozone, no nitroso- or nitrocompounds were found. The major products were NO_3^-, ammonia, CO_2 and cyanic acid.

The nature of oxidation byproducts and the efficiency of AOP treatment are related not only from the standpoint of the ability of byproducts to be treated by AOPs, but also in terms of their ability to promote the oxidation cycle. In this respect, and because of possible toxicity of intermediate byproducts, the identification of byproducts becomes very important.

The data available in the literature have been obtained primarily for byproducts in pinkwater treated with AOPs and related processes. TNT photolysis is known to produce highly colored products. Burlinson et al. (1979) found a variety of nitro-compounds resulting from photolysis of TNT solutions at different pH. Their data summarized in Table 2-4 show that UV irradiation alone does not break the benzene ring, but rather leads to formation of nitro- and aminonitro-benzenes, such as 1,3,5-TNB, 2,4,6-trinitrobenzoic acid (TNBA), 2-amino-4,6-dinitrobenzoic acid, etc., as well as nitroazoxy benzenes, apparently formed by coupling of nitroso-compounds. The same type of products were identified by Miaoqin et al. (1987) and Spanggord et al. (1980).

When TNT solutions were treated with O_3/UV (Spanggord et al. 1980) the byproduct distribution was different: TNB, 2,4,6-trinitrobenzaldehyde, dinitrophenols, dinitrodihydroxybenzenes, and oxalic acid. These compounds may be formed in the hydroxyl radical attack on aromatic ring or in oxidation of methyl group. Burrows, Jackson, and Lachoswki (1984) found only TNBA as an intermediate byproduct of TNT destruction when O_3/UV was applied.

DeBerry, Viehbeck, and Meldrum (1994) have found TNB to be the major product of TNT decomposition in its aqueous solutions treated with H_2O_2/UV or O_3/UV. Although TOC was relatively high at the point when TNB was gone, no nitro-and polynitrophenols or other nitro-compounds were found at this point, and acetic and formic acids were the only identified compounds that resulted from TNB destruction. Intermediate nitro-compounds resulting from hydroxyl radical attack are expected to be formed, but they apparently react quickly with ozone or with additional radicals constantly generated during the treatment, to produce smaller compounds.

Table 2-4. Photodegradation products of TNT.

1,3,5-Trinitrobenzene (TNB)
4,6-Dinitroanthranil (4,6-Dinitro-1,2-benzisoxazole)
2,4,6-Trinitrobenzaldehyde
2,4,6-Trinitrobenzyl alcohol
3,5-Dinitrophenol
4,6-Dinitroisoanthranil (4,6-Dinitro-2,1-benzisoxazole)
syn-2,4,6-Trinitrobenzaldoxime
anti-2,4,6-Trinitrobenzaldoxime
2,4,6-Trinitrobenzonitrile
1,3,7,9-Tetranitroindazolo-2,1-a-indazol-6-ol-12-one
2,2'-Dicarboxy-3,3',5,5'-tetranitroazoxybenzene
2,2'-Dicarboxy-3,3',5,5'-tetranitroazoxybenzene
2-Carboxy-3,3',5,5'-tetranitro-NNO-azoxy benzene
2,4,6-Trinitrobenzoic acid
N-(2-Carboxy-3,5-dinitrophenyl)-2,4,6-trinitrobenzamide
2-Amino-4,6-Dinitrobenzoic acid

The nitrate appearance in the solution initially followed the TNB destruction. In the latter stages of the experiment, the nitrate concentration appeared to reach a steady state or even decrease somewhat. Since no nitro-organics were detected, it was speculated that the nitrate might be undergoing photolysis and lost via some gaseous product. That seems unlikely, in view of the rapid rate of reaction of the photolysis product, NO_2, with water.

According to studies performed in Naval Weapons Support Center, IN (1985) H_2O_2/UV treatment of TNT resulted in the production of TNB, acetic acid, NH_4^+ and NO_3^-. Andrews and Osmon (1977) identified only TNB, NO_3^- and NH_4^+, but

they also reported nitrogen mass balance problems. On the whole, the nitrogen and carbon mass balance data that are available in literature are confusing and sometimes contradictory, which indicates another information gap that needs to be filled. In this respect, more attention should be paid to the analysis of gases. A similar situation exists in the wet air oxidation of redwater.

Glover and Hoffsommer (1979) have reported the byproducts from RDX treated by AOPs and related processes. Their findings were discussed in the beginning of this section. Nitramines, in general, are susceptible to photodegradation; therefore, photolysis may be an important part of the treatment. According to Kubose and Hoffsommer (1977), RDX photolysis proceeds via production of nitroso-compounds, but they are formed in the first minutes of the reaction and cannot be detected after RDX is gone. Smetana and Bulusu (1979) did not find nitroso-compounds, apparently because they investigated the final products of RDX photolysis. Another proposed intermediate byproduct of RDX decomposition was triazine (Glover and Hoffsommer 1979). Spanggord et al. (1980) identified formaldehyde, NO_2^- and NO_3^- as RDX photolytic products but, unlike Glover and Hoffsommer, they did not find any nitro-compounds. They also determined the final products of HMX photolysis and found them to be the same as for RDX (Spanggord et al. 1983).

Photolysis of 2,4-DNT resulted in a number of byproducts analogous to those observed in TNT photolysis, primarily single aromatic ring nitro- and nitroaminocompounds (Burlison et al. 1979). Similar to TNT studies, a different product distribution was found when the treatment involved an oxidant as well as UV light. Ho (1986) identified byproducts in 2,4-DNT solutions treated with H_2O_2/UV. The reaction scheme based on identified products was proposed as follows:

$$\text{2,4DNT} \xrightarrow{H_2O_2/UV} \text{2,4-dinitrobenzyl alcohol} \rightarrow$$

$$\text{2,4-dinitrobenzaldehyde} \rightarrow \text{2,4-dinitrobenzoic acid} \rightarrow$$

$$\text{1,3-dinitrobenzene} \rightarrow$$

$$\text{3-nitrophenol + dinitrophenols } (+ NO_3^-) \rightarrow$$

$$\text{dihydroxynitrobenzenes} \rightarrow \text{trihydroxynitrobenzenes} \rightarrow$$

$$\text{nitromuconic acid derivatives } (+ NO_3^-) \rightarrow \text{maleic acid + nitro- and hydroxymaleic acid derivatives +}$$

$$\text{glyoxal + glyoxic acid } (+ NO_3^-) \rightarrow$$

$$\text{oxalic acid + formic acid } (+ NO_3^-) \rightarrow CO_2 + H_2O$$

It is worth noting that many compounds shown in this scheme may result from photolysis reactions, as well as the hydroxyl radical attack on DNT.

The data discussed above show that the intermediate byproducts may be quite different at any of the sequential oxidation steps, and that the product distribution may depend on the moment the treatment is stopped. This

observation can, in part, explain the difference in byproducts reported in different studies on the same treatment process. Note that there are, however, other factors responsible for this difference, such as experimental conditions, the chemistry of a particular AOP, methods used to analyze for byproducts, etc.

Less work has been done to identify byproducts formed in AOP treatment of the energetic contaminants other than nitro-compounds. A variety of products was found (Sierka and Cowen 1980; Cowen, Sierka, and Zirolli 1981) in solutions of hydrazine fuels treated with O_3/UV at the point of complete removal of the target compounds. Methanol was the major organic oxidation product that resulted from monomethyl hydrazine destruction. Methanol, formaldehyde dimethylhydrazone, formaldehyde monomethylhydrazone, N-nitrosodimethylamine, dimethyl formamide and tetramethyl tetrazene were identified as products from unsymmetrical dimethyl hydrazine. Methanol decomposition produced formaldehyde and formic acid. Ozone/UV treatment of isopropyl alcohol produced acetone as a major intermediate byproduct (Judeikis and Hill 1991; Kuo, Chian, and Chang 1977). Photolytic ozonation of acetone results in formation of formaldehyde, oxalic, acetic, and formic acid (Kuo, Chian, and Chang 1977). Further treatment is likely to lead to the production of CO_2 and H_2O.

Polychlorinated organics were found to release chloride ions during the ozonation and O_3/UV treatment (Leitis et al. 1981). Glaze et al. (1979), elucidated the byproduct chain during the ozone/UV destruction of a symmetrical hexachlorobiphenyl (HCB), and found that the oxidation reaction proceeded by cleavage of one ring, followed by preferential dechlorination of the remaining carbon chains. The other ring was left intact until the first cleavage products were removed. Some isomerization of the HCB due to photolysis was also found.

UV-ozonation of nitrobenzene resulted in the formation of intermediate nitrophenols and, eventually, oxalic and formic acids (Leitis et al. 1981). Dimethylamine and NO_2^- were identified as major byproducts in dimethylnitrosoamine photolysis (Hunter, Sotsky, and Carraza 1983).

Products of hydroxyl radical reactions with organic contaminants not containing heteroatoms such as nitrogen or halogens are relatively well understood, primarily from radiochemical studies during the 1970s and 1980s. Hydroxyl radical attacks by hydrogen atom abstraction or addition to an aromatic ring or double bond if present. The resulting carbon-centered radical degrades through the formation of a peroxyl radical, as described in a following section on AOP chemistry, with the product of one step becoming the substrate of the next.

AOP Kinetics. The literature data on AOP kinetics are limited and inconclusive. Since many of AOP studies were carried out with the use of oxidant excess, contaminant disappearance was frequently observed to be of first order with respect to the compounds of interest (Naval Weapons Support Center 1985; Heffinger and Jake 1991; Noss and Chyrek 1984). Burrows (1983), however, found the reaction order to be between zero and first for TNT and nitramines, when the actual wastewater was treated with O_3/UV. Zero order kinetics was observed in O_3/UV treatment of hydrazine fuels (Sierka and

Cowen 1980) and the mixture of the first and zero order was found for photolysis of TNT and nitramines (Burrows, Jackson, and Lachowski 1984). AOP treatment is often observed to have both a zero- and first-order stage.

DeBerry, Viehbeck and Meldrum (1984) have used a reaction scheme based on competition reactions of H_2O_2 (or O_3), $OH\bullet$, $HO_2\bullet$ and organics to develop a kinetic equation describing the rate of disappearance of TNT and TNB treated with different AOPs. A mathematical model was developed to interpret the data and relate TNT and TNB removal to H_2O_2 loss. Unfortunately, it was incorrectly assumed that ozone photolysis directly yielded OH, rather than H_2O_2 (Taube 1956; Peyton and Glaze 1988). In addition, the proposed model did not include many important pathways such as the known regeneration of hydrogen peroxide following OH attack on organic compounds, etc. (Baxendale and Wilson 1957).

The differences found between studies for the empirical kinetic expressions describing the rate of disappearance of target compounds are due to several factors, including specific reaction conditions, competition for photons and OH radicals by other matrix components, and the interaction of multiple independent reaction pathways. The overall rate constants calculated from the observed disappearance rates may to some extent characterize the ability of contaminants to be treated by AOPs, but since they are system-specific, they cannot be used for process design purposes, or in prediction of treatment efficiency. On the whole, the lack of continuity in kinetic data seems to result from a lack of understanding of AOP chemistry and incomplete data analysis rather than incorrect experimental arrangements. Once again it should be emphasized that the solution to the problem is mathematical modeling of the treatment process in terms of fundamental principles.

AOP Economics. Like many other types of literature data on AOP application to Army wastewaters (as well as other waters), the data on treatment cost are limited and not always consistent. Estimated treatment costs are not directly comparable between processes and investigators, due to the difference in wastewater composition, constituent concentration, experimental conditions, scale, and cost assumptions.

Fischer, Jackson, and Lachowski (1982) have done a comparative cost analysis for O_3/UV and carbon adsorption (CA) treatment of RDX-contaminated wastewaters. They used the data obtained with the use of a ULTROX P602 unit to calculate the treatment cost for a UV-ozone system sized up to meet the mobilization requirements for the Kansas AAP production facility (5,000 gpd). The estimated cost was \$18.29/Kgal and \$68.00/Kgal for O_3/UV and CA, respectively. The authors claimed that, for the treatment facility able to accommodate 100,000 gpd, the cost may drop to \$7.14 and \$4.22. According to Andrews (1980) the capital cost of H_2O_2/UV, O_3/UV and CA treatment of explosive-contaminanted (RDX and TNT) wastewaters was \$683K, \$750K, and \$856.3K, respectively (based on ~20,000 gpd). Operating cost was estimated as \$3.69 to 4.69, \$4.93 and \$7.11 per thousand gallons for H_2O_2/UV, O_3/UV and CA, respectively (total treatment cost is not available). (Note that these are in 1980 dollars and do not represent today's costs.)

Arisman et al. (1980) estimated the cost of O_3/UV treatment of PCBs at the ULTROX pilot plant. The calculated cost was not shown in the report, but the authors claimed that it was about a $1.50 less per thousand gallons than actual cost of CA treatment on the same scale.

The costs of biological, CA, and O_3/UV treatment of DNT-contaminated wastewaters as estimated by Ordnance group of Hercules Aerospace Corp. (Heffinger and Jake 1991) were $0.49/Kgal, $0.75/Kgal (without operating cost of carbon regeneration), and $1.63/Kgal, respectively, although some aspects of their calculations are not clear. They also reported that the cost of O_3/UV treatment might have been negatively impacted due to the laboratory ozone generator not operating as designed. Ozone production was estimated from the manufacturer's specifications, and ozone transfer efficiency into solution was not taken into account. Herlacher and McGregor (1987) found that the cost of alkaline chlorination and photo-ozonation of cyanide wastes was practically the same ($8.23 and $8.05 per pound of cyanide destroyed, respectively).

The data discussed above, as well as several cases from the drinking water and groundwater remediation literature, indicate that the cost of AOP treatment of Army wastes and related wastewaters in some cases may be comparable or even less than that for carbon adsorbtion treatment, the current "baseline" cleanup technology. From the point of view of OH radical generation, O_3/UV seems less economical than H_2O_2/UV treatment, mainly due to its complexity in installation and maintenance, and high power requirements. However, the O_3/UV system often provides more effective treatment, particularly for wastewaters containing strongly UV-absorbing contaminants, such as most nitrocompounds. Perhaps most importantly, however, the majority of studies has not been conducted under optimal treatment conditions.

Comparison of Treatability Data

The majority of treatability data found have been obtained in quite different experimental conditions such as UV intensity, ozone and hydrogen peroxide doses and concentrations, pH, etc., which makes these data difficult to compare. To summarize and analyze the existing information for various groups of Army wastewaters treated by AOPs and related methods (photolysis, ozonation and treatment with H_2O_2), the following quantities were calculated whenever possible from the information given in the papers that were reviewed:

1. Amount and percent of target compound removal
2. Amount and percent of TOC removal
3. UV light dose rate (Watt/L)
4. Oxidant dose and concentration
5. Treatment efficiency, defined as a ratio of TOC and/or contaminant removal to amount of oxidant used
6. Cost.

Table 2-5 lists the calculated values. Treatment "efficiency" depends, in general, on properties of the wastewater to be treated and the process variables of the treatment method. On the other hand, the conclusion as to whether or not treatment is "effective" depends on treatment goals. To define treatment goals, questions such as the following should be addressed:

1. Are the goals the elimination of specific classes of compounds or complete mineralization of TOC?
2. What level of treatment is required for a particular constituent or a class of compounds?

However, the answers to such questions are often not simple, since they must address not only the current regulatory situation, but possible future changes as well. This applies not only to regulations, but also to economics. A recent example serves to illustrate the type of considerations that are necessary. Investigators at one Department of Defense site currently under study are comparing AOP treatment of ordnance compound-contaminated groundwater to carbon adsorption (Peyton, unpublished results 1992). The calculated treatment costs of the two processes are practically the same, within the accuracy of the calculation. On the basis of this information alone, GAC adsorption seems attractive because it is a more proven technology; however, AOP treatment is a final solution to the problem because it destroys contaminants rather than simply relocating them. In addition, since on-site GAC regeneration is not an option, selection of carbon adsorption assumes the continued willingness of the carbon vendor to transport and regenerate the carbon at the present price. Even a future change in the allowable loading rate of energetic compounds on the carbon prior to transporting and regeneration can have a drastic effect on the economics of the carbon adsorption process. On the other hand, AOP operating costs are sensitive to the cost of electricity, since both UV light and ozone generation require significant amounts of electricity.

Since AOPs proved effective in the destruction of numerous classes of chemicals down to the analytical detection limits, some means is required to evaluate and compare their treatment potential. Treatment efficiency and cost are crucial points in any technology evaluation and its further implementation. In the case of AOPs both efficiency and cost are strongly affected by the way the oxidant is applied. In this respect the data on oxidant behavior in the system (initial concentration, amount used, mass transfer problems, etc.) become very important, particularly in studies involving ozone. The data in Table 2-5 show a significant gap in existing data in this respect, which needs to be filled. The objective for the majority of investigators (especially at early stages of AOP studies) was to demonstrate removal of target compounds and sometimes byproducts, which led them to use an excess of oxidant.

Table 2-5. Treatability data.

Wastewater, solution etc.	Substance	Reference	Process	TOC_o mg/L	ΔTOC	Extent of TOC removal ξ_{TOC} $\Delta TOC/TOC_o$	Conc. of target compound, μ_o, mg/L	Target compound removal $\Delta\mu$
Pink water, aqueous solutions	TNT	NAVWPNSUPPGEN WQEC/C 85-297 AD A159 416 [1985]	UV/H_2O_2	40	35.8	0.895	98	97.9
Aqueous solutions, bomb-loading effluent	TNT	C. C. Andrews & J. L. Osmon [1977]	UV/H_2O_2	40	37	0.925	100	99.99
	RDX		•	12.8	-12.8	-1.0	50	49.5
	Explosive D		•	168	165.8	0.987	500	499
	2,4-DNT		•	38.4	-38.4	-1.0	100	99.5
	2,6-DNT		•	45.3	-45.3	-1.0	100	99.5
Aqueous solutions (synthetic pink water)	TNT*	C. C. Andrews [1980]	UV/H_2O_2	34.0	27	0.794	41.5	41.48
	RDX*						24.9	24.8?
Pink water from bomb LAP operations (diluted 1:3)	TNT*	M. Roth & J. M. Murphy [1979]	UV/H_2O_2	24.8	23.2	0.935	30.0	29.99
	RDX*						26.8	26.79
	HMX*						3.0	2.98
Pink water (economic analysis)	TNT*	B. Jackson & J. M. Lachowsky [1983]	UV/H_2O_2	–	–	–	100-120	–
	RDX*						30-40	–
	TNT*		UV/H_2O_2 catalyst	–	–	–	100-120	–
	RDX*						30-40	–

cess	TOC_o mg/L	ΔTOC	Extent of TOC removal ξ_{TOC} $\Delta TOC/TOC_o$	Conc. of target compound, μ_o, mg/L	Target compound removal $\Delta\mu$	Extent of target compound removal ξ_μ $\Delta\mu/\mu_o$	Efficiency ϵ, $\Delta TOC/\Delta O_3$ or $\Delta TOC/\Delta P$***	Efficiency ϵ (target compound) $\Delta\mu/\Delta O_3$ or $\Delta\mu/\Delta P$***	Experimental Conditions				Cost		
									pH	I_o Watt/L	Applied ozone dose rate D_e, mM/min	H_2O_2 concentration P_z, mM	Capital cost KS	Operational cost S/Kgal	T c S/
H_2O_2	40	35.8	0.895	98	97.9	0.999	0.103	0.029	7	4.86	–	30	–	–	
H_2O_2	40	37	0.925	100	99.99	0.999	0.105	0.015	–	50	–	30	–	–	
	12.8	-12.8	-1.0	50	49.5	0.99	0.0363	0.007	–	50	–	30	–	–	
	168	165.8	0.987	500	499	0.998	0.469	0.068	–	50	–	30	–	–	
	38.4	-38.4	-1.0	100	99.5	0.995	0.109	0.019	–	50	–	30	–	–	
	45.3	-45.3	-1.0	100	99.5	0.995	0.128	0.019	–	50	–	30	–	–	
H_2O_2	34.0	27	0.794	41.5	41.48	0.999	0.096	0.008	7	1.16	–	30	683	3.69-4.69	
				24.9	24.8?	0.997		0.005							
H_2O_2	24.8	23.2	0.935	30.0	29.99	0.999	0.0698	0.0047	7.3	2.35	–	30	–	–	
				26.8	26.79	0.999		0.0044							
				3.0	2.98	0.993		0.0004							
H_2O_2	–	–	–	100-120	–	0.99	–	–	–	1.87	–	3.0	561.5	2.56	
				30-40	–	0.99		–					343.19	1.46	
H_2O_2 st	–	–	–	100-120	–	0.99	–	–	–	*	–	3.0	425.0	1.60	
				30-40	–	0.99		–							

(2)

Efficiency ϵ (target compound) $\Delta\mu/\Delta O_3$ or $\Delta\mu/\Delta P$****	Experimental Conditions: pH	I_o Watt/L	Applied ozone dose rate $D_{e'}$ mM/min	H_2O_2 concentration P_3, mM	Cost: Capital cost KS	Operational cost S/Kgal	Total cost S/Kgal	Comments
0.029	7	4.56	–	30	–	–	–	Bench scale t_{res}***** = 8 hr (TNT); t_{res} = 24 hr (TOC)
0.015	–	50	–	30	–	–	–	Bench scale, V_r****** = 0.2 L In all cases all H_2O_2 was gone
0.007	–	50	–	30	–	–	–	
0.068	–	50	–	30	–	–	–	
0.019	–	50	–	30	–	–	–	
0.019	–	50	–	30	–	–	–	
0.008	7	1.16	–	30	683	3.69-4.69	–	Pilot scale V_r = 550 gal
0.005								
0.0047	7.3	2.35	–	30	–	–	–	Vr = 2.84 L Commercial units UV-200
0.0044								
0.0004								
–	–	1.87	–	3.0	561.5	2.56	4.84	Carbon adsorption cost-$4.22
–					343.19	1.46	3.08	$3.08-at flow rate ~2 times higher
–	–	*	–	3.0	425.0	1.60	3.34	
–								

③

Table 2-5. Treatability data (cont'd).

Wastewater, solution etc.	Substance	Reference	Process	TOC_o mg/L	ΔTOC	Extent of TOC removal ξ_{TOC} ΔTOC/TOC_o	Conc. of target compound, μ_o, mg/L	Target compound removal Δμ
Synthetic munitions mixtures	TNT*	C. I. Noss et al. [1984]	UV/H_2O_2	–	–	–	15.5	13.76
	RDX*						18.9	17.87
	TAX*						19.7	18.67
	HMX*						1.88	1.42
	SEX*						3.69	2.24
Explosive contaminated wastewater, aqueous solutions	RDX*	W. D. Burrows & E. E. Brueggemann [1986]	UV	–	–	–	2.504	2.434
	TAX*						0.162	0.092
	HMX*						1.201	1.131
	SEX*						1.966	1.896
Synthetic pink water (aqueous solution of TNT)	TNT	E. G. Fochtman & J. E. Huff [1975]	UV/O_3	53	26	0.49	–	–
				53	8	0.151		
				–	–	–		
Aqueous solutions	TNT	W. S. Layne et al. [1982]	UV/O_3	60.74	45.9	0.756	124	120
Pink water with composition A5 (99% RDX)	RDX	G. Fischer et al. [1982]	UV/O_3	–	–	–	9.7	9.5

	TOC_o mg/L	ΔTOC	Extent of TOC removal ξ_{TOC} $\Delta TOC/TOC_o$	Conc. of target compound, μ_o, mg/L	Target compound removal $\Delta\mu$	Extent of target compound removal ξ_μ $\Delta\mu/\mu_o$	Efficiency ϵ, $\Delta TOC/\Delta O_3$ or $\Delta TOC/\Delta P$***	Efficiency ϵ (target compound) $\Delta\mu/\Delta O_3$ or $\Delta\mu/\Delta P$***	Experimental Conditions: pH	I_o Watt/L	Applied ozone dose rate D_t, mM/min	H_2O_2 concentration P_i, mM	Cost: Capital cost KS	Operational cost $/Kgal	Total cost $/Kg
$)_2$	–	–	–	15.5	13.76	0.888	–	0.02	7	1.33	–	3.0	–	–	–
				18.9	17.87	0.946		0.027							
				19.7	18.67	0.945		0.028							
				1.88	1.42	0.755		0.0016							
				3.69	2.24	0.607		0.0025							
	–	–	–	2.504	2.434	0.972	–	–	–	0.89	–	–	5.775	0.24	0.4
				0.162	0.092	0.568									
				1.201	1.131	0.942									
				1.966	1.896	0.964									
	53	26	0.49	–	–	–	0.02	–	–	2.5	0.24	–	–	–	–
	53	8	0.151				0.06				0.024				
	–	–	–				0.09				0.012				
	60.74	45.9	0.756	124	120	0.968	3.5	0.489	8.3	0.22	0.0066**	–	1,033	6.53	10.-
													530.7	4.01	7.-
	–	–	–	9.7	9.5	0.979	–	–	7.5	1.41	33.04	–	129.45	6.26	18.-
															7.-

(2)

Efficiency ϵ (target compound) $\Delta\mu/\Delta O_3$ or $\Delta\mu/\Delta P$***	Experimental Conditions: pH	I_o Watt/L	Applied ozone dose rate D_e, mM/min	H_2O_2 concentration P_a, mM	Cost: Capital cost KS	Operational cost S/Kgal	Total cost S/Kgal	Comments
0.02	7	1.33	–	3.0	–	–	–	V_r = 20 L
0.027								
0.028								
0.0016								
0.0025								
–	–	0.89	–	–	5.775	0.24	0.41	t_{res} = 10 min
–	–	2.5	0.24	–	–	–	–	50 lb O_3/1 lb TOC removed
			0.024					17 lb O_3
			0.012					12 lb O_3
0.489	8.3	0.22	0.0066**	–	1,033	6.53	10.71	Ultrox P-801
					530.7	4.01	7.41	Ultrox P-801 O_3 from oxygen
–	7.5	1.41	33.04	–	129.45	6.26	18.29	5,000 gal of wastewater per day
							7.14	100,000 gal/day

(3)

Table 2-5. Treatability data (cont'd).

Wastewater, solution etc.	Substance	Reference	Process	TOC_o mg/L	ΔTOC	Extent of TOC removal ξ_{TOC} = ΔTOC/TOC_o	Conc. of target compound, μ_o, mg/L	Target compound removal $\Delta\mu$	c
Synthetic munitions mixture	TNT*	W. D. Burrows et al. [1984]	UV/O_3	–	–	–	24.05	1995	
	RDX*						24.39	22.69	
	TAX*						25.84	24.07	
	SEX*						5.60	5.0	
	HMX*						3.82	2.98	
Pink water	TNT*	F. C. Farrell et al. [1977]	UV/O_3	70	67	0.957	140	139	
	RDX*						72	71	
	WAX*						10	unch.	
Aqueous solutions	TNT	D. W. DeBerry et al. [1984]	UV/O_3	–	–	–	90.8	90.8	
	"		UV/H_2O_2	–	–	–	90.5	88.5	
	TNB		O_3	14.4	8.4	0.58	42	32.55	
	"		O_3/UV	14.4	8.4	0.58	42	37.8	
	"		H_2O_2/UV	14.4	8.4	0.58	42	39.06	
	"		O_3/H_2O_2	14.4	6.4	0.444	42	35.7	
	"		$O_3/H_2O_2/UV$	14.4	9.9	0.688	42	41.79	

TOC_o mg/L	ΔTOC	Extent of TOC removal ξ_{TOC} $\Delta TOC/TOC_o$	Conc. of target compound, μ_o, mg/L	Target compound removal $\Delta\mu$	Extent of target compound removal ξ_μ $\Delta\mu/\mu_o$	Efficiency ϵ, $\Delta TOC/\Delta O_3$ or $\Delta TOC/\Delta P^{***}$	Efficiency ϵ (target compound) $\Delta\mu/\Delta O_3$ or $\Delta\mu/\Delta P^{***}$	Experimental Conditions: pH	I_o Watt/L	Applied ozone dose rate $\dot{D}_4$, mM/min	H_2O_2 concentration P_a, mM	Cost: Capital cost KS	Operational cost S/Kgal	Total cost S/Kg
–	–	–	24.05	1995	0.83	–	0.074	–	0.87	0.038	–	–	–	–
			24.39	22.69	0.93		0.089							
			25.84	24.07	0.932		0.096							
			5.60	5.0	0.893		0.015							
			3.82	2.98	0.78		0.009							
70	67	0.957	140	139	0.993	0.3	0.03	6.2	770	0.053	–	962.5	2.61	–
			72	71	0.986		0.017							
			10	unch.	0		–							
–	–	–	90.8	90.8	~1	–	0.05	1.9	6.55	0.396	–	–	–	–
–	–	–	90.8	88.5	0.975	–	0.017	1.9	6.55	–	50	–	–	–
14.4	8.4	0.58	42	32.55	0.775	0.147	0.033	2.1	6.55	0.04**	–	–	–	–
14.4	8.4	0.58	42	37.8	0.9	0.245	0.055	1.85	6.55	0.054**	–	–	–	–
14.4	8.4	0.58	42	39.06	0.93	0.0184	0.005	1.8	6.65	–	50	–	–	–
14.4	6.4	0.444	42	35.7	0.85	0.106	0.034	1.8	–	0.053**	1.0	–	–	–
14.4	9.9	0.688	42	41.79	0.995	0.168	0.041	1.8	6.55	0.066**	1.0	–	–	–

(2)

Experimental Conditions				Cost			
pH	I_o Watt/L	Applied ozone dose rate $\dot{D}_e$, mM/min	H_2O_2 concentration P_a, mM	Capital cost KS	Operational cost S/Kgal	Total cost S/Kgal	Comments
–	0.87	0.038	–	–	–	–	Bench scale
6.2	770	0.053	–	962.5	2.61	–	Ultrox P602 (1 kgpd) Cost estimate for 100 kgpd plant
1.9	6.55	0.396	–	–	–	–	Bench scale V_r = 0.2 L
1.9	6.55	–	50	–	–	–	
2.1	6.55	0.04**	–	–	–	–	
1.85	6.55	0.054**	–	–	–	–	
1.8	6.65	–	50	–	–	–	
1.8	–	0.053**	1.0	–	–	–	
1.8	6.55	0.066**	1.0	–	–	–	

(3)

Table 2-5. Treatability data (cont'd).

Wastewater, solution etc.	Substance	Reference	Process	TOC_o mg/L	ΔTOC	Extent of TOC removal ξ_{TOC} $\Delta TOC/TOC_o$	Conc. of target compound, μ_o, mg/L	Target compound removal $\Delta\mu$ *
Aqueous solutions	MMH	R. A. Sierka & W. F. Cowen [1980]	UV/O_3	32	7	0.219	114	113.8
Aqueous solutions	Hydrazine	W. F. Cowen et al. [1981]	UV/O_3	–	–	–	122	121.95
	UDMH		*	54	17	0.315	122	121.3
Groundwater	DIMP******	D. W. Thompson et al. [1979]	UV/O_3	9.6	7.8	0.812	1.82	1.78
Wastewater from propellants production	2,4 DNT	J. Heffinger and C. Jake [1991]	UV/O_3	–	–	–	190	190
Aqueous solutions	NB	E. Leitis et al. [1980]	O_3/UV	58	58	1	98.5	98.5
	*		O_3	58	28	0.48	98.5	98.5
	1,3,5 TNB		O_3/UV	–	–	–	93.7	89.3
	*		O_3	–	–	–	93.7	89.3
	TNT		O_3/UV	37	32.5	0.878	100	100
	*		O_3	37	1.5	0.04	100	21.5
	*		O_3/UV	37	9	0.243	100	100

* – compounds were treated in mixture
** – utilized ozone dose rate
*** – utilized H_2O_2 dose
**** – residence time
***** – reactor volume
****** – DIMP was treated in the mixture with DCPD but no data for DCPD, except its initial concentration (<10 ppm), were not

ess	TOC_o mg/L	ΔTOC	Extent of TOC removal ξ_{TOC} $\Delta TOC/TOC_o$	Conc. of target compound, μ_o, mg/L	Target compound removal $\Delta\mu$	Extent of target compound removal ξ_μ $\Delta\mu/\mu_o$	Efficiency ϵ, $\Delta TOC/\Delta O_3$ or $\Delta TOC/\Delta P$***	Efficiency ϵ (target compound) $\Delta\mu/\Delta O_3$ or $\Delta\mu/\Delta P$***	Experimental Conditions				Cost		
									pH	I_o Watt/L	Applied ozone dose rate D_e, mM/min	H_2O_2 concentration P_a, mM	Capital cost KS	Operational cost S/Kgal	To co S/K
3	32	7	0.219	114	113.8	0.998	0.125	0.123	9.1	–	0.078**	–	–	–	-
3	–	–	–	122	121.95	0.999	–	0.112	9.1	–	–	–	–	–	-
	54	17	0.315	122	121.3	0.994	0.409	0.166	9.1	–	0.098	–	–	–	-
3	9.6	7.8	0.812	1.82	1.78	0.976	0.098	–	7.6	1.19	0.044	–	–	–	-
3	–	–	–	190	190	~1	–	0.008	–	2.8	0.75	–	–	–	
	58	58	1	98.5	98.5	1	0.187	0.06	–	4.6	0.43	–	–	–	-
	58	28	0.48	98.5	98.5	1	0.118	0.087	–	4.6	0.306	–	–	–	-
	–	–	–	93.7	89.3	0.953	–	0.023	–	4.6	0.243	–	–	–	-
	–	–	–	93.7	89.3	0.953	–	0.023	–	4.6	0.243	–	–	–	-
	37	32.5	0.878	100	100	1	0.148	0.048	–	4.6	0.243	–	–	–	-
	37	1.5	0.04	100	21.5	0.205	0.007	0.005	–	4.6	0.243	–	–	–	-
	37	9	0.243	100	100	1	0.082	0.048	–	4.6	0.243	–	–	–	-

DCPD, except its initial concentration (<10 ppm), were not provided.

(2)

Efficiency ϵ (target compound) $\Delta\mu/\Delta O_3$ or $\Delta\mu/\Delta P$***	Experimental Conditions: pH	I_o Watt/L	Applied ozone dose rate $\dot{D}_a$, mM/min	H_2O_2 concentration P_a, mM	Cost: Capital cost KS	Operational cost S/Kgal	Total cost S/Kgal	Comments
0.123	9.1	–	0.078**	–	–	–	–	ΔO_3 is approxim.
0.112	9.1	–	–	–	–	–	–	
0.166	9.1	–	0.098	–	–	–	–	$\dot{D}_a$ - assumed
–	7.6	1.19	0.044	–	–	–	–	Two-reactor flow system
0.008	–	2.8	0.75	–	–	–	1.63	
0.06	–	4.6	0.43	–	–	–	–	
0.087	–	4.6	0.306	–	–	–	–	
0.023	–	4.6	0.243	–	–	–	–	
0.023	–	4.6	0.243	–	–	–	–	
0.048	–	4.6	0.243	–	–	–	–	t_{res} = 120 min TNT N/D at 60 min
0.005	–	4.6	0.243	–	–	–	–	
0.048	–	4.6	0.243	–	–	–	–	t_{res} = 60 min

(3)

In many cases, the actual amount of oxidant used was unknown. Our calculations indicate that although the *effectiveness* (i.e., the capability of the process to remove the contaminant) of target compound and even TOC removal was often high, overall treatment *efficiency* (moles of contaminant removal per mole of oxidant used) in terms of oxidant spent was highly variable, and, in general, poor.

Little has been said in the AOP literature about treatment efficiency, despite the fact that it is directly linked to treatment cost. This is due in part to the myth that when ozone decomposes, it simply disappears without a trace, making ozone mass balance impossible. Due to the work of Hoigné and Bader (1983), that position is now known to be untenable, and the effects of various factors, including the composition of the water matrix, on efficiency are quantifiable. This exposes another data gap in the information from literature reports: the identities and concentrations of other species in the water matrix that may act as radical scavengers. The widely varying efficiencies seen in Table 2-5 indicate that the factors that are involved in AOP optimization and efficiency have not been widely appreciated.

TNT and RDX Photolysis

In the above literature review it was noted that RDX was observed to facilitate the photolytic destruction of TNT. In this section, a more focused analysis of RDX photochemistry is performed to find information that could help in the hypothesis of an intermediate radical (or radicals), generated from RDX, that might be responsible for enhancing TNT decomposition by attacking it.

The extinction coefficient and quantum yield are important photochemical parameters that must be determined for modeling. Kubose and Hoffsommer (1977) found that the extinction coefficient ϵ_{RDX} was 10^4 M^{-1} cm^{-1} at 220 nm and monotonically decreased to a value of 10^3 at 280 nm. Smetana and Bulusu (1979) reported a value of 1.1×10^4 at 238 nm. A value of $(7.3 \pm 0.7) \times 10^3$ at 254 nm was determined in the present work. Syracuse Research Corporation (1978) reported a quantum yield, ϕ_{RDX}, of 0.67 for photolysis of RDX at 254 nm in aqueous solutions at pH 8.1 and Spanggord (1980) found 0.16 at 313 nm.

Kubose and Hoffsommer (1977) studied the photolysis of RDX in aqueous solution using a 450-watt, medium pressure lamp (~max = 220 to 1370 nm) and identified several reaction byproducts. Table 2-6 lists the amounts of the various products found, normalized to the amount of RDX that was photolyzed. Nitrogen and carbon mass balance would have been achieved if the sum of the percentage values listed in Table 2-6 for nitrogen-containing species and the sum of the carbon-containing species, respectively, equaled 100 percent. It can be seen that only about 55 percent of the nitrogen and 27 percent of the carbon was found by these investigators.

Table 2-6. Byproduct yield from RDX photolysis and thermolysis (as % of possible nitrogen or carbon available from RDX).

	Product							
Investigators/Technique	NO_3^-	NO_2^-	N_2O	N_2	NH_3	CH_2O	CO_2	CO
Kubose and Hoffsommer photolysis (aq.)	trace	40	2	4	10	27	--(*)	--
Glover and Hoffsommer photolysis (aq.)	5	53	na(**)	na(**)	34	14	42	3
Smetana and Bulusu(†,‡)photolysis (solid)	na(**)	na(**)	13	53	--	2	8	11
Rauch et al.(†,§) thermolysis	na(**)	na(**)	45	33	--	32	20	17
Oxley et al.(†,D)thermolysis (solid)	na(**)	na(**)	41	46	--	--	29	29
Oxley et al.(†,D)thermolysis (acetone)	na(**)	na(**)	1	16	--	--	5	9

Notes:

(**)na = not analyzed.

(*) Another gaseous product was detected that was probably CO_2.

(†) Only gaseous products were determined in these experiments.

(‡) In addition, 18% NO and 1% HCN were detected.

(§) In addition, 15% NO and 1% HCN were detected.

(D) NO, HCN and NH_3 would have been detected, if present.

Kubose and Hoffsommer also found that a minor product from photolysis of RDX at λ >280 nm in acidic aqueous solution was the mononitroso analog of RDX, 1-nitroso-3,5-dinitro-1,3,5-triazine (identified by comparison with the authentic standard, using GC-MS). The presence of nitroso compounds is of interest because many nitroso compounds have been shown to be carcinogens. Although this was the largest peak in the chromatogram from GC/MS analysis of a benzene extract of the photolyzed RDX solution, it represented less than 1 percent of the initial RDX concentration. The mass-spectra of minor byproducts implied the presence of other similar compounds, but in amounts too small to allow identification. The formation of mononitroso compound was independent of oxygen concentration in solution. This product was not found when RDX was photolyzed in neutral or basic media. The authors suggested the initial step of RDX photolysis was the release of NO_2 group leaving a nitrogen-centered radical, followed by disproportionation of HNO_2 to yield NO, which was hypothesized to react with the previously-formed nitrogen radical to form the observed nitroso compound. Figure 2-1 (Scheme I) shows this sequence of reactions.

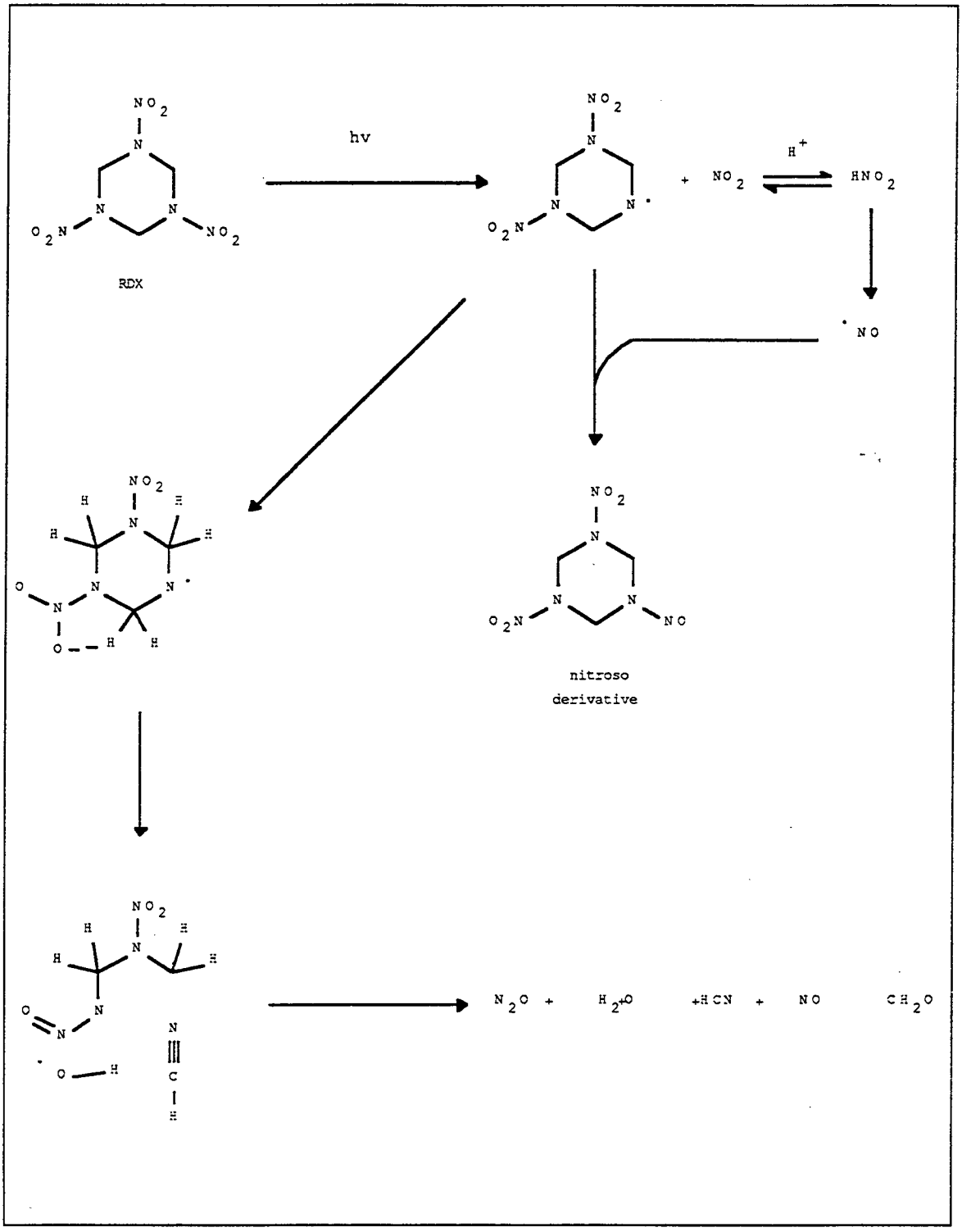

Figure 2-1. Scheme I: The initial step of RDX photolysis.

The addition of a fivefold excess of HNO_2 increased the yield of the nitroso compound by a factor of 10. Kubose and Hoffsommer also reported that several products were formed during the photolysis of RDX at λ >220 nm and their formation under these conditions was independent of the pH of the solution. The addition of HNO_2 only slightly affected the yield of byproducts at this wavelength. Kubose and Hoffsommer interpreted their data to mean that N-N bond cleavage may be the primary photochemical process at wavelengths greater than 280 whereas N-O cleavage occurs at shorter wavelengths.

Botcher and Wight (1993) performed laser pyrolysis experiments on thin films of RDX and inferred that the first step in degradation was the breaking of the N-N bond to yield NO_2. They identified N_2O_4 (the dimer of NO_2) as the primary product, and N_2O, NO, and HCN as secondary products. No evidence was found for a concerted depolymerization pathway forming methylene nitramine, CH_2NNO_2. Later studies by Botcher and Wight (1994) confirmed the initial degradation step and postulated the fragmentation mechanism of the nitrogen-centered radical shown in Figure 2-1. Whether this mechanism applies to aqueous phase photolysis is questionable, however, since the effective temperature at the time of laser photolysis was 1200 °K.

Glover and Hoffsomer (1979) also studied the aqueous photolysis of RDX and identified several byproducts, some of which are shown in Table 2-6. It can be seen that between nitrate (NO_3^-), nitrite (NO_2^-), and ammonia (NH_3), a nitrogen mass balance of greater than 92 percent was achieved. Although only 14 percent of the RDX carbon was identified as formaldehyde (CH_2O), by using ^{14}C-labeled RDX it was found that all of the carbon was still in solution at the end of the experiment. When oxygen was bubbled through the solution during the 12-minute experiment, and the gas passed through traps to determine CO and CO_2 formation, carbon dioxide accounted for another 42 percent of the carbon and CO for 3 percent of the carbon, bringing the carbon balance in that study to 59 percent.

During the GC-MS analysis of photolyzed aqueous solutions of RDX, Glover and Hoffsommer (1979) found a transient product (m/e=44) that was speculated to be formamidine ($NH=CH-NH_2$). The latter has been reported as a decomposition product of triazine in water (Grundmann and Kreutzberger 1954). Triazine itself could possibly be formed as a product of complete RDX denitration by three successive eliminations of HNO_2. Hunter, Sotsky and Carrazza (1983) stated that methyl- and dimethyl amine were the byproducts of RDX/HMX photolysis, but they did not specify the method by which those compounds were identified.

Several groups have investigated the thermolysis of RDX in thin films, melts, or aprotic solvents as a means of determining decomposition pathways. Smetana and Bulusu (1979) performed photolysis of aqueous solutions and solid poly-crystalline RDX and compared these results to thermolysis results reported by Rauch et al., (1969, 1970, and 1971, as cited in Smetana and Bulusu 1979). Product data was not quantitative for the aqueous solution photolysis, but Table 2-6 gives the solid and thermolysis data. Since only gaseous products were

measured in the solid photolysis, the amounts are normalized to 100 percent of the possible amount for carbon or nitrogen, but may not represent 100 percent of the products. In addition to the entries shown in Table 2-6, an NO yield of 18 percent and an HCN yield of 1 percent were detected. It can be calculated from the data in Table 2-6 that the carbon balance for these data is only about half as good as the nitrogen mass balance. The data of Rauch et al. (as quoted by Smetana and Bulusu 1977) indicates 94 percent mass balance for nitrogen and 70 percent for carbon. These investigators also found 15 percent of the nitrogen as NO and 1 percent of the carbon as HCN.

Other data on nitramine thermolysis in melts and organic solutions (Oxley et al. 1992) also indicate the cleavage of N-N bond, although in the case of nitramines containing methyl groups, a hydrogen transfer from methyl group to NO_2 group resulting in HONO loss was also suggested (Oxley et al. 1994). Oxley et al. (1994) studied laser-pyrolysis of various acyclic and cyclic nitramines, including RDX and HMX. They found significant differences in the amounts of gaseous products resulting from thermolysis of solid RDX, as compared with thermolysis of RDX in an acetone solution (Table 2-6). Much smaller quantities of gaseous products were liberated from the solution phase thermolysis, where 17 and 14 percent of the RDX nitrogen and carbon were found, compared to 87 and 58 percent, respectively, from solid phase thermolysis. This result implies secondary reactions of products and/or different pathways in the two systems.

Oxley and coworkers (1994) also found that the decomposition activation energies for all nitramines varied in the range of 40 to 50 Kcal/mol. This value corresponds to an activation energy for N-N bond dissociation of 205 kJ/mol (~50 Kcal/mol). Upon photolysis in acetone solution, all nitramines produced nitroso--amines (identified by GC-MS) and for all nitramines except RDX, they were found to be the principal byproducts. After 71 percent decomposition of RDX, 24 percent was found as the mononitroso derivative. Mono-, di and trinitroso compounds were all found during RDX thermolysis, but after complete removal of RDX, only numerous unidentified products were left, as well as some N_2, N_2O, CO_2, and CO.

According to the authors (Oxley et al. 1994), the first step of thermolysis of nitramines appears to be N-N bond scission. In the case of relatively simple nitramines, the amino radical formed as a result of N-NO_2 break was postulated to be stable enough to resist further decomposition and to react with NO trapped in the solution or melt (the authors did not specify the mechanism of NO_2 reduction to NO) yielding nitroso compounds. When RDX was heated under an NO_2 atmosphere, the rate of its decomposition increased. For complex nitramines such as RDX and HMX in the vapor phase, amino radicals were suggested to be unstable due to a strained structure of the heterocycle, which may lead to the ring breakdown after the loss of the first NO_2 group:

$$HMX \rightarrow NO_2 + HCN + 3H_2C{=}N{-}NO_2$$

$$H_2C{=}N{-}NO_2 \rightarrow N_2O + H_2CO$$

However, to be consistent with their data, the RDX radical would have to survive in the solution phase decomposition.

In addition, kinetic isotope effect experiments using deuterium-labeled RDX and HMX were cited, which showed that the decomposition path of these nitramines involved intramolecular hydrogen transfer. This result, confirmed by Oxley et al. (1994) for the simpler dimethyl nitroamine, suggested that a second pathway may also be available that involves H-atom transfer to an NO_2 group, with subsequent loss of HNO_2. This pathway probably deserves a closer look than the authors gave it, since their proposed mechanism for the production of the nitroso compound seems unlikely. Sufficiently increased stability of the N-centered radical in solution to allow reaction with NO seems questionable, particularly since no NO was detected by these investigators.

Several observations can be made concerning the data in Table 2- 6 that allow some conclusions to be drawn concerning similarities and differences between aqueous and nonaqueous photolysis and thermolysis:

1. Nitrate and nitrite would not be detected in the gas phase because, being ions, they would not volatilize. It is possible that the protonated forms HNO_3 and HNO_2 could volatilize under some circumstances, but their presence was not reported. It is likely that these ions were not even formed in nonaqueous systems, because of the energy associated with charge separation in nonpolar solutions.

2. If formed, NO_2 would not be detected in aqueous systems because it reacts quickly with water to produce nitrate and nitrite. NO_2 would probably not be detected in neat and nonaqueous systems because its reactivity makes gas chromatographic detection almost impossible. Thus, if NO_2 were formed initially, it would probably appear as other gaseous reaction products (from reactions with other gases) that were observed in solid or melt thermolysis, or as nitrate/nitrite that would be observed in aqueous solution.

3. Water formation was observed in some cases during RDX melt or thin film thermolysis or pyrolysis. Water can arise from the degradation of RDX, or air oxidation. Water formed by this process could also react with NO_2.

4. No NO formation was reported to result from any solution-phase decomposition. Thus, the recombination of NO with the nitrogen-centered radical seems unlikely as a route to the nitroso compound.

5. Nitrogen (N_2) is an unreactive product that, once formed, should not participate in further reactions. It is also not very soluble in water, so the low amount found by Kubose and Hoffsommer (1977) by GC analysis of the water might be less than was formed, due to outgassing from solution. However, Glover and Hoffsommer (1979) attained 92 percent mass balance with just the species NO_3^-, NO_2^-, and NH_3, so N_2 and N_2O do not appear to be important aqueous phase products. Exclusion of nitrogen as an important product eliminates denitrogenation of diazonium ions from consideration as

an important pathway. Diazonium salts can be formed by the action of nitrite on aromatic amines in acidic solution.

6. Since NO_2 disproportionates rapidly (tens of microseconds) in water, to yield equal quantities of nitrate and nitrite, and nitrate is relatively unreactive, the low nitrate yield observed in both aqueous photolyses Kubose and Hoffsommer (1977) and Glover and Hoffsommer (1979) indicate that NO_2 ejection may not be the most important first step in the aqueous photolysis of RDX. Balanced against that observation is the fact that the nitrate and nitrite analytical methods used by Kubose and Hoffsommer and Glover and Hoffsommer were indirect methods in which: (a) the nitrate is used to produce nitrobenzene, which is then measured by GC, and (b) nitrite is used in a reaction to produce a dye that is then measured colorimetrically. Although one version of the latter method has been adopted as a Standard Method, a more direct method such as ion chromatography (not generally available at the time of those publications) is preferable, and was therefore used in the present study.

From these data as well as newer gas phase data discussed by Botcher and Wight (1994), it is clear that the decomposition mechanism and products depend on the physical state (i.e., gas phase, solid, aqueous solution) of the material.

Although TNT and RDX have been the focus of numerous AOP investigations, not much is known about AOP application to the treatment of DNT. Andrews and Osmon (1977) treated 2,4-DNT and 2,6-DNT aqueous solutions with UV light in a continuous flow system and with H_2O_2/UV in a batch system. A germicidal 30 watt lamp was used as a UV source. Photolysis alone was successful in the elimination of DNT, but this may, in part, be attributable to the presence of acetone, since DNT solutions were prepared from its acetone concentrates. Photolysis of acetone can result in the production of methyl and acetyl radicals, which in turn may promote DNT oxidation. The authors did not perform a detailed investigation of the effect of acetone concentration on the DNT destruction rate, but they found that the rate of TNT photolysis increased with an increase in the acetone concentration from 0.01 to 1 percent. After 6 hours of irradiation, 2,4- and 2,6-DNT were practically gone, but in the case of 2,4-DNT a fluorescent product was detected. However, even after 78 hours of photolysis only ~6 percent of initial nitrogen was mineralized (primarily as nitrate and ammonia). These results indicate that DNT was converted to other nitrocompounds that apparently remained in the solution, but were not identified. When DNT was treated with H_2O_2/UV, the target compound and TOC were eliminated after 1 and 2 hours of the treatment, respectively.

P. Ho (1986) studied photo-oxidation of 2,4-DNT in aqueous solutions in the presence of H_2O_2. A 400-Watt, medium pressure mercury lamp with various types of filters was used as a UV source. The DNT concentration range was from 75 to 205 mg/L. The results obtained in this study indicated that the optimum concentration of H_2O_2 was ~0.1 percent. At this concentration, the complete DNT destruction was achieved in 30 and 90 minutes for DNT concentration, 75 and

205 mg/L, respectively. The data obtained in this study indicate that better DNT removal was achieved at shorter UV wavelength.

The Ordnance Group from Hercules Aerospace Co. studied feasibility of AOPs for 2,4-DNT treatment (Heffinger and Jake 1991). Preliminary laboratory-scale experiments were conducted in small quartz cells or test tubes. It was found that ozonation, photolysis, and H_2O_2 treatment were not effective for DNT solutions. The application of H_2O_2/UV showed a significant improvement in DNT degradation and O_3/UV treatment resulted in nearly complete destruction after 5 minutes. When O_3/UV was applied to actual wastewater, the DNT degradation proceeded at a lower rate, apparently due to other components of the wastewater competing for hydroxyl radicals. The O_3/UV bench-scale studies were carried out using a Normag photoreactor (~400 mL capacity) with two options of UV source. One source was a 15-Watt, mercury low-pressure lamp with 254 nm resonance emission; the other was a mercury high pressure lamp (typically ≥100 watt) that emitted in the region from ~240 nm to well into the visible range, with the strongest line at 366 nm. The results of these studies indicated that 254 nm radiation was more effective. No difference in the rate of DNT destruction was observed at various ozone flow rates. No effect of a high concentration of solvents (2-percent ether, 2-percent ethanol) on DNT removal in aqueous solutions was found, but these experiments were conducted in a short period of time (10 min). In many cases, however, the precision of the data was close to the magnitude of the effect being observed. Under these circumstances, it is difficult to know whether a real effect or random experimental error is being measured. The O_3/UV treatment of the actual wastewater containing ~200 mg DNT resulted in the complete removal of DNT over the period of 4 hours. At the end of the experiment all the byproducts (tracked as peaks in the HPLC chromatogram) had been eliminated. No byproducts were identified in this study, and TOC changes were not monitored.

According to Burlinson et al. (1979) photolysis of DNT resulted in a number of byproducts, primarily single aromatic ring nitro- and nitroaminocompounds. Table 2-7 summarizes the data obtained in their work. In the study discussed earlier in this section Ho identified byproducts in DNT solutions treated with H_2O_2/UV and proposed the scheme shown in Figure 2-1. It is worth noting that many compounds produced in the scheme may result from photolysis reactions, as well as the hydroxyl radical attack on DNT.

The large amount of 2,4-dinitrobenzoic acid found in this study at short reaction times may indicate that the degradation of 2,4-dinitrotoluene starts with side-chain oxidation. The product distribution implies that nitrogen mineralization may proceed by multiple pathways. A nitro group may be removed from benzene ring by replacing with a hydrogen atom or hydroxyl group. The attack of hydroxyl radical on the ring may lead to the ring cleavage with a nitro group staying on the resulting carbon chain. Nitro groups of nitroacids may be oxidized to NO_3^-. On the whole, information available in the literature is

Table 2-7. Photodegradation products from DNT (Burlinson et al. 1979).

Products	Relative amounts
2,4-Dinitrobenzaldehyde	6
2,4-Dinitrobenzonitrile	3
2-Amino-4-nitrobenzaldehyde	10
5,5'-Dinitro-azoxybenzene-carboxaldehyde	3
2,4-Dinitrobenzoic Acid	7
2-Amino-4-nitrobenzoic Acid	16
2,2'-carboxy-5,5'-dinitro-azoxybenzene	10

consistent with respect to AOP feasibility to treat DNT. However, many aspects of treatability remain to be explored.

The DNT wastewater at RAAP contains large amounts of ethanol and diethyl ether (DEE), which may affect treatment efficiency for the target compound. Data obtained from pulse radiolysis studies provide information on the rate constants and byproducts of hydroxyl radical attack on ethanol and DEE. Schultze and Schulte-Frohlinde (1975) found the major byproducts resulting from the ethanol reaction with OH• radicals to be acetaldehyde and acetic acid. The latter is known to be resistant to AOP treatment. A more detailed mechanism of ethanol oxidation was developed by Bothe et al. (1982). The hydroxyl radical rate constants for ethanol, acetaldehyde, and acetic acid are well established (Buxton et al. 1988). Oxidation byproducts resulting from pulse and γ -radiolysis of DEE were ethanol, various aldehydes, esters of carboxylic acids, and hydroperoxides such as acetaldehyde, formaldehyde, ethyl acetate, hydrogen peroxide, etc. (Schuchmann and von Sonntag 1982).

3 Experimental Details

Experiments were designed to obtain information on the treatability of wastewaters containing DNT, ethanol and ether, and pinkwater containing TNT and RDX. The experimental information will be used to develop a model for AOPs.

The Ozonation System and the Reactor

Figure 3-1 shows the experimental setup. Ozone was generated from extra-dry grade oxygen using a model GTC-0.5C 0.5 lb/day ozone generator from Griffin Technics Corporation. The ozone stream was split and sent to two mass flow controllers (Unit Instruments), which regulated the flow of ozone-containing gas to the reactor and the ozone monitor. The gas-phase ozone concentration monitor (PCI Ozone Corporation) employs ultraviolet absorbance to measure ozone concentration in the gas stream. Gas flow through the generator was kept constant at all times to ensure that reactor feed gas concentrations were stable. A solenoid valve controlling flow to the reactor can be switched to bypass the reactor. Using a pair of three-way solenoid valves, the monitor was configured to follow either reactor feed gas concentration or off gas concentration.

Ozone concentration and flow rate data were acquired in real time by a computerized data acquisition system. The computer collecting the data was a 12.5 MHz Dell AT-compatible computer with one megabyte of RAM, 86 Mb of disk storage and multi-mode VGA monitor. The data acquisition system was a 16 channel, 12-bit, auto-ranging Metrabyte DAS-16 G1 A/D board and a daughter board holding optically-isolated relays. The data acquisition software was Labtech Notebook® (Laboratory Technologies Corporation, Wilmington, MA). The data collected were imported into Lotus 1-2-3® (Lotus Development Corporation) for post-run analysis.

The reactor used was a stirred-tank reactor, constructed from glass and polytetrafluoroethylene (PTFE). In most cases, it was operated as a continuously-stirred reactor in the semi-batch mode, but could also be configured to operate in a flow mode. It was usually operated with a 10.7-L liquid volume. Liquid sampling was done by opening a glass and PTFE stopcock at the bottom of the reactor. All the tubing and fittings in the system were PTFE, except for the mass flow controllers and two stainless steel components inside the ozone monitor. Four ultraviolet lamps (American Ultraviolet) were contained in quartz housings that extend through the Teflon® headplate of the reaction vessel. The lamps used were rated at 5.3 watts of emitted UV power at 254 nm. One of the lamps was partially shrouded to allow "half lamp" intensities to be used, giving a range of seven intensity levels from different

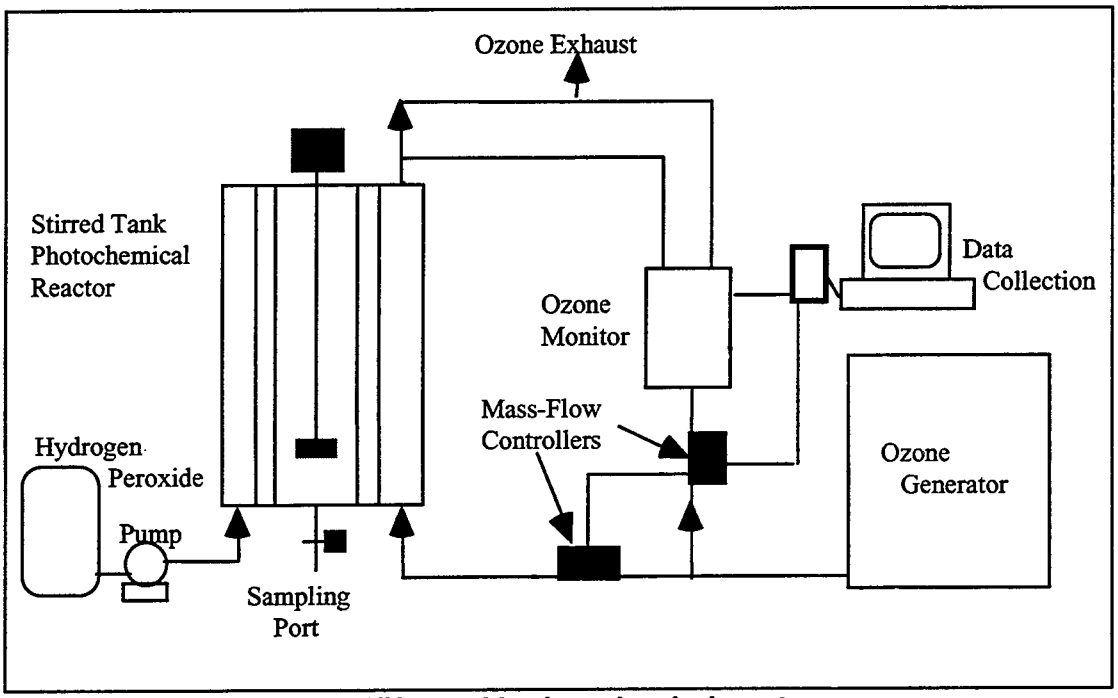

Figure 3-1. Laboratory-scale UV/peroxide photochemical reactor.

combinations of the four lamps. Each lamp could be turned on or off individually.

As an experiment proceeded, the headspace in the reactor grew larger due to sample removal (a typical sample size was ~70 mL). It was found that, depending on the size of the headspace and the rate of introduction of gas into the reactor from the ozone generator, it may be necessary to sweep the headspace of the reactor with makeup oxygen to ensure that the residence time of ozone in the reactor is short enough so that decomposition of ozone in the gas phase does not occur. Decomposition of ozone results in artificially low readings of off-gas ozone concentrations and therefore gives inaccurate (high) calculated ozone-utilized doses. This appears to be a general problem in many laboratory-scale and most pilot- or full-scale reactors. Gas flow from a makeup oxygen line was sent through a third mass flow controller that regulates the rate of flow of makeup gas to the headspace. The off-gas concentration measured by the ozone monitor was then corrected for the makeup gas addition during the post-run data analysis. The utilized ozone dose was corrected for the volume change of the reactor charge during this post-run calculation.

High-Power Lamp Reactor

Several of the experiments used a high-power lamp for the generation of radiation in the ultraviolet range. All of these experiments were performed in a recirculating batch reactor that houses this lamp. All wetted surfaces within the reactor are either glass or Teflon®. The operating capacity of the reactor was

initially 5.1 L. Its contents are recirculated at 8 to 9 L per minute. Oxygen was introduced at approximately 2 standard L per minute through a coarse frit. The radiation source is a 1 kW lamp that generates ultraviolet photons with 20 percent efficiency. A large portion of the photons are emitted at a wavelength of 200 to 250 nm. Ozone was introduced through the oxygen influent gas line. Ozone flow to the reactor was regulated by a UFC-1000 mass flow controller with digital readout. The percent of ozone in the feed stream and the off gas was monitored spectrophotometrically by a PCI model HC ozone monitor. Information from both the mass flow controller and the ozone monitor were fed into the computerized data acquisition system described above.

An Orion Model 820 dissolved oxygen (DO) meter was used to continuously monitor the amount of oxygen in the reactor charge by passing a small stream from the reactor through a sealed flow cell containing the sensor of the DO meter. The meter was calibrated against water-saturated air and automatically compensated for temperature and pressure. Hydrogen peroxide was added to the reactor as a concentrated (30 percent) solution before the experiments. Three and one-half lamps were used in all experiments, providing a total 254-nm UV flux of 2.75×10^{-6} E/L•sec out of the lamp wells and into solution.

Use of the high-power lamp in the semi-batch reactor for extended periods of time led to significant heating of the reactor contents. After treatment for 45 minutes the temperature of the reactor charge reached 79 °C. Before that time, a water/ethanol/acetaldehyde azeotrope began to distill from the reactor through the off gas line and were collected for analysis. Under these conditions, the off gas line was only intermittently connected briefly to the ozone monitor for off gas measurement, then again disconnected. The organic vapors probably interfered with ozone measurement in the one ozonation experiment using the high-power lamp. This interference would cause the apparent consumed ozone dose to be lower than the actual dose, and therefore lead to higher calculated efficiencies. Ozone data from this experiment was not used in the data analysis. The distillate was also noted to contain some DNT, which presumably codistilled with the azeotrope.

During the later part of experiments, a third photoreactor having a smaller volume was used because of the reduced availability of ordnance compounds. The reactor was constructed from a 1-L borosilicate resin kettle, having a matching head fitted with three, 24/40, standard taper ground glass female joints as ports. Two of these joints held quartz male through-joints that had been sealed at the bottom to produce lamp wells that were immersed in the reactor charge when in place. The third port held a combination of adapters to allow gas sparging, sample withdrawal, and inlet and outlet tubes for a recirculated slipstream for dissolved oxygen (DO) measurement. Except for the silicone rubber gasket between the reactor head and body, and a viton o-ring in the DO cell, all exposed parts were made of borosilicate glass, quartz, or polytetrafluoroethylene (PTFE).

Materials

2,4-Dinitrotoluene (97 percent) and acetaldehyde (99 percent) were obtained from Aldrich Chemical Company, Inc. Absolute ethanol (100 percent purity) was purchased from McCormick Distilling Company. Diethyl ether of high performance liquid chromatography (HPLC) grade was obtained from Baxter Scientific. Both hydrogen peroxide (30.5 percent aqueous solution) of certified A.C.S. grade and glacial acetic acid were obtained from Fisher Scientific. Methanol and acetonitrile of HPLC and spectroscopic grade were also purchased from Fisher Scientific and were used for liquid chromatography. Deionized water was produced in the laboratory using a Millipore system.

Analytical Methods

Analysis of various components of the wastewater and the products of the AOPs are conducted with well designed and established methods. Details of the analytical methods will be described in detail in the following section. However, Table 3-1 summarizes the methods.

Organic Analytes

Ordnance Compound Analysis. Aromatic organic compounds were determined by HPLC, while low-boiling aliphatic compounds such as ethanol and acetaldehyde were quantitated by GC/FID. Samples of DNT wastewater were supplied by RAAP and analyzed in this laboratory for various organic and inorganic constituents. DNT was measured by HPLC. Despite some sensitivity limitations compared to GC, HPLC also provides information on many oxidation byproducts that are formed during treatment. HPLC is a more appropriate method for determining these compounds than is gas chromatography, because oxidation byproducts tend to be more polar, hydrophilic, and thermally unstable than their parent compounds. Since gas chromatography requires thermal volatilization of the analytes, decomposition of sensitive compounds can occur.

An adaptation of the EPA Method 8330 was used as the HPLC protocol for the separation and quantitation of ordnance compounds. It consisted of an isocratic separation using a mobile phase of methanol and water (40:60, v:v) at a flow rate of 1 mL/min. The analytical column was a Supelco LC-18, which was preceded by a C18 guard column. Quantitation of analytes was done by monitoring UV absorbance at 254 nm.

An additional HPLC method was used to analyze samples for byproducts. This procedure used an anion exchange/reverse phase separation on a mixed-mode column which improved the separation of explosives and their polar and ionic degradation products such as 2,4-dinitrobenzoic acid (DNBA). The method was developed using a mixed-mode HPLC column in which the phase bonded to the silica contains an octyldecylsilane (reversed-phase function) and a secondary amine (anion exchange function) incorporated into a single ligand in a 1:1 ratio.

Table 3-1. Analytical methods.

Analyte/parameter	Method	Comment
2,4-DNT	HPLC	EPA method 8330 (Basis), Supelco LC-18 column, estimated quantitation limit = 25 ppb.
2,4-dinitrobenzoic acid, and other byproducts	HPLC	Anion exchange/reverse phase separation.[37]
Total Organic Carbon (TOC) Ethanol, Diethyl ether, GC		OI Corp. model 700 TOC analyzer Varian 3700 GC, FID detector, acetaldehyde, acetic acid Supelco Chromosorb 102 column, isothermal, internal standards used.
Nitrate/Nitrite	IC	Dionex 2000i/SP, Anion membrane suppresser, IonPac AS4A/Metachem SARASep An300 columns
Ammonia	Wet Chemistry	Automated wet chemistry method,[38] Absorbance at 630nm, Quick Chem IV system.
Ozone	Indigo Method	Reference 39.
Hydrogen peroxide	Ti(IV) Complexing	Colorimetric measurement.[40]
pH		Beckman Ø-21 pH meter with temperature compensation
Ultraviolet Absorbance		LKB model 4050 UV/VIS Spectrophotometer

The dual nature of this chromatographic resin permits the separation of a mixture of compounds with a wide range of polarities. The ternary gradient separation used three eluting solvents. The aqueous solution, A, contained phosphate at 0.015 M adjusted to pH 5.1 in a 10:90 methanol:water solution. Solvent B was methanol and solvent C was acetonitrile. The gradient initializes with the solvent A for 10 minutes before gradual incorporation of additional organic portions reaches a final 98 percent organic composition within 31 minutes. This separation is an adaptation of a method published by Griest and co-workers (Griest et al. 1990).

The HPLC procedures were modified slightly during later stages of experiments, including that for carbonyl compound analysis, which was simplified to shorten sample preparation and analysis time, decrease the risk of thermal decomposition or rearrangement of derivatives, reduce solvent consumption, convert to a more "friendly" solvent (methanol instead of DMF), and prevent loss of volatiles due to a solvent exchange step in the procedure.

Sample Handling. Reactor samples were removed at timed intervals from the stirred tank photolytic reactor (STPR). For HPLC analysis, a 5 mL aliquot was placed in a 10 mL volumetric flask and brought up to volume with methanol. After careful and complete mixing by inversion a 2 mL portion was removed from the vial and placed in an HPLC autosampler vial. HPLC analyses were performed with a minimum of triplicate injections of a sample that represented a single time point. Occasionally, triplicate samples were drawn at a single time and were analyzed with triplicate injections of each sample.

Estimated quantitation limit (EQL) for DNT was 25 ppb in the aqueous sample using this method. The method is discussed in more detail elsewhere (Peyton et al. 1992).

Total Organic Carbon

Total Organic Carbon (TOC) was determined using an OI corporation model 700 TOC analyzer with the purgeable organic carbon option. The sample is introduced into a heated reaction chamber where it is acidified with phosphoric acid and purged with a nitrogen stream. Inorganic carbon is liberated as carbon dioxide and detected with a nondispersive infrared detector. Purgeable organic carbon is removed from the gas stream on a Tenax® trap, and is then thermally desorbed and oxidized to carbon dioxide on a heated catalyst under an oxygen stream. Potassium persulfate is added to the heated reaction chamber to oxidize any remaining carbon to carbon dioxide, which is subsequently detected.

Gas Chromatography

Ethanol, diethyl ether, acetaldehyde, and acetic acid were analyzed by direct aqueous injection gas chromatography. A Varian model 3700 GC with a 6-ft glass Supelco 100/120 Chromosorb 102 column was used to separate the compounds. Detection was accomplished with a flame ionization detector and results quantified with a Hewlett-Packard 3390A integrator. For all analyses, the following were kept constant: 2 µL sample injected, injector temperature 160 °C, detector temperature 190 °C, carrier gas (UHP nitrogen) flow at 20 mL/min. To optimize analytical time, oven temperature program and internal standard were varied. All programs were isothermal, ranging from 120 to 150 C. Internal standards included isopropanol (which cannot be used with diethyl ether), tert-butyl alcohol (which cannot be used with acetic acid), and isobutanol.

Inorganic Analytes

Nitrate/Nitrite (NO_3^-/NO_2^-) Analysis

The nitrate (NO_3^-) and nitrite (NO_2^-) analysis was performed on a Dionex 2000i/SP ion chromatograph that was equipped with an ISCO autosampler and a conductivity detector (Dionex Anion Membrane Suppressor). Anion separations were carried out isocratically on either a Dionex IonPac AS4A (4 mm x 250 mm) column or a Metachem SARASep An300 (7.5 mm x 100 mm) column using an eluent composed of 1.80 mM sodium carbonate/1.70 mM sodium bicarbonate.

Aqueous samples of 50 µL were used for the analysis. Calibration was achieved with a five-point external standard curve.

The use of ion chromatography was extended to the analysis of cyanate, cyanide (by conversion to cyanate using alkaline chlorination), and small organic acids such as formate and acetate.

Metals Analysis

Analysis of metals was added for a more complete characterization of the wastewater. The concentrations of metals in the samples were measured by inductively coupled argon plasma spectrometry (ICP) using a Thermo Jarrell-Ash MARK III Model 1100 vacuum direct reader.

Ammonia (NH_3) Analysis

Flow injection analysis is an automated wet chemistry method used for the analysis of ionic parameters in a liquid matrix (Grasshoff 1976). This method is based on the Berthelot reaction. Sodium EDTA was added as a complexing reagent to reduce formation of hydroxide precipitates. Ammonia in the sample was reacted with alkaline phenol, then with sodium hypochlorite to form indophenol blue. Sodium nitroprusside was added to enhance the sensitivity. The absorbance of the reaction product was measured at 630 mn, and is directly proportional to the original ammonia concentration.

The Quik Chem IV system from Lachat Instruments of Milwaukee, WI, is directed to introduce a 2.5 mL sample into an unsegmented continuous flowing carrier stream. A 180 µL portion of the sample is then injected into the reagent stream and mixed as the chemical reaction occurs. The sample stream is then passed through a 10 µL flow cell where color detection occurs at the absorbance wavelength of 630 nm. Analysis time from initial sampling to real-time data reporting is approximately 1 minute per sample. This method had an analytical range of 0.02 to 2.00 mg/L of NH_3. A blank sample plus five calibration standards were used to determine the calibration curve.

Total Inorganic Carbon Analysis

Total inorganic carbon (TIC) measurement was obtained automatically during the course of TOC measurement using the OI-700. In previous projects, these measurements have been compared to results obtained by titration and the use of Gran plots (Gran 1952), and found to give comparable values. In the presence of interferences such as iron, the TIC measurement provided a better measure of bicarbonate than did the standard alkalinity titrations.

Oxidants

Ozone was measured by the indigo method of Bader and Hoigné (1982). Hydrogen peroxide was determined by formation of the Ti(IV) peroxy complex, followed by colorimetric measurement (Parker 1928). Both of these methods are insensitive to most interferences and have been in use in the Aquatic Chemistry Laboratory at the Illinois State Water Survey for 13 years.

pH

Solution pH was measured using a Beckman Ø-21 pH meter with temperature compensation, with a two-point calibration against commercial standard buffers. All solutions were magnetically stirred during pH measurement.

Ultraviolet Absorbance at 254 nm (UV)

Ultraviolet absorbance at 254 nm was measured using an LKB model 4050 UV/VIS spectrophotometer. Absorbance at this wavelength was of interest primarily because of the effect of competition of the solution components for 254 nm photons during photolytic studies.

Selection of AOPs To Be Investigated

The three most common AOPs, ozone/UV, ozone/H_2O_2, and H_2O_2/UV, were considered in the present study. Peyton and Glaze (1988) have pointed out the chemical similarities of these processes. Other processes such as gamma irradiation, electron beam treatment, semiconductor photocatalysis, sonication, cavitation, and combustion also produce free radicals. However, in the present work, only processes where OH is generated from combinations of ozone, hydrogen peroxide, and UV are considered.

One factor known to be detrimental to the effectiveness of H_2O_2/UV treatment is high UV absorbance of the solution to be treated. The extinction coefficient of hydrogen peroxide at 254 nm is low, so that for peroxide to be competitive for photons, it must be used at such a high concentration that it is also competitive for OH radicals. This detriment is even more serious in the treatment of DNT since the reaction rates of OH radical with multinitrated compounds tend to be significantly lower than for typical organic compounds. This is consistent with the results of Heffinger and Jake (1991), who found H_2O_2/UV treatment to be slower than treatment by O_3/UV. Accordingly, H_2O_2/UV treatment was not initially considered in this study, and the first few sets of experiments were carried out using ozone/H_2O_2 and ozone/UV. The UV lamps used emitted at 254 nm, which is characteristic of many commercial units.

Flow-Through Treatment Studies

The purpose of this part of the study was to demonstrate results similar to those of DNT batch studies in a flow reactor and to determine if the kinetic model developed for batch studies could be extended to flow conditions.

Flow Reactor

The flow experiments were carried out in a smaller (1-L liquid volume) photochemical reactor than was used for the batch studies (10-L volume) because of the large volume of liquid required for each experiment. One limitation imposed by the use of this reactor was that the UV intensity was sufficiently low

so that a long residence time (>60 minutes) was required for sufficient radical generation to achieve reasonable DNT removal. In principle, a 95 percent equilibration can be reached by flowing three reactor volumes (V_R) through a perfectly-mixed stirred-tank reactor, but in practice, it was often necessary to flow twice that amount or more through the reactor before the effluent DNT concentration stabilized.

The 10-L reactor (labeled "reservoir CSTR" in Figure 3-2) served as a gas-spargable reservoir. The continuous stirred-tank photochemical reactor (CSTPR in Figure 3-2) was fed with a mixture of synthetic DNT wastewater and hydrogen peroxide solution through pumps P1 and P2, respectively. The hydrogen peroxide solution was approximately 100 times more dilute than the commercial 30 percent H_2O_2 so that decomposition in the H_2O_2 reservoir would not be sufficiently rapid to affect quantitation of peroxide usage. Therefore, the flow rate of the H_2O_2 stock solution (2 mL/min, nominal) was about 12 percent of the total flow to the reactor (about 16 mL/min, nominal). Under these

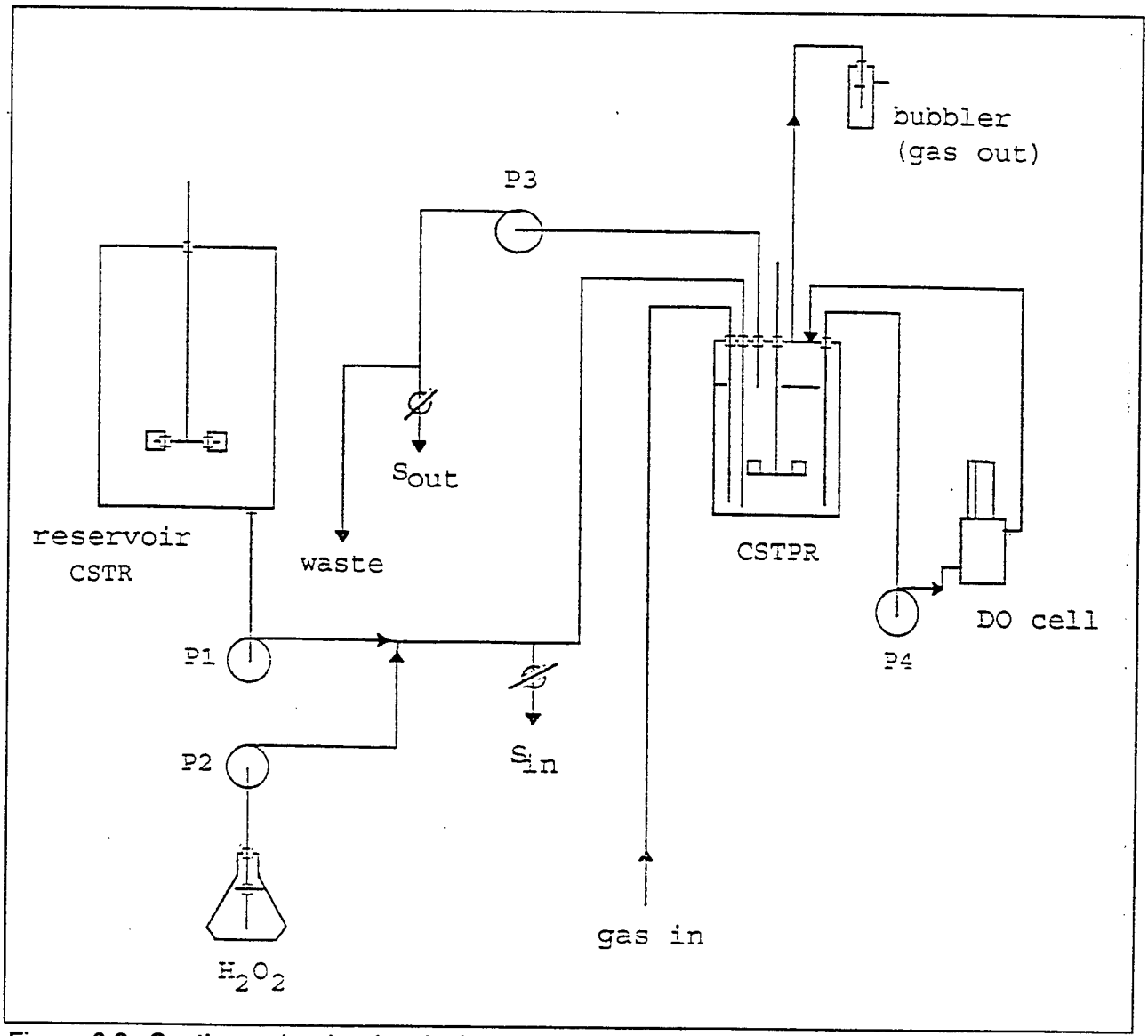

Figure 3-2. Continuously stirred-tank photochemical reactor.

conditions, the peroxide stock solution was capable of carrying 100 times more dissolved oxygen into the reactor than would the peroxide feed solution in an actual application, so the peroxide stock solution was always continually sparged with nitrogen or the oxygen/nitrogen mixture being used for the particular experiment.

The effluent pump P3 was operated at a pumping rate greater than the sum of P1 and P2 to ensure that the reactor never fills above the intake and thus maintains a constant liquid level. Thus the retention time depends only on P1 and P2, and is independent of P3. This procedure resulted in a net removal of gas from the reactor, so the headspace of the CSTPR was swept with nitrogen when no gas sparging of the reactor contents was occurring. The excess sparge gas was released through a bubbler to prevent backflow of air into the reactor. Pump P4 recirculated reactor solution over the DO probe for continuous real-time DO measurement. Reactor feedstock was sampled at S_{in} and effluent was sampled at S_{out} at 30-minute intervals from the time flow began until the effluent DNT concentration had stabilized at the end of the experiment. The DO content of the water had usually stabilized by the time the reactor had filled (about 1 hour), whereupon the lamps were turned on at t=0.

Gas Manifold

Initially, nitrogen and oxygen gas streams were regulated by needle valves and mixed before being sent to the reactor. Because of an inability to maintain certain DO concentrations, the gas manifold from the laboratory ozonation system was replumbed to allow regulation of the gas flow rates using mass flow controllers (thermal conductivity). The gas manifold is shown in Figure 3-3. The lines going to and from "Reactor" (the the reservoir CSTR during flow experiments) in Figure 3-3 were split to send streams to the CSTPR and the H_2O_2 stock solution reservoir. Solenoid valves (PTFE) labeled V1, V2, and V3 in Figure 3-3 provided connection of the center port to one or the other side port. Valve V_1 allowed either the liquid contents or the headspace of the CSTPR to be flushed with gas. The ozone-related components remained in place, but were not used.

Use of the gas manifold provided better control of the sparge gas flow rate and composition, and allowed control of the DO concentration at any desired value during subsequent experiments. These experiments (group B) gave somewhat different results than those carried out before the manifold was installed (group A), which tended to go toward particular values of DO concentration, regardless of the initial value. After installation of the manifold, it was noticed that continual changing of the mass flow controller settings was required to prevent the previous behavior and maintain constant DO values.

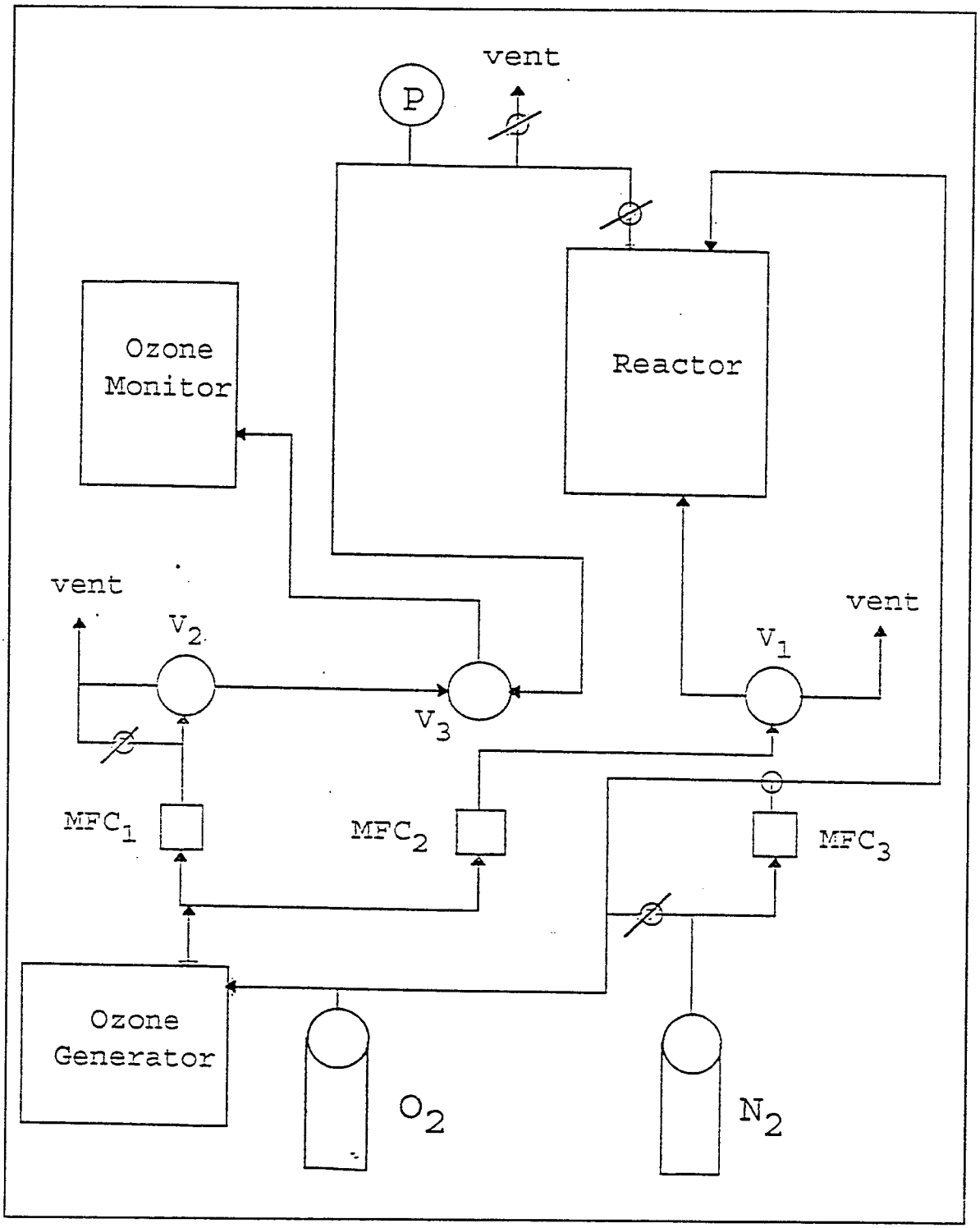

Figure 3-3. Gas manifold from the laboratory ozonation system.

Solutions, Chemicals, and Procedures

DNT was dissolved in warm ethanol and this solution was added to the appropriate volume of deionized water to prepare 10 L of reactor charge solution (0.16 mM DNT, nominal) to be placed in the reservoir, a 10-L stirred tank reactor equipped for sparging of the solution with oxygen/nitrogen mixtures (see "Gas Manifold," above). Pumps and gases were turned on and the CSTPR allowed to fill. When the reactor was full, the initial DO was noted, "zero-time" samples were taken, then the UV lamps were turned on to start the experiment. At this point, the DO concentration would drop drastically as oxygen was consumed by the photochemically-initiated reactions, then level out at a new steady-state value. A typical example is a steady-state value of 1.0 mg/L DO dropping to 0.5, or 0.6 dropping to 0.2 mg/L. The actual values of the DNT concentrations at times prior to steady-state (other than the zero-time value) are of little consequence other than to indicate the approach to steady-state, which was approximately exponential as expected. HPLC analyses for DNT and byproducts were performed in real time to follow this approach. Ethanol and acetaldehyde were monitored by gas chromatography on packed porous polymer columns (Chromosorb 101) by direct aqueous injection. Hydrogen peroxide was measured by the titanium IV method described previously, and pH and UV absorbance at 254 nm were measured periodically, as well. Experiments were continued until the DNT effluent concentration stabilized, sometimes requiring more than 400 minutes, even though the average reactor residence time was only about 1 hour. Occasionally, the DNT concentration would appear to have just stabilized, when another major drop would occur, requiring several hours to restabilize. The reasons for that unexpected behavior are currently unknown.

4 Experimental Results, Analysis, and Discussion

This chapter presents the results obtained using the experimental apparatus and procedures described in the previous chapter. The results are analyzed and explained to develop a process kinetic model. The model considers the dominant process occurring in the reactor. Later, the process and model concepts are used to study the DNT wastewater from RAAP, which is one of the main objectives of the study. Results of the flow-through study are also included.

The DNT wastewater from RAAP contains mainly DNT, ether and ethanol. The concentrations of these components vary widely based on the production process and ambient discharge conditions. Table 4-1 lists typical concentrations of the wastewater discharge from the water dry process. Table 4-2 gives a detailed characterization of a representative sample of the wastewater.

During the AOP application, the reactants (waste components and the oxidation/reducing agents) are brought into contact causing the reaction process. Therefore, both the mass transfer and chemical reaction parameters are important in studying and developing a AOP application.

Coupling of Mass Transfer and Chemical Reactions

A complete description of ozone behavior by use of the rate equation requires the inclusion of the mass transfer term as the ozone source, as well as the chemical reactions it undergoes (sinks). However, that information is rarely given in the literature when ozonation research is reported, and most of the published ozonation literature suffers from the fact that the findings are not quantitatively transferable to another system. This problem is so severe that most of the existing (water treatment) ozonation literature is only useful in a qualitative "feasible/not feasible" way.

Table 4-1. Typical concentrations of organic constituents of RAAP DNT wastewater.

Concentration	DNT (mg/L)	Ether (mg/L)	Alcohol (mg/L)
Averages	142	377	2413
Low	50	0	60
High	208	2058	9212
Standard Deviation	33.8	404	1844

Table 4-2. Chemical characterization of RAAP DNT wastewaters.

Species	Concentration (mg/L)[a]	Method[b]
DNT	183.5	HPLC
Ethanol	81	GC
Acetaldehyde	2.5	GC
Ether	64	GC
Nitrite	0.58	IC
Nitrate	0.27	"
Ammonia	0.04	"
Sulfate	34.92	"
Chloride	5.9	"
Fluoride	0.1	"
Phosphate	0.118	"
Alkalinity[c]	52.5	Autotitration
Calcium	18.3	ICP
Potassium	15.2	"
Magnesium	6.2	"
Sodium	5.53	"
Manganese	0.53	"
Lead	0.256	"
Iron	0.13	"
Strontium	0.087	"
Aluminum	0.054	"
Zinc	0.045	"
Barium	0.038	"
Copper	0.036	"
Lithium	0.017	"
Sulfur	11.06	"
Silicon	3.87	"
Organic Carbon (TOC)	217 ± 19	TOC analyzer
Inorganic Carbon (TIC)	16	"

[a] Data obtained in this laboratory.
[b] See text for abbreviations.
[c] As $CaCO_3$

In studying the complex chemistry of ozone/hydroxyl radical systems, it is convenient to separate the mass transfer process from the fundamental chemical reactions that are occurring. The former is very much a function of the reactor and operating conditions, while the fundamental reactions can be described by reaction rate constants that are constants of nature, independent of the experimental apparatus and protocol. The philosophy behind this separation is that, if the reaction system can be elucidated, then the process design engineer

can combine this information with the mass transfer characteristics of the reactor that is most suitable for the application. Although situations can arise where the "coupling terms" between mass transfer and chemical reaction can be important, such as the case where reaction is so fast as to take place in the liquid film surrounding the bubble, the assumption is that the simple approximate model that is the ultimate goal of this research is sufficiently flexible to accommodate these effects. The test of this assumption is whether the model works.

Therefore, great care is taken to measure the "dose" of ozone that is taken out of the gas stream and assumed to be transferred to the liquid. This amount of ozone (normalized to the liquid volume, so as to represent a concentration in the liquid) is the "utilized ozone dose," and the (liquid volume-normalized) rate at which it is removed from the gas stream is defined as the "utilized ozone dose rate." These quantities are used as the basis for all ozone accounting processes. The utilized ozone dose rate is also the mass transfer rate, but the assumption is that once the ozone has been transferred into solution, its history is unimportant. The ozone accounting (mass balance) process is crucially important, because it is the only way of drawing conclusions concerning the fate of dissolved ozone in treatment experiments. One of the most important contributions of Hoigné and co-workers was to demonstrate that ozone did not simply disappear when it decomposed in solution, but that it participated in well-defined chemical reactions, knowledge of which allowed this accounting process to take place. The efficiency model described below is simply an extension of this accounting process.

Origin of the Model

Consideration of the DNT wastewater characteristics led to the preliminary conclusion that because of the presence of high concentrations of solvents in the water, free-radical scavengers would be most significant factor affecting process efficiency. Although DNT undergoes photolysis by UV radiation, the rate was found to be considerably below that of removal by hydroxyl radical attack, so ultraviolet (UV) intensity was initially considered to be of secondary importance with regard to process efficiency for this system.

The first model tried during the present investigation was one that was developed based on earlier work of Hoigné and co-workers (Hoigné and Bader 1977; 1978) in the late 1970s. Those authors used rather simple models to successfully describe the effects of Natural Organic Material (NOM) and bicarbonate on the treatment of pollutants by ozone under conditions where hydroxyl radical was formed. The starting point for the model developed here is the mass balance relationship (similarly to Hoigné and Bader 1978), in the form of the statement that the number of contaminant molecules destroyed is equal to the number of OH molecules that successfully attack contaminant, which is equal to the amount of ozone decomposed ($\dot{D}_u$), times the OH yield per ozone

molecule decomposed (η), times the fraction of OH radicals that react with contaminant R (f_{OR}). The differential form of the above statement is

$$\dot{R} = \eta f_{OR} \dot{D}_u \quad \text{(4-1)}$$

while the integrated form is

$$\Delta R = \eta f_{OR} D_u \quad \text{(4-2)}$$

The ηf_{OR} indicates the average value of the product of η and f_{OR} over the time period of interest. The fraction of radical A captured by species B is defined as the "competition function" f_{AB}:

$$f_{AB} = \frac{k_{AB}BA}{\sum_i k_{Ai}S_iA} = \frac{k_{AB}B}{\sum k_{Ai}S_i} \quad \text{(4-3)}$$

where the k's are second-order rate constants and the S_i are all species that scavenge radical A. The competition function is not new (e.g., Hoigné and Bader 1977; Larson and Zepp 1988); however, formalization of the symbology simplifies the manipulation of complex equations.

In summary, the above formalism is a generalized and extended version of ideas and techniques that have already been published by Hoigné and Bader. This technique has been used to evaluate rate constants of various organic species with both hydroxyl and carbonate radical, and has been shown to work well in describing the competition between target and nontarget species for radicals generated during the application of AOPs.

Determination of $k_{OH,DNT}$

The theoretical basis for analyzing experimental results in which substrates compete for free radicals was described in a previous section. The use of the fundamental competition relationship, equation (4-3), requires concentration data and values of the rate constants for the competing species. The experiments carried out during the initial stage of the project are summarized in Table 4-3. Molar units are used throughout this report because they represent the proportions in which substances react. Conversion factors from millimolar (mM = 10^{-3} M, M = moles/L) are given in Appendix A. Three experiments were performed (A03, A04, and A05) to evaluate the rate constant for the reaction between OH and DNT, for use in these kinetic equations. Ozone/H_2O_2 treatment was used to generate OH radicals, to avoid photolysis reactions and ensure that only OH radical reactions were being observed. Ethanol was used as a probe compound (a compound competing with a target compound for hydroxyl radicals) because the rate constant and byproducts of its reaction with OH• were known. In addition, ethanol is one of the major components of the DNT wastewater and its use in these experiments might provide some additional information on the

system behavior under AOP treatment conditions. The results were analyzed using equation (4-4), by solving for $k_{OH,EtOH}$.

$$\frac{\dot{E}}{\dot{D}} = \frac{Rate\ of\ ethanol\ disappearance}{Rate\ of\ DNT\ disappearance} = \frac{k_{OH,EtOH}[\cdot OH]E}{k_{OH,DNT}[\cdot OH]D} = \frac{k_E^{'}E}{k_D^{'}D} \qquad (4\text{-}4)$$

Table 4-3. DNT treatability experiments.

Experiment No.	Method	DNT concentration, mM	Ethanol concentration, mM	Ether concentration, mM	Utilized ozone dose rate, mM/min	H_2O_2 concentration, mM
A01	UV	0.561	--	--	--	--
A02	Sparge	--	63.25	6.25	--	--
A03	O_3/H_{2O2}	0.512	0.073	--	0.026	0.18
A04	O_3/H_2O_2	0.456	0.071	--	0.025	0.15
A05	O_3/H_2O_2	0.517	0.098	--	0.021	0.18
A06	O_3/H_2O_2	0.451	4.05	--	0.105	0.20
A07	O_3/H_2O_2	0.515	--	--	0.08	0.25
A08	O_3/UV	0.594	--	--	0.09	--
A09	O_3/UV	0.551	4.8	--	0.08	--
A10	O_3/UV	0.568	442.0	--	0.230	--
A11	O_3/UV	0.893	74.39	6.06	0.205	--
A12	O_3/UV	0.723	--	4.22	0.105	--
A13	Sparge	--	--	5.20	--	--
A14	O_3/UV	0.543	16.26	--	0.16	--
A15	O_3/UV	0.841	69.5	4.57	0.315	--
A16	O_3/UV	0.524	4.54	--	0.19	--
A17	UV/(HP)	0.504	17.84	--	--	--
A18	UV/(HP)	0.517	--	--	--	--
A19	O_3/(HP)	0.504	13.3	--	0.47	--

(HP) High-power 1-kw lamp. All other experiments as in Experimental section.

The pseudo first-order rate constants were the slopes of plots of the logarithm of the ethanol and DNT concentrations versus time, as obtained from linear regression. These calculations led to a value of $k_{OH,DNT}=(2.5 \pm 1.3) \times 10^8\ M^{-1}s^{-1}$, where the range is the standard deviation for three determinations. Although the precision of this measurement is not particularly good, the result seems reasonable, since hydroxyl radical is an electrophilic reactant and nitro groups

deactivate aromatic rings by withdrawing electrons. It should therefore react with OH much more slowly than does ethanol, for example, which has a rate constant of $1.9x10^9$ $M^{-1}s^{-1}$ (Buxton et al. 1988). A value of $k_{OH,DNT}=4.6x10^8$ was estimated on the basis of $k_{OH,nitrobenzene} = 3.9x10^9$ (Buxton et al. 1988) and a value of $K_{OH,TNT} = 5.5x10^7$, reported by DeBerry et al. (1984), assuming a linear free energy (Hammett) relationship (Gould 1959). However, this value seems too high compared to typical non-nitrated organic compounds.

Comparison of Ozone/UV and Ozone/H_2O_2

Figure 4-1 shows a comparison of the DNT disappearance curves for ozone/UV and ozone/H_2O_2 treatment (Experiments A08 and A07) of 100 mg/L (nominal) DNT in purified water, at similar applied ozone dose rates. The applied and utilized ozone doses were actually both slightly larger for the ozone/UV experiment, so the relative disappearance rate in the O_3/H_2O_2 and O_3/UV experiments is difficult to interpret without the aid of a model. The initial disappearance rates are probably within experimental error of each other. As discussed in the previous sections, contaminant destruction relative to the amount of ozone used is of greater importance than simply contaminant destruction rate. Figure 4-2 shows a plot of efficiency, ϵ, defined in the following equation,

$$\epsilon = \frac{\Delta R}{D_U} = \overline{\eta} f_{OR} \qquad \textbf{(4-5)}$$

versus the extent (as a decimal fraction) of contaminant removal. It can be seen that contaminant destruction is somewhat more efficient in the later stages of the ozone/UV experiment. Competition kinetic analysis using equation 4-3 indicates that one reason for the difference is that peroxide may be scavenging 1 to 8 percent of the OH radicals that are produced, depending on the true value of $k_{OH,DNT}$.

Another potential reason for the higher efficiency of ozone/UV is that UV photolysis of DNT was contributing to DNT removal. Figure 4-3 shows the DNT disappearance curve during UV photolysis (Experiment A01) using the same lamp arrangement as was used in the previously discussed ozone/UV experiment. The initial photolysis rate is approximately 0.3 mg/L/min, so photolysis during the ozone/UV experiment may account for the destruction of perhaps 6 to 12 mg/L of DNT over 45 minutes of treatment. Photolysis rate decreases with concentration, and therefore slows as treatment progresses.

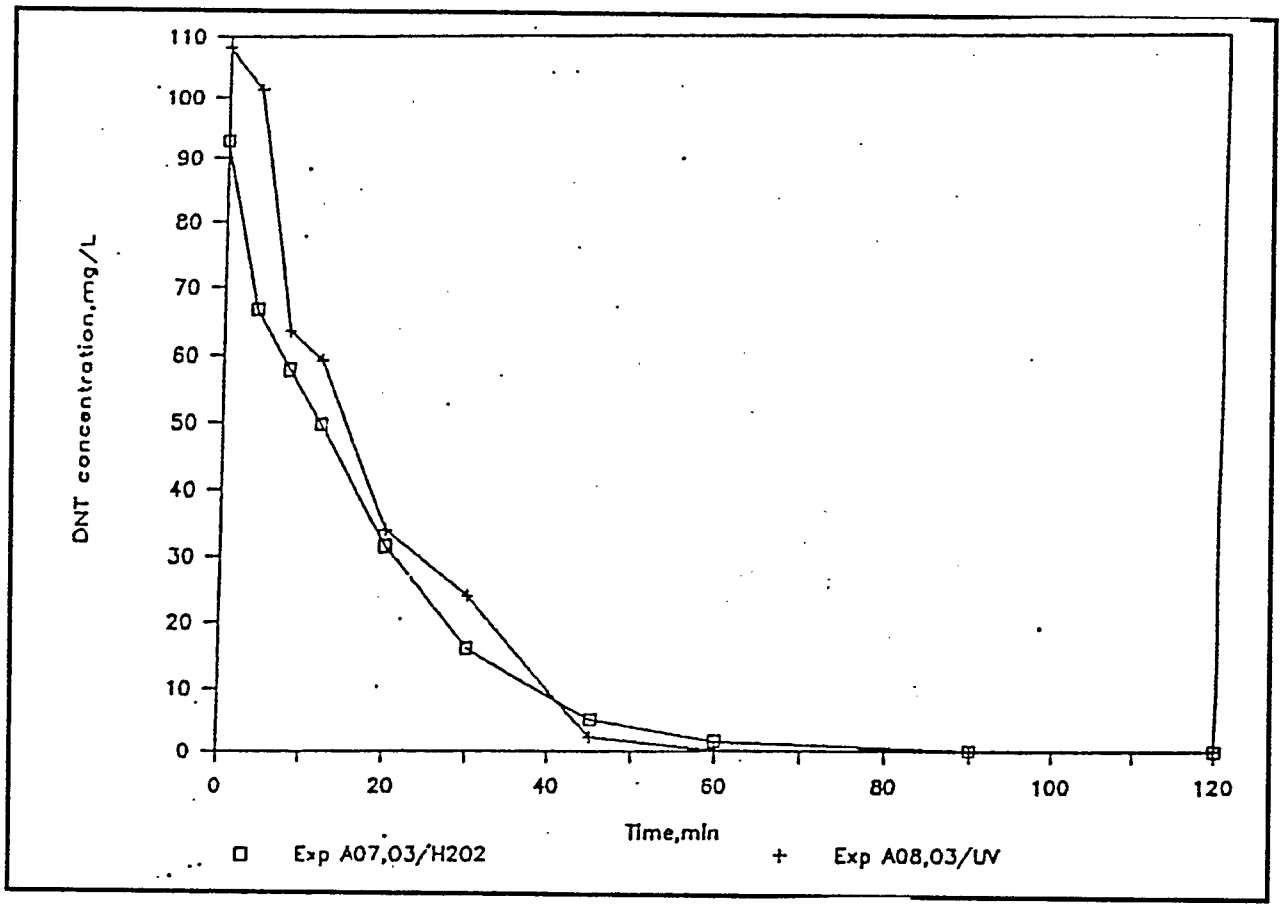

Figure 4-1. DNT removal by O_3/H_2O_2 treatment (no ethanol present).

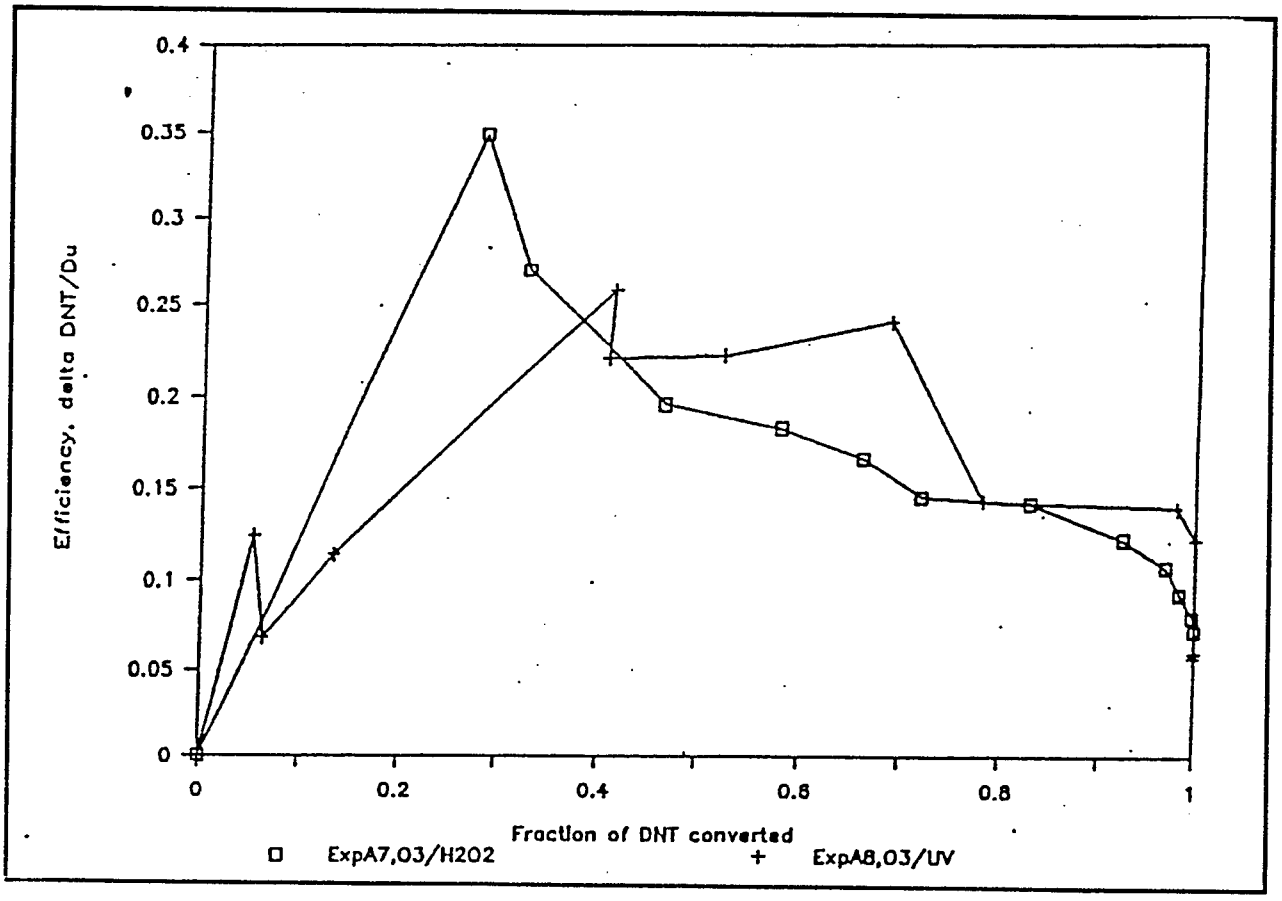

Figure 4-2. Efficiency of DNT removal by O_3/UV and O_3/H_2O_2 (no ethanol present).

The actual wastewater contains high concentrations of ethanol and diethyl ether, which would be expected to act as radical scavengers and reduce the efficiency of DNT removal by OH radical. However, the results reported by Heffinger and Jake (1991) did not show a significant detrimental effect on the DNT removal rate when ethanol and ether were present. This type of radical scavenging effect is usually well predicted by the preliminary model discussed in a previous section, so experiments were designed to investigate this phenomenon. A sampling of wastewater analytical data from RAAP was used to generate an approximate concentration range of interest for the present study. The mean concentrations and their standard deviations were given in Table 4-1.

Experiments were performed (using the reactor in Figure 3-1) to compare the efficiencies in the presence of a ten-fold (molar) excess of ethanol to those in purified water, for both ozone/UV and ozone/H_2O_2. Figure 4-4 shows the DNT disappearance curves for ozone/UV and ozone/H_2O_2 treatment (Experiments A09 and A06) of DNT in the presence of ethanol. Although 6 percent more DNT was removed by ozone/H_2O_2 in the first 100 minutes, that process also consumed 25 percent more ozone, and was therefore less efficient (Figure 4-5). Comparison of Figures 4-2 and 4-5 shows that, at 80 percent DNT removal, the efficiency (eq 4-5) of DNT removal was 3.5 to 4.5 times lower for O_3/UV and O_3/ H_2O_2 treatment, respectively, in the pressure of excess ethanol, than in its absence. The considerable efficiency drop in the presence of ethanol was not in agreement with the results of Heffinger and Jake (1991), and would have a significant impact on the treatment cost. The observed efficiency drop implied a DNT rate constant of two to four times that of ethanol, which is quite inconsistent with either the estimated value or the value calculated from earlier experiments. It was concluded that some unexpected effect was operative in this reaction system and therefore that the previously-determined rate constant was incorrect. Since the effect appeared in both ozone/UV and ozone/H_2O_2 experiments, UV light is not necessary to cause the effect. A set of experiments was designed to investigate that effect.

Effect of High-Power UV Lamp on DNT Removal

Three experiments were performed in which a 1-kw lamp was used. This lamp differs from the usual 13-watt 254 nm 30 percent-efficient "germicidal" lamps that were used in most of the experiments, in that the higher-power lamp is 20 percent efficient, but emits 25 percent of its radiation between 200 and 250 nm. The use of higher UV power should speed up the photochemical reactions, but have little effect on the efficiency of the hydroxyl radical processes.

Figure 4-6 shows the results of UV photolysis of DNT in the absence (Exp A18) and presence (A17) of ethanol, using the higher-powered lamp. As discussed earlier, it was found that the presence of 17.8 mM (819 mg/L) ethanol had little effect on the DNT disappearance rate during this photolysis, indicating that the enhancement phenomenon apparently required ozone or OH radical. Also shown for comparison is the DNT disappearance curve for photolysis by the lower energy 254nm lamps (Experiment A01).

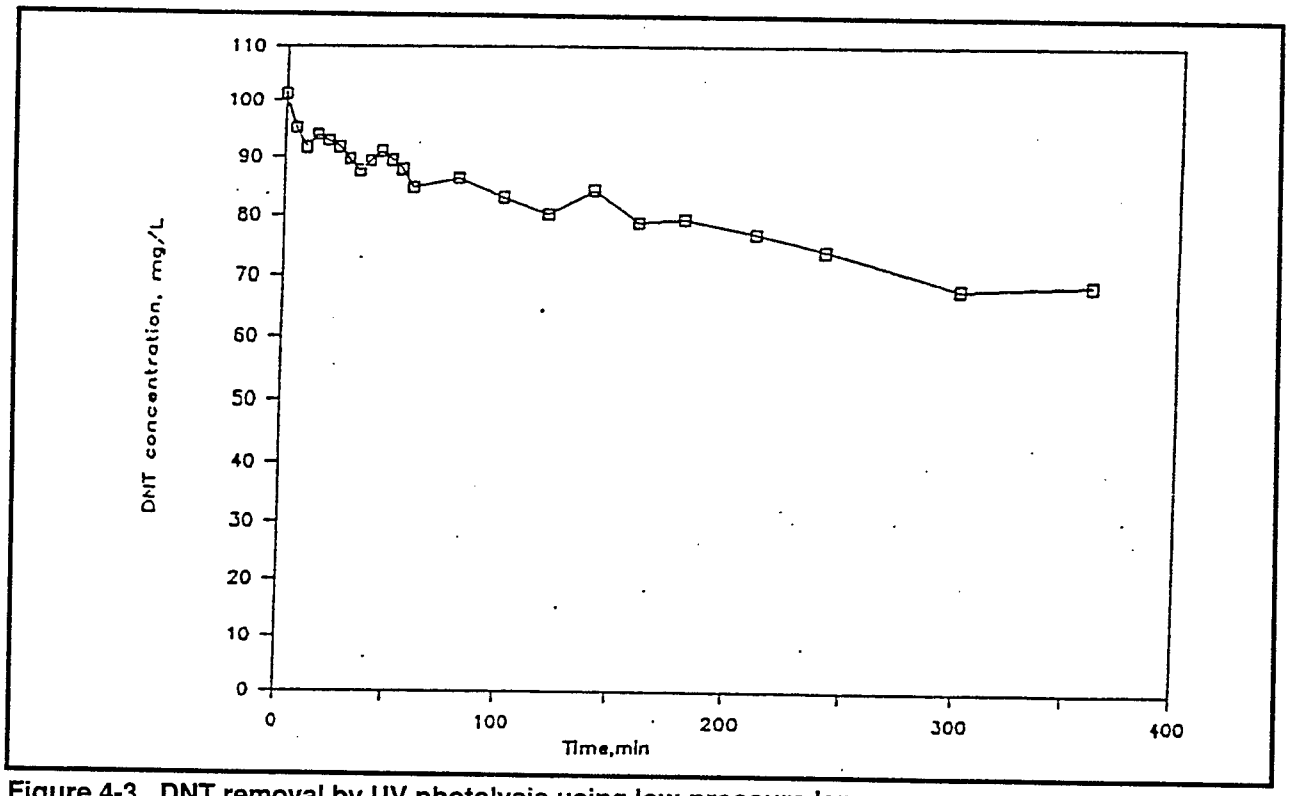

Figure 4-3. DNT removal by UV photolysis using low-pressure lamps.

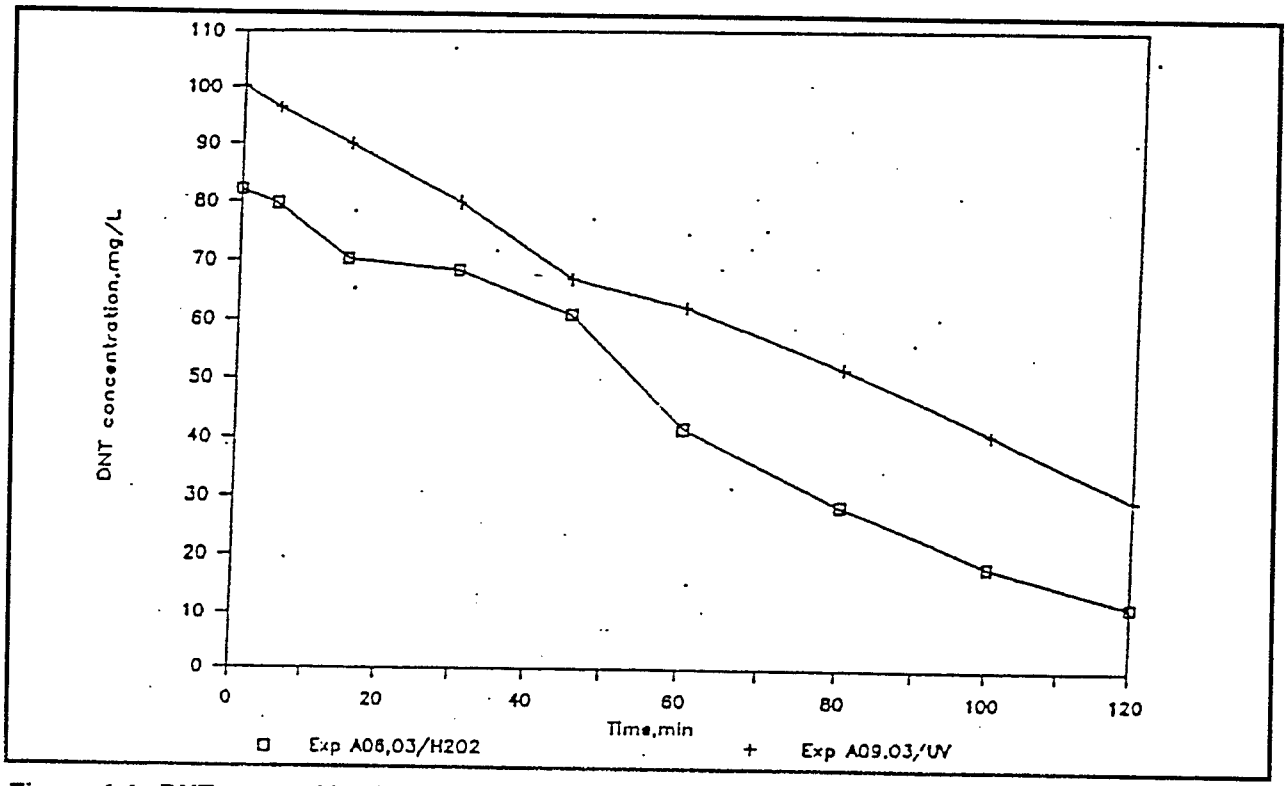

Figure 4-4. DNT removal by O_3/UV and O_3/H_2O_2 treatment in the presence of ethanol.

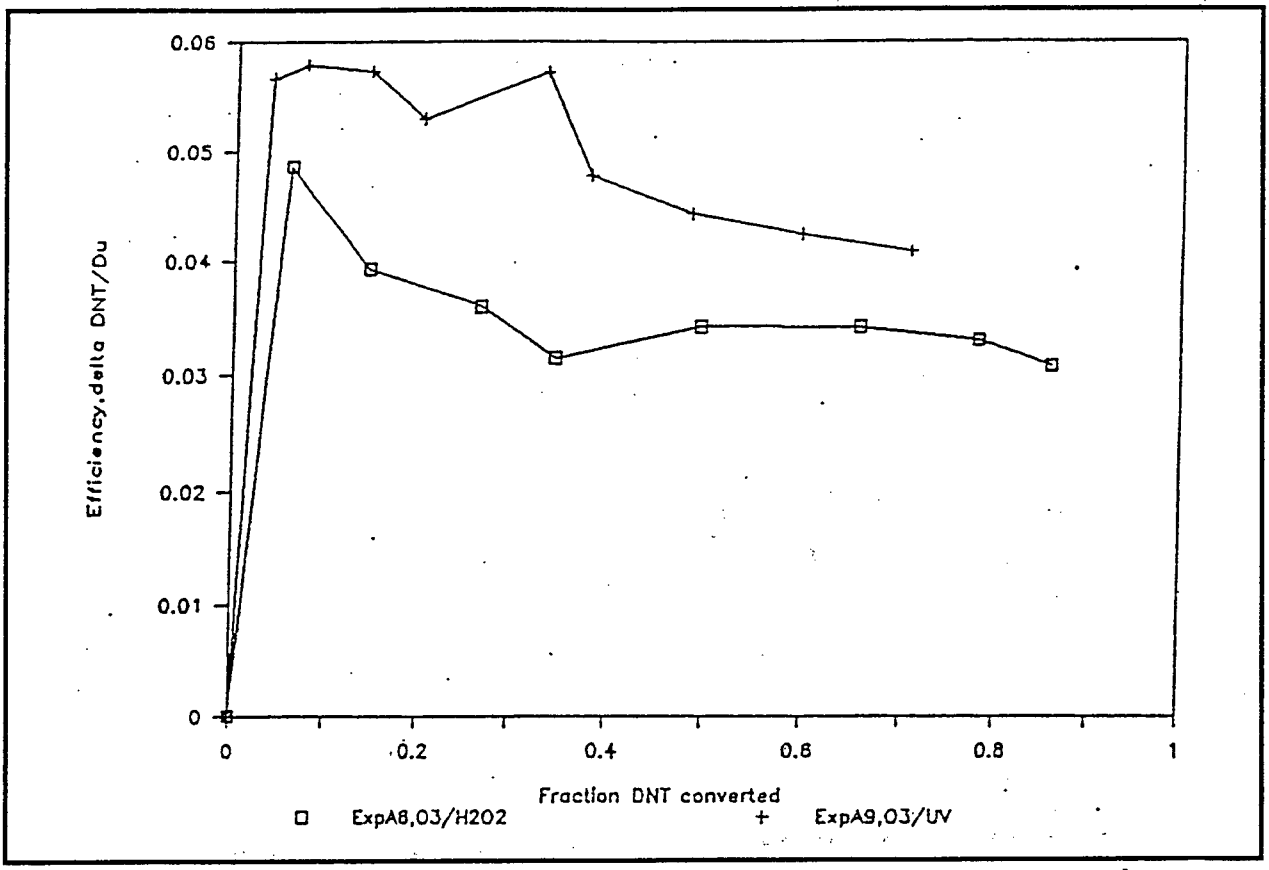

Figure 4-5. Efficiency of DNT removal by O_3/UV and O_3/H_2O_2 treatment in the presence of ethanol.

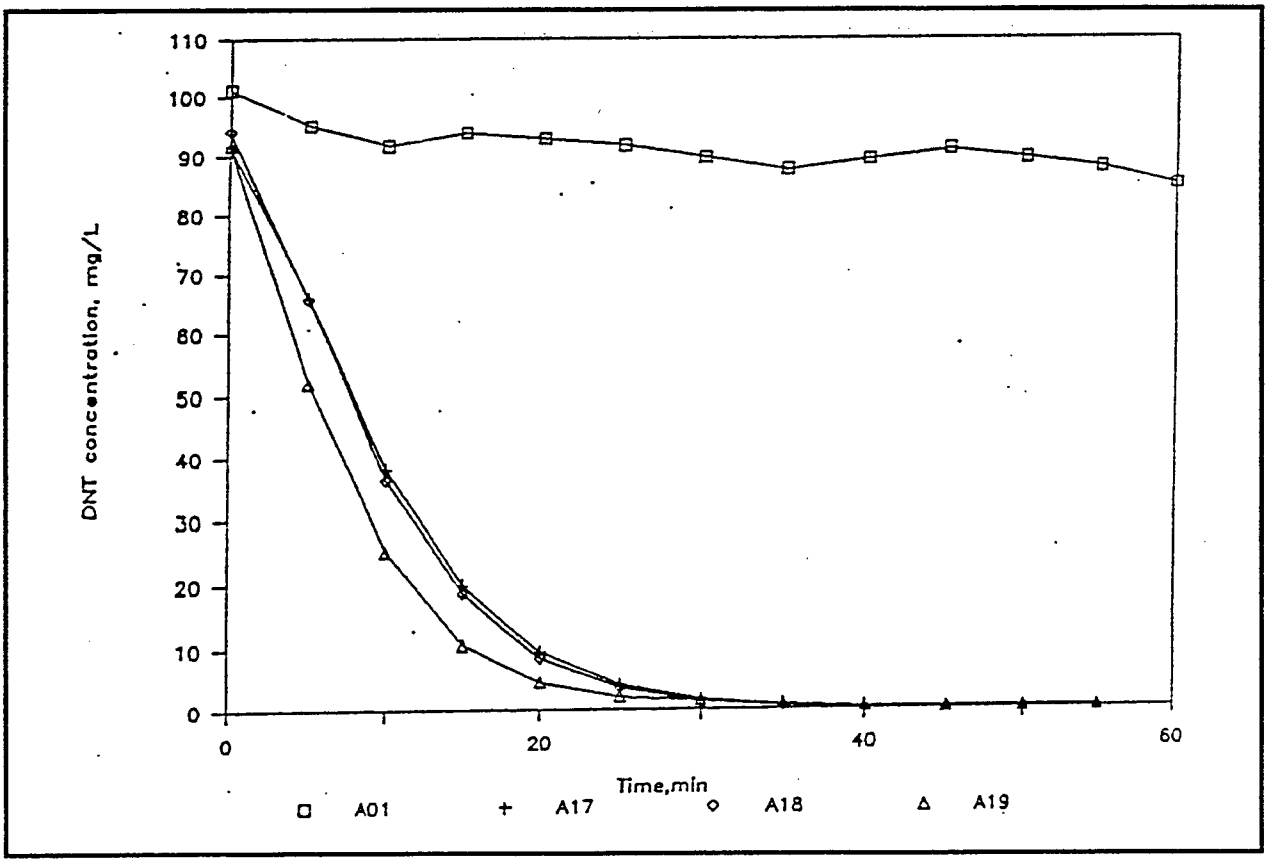

Figure 4-6. DNT removal by UV photolysis and O_3/UV treatment using a high-power lamp: exp A01-photolysis with 13-Watt lamps (presented for comparison); exp A17-photolysis, ethanol 17.8 mM; exp A18-photolysis; exp A19-O_3/UV, ethanol 13.3 mM.

The twenty-fold increase in photon dose (moles photons/L-sec) provided by the 1-kw lamp produces a similar increase in DNT removal rate, and in both cases absorbance measurements indicate 99+ percent photon absorption, so that an insignificant fraction of the photons are lost to the reactor wall. Also shown for comparison is the DNT disappearance curve for an O_3/UV experiment (A19) carried out using the higher-powered lamp in the presence of 13.3 mM (612 mg/L) of ethanol. The ozone efficiency at high extent of conversion for this experiment was seen in Figure 4-6 to be comparable to that of the experiments carried out with the low pressure (254nm) lamps, even though the apparent efficiency at intermediate conversion was more than seven times higher than the corresponding low-pressure lamp experiment.

Oxidation Byproducts

The knowledge of byproducts formed in the treatment process is important, in general, since they may be more resistant to treatment and more toxic than original target compounds. For AOPs, in particular, the nature of oxidation byproducts is related to treatment efficiency not only from the standpoint of their ability to be treated, but also in terms of the ability to promote the oxidation cycle. In this respect, identification of as many compounds as possible is of great interest. On the other hand, for many of the byproducts routinely tracked during the analysis of treatment samples, identification may not be as important since they disappeared in the course of treatment. Since the goal of this project has been to evaluate the whole complex of factors affecting AOP efficiency, basic trends in byproduct accumulation and destruction were noted for a variety of treatment conditions and, therefore, because of time constraints, byproduct identification was limited to major persistent components.

Organic Byproducts

Regardless of the composition of DNT solutions or AOP applied, the same two major groups of byproducts were found in the HPLC chromatogram obtained using the C_{18} column. As it can be seen from Figure 4-7 (a & b), one group was a cluster of several polar products around the solvent front. The other group consisted of a few peaks with retention times between 10 and 15 minutes (DNT eluted last at 23 to 25 minutes). One of the largest peaks in the first group was identified by its retention time on the mixed-mode column and UV spectrum as 2,4-dinitrobenzoic acid (DNBA). Major components in the second group were 2,4-dinitrobenzaldehyde (DNBAL) and m-dinitrobenzene (DNB) tentatively identified by retention times. These assignments are consistent with the findings of Ho (1986).

UV photolysis of DNT solutions, in general, resulted in a significant number of early eluting products, and this number was greater when the high-power UV lamp was used. In both cases, these products as well as DNB were seen to be resistant to UV treatment. Dinitrobenzaldehyde was practically eliminated at the end of treatment with the high-power lamp.

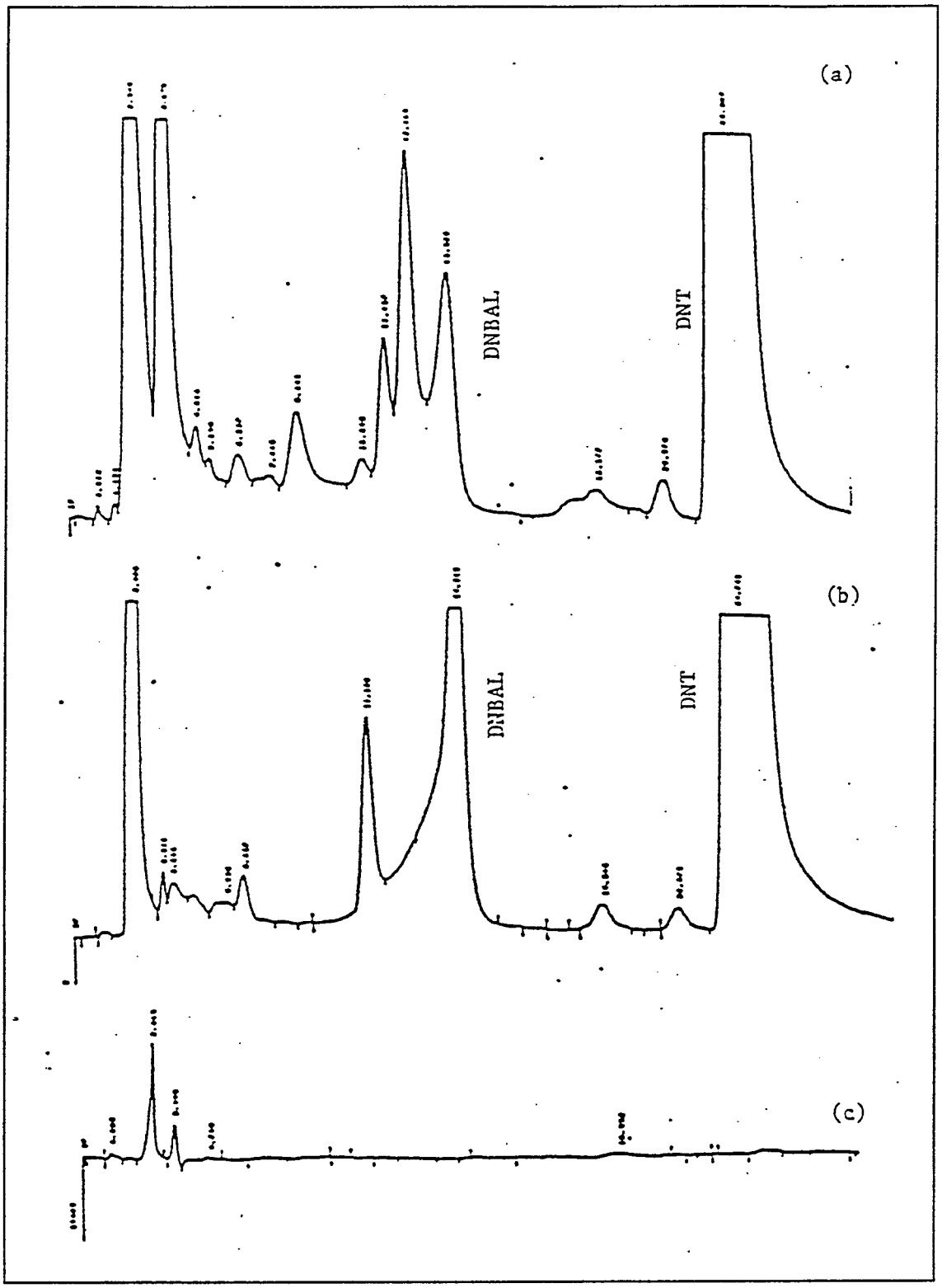

Figure 4-7. DNT byproduct distribution on C18 column: (a) after 360 min of photolysis; (b) after 20 min of O_3/UV treatment; (c) after 120 min of O_3/UV treatment; DNBA elutes as an unretained peak at ~2 mn on this column.

When DNT was photolyzed with the high-power lamp in the presence of ethanol, the byproduct distribution was found to be similar to that in the absence of ethanol, but ethanol slowed byproduct formation and disappearance, apparently due to ethanol competition with DNT for photons or transient radicals.

In the O_3/UV treatment of DNT solutions the overall number of byproducts was reduced in comparison to the photolysis alone, particularly for early eluting compounds, although the major peaks appeared to be the same (Figure 4-7b). Only a small amount of DNBA was left after 2 hours of treatment. When DNT was treated with O_3/H_2O_2, the byproducts distribution at early stages of the experiment was surprisingly much more similar to that for photolysis alone than in O_3/UV system. However, in the end of the 90-minute experiment, all the byproducts with the exception of DNBA were eliminated as in O_3/UV treatment.

Similar to the effect seen during photolysis, the addition of ethanol (4 to 5 mM) slowed down the transformation of byproducts for both O_3/UV and O_3/H_2O_2, and practically none of the tracked byproducts were eliminated in the 2-hour experiment. In this experiment, however, ethanol apparently competes with DNT (and, possibly, byproducts) primarily for OH radicals. In the prolonged O_3/UV treatment at the same ethanol concentration, all the byproducts were destroyed, with only traces of DNBA found after 330 minutes of treatment. The same competition effect was observed when DNT was treated with O_3/UV in the presence of diethyl ether. No difference in the suite of byproducts was found in comparison with that found when ethanol was present.

The dependence of the extent of byproduct removal on ethanol concentration was also investigated (experiments A14-A16). The increase in the ethanol-to-DNT ratio from ~9 to ~80 had little effect on byproduct accumulation and destruction in the early or middle part of treatment (i.e., for $\xi \leq 0.5$); however, the difference in the extent of byproduct removal toward the end of the experiment (330 minutes) was drastic, as can be seen from Figure 4-8. The observed effect can be explained on the basis of the competition between ethanol, acetaldehyde, and ether (if present) with byproducts, similar to that discussed early in this report with respect to DNT removal.

The concentration of ethanol oxidation byproducts such as acetaldehyde and acetic acid were routinely measured in the course of treatment. Although acetic acid has a much lower rate constant for reaction with OH radical (1.6×10^7 $M^{-1}s^{-1}$) than does ethanol (1.9×10^9), that of acetalaldehyde (2.4×10^9) is comparable. The amount of acetalaldehyde in the solution was thus high enough to participate in competition in many uses.

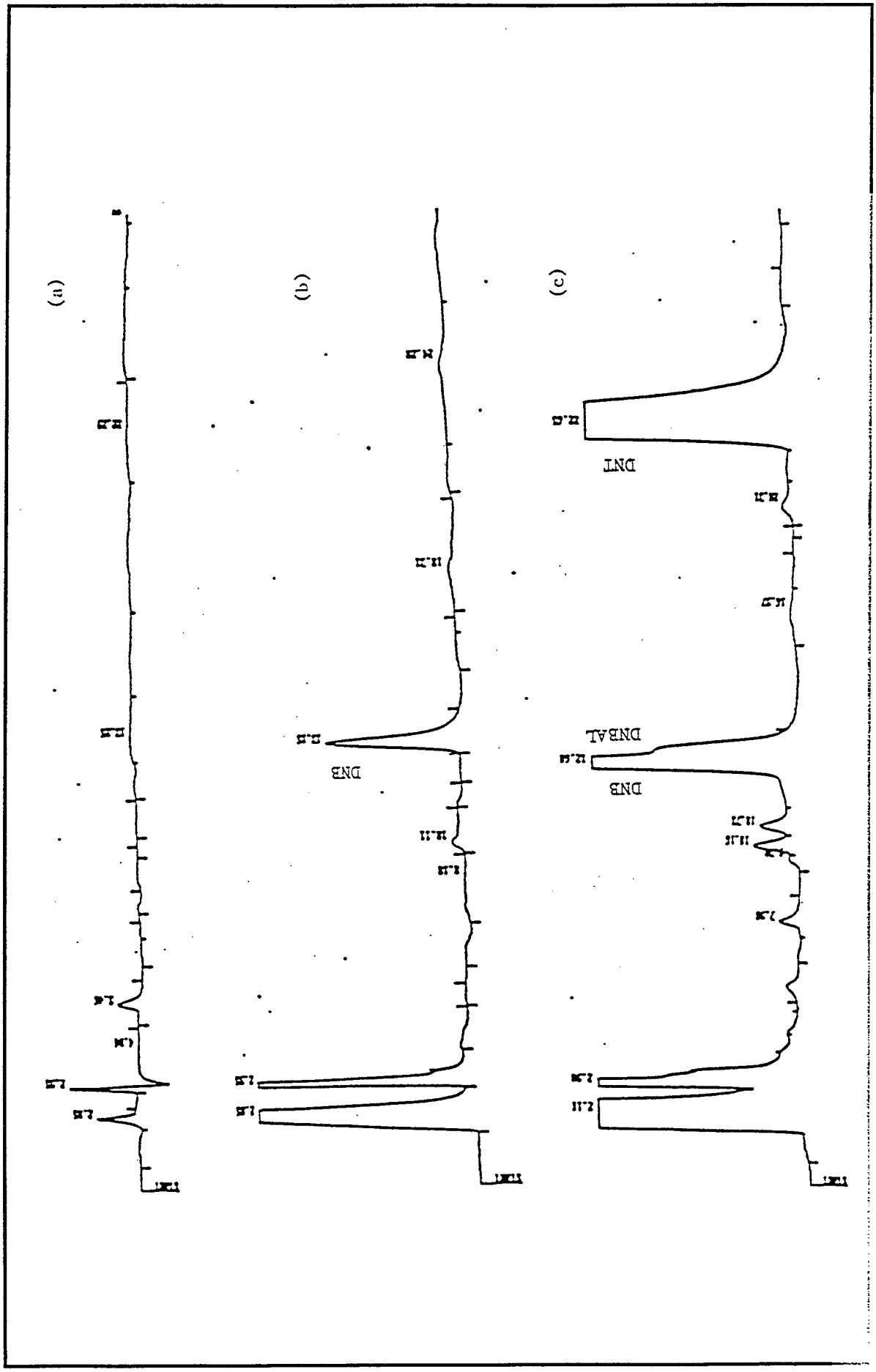

Figure 4-8. DNT byproduct distribution on C_{18} column after 330 min of O_3/UV treatment at various ethanol concentrations (mM): (a) 4.5; (b) 16.3; (c) 69.5; DNBA elutes as an unretained peak at ~2 min on this column.

Nitrite and Nitrate

Nitrite and nitrate accumulation was also monitored during treatability experiments as a measure of nitrogen mineralization. The data on nitrogen mass balance are presented in Table 4-4. Nitrogen mineralization was found to be insignificant (~1 percent in a 360-minute experiment) when DNT was photolyzed using low pressure lamps, despite the destruction of ~3.0 percent of DNT, but nitrogen mineralization was more effective (~13 percent in a 60-minute experiment) when a high-power UV lamp was used. However, the extent of nitrogen mineralization in the latter experiment was also low in comparison with the extent of DNT removal (99.9 percent). These results imply that during photolysis, the major part of DNT was converted to other nitroaromatic compounds that presumably remain in solution.

It can be seen from experiments A08, A14, A17, and A19 that, in the absence of ethanol, nitrogen mineralization proceeds very effectively in both O_3/H_2O_2 and O_3/UV treatment. The addition of ethanol leads to a noticeable decrease in the amount of nitrogen released as nitrite and nitrate. Dependence of the extent of nitrogen mineralization on ethanol concentration (experiments A9-A11, A14, A15) shows the same trend as DNT and byproducts removal discussed earlier.

Dependence of DNT Removal on Ethanol Concentration

A set of experiments was performed in which 0.5 to 0.9 mM DNT (90 to 164 mg/L) was treated with ozone/UV in the presence of various concentrations of ethanol covering the range of 4.8 to 442 mM (221 to 20,300 mg/L). The DNT disappearance curves for these experiments are shown in Figures 4-9 through 4-14. Observed removal efficiencies are compared in Figure 4-15 to those calculated from equation 4-4. The observed efficiencies are more than an order of magnitude higher than those predicted for simple removal of DNT by hydroxyl radical at *high* ethanol concentrations, using the DNT/OH rate constant calculated in an earlier section, and a factor of 2 too low at *low* ethanol concentrations, confirming the inability of the simple OH-scavenging model to predict performance of this system. It is clear from these results that some process other than simple competition for OH radical is taking place, i.e., DNT removal is enhanced by attack on DNT by some species other than OH radical. Therefore, equation 4-4 and the method used to calculate the rate constant are inappropriate, and equations based on a more suitable model must be used.

Table 4-4. Nitrogen mass balance.

Experiment	AOP	Ethanol concentration mmol/L	Initial nitrogen concentration (in DNT) mmole/L	Final nitrogen concentration (as NO_2^- + NO_3^-) mmole/L	% Nitrogen mineralization	Experiment length, min
A1	UV	--	1.12	0.013	~1	400
A6	O_3/H_2O_2	4.05	0.902	0.52[a]	58	120
A7	O_3/H_2O_2	--	1.03	0.75	75	90
A8	O_3/UV	--	1.19	1.13[b]	96.7	120
A9	O_3/UV	4.8	1.1	0.42	38	120
A10	O_3/UV	442.0	1.13	0.027	2.4	120
A11	O_3/UV	74.4	1.796	1.14	7.7	120
A12	O_3/UV	4.2[c]	1.45	0.69	48	120
A14	O_3/UV	16.3	1.09	1.16	100	360
A15	O_3/UV	69.5	1.68	1.98	100	615
A17	UV[f]	17.8	1.01	0.034	3.4	60
A18	O_3/UV[f]	--	1.03	0.14	13.0	60
A19	O_3/UV[f]	13.3	1.01	0.38	38.	60

[a] Last sample for NO_2/NO_3 analysis was taken at 100 min.
[b] The same value was at 100 min. May be within experimental error.
[c] Diethyl ether
[d] 25.3% at 120 min.
[e] 16.3% at 120 min.
[f] High-power lamp

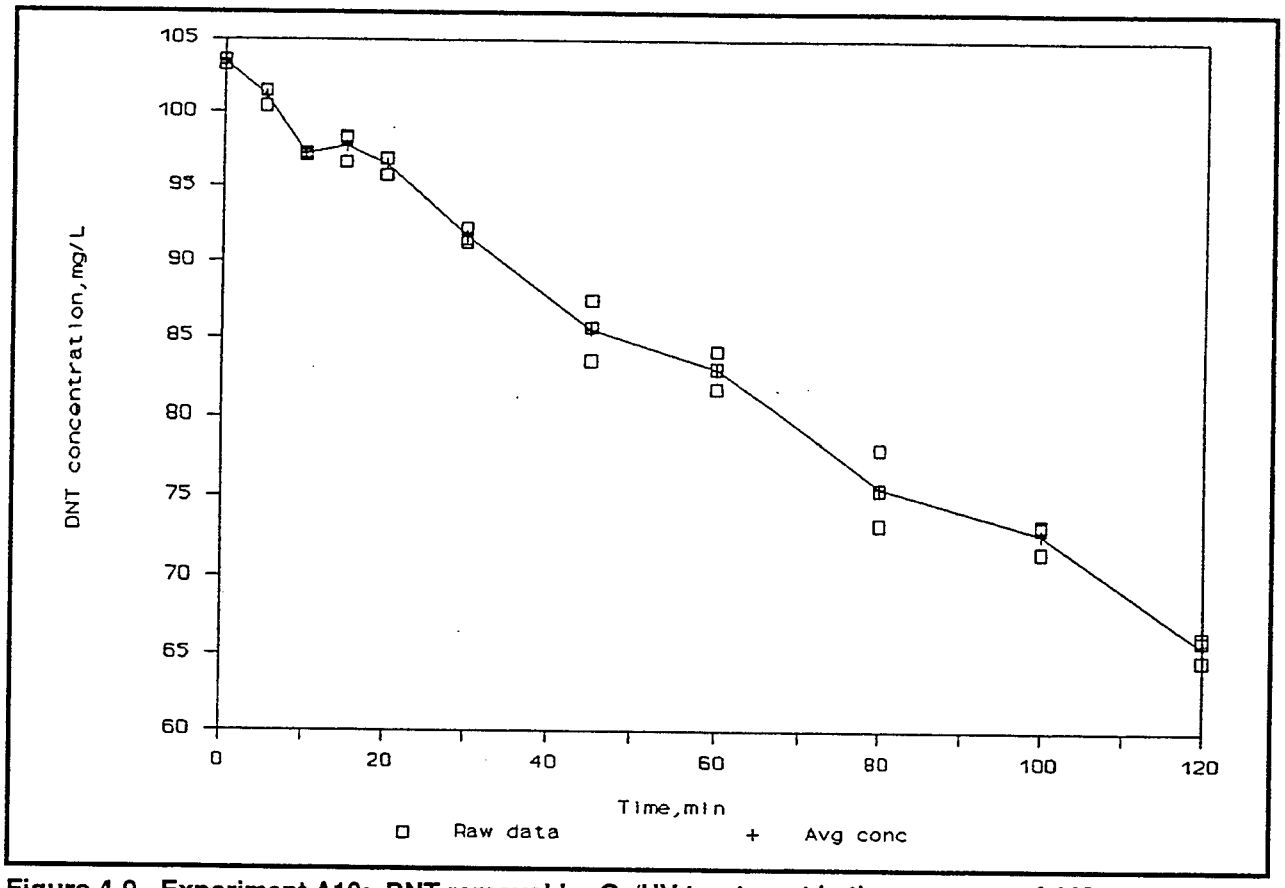

Figure 4-9. Experiment A10: DNT removal by O_3/UV treatment in the presence of 442 mM of ethanol.

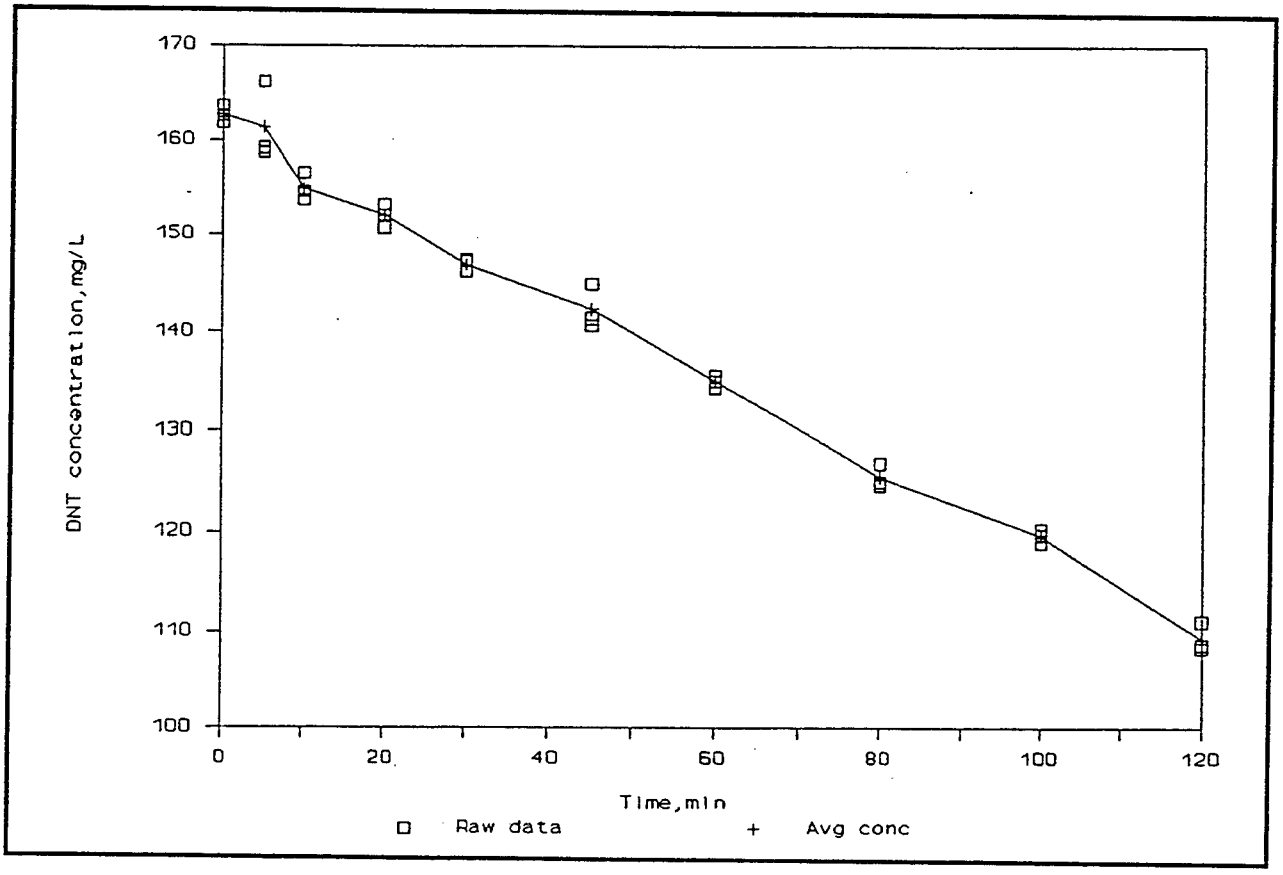

Figure 4-10. Experiment A11: DNT removal by O_3/UV treatment in the presence of 74.4 mM of ethanol and 6.1 mM of ether.

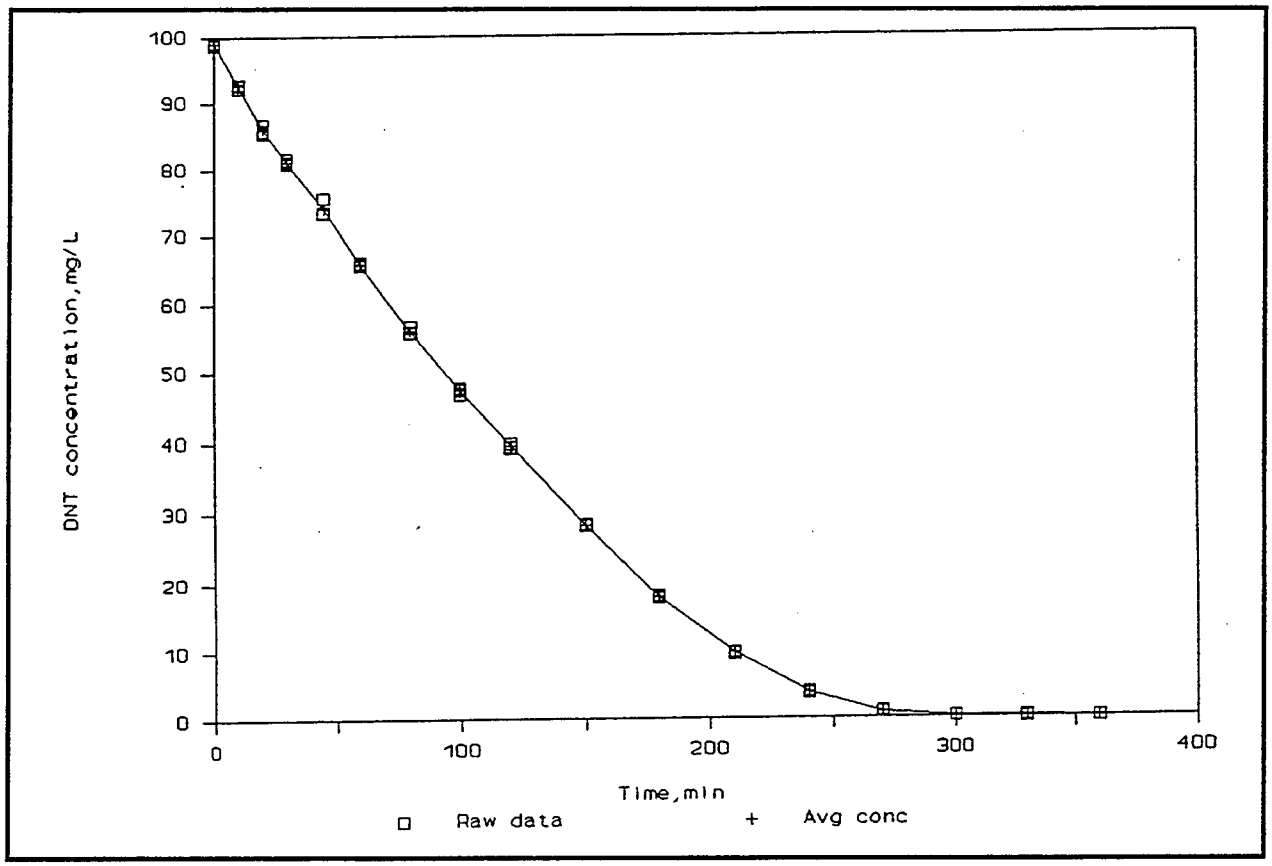

Figure 4-11. Experiment A14: DNT removal by O_3/UV treatment in the presence of 16.3 mM of ethanol.

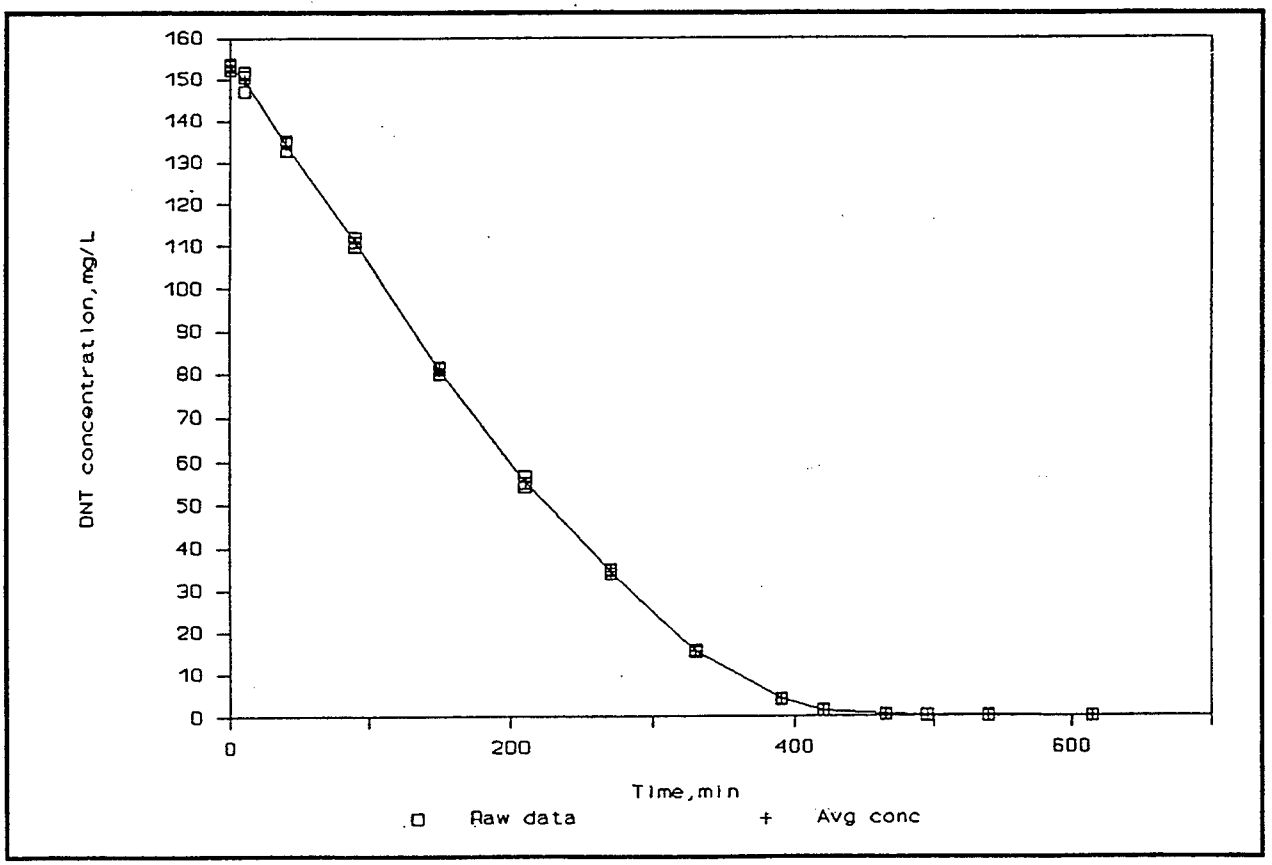

Figure 4-12. Experiment A15: DNT removal by O_3/UV treatment in the presence of 69.5 mM of ethanol and 4.5 mM of ether.

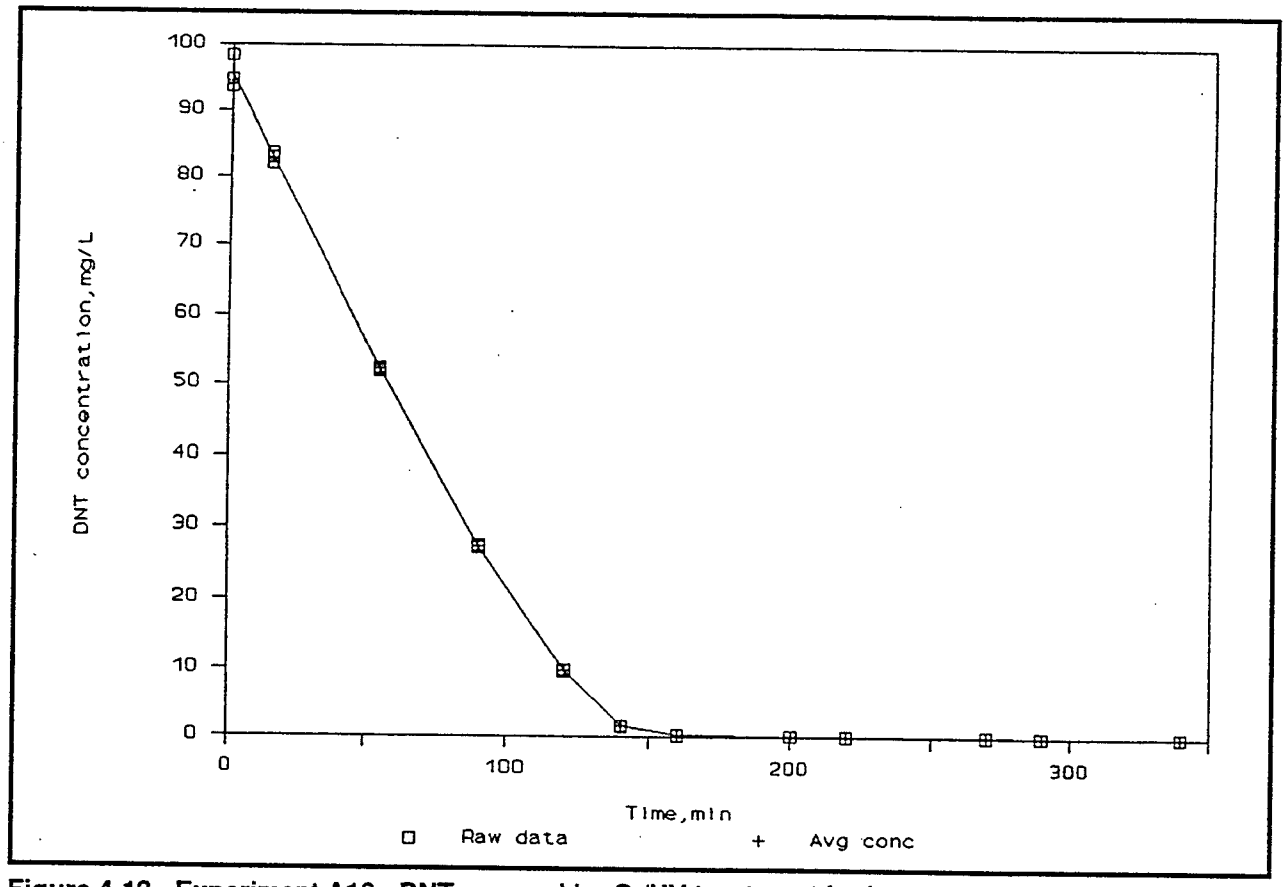

Figure 4-13. Experiment A16: DNT removal by O_3/UV treatment in the presence of 4.5 mM of ethanol.

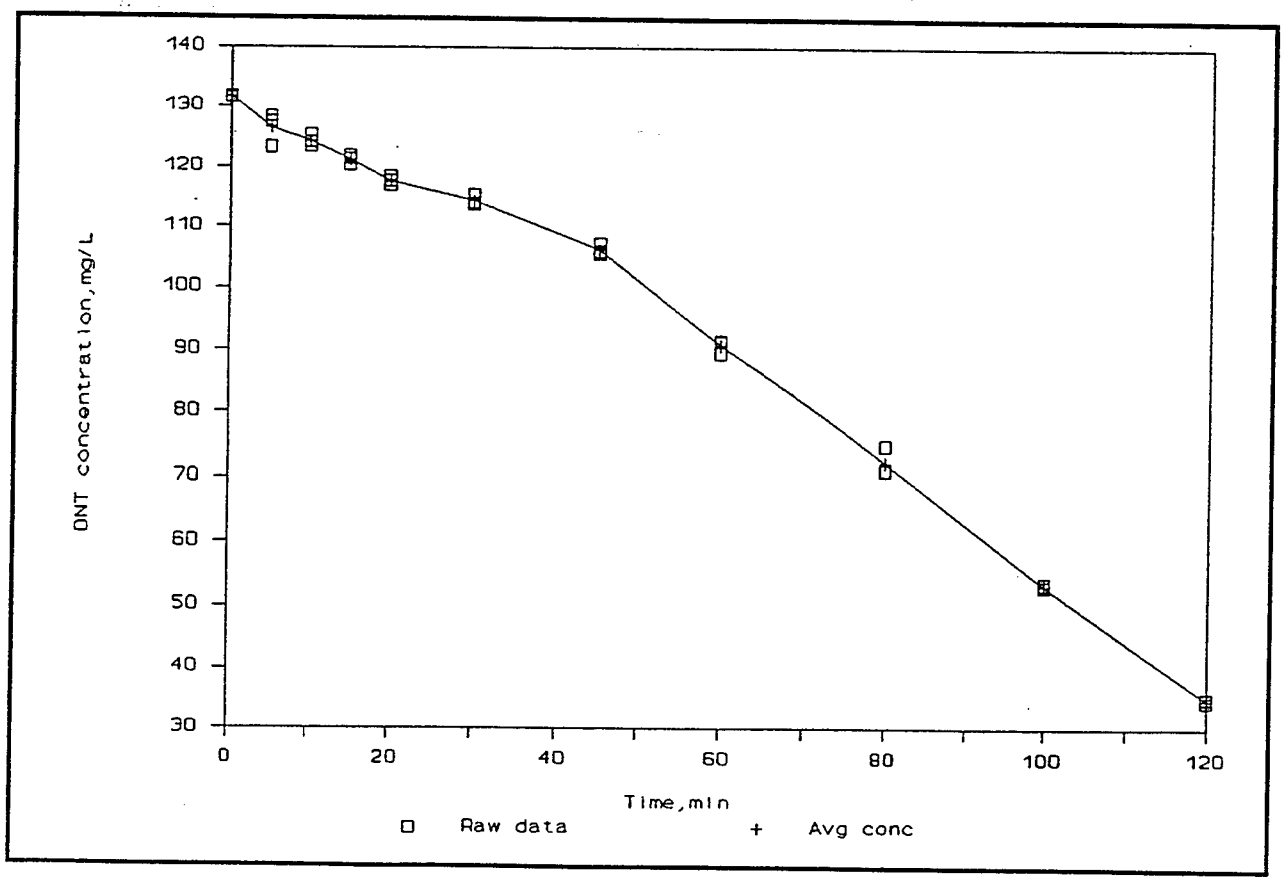

Figure 4-14. Experiment A12: DNT removal by O_3/UV treatment in the presence of 4.2 mM of DEE.

The apparent lack of direct correlation of efficiency with ethanol concentration can be seen in Figure 4-16, which shows the efficiency of DNT removal as a function of extent of conversion (ξ) of DNT for the experiments in this set. Although some irregularity is seen in the early part of the efficiency curves due to lower precision at low degrees of conversion, the relative flatness of these plots out to 90 percent conversion is striking. This figure emphasizes the fact that the efficiency ranged by a factor of 7.25 (from 0.008 to 0.058) for an ethanol concentration range of a factor of 100 (from 4.0 to 442 mM).

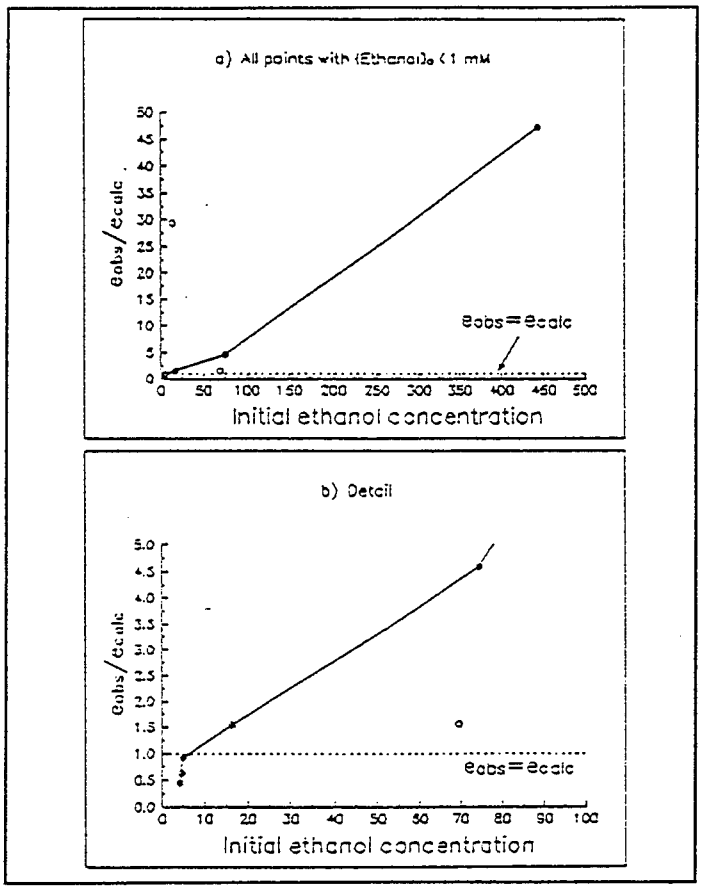

Figure 4-15. Comparison of observed and calculated DNT destruction efficiencies, as a function of initial ethanol concentration (mM).

Likely processes for enhancement of DNT destruction include photochemical and nonphotochemical processes involving transient species produced from ethanol. In the absence of hydrogen peroxide, photolysis of DNT in the absence and presence of ethanol resulted in the same DNT disappearance rate, indicating that a strictly photochemical process involving DNT and/or ethanol and its photo-oxidation products was not responsible for the observed behavior. Thus, it appears that ozone or hydroxyl radical must be present for the enhancement reaction to occur. The oxidation products of ethanol (acetaldehyde and acetic acid) were found to be present in the photolysis mixture (from use of the high-powered lamp), indicating that the more powerful UV lamp used for these experiments was capable of initiating oxidation processes even without the addition of ozone or hydrogen peroxide. Whether these oxidation processes occur by similar pathways as the AOP reactions is not known, but the absence of enhanced removal seems to indicate that OH radicals are not involved in DNT removal during UV photolysis.

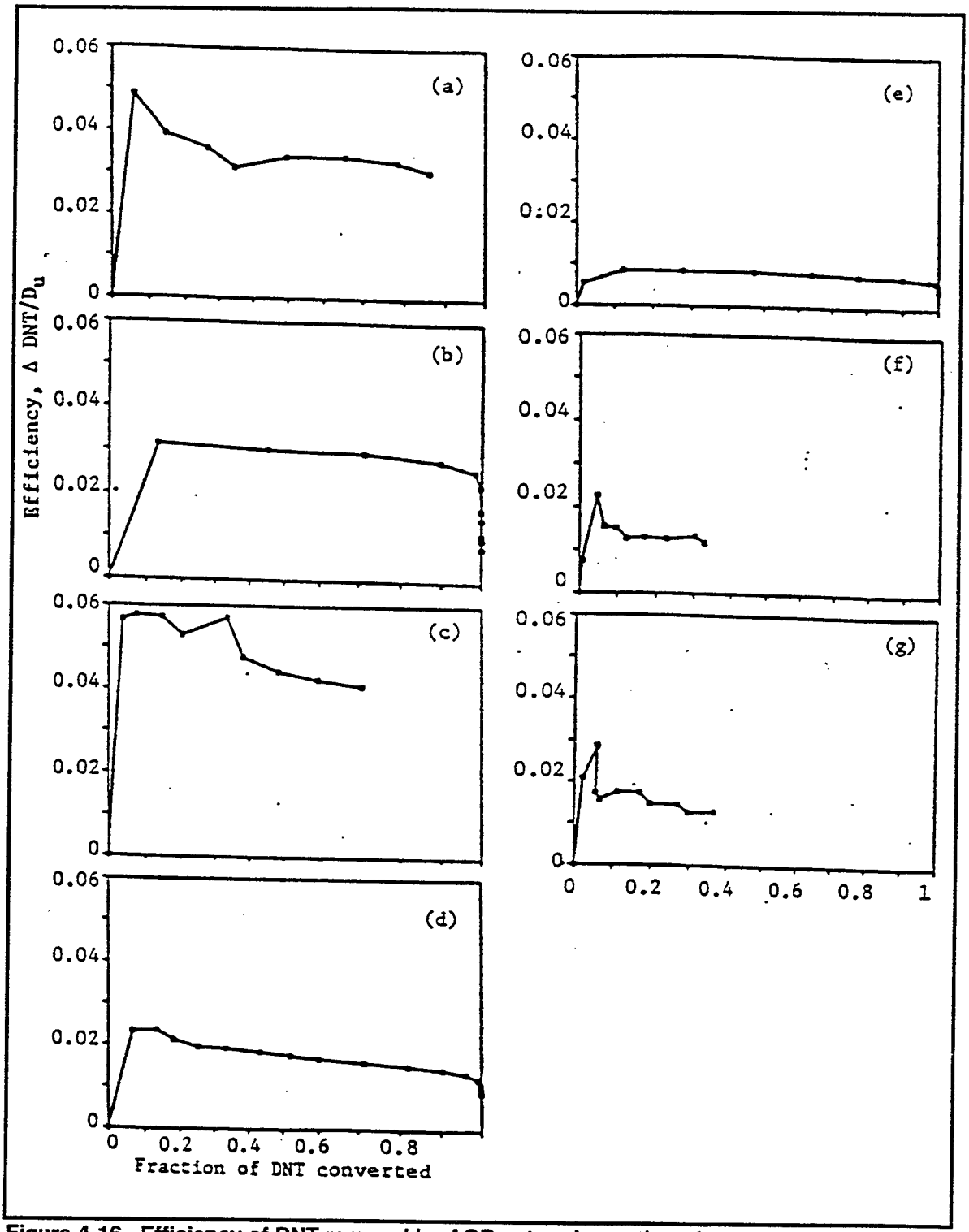

Figure 4-16. Efficiency of DNT removal by AOPs at various ethanol concentrations (mM): (a) 4.0; (b) 4.5; (c) 4.8; (d) 16.3; (e) 69.5; (f) 74.4; (g) 442; all experiments were O_3/UV except (a), which was O_3/H_2O_2.

Modeling of Ethanol Oxidation

Hydroxyl radical was thought to be at least partly responsible for DNT destruction, in competition with OH-radical attack on ethanol. In addition, the unknown active species was thought to originate from ethanol. Therefore, complete a priori modeling of the system would require modeling of the ethanol behavior. Although seemingly a simple system, a review of the pulse radiolysis work on ethanol and its reaction byproducts revealed complications. A few experiments were performed on ethanol oxidation, to provide good AOP data on which to test the principles obtained from radiolysis studies. Numerical modeling of the ethanol data was begun, considering only the degradation steps up to and including conversion to acetic acid. The difficulties encountered are described below, following a review of the known ethanol oxidation chemistry.

Hydroxyl Radical Chemistry of Ethanol

The reaction of hydroxyl radical with ethanol in the presence of oxygen has been studied by a number of investigators including Schultze and Schulte-Frohlinde (1975). Previous mechanistic conclusions were not found to be entirely satisfactory, and the system was investigated later in more detail by von Sonntag and co-workers (1983) at the Max Planck Institut für Strahlenchemie. In this study it was found that, after the initial steps that produced a peroxyl radical, it was necessary to hypothesize several parallel reaction pathways to explain the data. This manifold of reactions for the peroxyl radical is shown in Scheme I (Figure 4-17). The proposed scheme is considerably more complicated than the simple intuitive stepwise schemes that are often proposed to explain treatability data. An example of such a scheme for the present system would be

$$ethanol \xrightarrow{HO^{\bullet}} acetaldehyde \xrightarrow{HO^{\bullet}} acetic\ acid \qquad \textbf{(4-6)}$$

Numerical modeling using the system shown in Scheme I is used to attempt to determine if it is consistent with experimental data from this laboratory, but was complicated by data gaps and other factors such as product (e.g., acetaldehyde) reactions and direct (as opposed to free-radical) ozone reactions, described below. A summary of our observations from detailed kinetic modeling performed to date on the ethanol system follows.

Ethanol is attacked by hydroxyl radical primarily in the α-position (carbon attached to the O-atom of the -OH group). Abstraction of the hydrogen atom forms the α-hydroxyethyl radical (reaction 1, Scheme I [Figure 4-17]). This carbon-centered radical reacts with oxygen at nearly diffusion-controlled rates ($k=4.6 \times 10^9\ M^{-1}s^{-1}$), forming the α-hydroxyethylperoxyl radical (reaction 2). If during the AOP treatment of ethanol solutions, the pH stayed above approximately 5, the dominant fate of the ethanol peroxyl radical would be reaction 4 in Scheme I, producing acetaldehyde and superoxide.

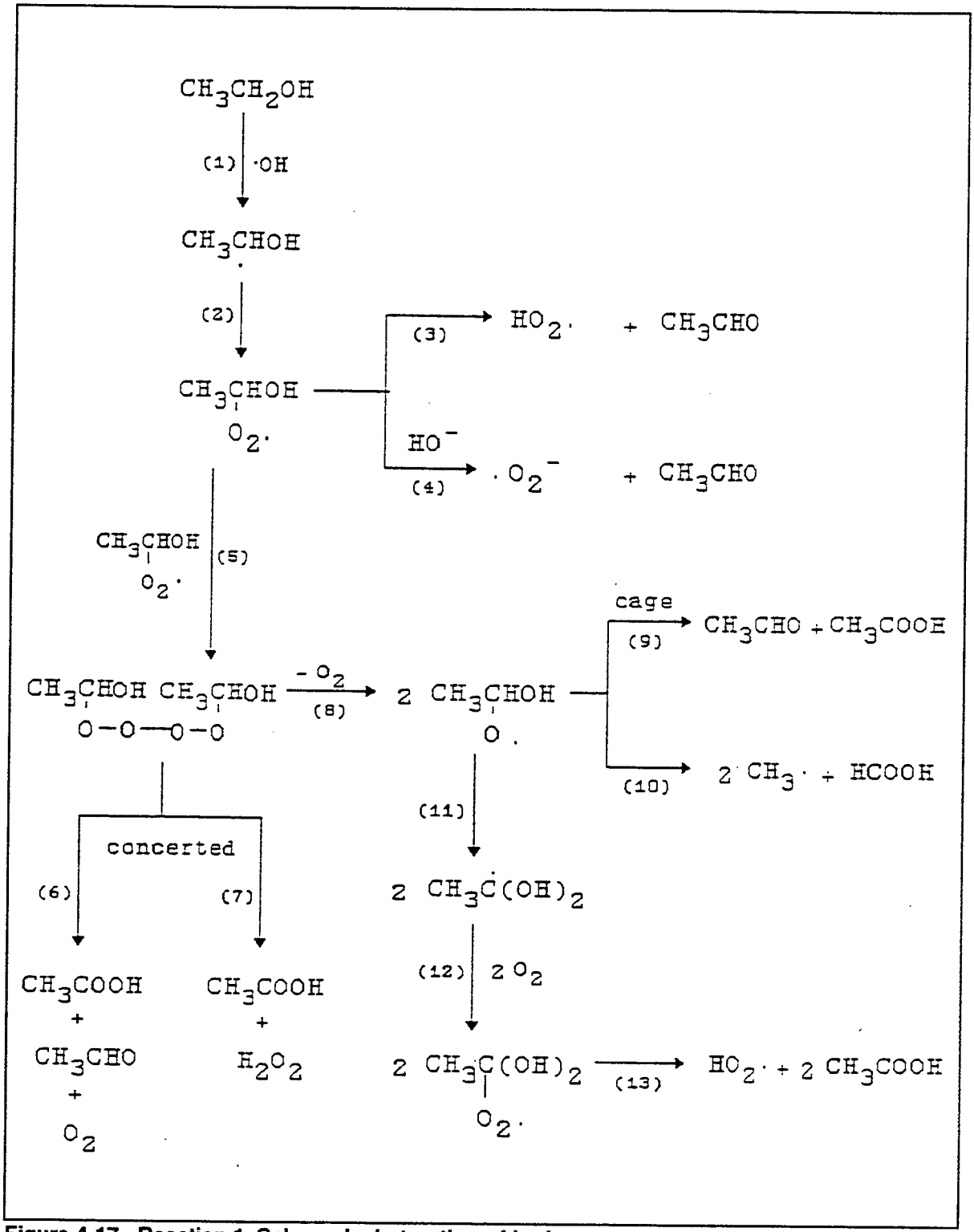

Figure 4-17. Reaction 1, Scheme I, abstraction of hydrogen atom.

Oxidation of the organic would advance by one step (ethanol to acetaldehyde) while in ozonation-based treatment systems, superoxide would react with ozone to produce more hydroxyl. However, some occurrence of the bimolecular pathway (reaction 5, Scheme I), in addition to further oxidation of acetaldehyde to acetic acid, leads quickly to the accumulation of acetic acid, which lowers the pH to the point that the base-catalyzed reaction 4 is suppressed, allowing greater flux through the bimolecular pathway. Since most of these channels (reactions 6, 7, 9, and 13) bypass acetaldehyde and go directly to acetic acid, the pH drops even faster than if the reaction were purely stepwise. Simultaneously, the pH decrease also suppresses the promotion reactions that convert ozone to hydroxyl radical, allowing ozone to build up in solution to the point that direct reaction of ozone with ethanol could dominate the fate of ozone (and ethanol), if the literature value (Hoigné and H. Bader 1983) of the ozone/ethanol rate constant of 0.37 $M^{-1}s^{-1}$ is correct. The possibility of direct reaction of ethanol with ozone introduces an additional problem into the modeling, since the products of that direct reaction are not known. In addition, preliminary computer simulations based on the experimental conditions of Hoigné and Bader (1983) have indicated that under the conditions used, hydroxyl radical reactions would not have been suppressed as the authors claimed, but would have still been occurring, contributing to the destruction rate of ethanol. Therefore, the value of the rate constant reported by Hoigné and Bader (1983) is probably too high, as it includes some destruction of ethanol by hydroxyl radical as well.

Numerical modeling of the data gave preliminary evidence that even at the low pH values observed in these experiments, destruction of ethanol is due primarily to hydroxyl radical, and that the almost complete change to free-radical reactions can take place within the first few seconds of treatment. This switch can be initiated by direct reaction of ozone with even the smallest of impurities in the water, provided some free-radical product is produced by that reaction.

Hydroxyl Radical Chemistry of Acetaldehyde

The hydroxyl radical chemistry of acetaldehyde has also been studied by Schuchmann and von Sonntag (1988), who performed pulse radiolysis kinetic spectroscopy/conductance experiments on aqueous acetaldehyde solutions. The conclusions of those investigators are summarized below.

Acetaldehyde hydrolyzes in aqueous solution to give a geminal diol

$$CH_3CHO + H_2O \underset{k_r}{\overset{k_f}{\leftrightarrow}} CH_3CH(OH)_2 \qquad \textbf{(4-7)}$$

where k_f is 9.0×10^{-3} s^{-1} at 25 °C ($t_{1/2}$=77 sec) and the equilibrium constant K=1.246 at 30 °C, which results in an equilibrium ratio of carbonyl form to hydrate of about 0.8. Hydroxyl radicals attack the carbonyl form to produce acetyl radical with a rate constant of 3.6×10^9 (all rate constants are in $M^{-1}s^{-1}$ unless otherwise specified):

$$OH + CH_3CHO \rightarrow CH_3C(O)\cdot \qquad \textbf{(4-8)}$$

and attacks the hydrate with $k=1.2x10^9$ to form the diol radical (dihydroxyethane radical, or DHE):

$$OH + CH_3CH(OH)_2 \rightarrow CH_3C(OH)_2\cdot \quad \textbf{(4-9)}$$

However, the acetyl radical hydrolyzes very rapidly ($k=2x10^4$ s^{-1}, or $2x10^6$ times more rapidly than the parent compound acetaldehyde) to the diol radical. The dehydration of the diol DHE radical back to acetyl radical is also fast. The rate constant was measured to be approximately $3x10^4$ s^{-1}, so that the equilibrium mixture contains slightly more acetyl radical than diol radical. The rapid establishment of this equilibrium (half-life of tens of microseconds) means that, if one radical was drawn off by reaction while the other remained unreactive, the equilibrium would shift so that both species were consumed through that channel. The diol radical was found to be a reducing radical while the acetyl radical was neither oxidizing nor reducing to the usual substrates tried by the authors. Only 5 to 10 percent of the OH attacks the ß-position of acetaldehyde and its hydrate to produce the formylmethyl radical:

$$\cdot OH + CH_3CHO \rightarrow \cdot CH_2CHO \quad \textbf{(4-10)}$$

Both acetyl and DHE radicals rapidly add oxygen to form peroxyl radicals, which suffer differing fates in solution. This reaction accounts for the fate of most the acetyl and DHE radicals in solutions containing oxygen. The DHE peroxyl radical (DHEP) rapidly loses superoxide and a proton to become acetic acid.

$$CH_3C(OH)_2O_2\cdot \rightarrow CH_3COOH + O_2^- + H^+ \quad \textbf{(4-11)}$$

The acetylperoxyl radical has no such pathway available to it, and is one of the most strongly oxidizing peroxyl radicals found so far, being capable of oxidizing superoxide with approximately $k=10^9$ $M^{-1}s^{-1}$ to form peracetate ($CH_3C(O)O_2^-$). This reaction is in competition with the expected bimolecular decay as well as other radical-radical reactions. The kinetic details of those steps have not yet been elucidated. Acetylperoxyl radical can undoubtedly oxidize some other solution species as well, perhaps including other organic species and H_2O_2. The formed peracetic acid can oxidize acetaldehyde ($k=1.2x10^{-2}$) to acetic acid.

$$CH_3C(O)O_2H + CH_3CHO \rightarrow 2CH_3COOH \quad \textbf{(4-12)}$$

For an acetaldehyde concentration of 0.1 mM (4 mg/L), the calculated peracetic acid half-life would be 160 hours, so peracetic acid should be detectable if formed, unless it reacts with another product.

The reactions discussed above are summarized in Scheme II (Figure 4-18). One unique feature of this reaction network is that an intermediate in the left-hand ladder (acetylperoxyl radical) is strongly oxidizing, while one in the right-hand ladder (DHE) is strongly reducing. Since the ladders are connected by a facile

equilibrium between acetyl radical and DHE, it is conceivable that the system might exhibit "opportunistic" behavior in response to the solution composition. DHE is likely to be reactive with nitro- compounds in the same manner as α-hydroxyethyl radicals produced from ethanol (described below). This reaction would be in competition with reaction of DHE with oxygen, which ultimately produces superoxide. The acetylperoxyl radical may react with organic compounds, but can also react with superoxide formed by decomposition of the DHE peroxyl radical. In H_2O_2/UV systems, that reaction may be an important sink for both acetyl radical and superoxide, resulting in the prevention of peroxide regeneration by superoxide disproportionation, and suppressing organic oxidation by acetyl radical. In ozonation systems, superoxide is consumed rapidly by ozone, leaving acetyl radical to attack other species, including, perhaps, intermediates in the reductive pathway for nitro- compound destruction (described below).

Acetaldehyde reacts with ozone, with a rate constant of 1.5 $M^{-1}s^{-1}$, compared to a value of 0.37 $M^{-1}s^{-1}$ for ethanol. As with ethanol, the immediate products of this reaction are not known, so that kinetic modeling of this system requires the assumption of possible pathways, testing of the hypotheses, and finally a sensitivity analysis to evaluate the importance of that part of the reaction mechanism, to determine if it may safely be eliminated from the model. It seems likely that the reported ozone-acetaldehyde rate constant may also be too high, as is thought to be the case for ethanol.

Reactions of Acetic Acid and Subsequent Products

"Complete" numerical modeling requires that the fate of all products be described. It is therefore necessary to consider the chemistry of secondary products as well as that of parent compound and primary product. The reaction of acetic acid with hydroxyl radical has also been studied by von Sonntag and co-workers (Schuchmann, Zegota, and von Sonntag 1985). The degradation scheme (not shown) was found to be as complex as those for ethanol and acetaldehyde. Similarly to the α-attack described above, ß-attack of OH radical on ethanol (about 13 percent of the total) produces ß-hydroxyethyl radical. The chemistry of this radical has also been studied by von Sonntag and co-workers (Piesiak, et al. 1985), who produced it in a "cleaner" system by the reaction of OH radical with ethylene. A complicated reaction scheme (not shown) was determined, similarly to those described above for other parent compounds. The chemistry of a few of the stable secondary organic byproducts has also been studied, with similar conclusions, i.e., that degradation occurs by complicated branched pathways instead of simple stepwise routes.

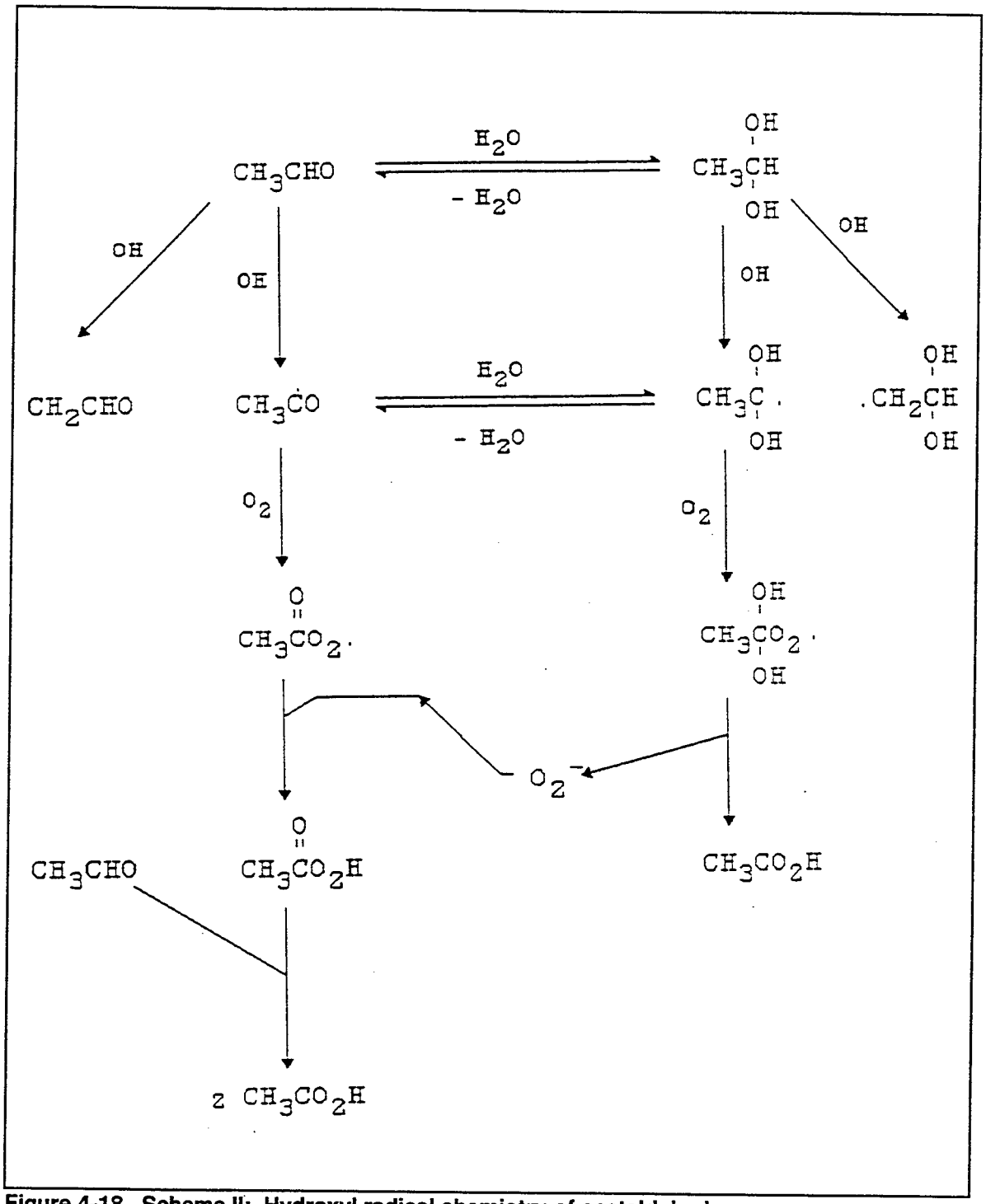

Figure 4-18. Scheme II: Hydroxyl radical chemistry of acetaldehyde.

Implications of Conclusions From the Pulse Radiolysis Literature

Since most of the current knowledge of free radical reactions is derived from pulse radiolysis, the data here are compared to data collected from the pulse radiolysis literature. It was seen from the above discussion that the free radical chemistry of even simple organic molecules such as ethanol and acetaldehyde can be extremely complicated. An extensive study of the free-radical literature has indicated that, for practically all organic compounds for which detailed pulse radiolysis studies have been made, the hydroxyl radical degradation routes have been found to be similarly complex. This situation poses severe problems for the detailed (i.e., "complete") kinetic modeling of even a single contaminant, because of the data gaps such as lack of knowledge of all reaction pathways, lack of required rate constants, and the sheer size of the mathematical problem to be solved. When rate constants are not available, it is tempting to attempt to determine them parametrically by fitting the data. However, when several different reactions lead to the same products in different proportions, there are not enough measurables to uniquely determine parameter values. Although many contemporary software packages are sold as fitting routines, they balk at large, complex problems. Unfortunately, these problems are also too complex to allow determination of parameter values by trial and error. If a satisfactory fit could be found, there is no guarantee that the determined parameters represent a unique solution or physical reality. Thus, complete and reliable fundamental kinetic and mechanistic data are needed as input to the kinetic software.

The problems discussed above are very important to the overall goals of this project, because the data gaps (such as direct ozonation rate constant and products) exist in the ethanol system that may or may not be important, depending on whether the direct reaction can be shown to be unimportant. In addition to being of practical interest because of its presence in the DNT manufacturing wastestream, ethanol was chosen for detailed numerical modeling precisely because there was more kinetic and mechanistic information available for ethanol and its oxidation products than for most matrix components that will be encountered in treatability studies.

Probably only in cases where the size of the problem is first reduced by demonstrating that particular suites of reactions can (under certain circumstances) be ignored, can the data gaps be filled by model parameterization. This can be sometimes be accomplished, for example, by showing that the (unknown) rate constant required for a particular reaction would have to be unrealistically high (typical ranges are known for some types of reactions) for that reaction to be important. This cannot always be done, and it is a complicated procedure, at best.

The only route to general prediction of the outcome of treatment is kinetic modeling of the process. To be of use for process optimization, the kinetic model must be cast in a form that can be related to process variables. These facts and observations from literature sources lead to the next series of experiments.

Identification and Modeling of the Unknown Active Species

A set of experiments was designed to distinguish between oxidative and reductive attack on DNT. For that purpose, the AOP treatment of DNT aqueous solutions was performed in the presence of various oxygen concentrations by continually sparging with oxygen/nitrogen gas mixtures throughout the experiments to control the dissolved oxygen concentration. During application of the AOPs involving ozone, such as the O_3/UV system previously used for DNT treatability studies, an ozone/oxygen gas stream is bubbled through the solutions. As a result, the solutions are saturated with oxygen. Treatment using an ozonation process was not suitable for these experiments because it continuously adds oxygen to the water (Ozone is typically <4% by weight.) Therefore, photolysis of hydrogen peroxide was used to generate OH radicals. A low DNT concentration ($2x10^{-5}$ M) and a high ethanol concentration (0.5M) were used to ensure that essentially all OH radicals generated during the treatment were captured by ethanol. Experiments with nitrogen and oxygen sparging in the absence of ethanol were also performed for comparison. All the experiments carried out during this phase are summarized in Table 4-5.

Figure 4-19 shows the disappearance curves for DNT treated with H_2O_2/UV in the absence of ethanol in oxygen- and nitrogen-sparged solutions (Experiments A22 and A23, respectively). It can be seen that oxygen has no significant effect on the rate of DNT destruction by OH radical. On the other hand, in similar experiments with ethanol present, the rate of DNT disappearance was dramatically higher in the nitrogen-sparged (Experiment A24) solution than in the oxygenated solution (Experiment A25), as seen in Figure 4-20. The observed difference in the rates implies that DNT destruction was due to a reductive process rather than oxidation by ethanol peroxyl radical, since a lack of oxygen would preclude the formation of peroxyl radical. Comparison with Figure 4-19 shows that destruction in the N_2/ethanol experiment was faster than with N_2-sparging in the absence of ethanol. Since the added ethanol should be an efficient OH radical scavenger, these results confirm that a species other than hydroxyl radical is responsible for the majority of DNT destruction in Experiment A24. Since ethanol radical is known to be a reducing radical, and DNT should be easily reduced because of the presence of the electron withdrawing nitro groups on the ring, the proposed electron transfer mechanism of DNT destruction is reasonable.

Kinetic Experiments

A series of kinetic experiments was performed at different oxygen concentrations to test prototype mathematical models based on hypothesized reaction schemes. As in the preliminary experiments, a relatively low DNT concentration ($2x10^{-5}$M) was chosen for the experiments, to obviate hydroxyl radical attack on DNT, as well as for other reasons discussed below. A high ethanol concentration (0.5 M) was used so that essentially all of the OH radicals generated were captured by ethanol. As before, solutions were presparged and continually sparged throughout the experiments with nitrogen/oxygen mixtures to maintain constant

dissolved oxygen concentration. The DNT disappearance rate was found to be strongly inversely dependent on the oxygen concentration in solution (Figure 4-21), with more than two orders of magnitude difference between the rates observed in the oxygen- and nitrogen-sparged experiments.

Table 4-5. DNT treatability experiments: effect of oxygen concentration.

Experiment No.	Method	DNT Concentration, mM	Ethanol Concentration, mM	Oxygen Concentration, mM
A20	O_3/UV	0.809	25.8[a]	$O_3 + O_2$ sparge
A21	O_3	--	19.8	$O_3 + O_2$ sparge
A22	H_2O_2/UV[b]	0.021	--	O_2 sparge
A23	H_2O_2/UV	0.025	--	N_2 sparge
A24	H_2O_2/UV	0.023	500	N_2 sparge
A25	H_2O_2/UV	0.028	500	O_2 sparge
A26	Sparge	--	500	$N_2 + O_2$ sparge
A27	H_2O_2/UV	0.022	500	0.019
A28	H_2O_2/UV	0.022	500	0.042
A29	H_2O_2/UV	0.022	500	0.4
A30	H_2O_2/UV	0.022	500	0.075
A31	H_2O_2/UV	0.022	500	0.025
A32	H_2O_2/UV	0.024	500	0.006
A33	H_2O_2/UV	0.027	500	0.787
A34	H_2O_2/UV	0.021[c]	500	0.019
A35	H_2O_2/UV	0.021[c]	500	0.912
A36	H_2O_2/UV	0.067[d]	500	0.095
A37	H_2O_2/UV	0.097[d]	500	0.006
A38	H_2O_2/UV	0.439[d]	500	0.006
A39	H_2O_2/UV	0.51	468	0.011
A40	O_3/UV	0.461	13.7	0.225

[a] Diethyl ether, rather than ethanol
[b] H_2O_2 concentration in all H_2O_2/UV experiments was 500 mM (nominal)
[c] TNT, rather than DNT
[d] DNB, rather than DNT

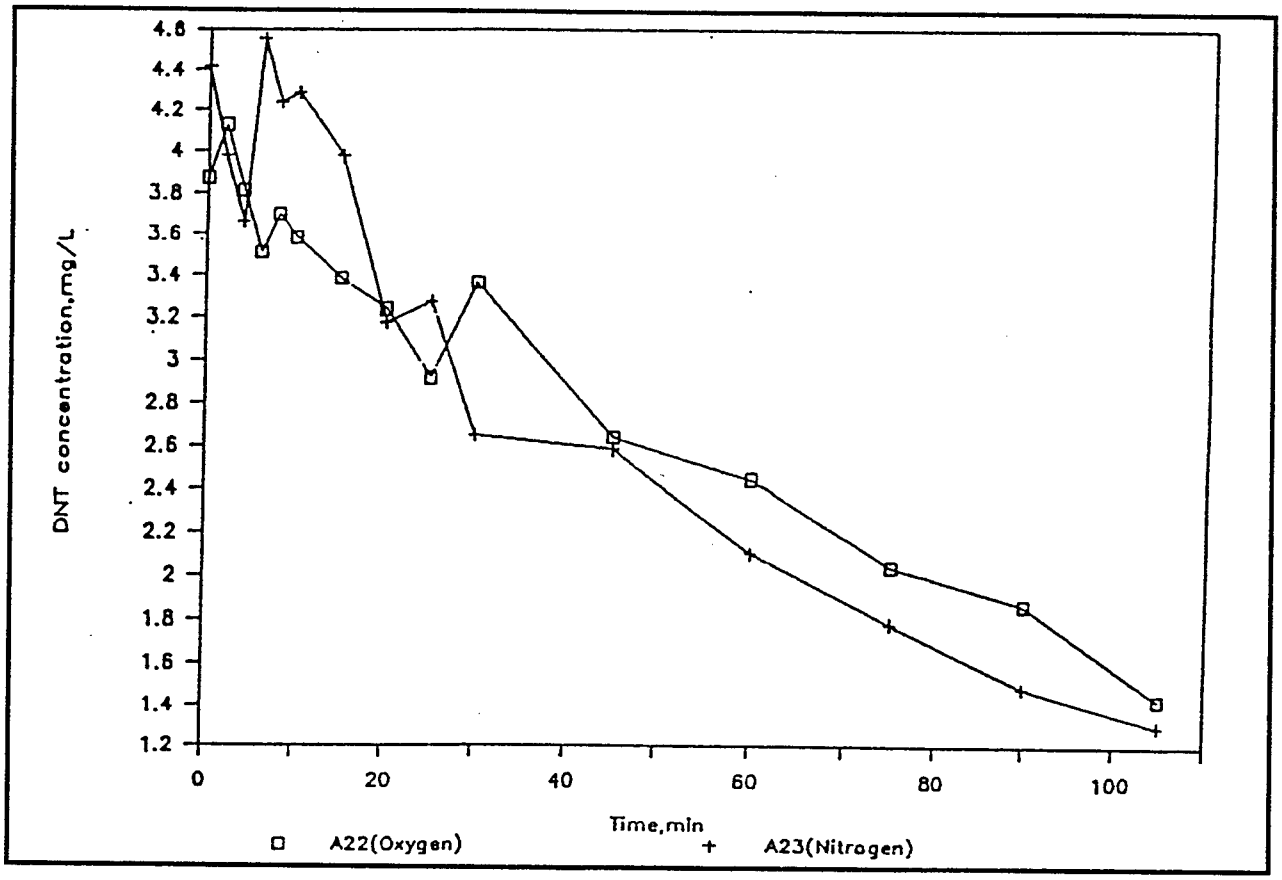

Figure 4-19. DNT removal by H_2O_2/UV treatment in oxygen- and nitrogen-sparged solutions (no ethanol present).

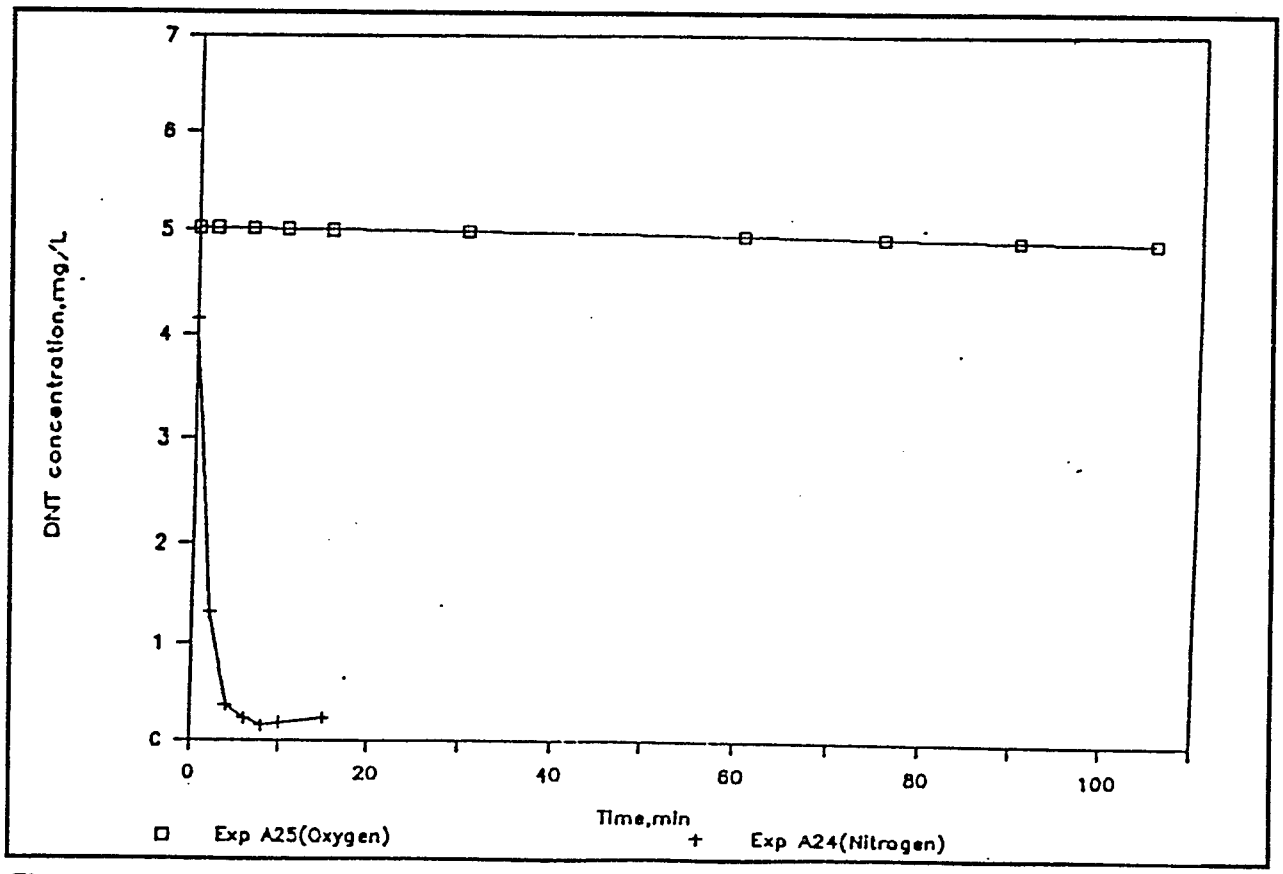

Figure 4-20. DNT removal by H_2O_2/UV treatment in oxygen- and nitrogen-sparged solutions in the presence of ethanol.

Ethanol radicals are known to be reducing radicals, and the rate constants for electron transfer reaction of these radicals with some para-substituted nitrobenzenes have been reported (Jagannadham and Steenken 1984), as has oxidation of the resulting radical anions by molecular oxygen, to regenerate parent compound (e.g., Wardman and Clark 1976). Two reaction schemes were assumed as the basis for mathematical models. In Scheme III (Figure 22), the radical anion of the nitro- compound "escapes" the reaction system by an unspecified pathway that operates in competition with oxidation of the radical anion back to parent compound by molecular oxygen. The rate of reduction of DNT by superoxide was demonstrated in separate experiments (ethanol absent-data not shown) to be insignificant, compared to the observed processes. The reaction scheme shown in Scheme IV (Figure 23) was obtained from Scheme III (Figure 22) by replacing the generic escape reaction with information from the findings of Asmus, Henglein, and co-workers (Asmus et al. 1966; Wigger, Henglein, and Asmus 1967; Grünbein, Fojtik, and Henglein 1969; Grünbein, Fojtik, and Henglein 1970). The one-electron half reactions labeled t_1 and t_2 in the lower part of Scheme IV (Figure 23) are driven by electron transfer from the radical anion (of the parent nitro- compound) shown in the upper right-hand part of the scheme.

The kinetic equations corresponding to the reaction pathways shown in Schemes III and IV were solved, yielding the rate equations for DNT (D) in terms of R_g, the rate of hydroxyl radical generation by an unspecified process. Both schemes gave equations of the form

$$\dot{D} = \nu_e \nu_D f_{OE} R_g \tag{4-13}$$

The factors f_{OE}, ν_D, and ν_e are the efficiencies of 1) hydroxyl radical capture by ethanol, 2) ethanol radical attack on DNT (in competition with the reaction of ethanol radical with molecular oxygen), and 3) DNT radical anion "escaping" to products, respectively. These quantities are defined as:

$$f_{OE} = \frac{k_{OE}E}{k_{OE}E + \sum k_{Oi}C_i} \tag{4-14}$$

$$\nu_D = \frac{k_{RD}D}{k_{RD}D + k_{RX}[O_2]} \tag{4-15}$$

and for Scheme I:

$$\nu_e = \frac{k_e}{k_e + k_r[O_2]} \tag{4-16}$$

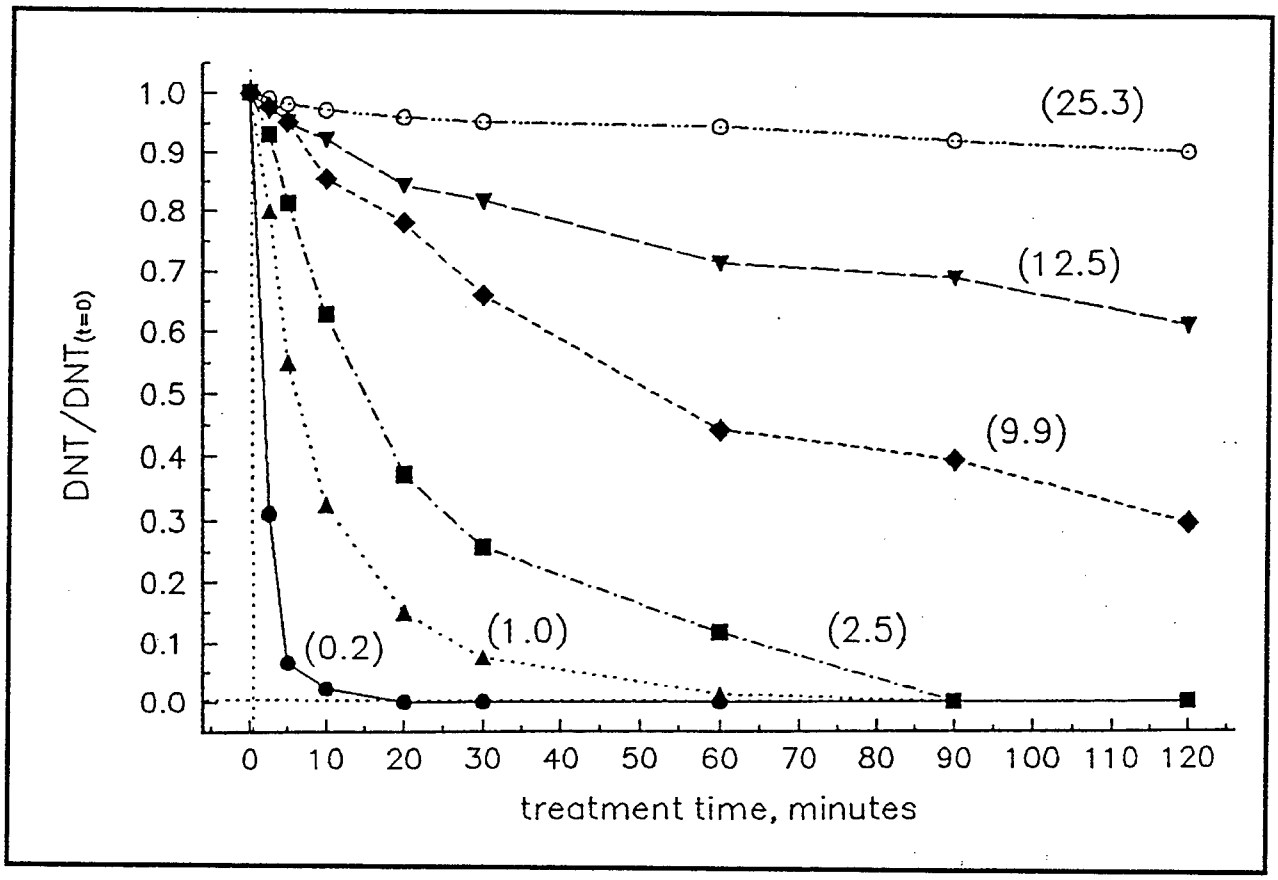

Figure 4-21. Effect of oxygen concentration on DNT removal by H_2O_2/UV treatment; oxygen concentration (mg/L) given in parenthesis.

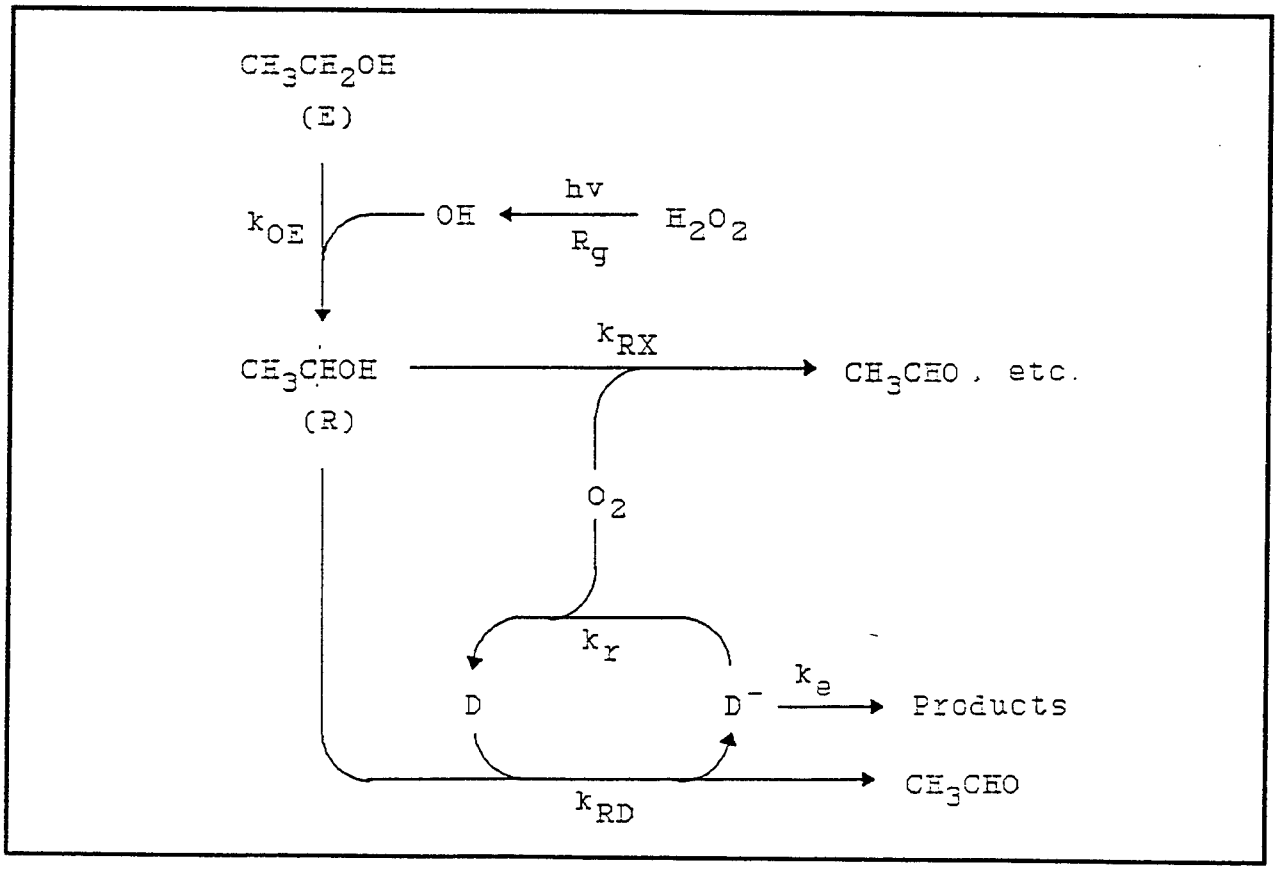

Figure 4-22. Scheme III: Radical anion of the nitro-compound "escapes" the reaction system.

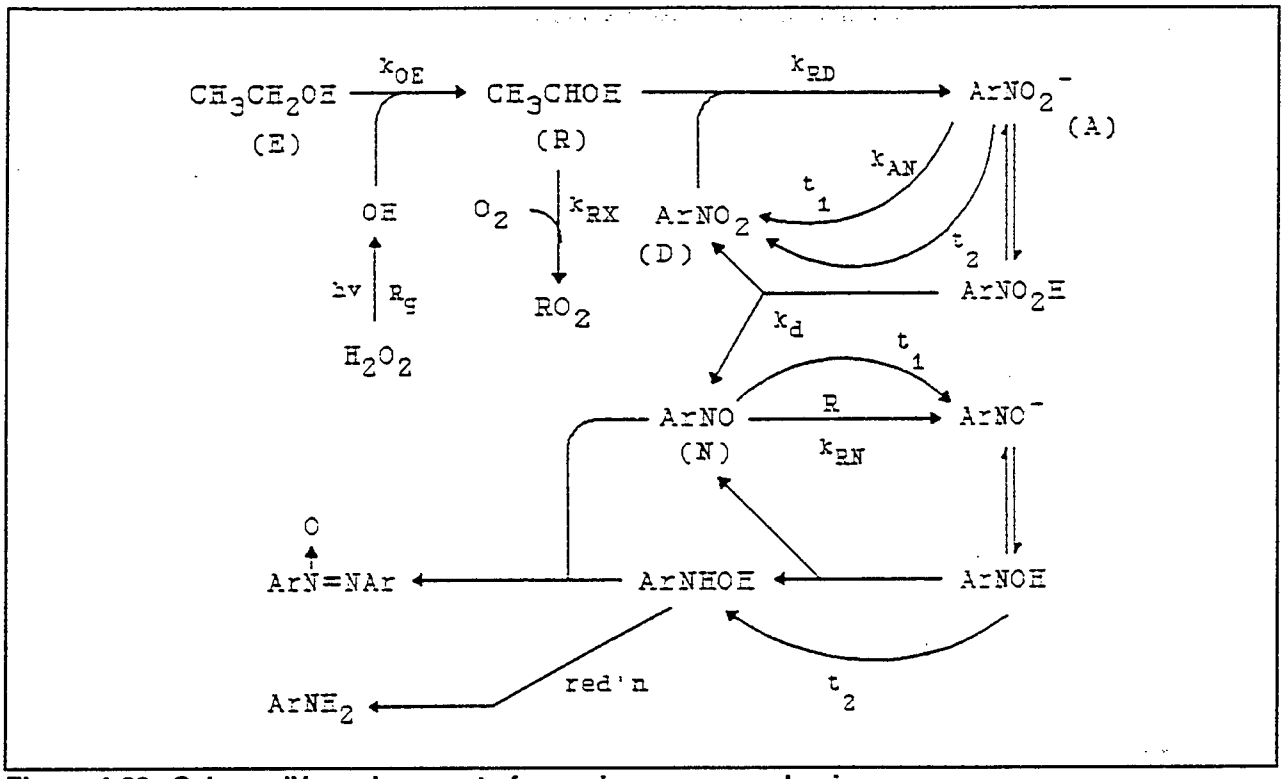

Figure 4-23. Scheme IV: replacement of generic escape mechanism.

The double subscripts indicate the reacting species (O=hydroxyl radical, E=ethanol, D=DNT, and X=oxygen) and single lower-case subscripts indicate function, i.e., e=escape, r=return to parent compound. All efficiencies take the usual form of the "competition function":

$$\frac{\textit{rate of process of interest for species } i}{\sum \textit{rates of all processes for species } i} \qquad \textbf{(4-17)}$$

Substitution and rearrangement of equation 4-13 to define the function Γ_D for Scheme III (Figure 4-22) yields

$$\Gamma_D \equiv -\frac{f_{OE} R_g}{\dot{D}/D} = (D + \frac{k_{RX}[O_2]}{k_{RD}})(1 + \frac{k_r[O_2]}{k_e}) \qquad \textbf{(4-18)}$$

where the identity sign defines Γ_D. The form of this equation implies that a plot of log Γ_D vs. log $[O_2]$ should yield a curve with three linear regions joined by transitional regions:

I. $k_{RX}[O_2]/k_{RD} >> D$, *and* $k_r[O_2]/k_e >> 1$, *with slope 2,*

II. $k_{RX}[O_2]/k_{RD} >> D$, *and* $k_r[O_2]/k_e << 1$, *or*

$k_{RX}[O_2]/k_{RD} << D$, *and* $k_r[O_2]/k_e >> 1$, *with slope 1,*

and

III. $k_{RX}[O_2]/k_{RD} << D$, *and* $k_r[O_2]/k_e << 1$, *with slope 0,*

with the additional possibility that regions might be overlapping, depending on the values of the various constants and the substrate concentration. Extrapolation of the linear regions, if identifiable, should provide values of k_{RX}/k_{RD} and k_r/k_e.

The disappearance curves were found to obey first-order kinetics, so that Γ_D in equation 4-18 simplified to R_g/k', where k′ is the pseudo-first-order rate constant for DNT disappearance. The results are plotted in Figure 4-24, along with a curve fit that yielded the value $k_{RX}/k_{RD}=46$ from extrapolation of the slope=1 region to the y-axis. It was not possible to determine the intercept of the Region I (slope=2) portion of the curve since the data fall entirely in Region II (slope=1), indicating that one-electron oxidation of the radical anion by oxygen is not competitive with escape to products at any but perhaps the highest oxygen concentration shown in Figure 4-24. Curve fits with various values of k_r/k_e indicated that this ratio is ≤ 400 M^{-1}. Using the value $k_{RX}=4.6\times10^9$ $M^{-1}s^{-1}$ (Adams and Wilson 1969) gives $k_{RD}=1.0\times10^8$ $M^{-1}s^{-1}$. This value seemed slightly low when compared with a Hammett plot (not shown) of the substituted nitrobenzene rate constants from Jagannadham and Steenken (1984). However, those rate constants were for the para-isomers only, so the extent to which direct comparison is valid is uncertain.

On the basis of the information obtained from the literature dealing with ethanol radical reaction with nitro- compounds, the "escape" reaction was investigated further, to determine the effect of a subsequent reaction network on the kinetic model. The system of rate equations corresponding to Scheme IV (Figure 23) was solved analytically, with some simplifying assumptions. The resulting rate equation for DNT was found to have the same form as equation 4-13, but with a different expression for ν_e:

$$\nu_e = \frac{1}{3+\nu_N} \tag{4-19}$$

where:

$$\nu_N = \frac{1}{1+\dfrac{k_{RN}R}{k_{AN}A}} \equiv \frac{1}{1+\gamma} \tag{4-20}$$

with:

$$\gamma = \frac{2k_{RN}}{k_{AN}\alpha}\left[\frac{k_d R_g}{k_{RD}k_{RX}[O_2]}\right]^{1/2} \tag{4-21}$$

In equations 4-20 and 4-21, A is the concentration of the DNT radical anion, k_D is the rate constant for disproportionation of the protonated DNT radical anion, and $\alpha=10^{(pH-pKa)}$, where pK_a is the pK-value of the protonated DNT radical anion. It is not possible to evaluate γ directly, since values are not known for the rate constants k_{RN}, k_{AN}, and k_d for DNT as the parent compound. However, progress in the evaluation of γ can be made by considering that since γ is a non-negative number, $0 \le \nu_N \le 1$, so that $1/4 \le \nu_e \le 1/3$. Therefore, $\nu_e = 0.29 \pm 0.04$. Thus, the accuracy with which ν_e is determined is probably as good as if literature values for the unknown rate constants were available, since such values are typically considered to be reliable within a factor of 2. The lower escape efficiency, ν_e, found from the Scheme IV model relative to that derived from Scheme III (Figure 22), reflects the fact that DNT, regenerated as the radical anion, drives subsequent processes by electron transfer. The pH-, DNT-, O_2-, and R_g-dependences of ν_e are imbedded in γ, and are thus seen to be weak. In this model, the intercept in Figure 4-24 leads to the value $k_{RD} = (3.5 \pm 0.5) \times 10^8\ M^{-1}s^{-1}$ where the range of values represents only the uncertainty in γ.

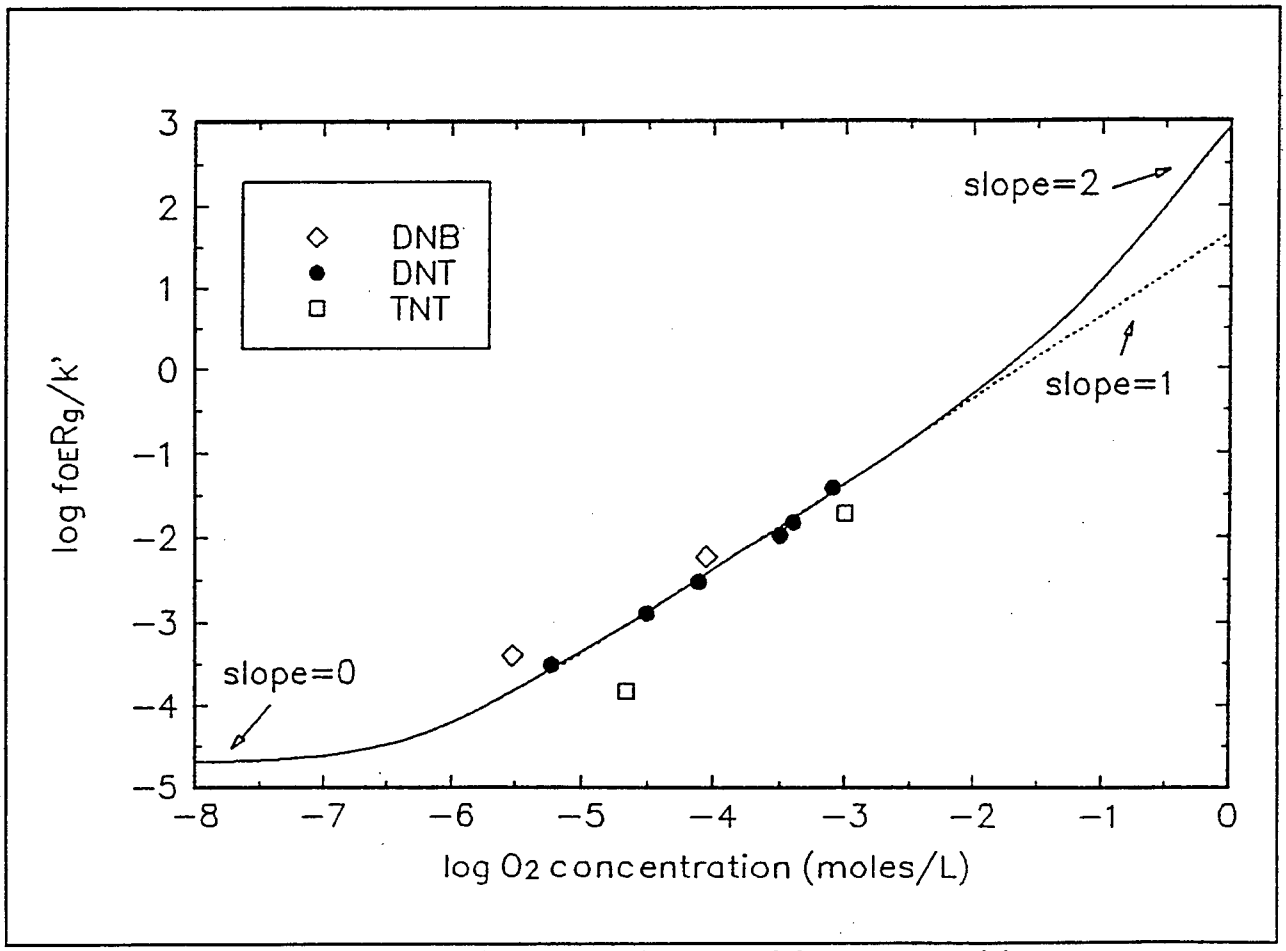

Figure 4-24 Ordnance compound initial rate data in terms of the escape model.

Also shown in Figure 4-24 are points obtained from preliminary initial rate data on 2,4,6-trinitrotoluene (TNT) and 1,3-dinitrobenzene (DNB), from experiments similar to those described above for DNT. The effect of oxygen concentration on the destruction rates of these compounds demonstrates that the "enhancement" effect is also operative for these nitro- compounds. It is therefore reasonable to hypothesize that the effect may be general for compounds having high electron affinity. The slope of approximately unity seen for each pair of points indicates that they also fall in Region II of their respective curves, but the deviation from unity may represent the fact that the upper TNT point and the lower point for DNB are in the edge of the transition regions. Extrapolation of a linear region of slope 1 would indicate that, as expected, TNT has a higher rate constant than DNT for reaction with ethanol radical. It is not clear why the DNB data fall above those of DNT in Figure 4-24, but variation in ν_e- values between compounds may be a contributing factor.

Testing on Other Types of Compounds

The question of whether the effect described above extends to other types of electron-affinic compounds is an important issue with respect to the generality of this AOP treatment improvement. Halogenated organic compounds are known to be reducible under some conditions, eliminating halide ions. Compounds that are polyhalogenated on the same carbon atom are completely dehalogenated at that site by virtue of the incompatibility of halogen and oxygen atoms attached to the same carbon atom. Although phosgene can be an intermediate product in chlorination in the presense of carbon, its hydrolysis in water is very fast. A half-life of about 0.1 second has recently been measured (Mertens, et al. 1994). Thus, AOP reduction may provide a rapid means of dehalogenating previously intractable contaminants.

A series of experiments was carried out to test this hypothesis, using carbon tetrachloride as the model contaminant. Carbon tetrachloride apparently reacts very slowly if at all with hydroxyl radical in water. Since carbon tetrachloride is very volatile, the sparged reactor used in the previous experiments could not be used, and a simple photochemical reactor was constructed from a borosilicate vial with a septum cap fitted with a small UV "pen-lamp" extending into the vial through a hole cut in the septum. The water or ethanol (0.16 M, 7.4 g/L) solution containing hydrogen peroxide (0.15 M, 5.1 g/L) was presparged with oxygen or nitrogen, then spiked with a deaerated carbon tetrachloride/ethanol solution to a nominal concentration of 22 µg/L, the vial quickly closed, and the UV lamp turned on. Oxygen concentrations were measured on the presparged water.

Figure 4-25 shows the fraction of carbon tetrachloride remaining after various treatment times. Several features stand out in these results:

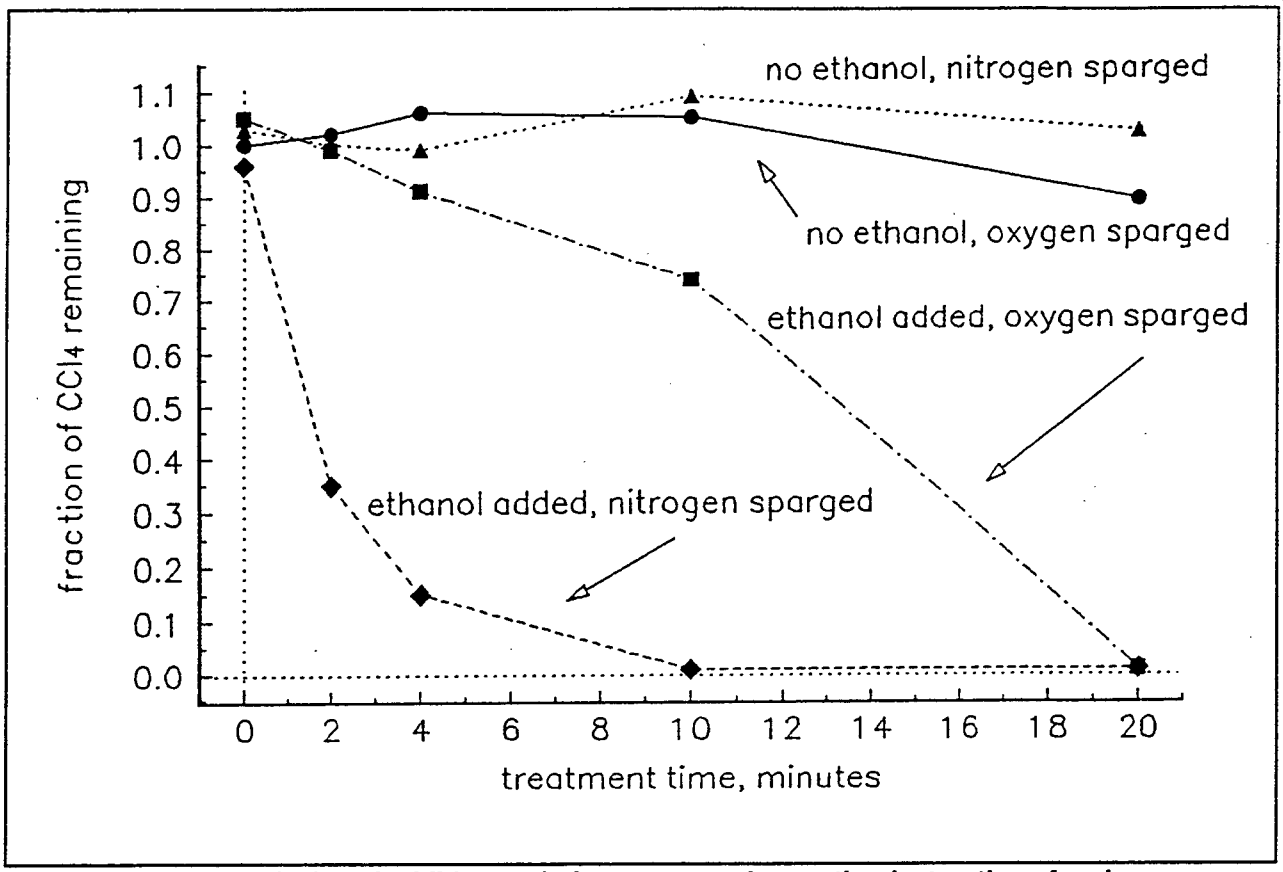

Figure 4-25. Effect of ethanol addition and nitrogen sparging on the destruction of carbon tetrachloride in water.

1. No carbon tetrachloride is removed in the absence of ethanol, indicating that the reaction of OH with carbon tetrachloride is very slow.

2. In the presence of ethanol, carbon tetrachloride removal is 14 times faster when the solution was sparged with nitrogen ($[O_2]$=1.2 mg/L) than when sparged with oxygen ($[O_2]$=35.3 mg/L), consistent with the electron-transfer mechanism discussed above.

3. Even in the oxygen-sparged system, removal still occurred in the presence of ethanol, whereas no significant removal was observed in the absence of ethanol. This indicates that results of AOP treatability experiments for substances such as carbon tetrachloride may be very dependent on the matrix, including solvents used to solubilize the model contaminants prior to spiking synthetic waters.

4. Most importantly, the results indicate that a means of removing previously AOP-intractable species such as carbon tetrachloride is now available. A similar effect is expected for other halogenated species such as PCBs, etc.

Application of Kinetic Model to Treatability Experiments

The model represented by equation 4-13 describes the disappearance of the target compound in terms of the hydroxyl radical generation rate, regardless of

the means of radical generation. To predict actual treatability data, it is necessary to mathematically specify the radical generation rate as a function of any process variables upon which it may be dependent. The form of this expression will of course be different for different AOPs. As is typically done in kinetic studies, the parameters (such as rate constants) for the model were determined from the initial DNT destruction rates in kinetic experiments, to avoid complications introduced by reaction byproducts that might accumulate later in the experiment. Thus, it is not assured that such a model will correctly describe target compound disappearance throughout the entire course of treatment. It was therefore necessary to evaluate the ability of the model to reproduce treatability data collected on DNT in aqueous ethanol solution.

An experiment (A-39) was performed using 0.5 mM DNT (93 mg/L) in 0.5 M (21 g/L) aqueous ethanol solution as the reactor charge, primarily to determine reaction byproducts (those results described in a later section). The results of this experiment were selected for modeling since H_2O_2/UV was used to generate hydroxyl radical, as was the case in the kinetic experiments used to define the model parameters. The initial peroxide concentration was 0.56 M (19 g/L). As in the kinetic experiments, this high peroxide concentration was chosen to maximize peroxide photolysis with a minimum of DNT photolysis. The rate of hydroxyl radical generation, R_g, is ϕ_0=2 (yield of hydroxyl radicals per hydrogen peroxide molecule photolyzed) times the rate of peroxide photolysis, R_p, so that:

$$R_g = \phi_0 R_P = \phi_0 \phi_P f_P F_T I_0 \qquad \textbf{(4-22)}$$

where Φ_P is the quantum yield (molecules dissociated per photon absorbed) of peroxide photolysis, I_o the UV dose rate in Einsteins (a mole of photons) per unit time, F_T the fraction of incident photons absorbed, and f_P the fraction of absorbed photons that are absorbed by peroxide. The fractions F_T and f_P are given by:

$$F_T = 1 - 10^{-A_T l_{eff}} \qquad \textbf{(4-23)}$$

and:

$$f_P = \frac{\varepsilon_P P}{\varepsilon_P P + \sum_i \varepsilon_i C_i} = \frac{\varepsilon_P P}{A_T} \qquad \textbf{(4-24)}$$

where the ε's are decadic extinction coefficients, P and C_i are molar concentrations of peroxide and other solution components, and the total (1-cm) absorbance, A_T is defined by the second equal sign in equation 4-24. The UV dose rate and the effective path length of the reactor (l_{eff}) were determined by using aqueous hydrogen peroxide as an actinometer, that is, by fitting equation 4-22 to results from peroxide photolysis experiments carried out in purified water.

The expression for the hydroxyl radical generation rate can now be substituted into equation 4-13, which is then integrated to give the target compound

concentration as a function of time, for comparison with experimental data. However, equation 4-22 requires that the dependence of the absorbance on treatment time be known. A thorough knowledge of solution component concentrations and extinction coefficients would be sufficient to calculate the absorbance, but would greatly complicate the integration, since the target compound rate equation would be coupled to the rate equations of all other components. In practical cases, that knowledge is not available, anyway, and suitable means of approximation are required to proceed with the integration. Four approximations were considered for an optically dense reactor charge, i.e., for the case in which A_T was sufficiently high that $F_T \rightarrow 1$. The mathematical expressions get considerably more complicated if this restriction is relaxed. The approximations were:

1. Absorbance of byproducts is insignificant ($\sum \varepsilon_i C_i = 0$). This assumption led to an integrable equation, but did not provide an adequate description of the system when modeling results were compared to the actual data.

2. Total absorbance does not change (A_T constant). This assumption gave reasonable results for the present example, where the majority of absorbance was due to peroxide, but would not be a good approximation at lower peroxide concentrations.

3. Absorbance can be represented as an empirical function of time. This is a flexible and relatively easy approach, but gives an integrated result that is a nonlinear function of time, which is difficult to visualize. For example, for the (simplified) case where the peroxide concentration is approximately constant (as it was in Experiment A-39), and the total absorbance is represented as a linear function A(t)/A(t=0)=(1-at), the integrated result is:

$$\Delta D + \beta \ln \frac{D}{D_0} = \frac{k}{a} \ln(1 - at) \qquad \textbf{(4-25)}$$

or, rearranged:

$$1 - \left[\frac{D}{D_0}\right]^{\frac{\alpha\beta}{k}} e^{\frac{\alpha}{k}\Delta D} = at \qquad \textbf{(4-26)}$$

where:

$$k = \frac{\phi \varepsilon_P Pl_{eff} I_0}{A(t=0)(3 + \kappa_N)} \qquad \textbf{(4-27)}$$

This method may prove to be more useful in future calculations at lower total absorbance, where method 4 (below) may be a poorer representation.

4. Average byproduct extinction coefficient remains constant. In this approach, it is assumed that attack on target compound leads to byproducts, the extinction coefficients of which do not change appreciably in subsequent conversion to secondary byproducts. Product absorbance is then

$$\sum_i \varepsilon_i C_i = -\Delta D\, \varepsilon_{products}) \tag{4-28}$$

The value of $\varepsilon_{products}$ may be obtained from the solution absorbance when all the target compound has been removed, corrected for remaining peroxide absorbance. Thus, this method requires calibration to experimental results, and is therefore presently of use only for verifying the general utility of the kinetic model, and not as an *a priori* prediction method. This is also true of Case 3, above. Further work will be required to determine what level of approximation is allowed/required. However, this approximation is only used to describe the effect of competition for photons on the OH radical generation rate by H_2O_2/UV, so agreement of the kinetic modeling results with experimental results, even with the absorbance calibration, is evidence for the applicability of the kinetic/mechanistic model. Insertion of equation 4-28 into equation 4-13, followed by integration, assuming $[H_2O_2]$ constant, leads to:

$$(a_1 + \beta a_2)\Delta D + \frac{a_2}{2}(D^2 - D_o^2) + \beta a_1 \ln\frac{D}{D_o} = -kt \tag{4-29}$$

where:

$$a_1 = 1 + \frac{2}{\varepsilon_P P} \tag{4-30}$$

$$a_2 = \frac{\varepsilon_D - \varepsilon_{products}}{\varepsilon_P P} \tag{4-31}$$

$$\beta = \frac{k_{RX}[O_2]}{k_{RD}} \tag{4-32}$$

and:

$$k = \nu_e \phi_P I_o \tag{4-33}$$

Values for a_1, a_2, ß, and k can be calculated from known physical constants, the parameter $\varepsilon_{products}$ found from the absorbance fit discussed above, v_e estimated from the kinetic model development, I_o measured by actinometry, and the value of k_{RX}/k_{RD} determined from the fit of the kinetic data. These values were used as starting values for a fit of equation 4-29 to the DNT disappearance data from Experiment A-39. The successful fit is shown in Figure 4-26. It is significant that the model fits the final as well as initial stages of treatment, implying that

the model is reasonable and that no other reactions either: (1) are important in, or (2) interfere with the destruction of DNT during the application of this treatment process. It is also significant that the parameter values giving the best fit were very close to the starting values calculated from the theoretical expressions in equations 4-30 through 4-33.

Theoretical and best-fit values are compared in Table 4-6. The values are seen to be quite similar, with the largest difference factor being in the value of $ß=k_{RX}[O_2]/k_{RD}$. Using the experimentally-measured oxygen concentration of 11 µM, the ratio of k_{RX}/k_{RD} is calculated from this fit to be 25, compared to 42, as was determined from extrapolation of the kinetic data shown in Figure 4-24. Figure 4-27 shows a similar log plot of the kinetic data with a line added to represent the extrapolation line that would result from the use of $k_{RX}/k_{RD}=25$. An extrapolation error of the magnitude represented by the difference between the two lines in Figure 4-27 is very likely, indicating that the curve fit just discussed may be a more accurate method of determining the rate constant ratio than is the extrapolation technique. This possibility was not explored in the present study.

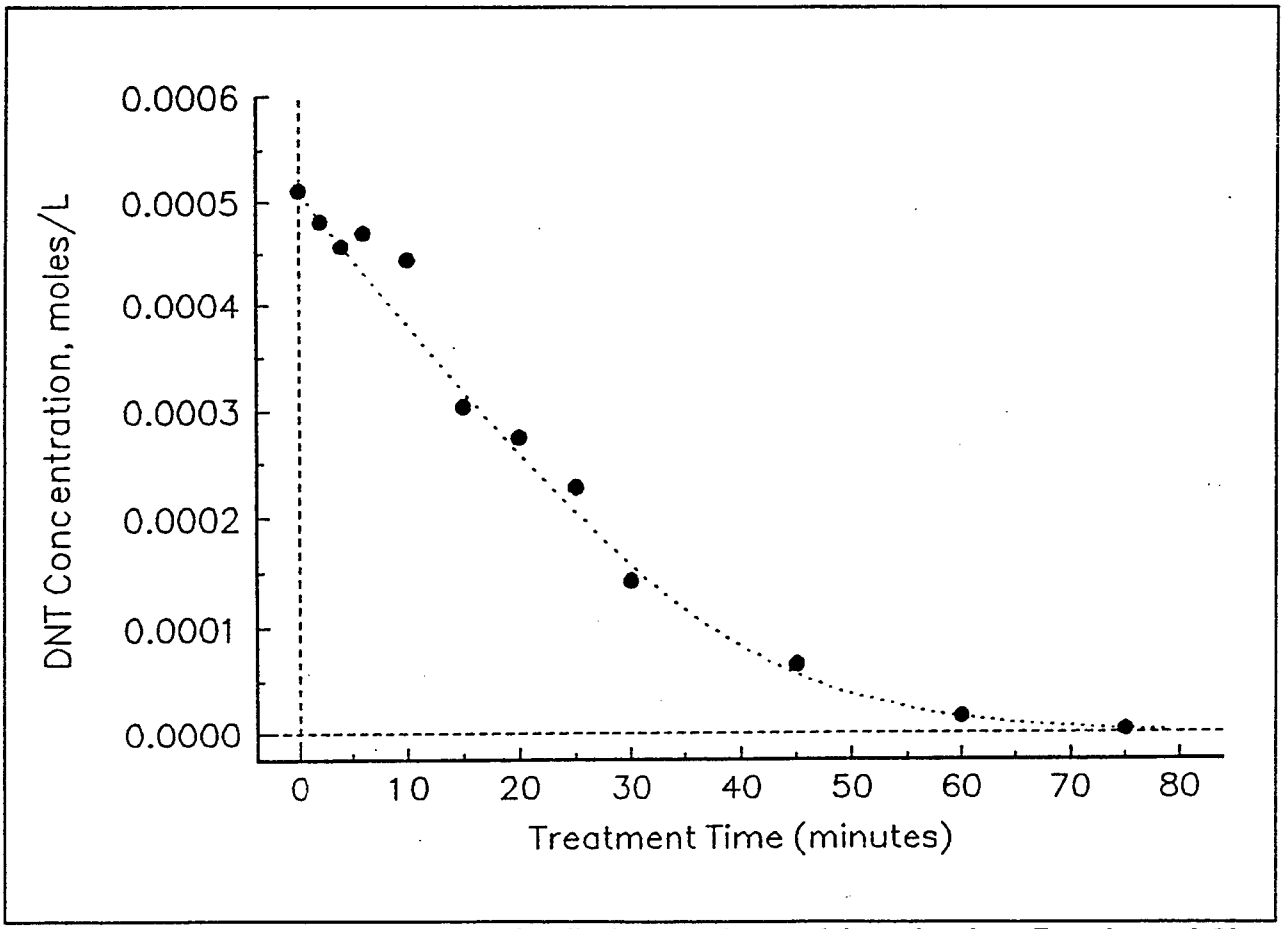

Figure 4-26. Fit of combined escape and radical generation models to data from Experiment A-39.

Table 4-6. Comparison of theoretical and "best-fit" values for parameters in kinetic model.

Parameter	Theoretical Value	Best-Fit Value
a_1	1.19	1.19
a_2	756	756
ß	1.4×10^{-4}	2.7×10^{-4}
k	3.4×10^{-5}	3.2×10^{-5}

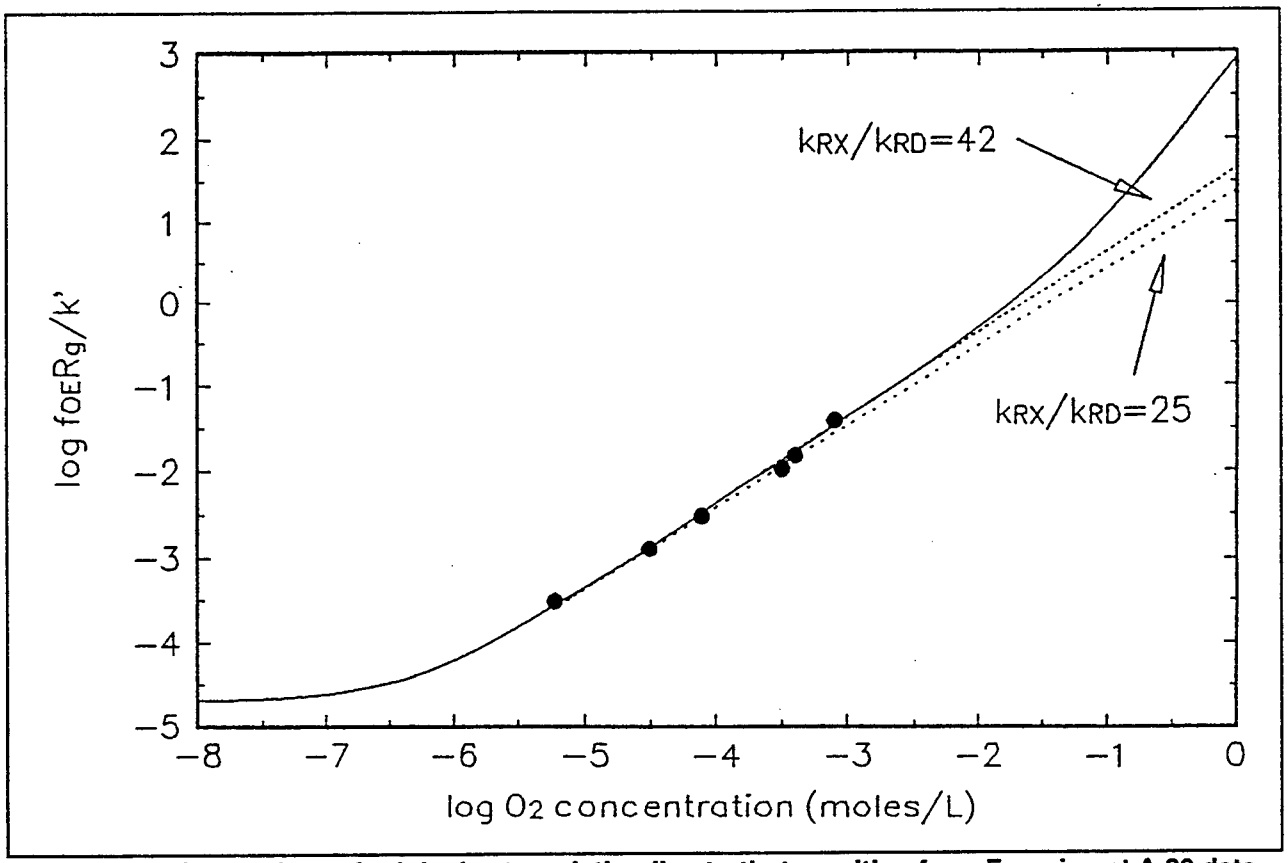

Figure 4-27. Comparison of original extrapolation line to that resulting from Experiment A-39 data fit.

Thus, the model calibrated for the initial rates observed in the kinetic experiments in one concentration range appears to describe the DNT disappearance data from another experiment in a different concentration range, over the entire disappearance curve (rather than just the initial rates). As will be seen in the section on treatment byproducts, the identified products from these experiments are different from those expected for hydroxyl radical reaction, and are consistent with those that would be produced by reduction of the target compound. We therefore conclude that the model is appropriate and adequately represents the progress of treatment under at least some conditions.

Reanalysis of Early Treatability Data

The action of an active species other than OH radical was initially discovered during kinetic analysis of data from treatability studies performed in an earlier phase of this investigation. The method used to calculate instantaneous DNT disappearance rates for the points in the competition plot shown in a previous report was refined to provide a more accurate value of the rate, by replacing values of $\Delta DNT/\Delta t$ calculated between two consecutive data points with $k'[DNT]$, where k' is the slope of a plot of ln[DNT] vs time (i.e., the pseudo-first-order rate constant). This was possible because the DNT disappearance curves were observed to all be first-order or nearly first-order. This procedure has the effect of smoothing normal random scatter in analytical data. The competition equation for this system is:

$$\varepsilon_i = \frac{\dot{D}}{\dot{D}_u} = \eta \left[\frac{\nu_e f_\alpha k_{RD}}{k_{RD} D + k_{RX}[O_2]} + \frac{k_{OD}}{k_{OE} E + k_{OA} A} \right] D \qquad \text{(4-34)}$$

where f_α is the fraction of hydroxyl radical attacks on ethanol that occur in the α-position (i.e., the carbon atom to which the OH group is attached), η is the OH yield per ozone molecule consumed and $\dot{D}_u$ is the ozone utilized dose rate. As discussed before, $\eta \rightarrow 1$ is a good approximation since ethanol is a very efficient superoxide producer. Slight rearrangement leads to:

$$\frac{\dot{D}/D}{\dot{D}_u} = \frac{k'}{\dot{D}_u} = \frac{\nu_e f_\alpha}{D + \frac{k_{RX}[O_2]}{k_{RD}}} + \frac{k_{OD}/k_{OE}}{E + \frac{k_{OA}}{k_{OE}} A} \qquad \text{(4-35)}$$

so that plotting $k'/\dot{D}_u$ versus $1/(E+k_{OA}A/k_{OE})$ should yield a straight line with slope k_{OD}/k_{OE} and intercept $\left[\frac{\nu_e f_\alpha k_{RD}}{k_{RD} D + k_{RX}[O_2]}\right]$.

The resulting revised competition plot is shown in Figure 4-28, which exhibits a better linear correlation than the corresponding previous plot. Using $\nu_e = 0.3$, $f_a = 0.87$, $k_{OE} = 1.9 \times 10^9$ and $k_{RX} = 4.6 \times 10^9$ gives the values $k_{RD} = 2.9 \times 10^8$ and $k_{OD} = 2.4 \times 10^8$ $M^{-1}s^{-1}$. This value of k_{RD} is intermediate between the other two determined values, giving an average value of $k_{RD} = (2.5 \pm 1.3) \times 10^8$ $M^{-1}s^{-1}$. Thus, the value of k_{RD} determined from these early ozone/UV experiments performed in a different DNT concentration range, at widely different ethanol concentrations, under conditions where OH-radical attack on DNT is also important, is in agreement with those calculated from other, very different experimental conditions.

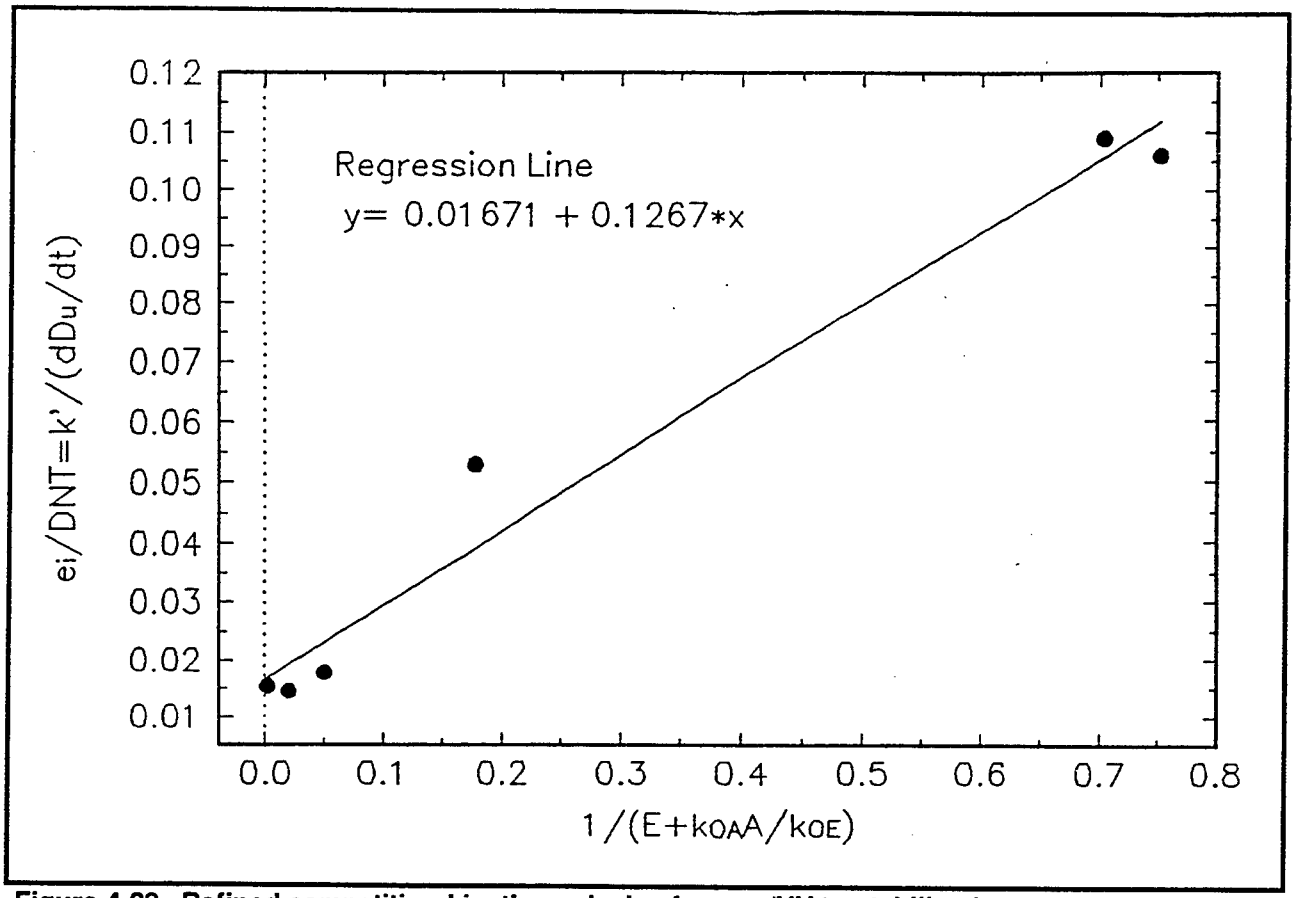

Figure 4-28. Refined competition-kinetic analysis of ozone/UV treatability data.

This agreement is supportive of the applicability and generality of the hypothesized mechanism and mathematical model, and indicates that extension of the model to ozonation-based AOPs, incorporating the specifics of radical generation in terms of process variables such as ozone mass transfer rate and ozone photolysis, looks promising.

Byproduct Study

To find additional evidence to support the model discussed above an attempt was made to identify byproducts arising from the reaction of DNT with ethanol radical and to compare them with byproducts predicted by the model. The basic trends were discussed for the accumulation and disappearance of oxidation byproducts formed during O_3/UV treatment of concentrated (0.5 to 0.9mM) DNT aqueous solutions in the presence of ethanol. The major products were 2.4-dinitrobenzoic acid (DNBA) identified by its retention time and UV spectrum and also 2,4-dinitrobenzaldehyde (DNBAL) and 1,3-dinitrobenzene (DNB) tentatively identified by retention times. These findings were consistent with the data of Ho (1986) who found these byproducts in DNT solutions treated with H_2O_2/UV. These are also the byproducts expected from oxidation of DNT, which occurs primarily at the methyl side chain, and can also occur during DNT photolysis. A

different suite of products is expected to arise from the reductive pathway. Figure 4-29 presents HPLC chromatograms for samples taken during the H_2O_2/UV treatment of nitrogen-and oxygen-sparged DNT solutions (Experiments A24 and A25). The example chromatograms were chosen for the samples with as similar extent of DNT conversion (ξ) as possible (the extent of DNT conversion after 2 min of treatment in oxygen-free solution was already higher than that at the end of DNT treatment in oxygen-sparged solution). The data indicate that greater absorbance due to polar byproducts (which elute early as unretained peaks on the LC-18 column) was found in oxygen-sparged solutions, although the identities of these products is unknown in both cases and may be different.

The apparent lack of byproducts (other than unretained products) in the HPLC chromatograms indicates their relatively low concentrations. In the nitrogen-sparged experiment, however, the smaller amount of byproducts may be due to the formation of coupling products similar to those proposed in Scheme IV (Figure 4-23). Azo and azoxy multiple-ring compounds have been shown in other work (Peyton, et al. 1997) to be retained longer than single-ring products on the LC-18 column used in this study, so they could not be tracked under these conditions. Furthermore, repeated coupling yields lower concentrations of larger products, which probably reduces their detectability. The method used was developed for high sample throughput to allow the collection of as many kinetic data points as possible, while still resolving the maximum number of products. However, it was also observed that the size of the unretained peaks grew with treatment time, even after DNT had been completely removed. This is seen in Figure 4-30, and may be, in part, due to compounds resulting from decomposition of various coupling byproducts (not detected during HPLC analysis) by continued treatment.

As can be seen from Figure 4-31, some additional byproducts were observed when samples from similar DNT experiments (A32 and A33) were analyzed under different HPLC conditions (higher organic content in the mobile phase) that were chosen to elute these compounds. More later-eluting compounds seem to be present in the nitrogen-sparged solution (Experiment A32), consistent with the coupling hypothesis. To identify those and other byproducts, an experiment (A39) was performed in which a high concentration of DNT (0.5mM) was treated by H_2O_2/UV in nitrogen-sparged solution. High concentration DNT was used to develop the highest concentrations of byproducts, allowing easier identification. At lower concentrations, many compounds produce response on an HPLC, but are too low in concentration to identify. The conditions for HPLC analysis were similar to those used in the Experiment A24 to achieve a better peak separation, but the analyses were carried to longer times to allow detection of later-eluting peaks. Figure 4-32 shows a byproduct distribution at DNT conversion ξ_{DNT} = 0.87. The data presented in the Figure 4-33 indicate that the majority of byproducts continued to grow when DNT was present, but started to decline when DNT was almost gone.

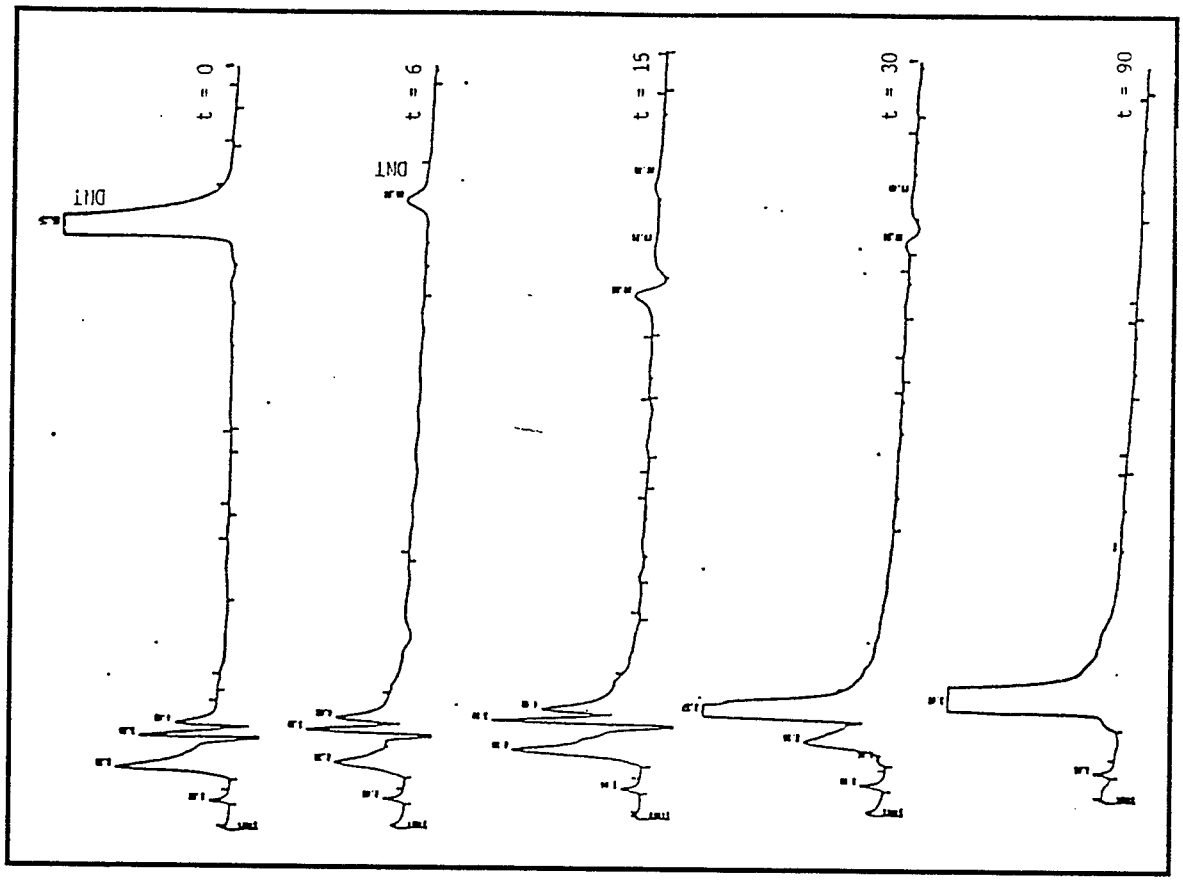

Figure 4-30. Chromatogram of successive samples from Experiment A24 (N_2-sparge). Peaks with retention times 18.26 min (chromato-gram at 15 min) and 19.30 min (chromatogram at 30 min) are artifacts.

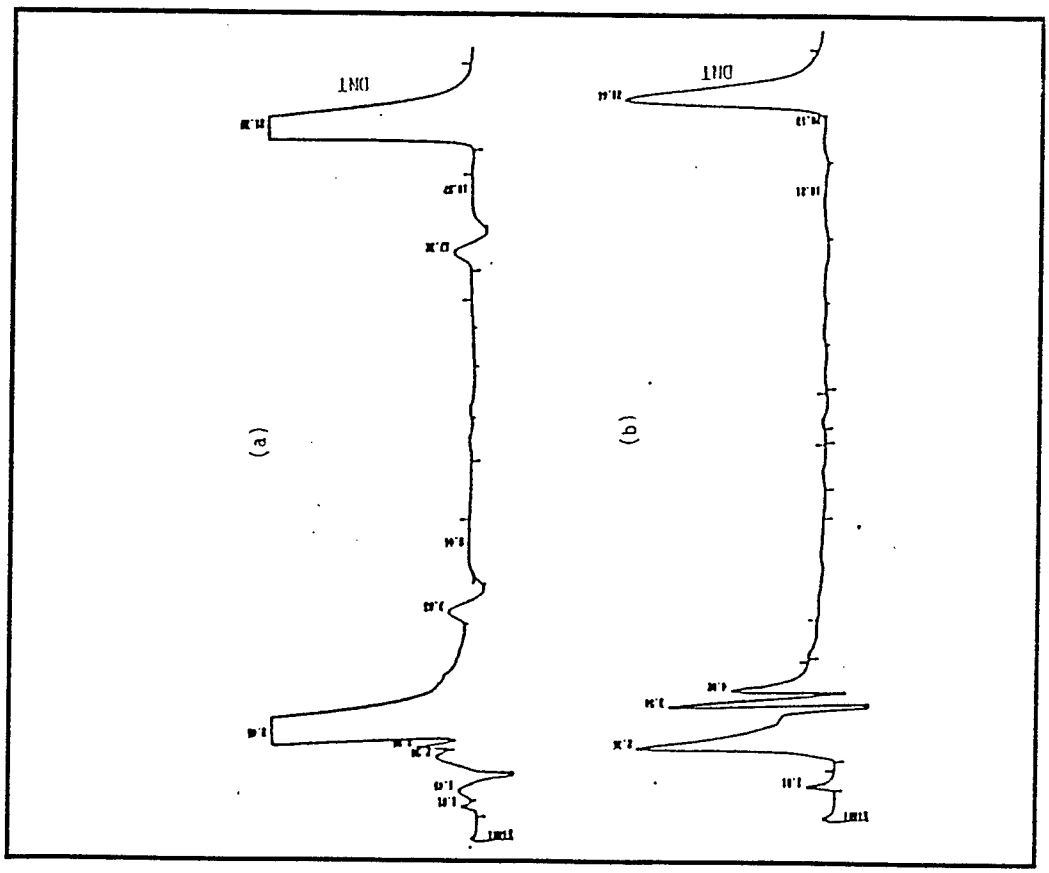

Figure 4-29. DNT byproduct distribution on C_{18} column: (a) after 90 min of H_2O_2 /UV treatment in O_2-sparged solution (ξ_{DNT} = 0.29); (b) after 2 min of H_2O_2/UV treatment in N_2-sparged solution (ξ_{DNT} = 0.68). Peaks at 7.03 and 17.32 min in chromatogram (a) are artifacts.

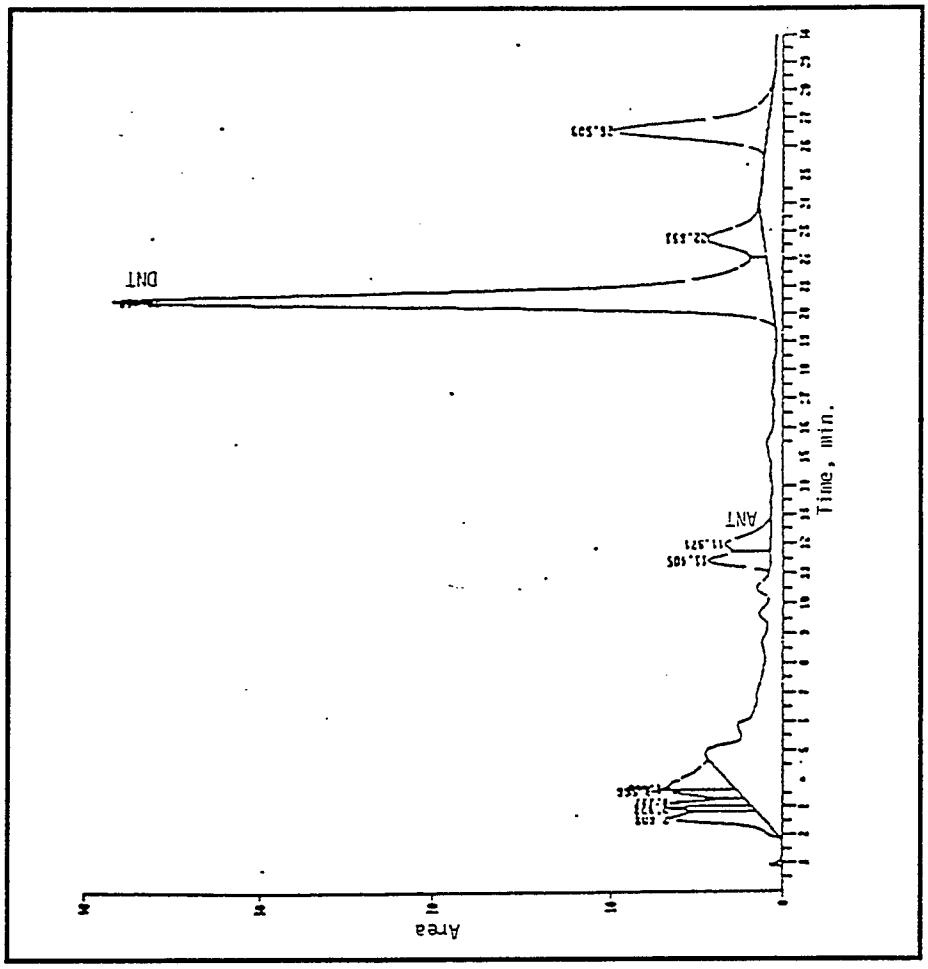

Figure 4-32. Chromatogram of 45-min sample from Experiment A39 (N_2-sparge).

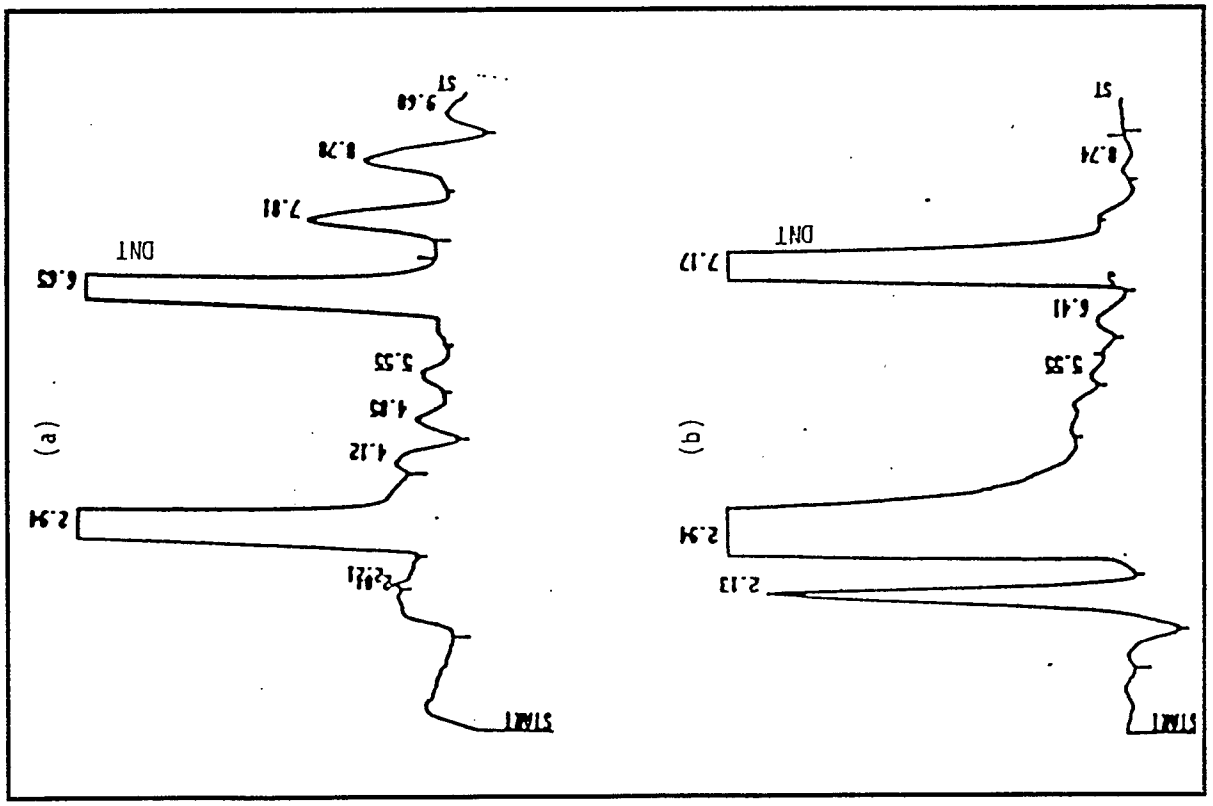

Figure 4-31. DNT byproduct distribution on C_{18} column: (a) after 1 mn of H_2O_2/UV treatment in N_2-sparged solution (ξ_{DNT} = 0.34), (b) after 220 min of H_2O_2/UV treatment in O_2-sparged solution (ξ_{DNT} = 0.16).

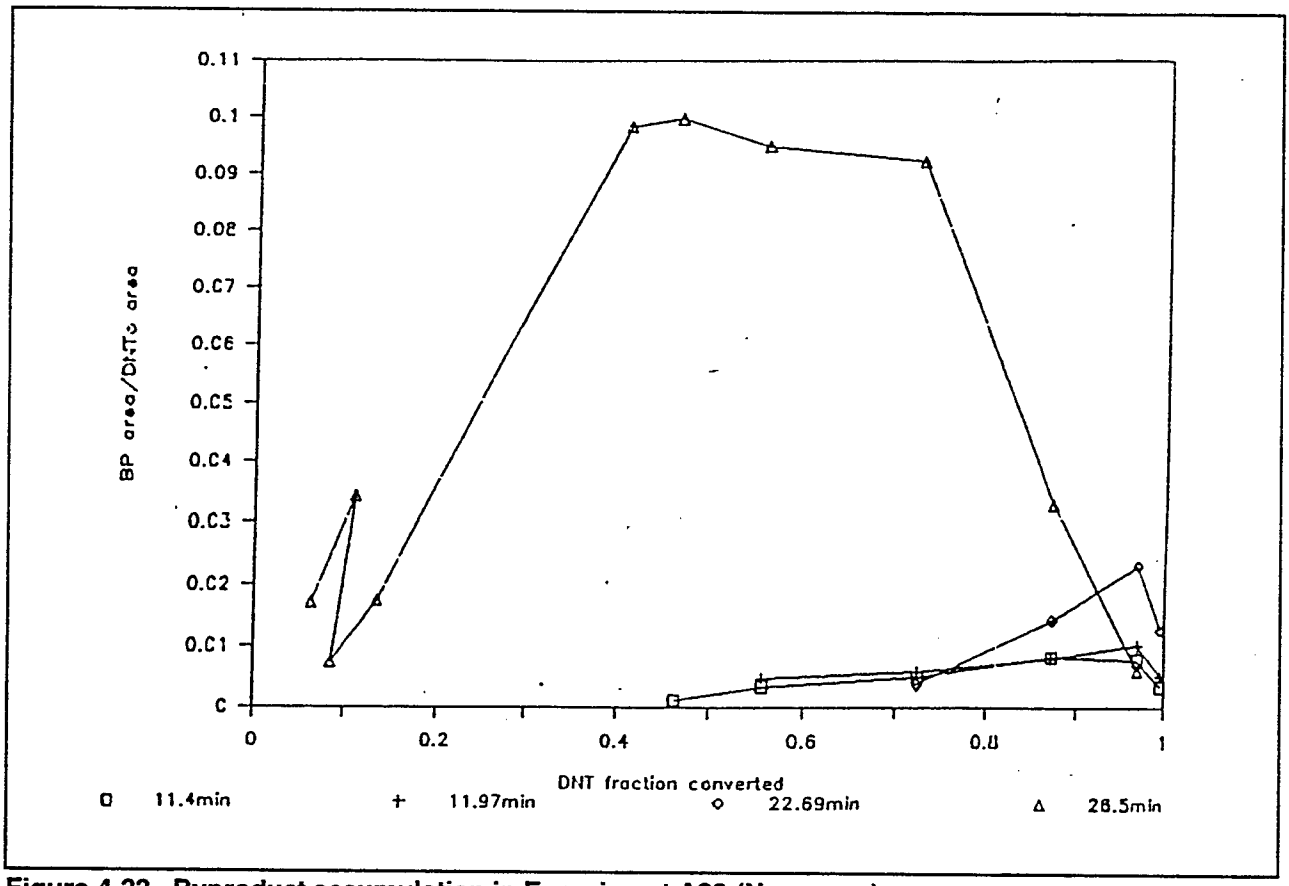

Figure 4-33. Byproduct accumulation in Experiment A39 (N_2-sparge).

However, unretained compounds (not shown) continued to grow beyond this point similar to observations during other nitrogen-sparged experiments (e.g., Figure 4-30). Although retention times for some peaks seen in Figure 4-30 were close to those for various nitrogen compounds used as standards, a match between the UV spectra of unknowns and standards was found only for the peak eluted at 11.97 minutes. Both the retention time and spectrum of this peak were very similar to those of 2-amino-4-nitrotoluene (ANT). The byproduct identification was, in general, difficult because many of the standards for the types of compounds postulated in Scheme IV were not commercially available. Under these conditions, byproduct identification represents a major effort involving synthesis and purification of suspected intermediates, characterization by MS, NMR, IR, etc. This effort alone would be a full-time multi-year project. The study was limited to the positive identification of products for which authentic standards are available.

The most probable means of ANT formation is reduction of one of the nitro groups of DNT. Detection of ANT is consistent with the proposed model that predicts the formation of amino compounds as a result of a reductive attack of ethanol radical on DNT. The low ANT concentration (0.004mM or $4x10^{-6}$M) observed in the experiment is also consistent with the model, since ANT

precursors (see Scheme IV [Figure 23]) are expected to participate in a variety of reactions including coupling. In addition, ANT itself may be susceptible to further reaction (including oxidation) during the course of treatment. For instance, many aromatic amines can be diazotized in the presence of nitrous acid, which is often present when nitro compounds are treated with AOPs, due to nitrite ejection in acidic solution. Diazotation may be followed by coupling to give azo compounds.

Since DNB is the most persistent product found in typical AOP treatment of DNT and it was also demonstrated to be easily reduced by ethanol radical, an experiment (A38) was performed at a high concentration of DNB to identify its reduction byproducts. Only two compounds could be identified using available standards. One of them was 3-nitroaniline (3NA), the retention time and UV spectrum of which almost perfectly matched those of the corresponding standard. The other compound had a retention time and a spectrum similar to those of 3-nitrophenol (3NP). Similar to ANT formation from DNT, nitroaniline results from DNB reduction. Although the identification of all byproducts has not been achieved, the detection of amino compounds alone may be considered as significant evidence of the reductive nature of DNT (and DNB) destruction under the conditions of our experiments, and is thus consistent with the proposed mechanism.

Study System I: RAAP Wastewater—DNT in Aqueous Ethanol

Mechanistic Determination

The mechanism of DNT destruction during the AOP treatment of DNT in aqueous ethanol solutions was determined to be a reductive step involving radicals produced by OH radical attack on ethanol, in parallel with direct OH radical attack on DNT. In the case of H_2O_2/UV experiments at high ethanol concentration, the reductive step was of primary importance in DNT removal. However, during O_3/UV treatment of DNT/ethanol solutions, most DNT removal was effected by OH radical, due to scavenging of ethanol radical by oxygen. The mechanism, its determination, and the resulting kinetic equation for the reductive part of treatment were discussed above in detail and also reported in a research communication (Peyton et al. 1995).

Results of modeling simultaneous ethanol- and hydroxyl-radical attack on DNT were successful in describing O_3/UV treatability experiments carried out in earlier stages of this project (discussed below). In addition, 1,3,5-trinitrobenzene, DNB, and TNT were shown to behave similarly to DNT in terms of susceptibility to the reductive reaction. This is significant since TNB removal is often the cost-determining step in the AOP treatment of groundwater contaminated by TNT. No evidence has emerged that calls the current mechanistic picture into question. The kinetic model resulting directly from the mechanistic model described the disappearance of DNT from the start of H_2O_2/UV treatment to well below 1 percent remaining. It is this crucial last stage of treatment that is usually the most difficult to model, but the most

influential on the treatment process optimization calculations and treatment cost estimate derived from the kinetic model.

Reductive Process vs. Oxidation by OH Radical

The model must also address system behavior at a "transition region" between conditions where the reductive process is the primary pathway for DNT removal, and the region in which reducing-radical precursors (e.g., ethanol and acetaldehyde) are depleted to the point that OH-radical reaction becomes the primary removal mechanism. Statement of the problem in this way implicitly assumes that two separate descriptions of behavior in each region must be joined by some model that blends one into the other in a transition region. Such descriptions are often used in science (and particularly in kinetics) when an acceptable but complicated model for behavior in each region is already established, but the complications of describing the entire system with a comprehensive model are prohibitive. Although this may turn out to be the case in some AOP systems, the comprehensive model approach was attempted first.

Model Development for O_3/UV Treatment of DNT

An earlier model was described for DNT removal by a reductive attack of ethanol radical formed in the reaction of OH radical with ethanol during H_2O_2/UV treatment. Equation (4-36) was derived to describe DNT disappearance ($\dot{D}_E$) due to reaction with ethanol radical:

$$\dot{D}_E = \nu_e \nu_D f_\alpha f_{OE} \eta \dot{D}_u \qquad \textbf{(4-36)}$$

where ν_D and ν_e are the efficiencies of ethanol radical capture by DNT and escape of the resulting radical to products, respectively. $\dot{D}_E$ is the utilized ozone dose rate (essentially, the rate of ozone transfer into solution) and f_α and f_{OE} are the fraction of ethanol molecules that are attacked at the alpha-position and the fraction of hydroxyl radicals that attack ethanol, respectively. This equation is discussed above in detail starting with equation 4-13.

To describe the DNT destruction during O_3/UV treatment where both oxidative and reductive processes may contribute to the overall removal of DNT, another term must be introduced:

$$\dot{D} = \dot{D}_E + \dot{D}_{OH} \qquad \textbf{(4-37)}$$

where $\dot{D}_E$ is the rate of DNT removal by ethanol radical and $\dot{D}_{OH}$ is the rate of DNT removal by OH radical.

$$\dot{D}_{OH} = f_{OD} \eta \dot{D}_u \qquad \textbf{(4-38)}$$

where f_{OD} is the fraction of OH radicals captured by DNT and η is the efficiency of OH production from ozone. Substitution of equations 4-36 and 4-38 into equation 4-37 and further rearrangements led to:

$$-\frac{\dot{D}}{D}=\left(\frac{2E}{\alpha}+1\right)\frac{\eta\dot{D}_u k_{OD}}{\sum_o} \quad \textbf{(4-39)}$$

where $\alpha = k_{RX}[O_2]/k_{RD} = 46[O_2]$, in which k_{RX} and k_{RD} are the rate constants for reaction of ethanol radical with oxygen (X) and DNT (D), respectively, and the ratio of the rate constants was determined experimentally. The term $2E/\alpha$ in equation 4-39 is the ratio of the ethanol radical to hydroxyl radical reaction rate with DNT. Calculation of this term reveals which active species is primarily responsible for contaminant removal. Integration of equation 4-39 gives:

$$-lnD/D_o = I \quad \textbf{(4-40)}$$

or:

$$\frac{D}{D_o} = e^{-I} \quad \textbf{(4-41)}$$

where:

$$I=\int_0^t \frac{\eta\dot{D}_u k_{OD}}{\sum_0}\left(\frac{2E}{\alpha}+1\right)dt \quad \textbf{(4-42)}$$

In this equation the abbreviation $\sum_0=\sum_i k_{oi}S_i$ has been used. The sum runs over all species S that react with OH radical.

The data from Experiment A-15 were used in Equation 4-42 to test the ability of the model to simulate treatment systems in which both hydroxyl radical and ethanol radical are important. This O_3/UV experiment (DNT_o=0.84 mM, $EtOH_o$=69.5 mM, $[\text{diethyl ether}]_o$=4.6 mM) was one of the two experiments for which sufficient byproduct measurements were made to enable the competition sum (Σ_o in equation 4-39) to be calculated. Assuming η = 1, $[O_2]$ = 25.5 mg/L (dissolved oxygen concentration was not measured) and using k_{OD} value 2.4×10^8 M^{-1} sec^{-1} determined above, the values D/D_o were calculated for the conditions of experiment A15 and compared with actual experimental data. At the time of the experiment, the dissolved oxygen concentration was not measured because the importance of oxygen concentration was still unrecognized. The results are presented in Figure 4-34, together with several profiles calculated assuming various reduced concentrations of oxygen (50 and 80 percent saturated). It can be seen from Figure 4-34 that the calculated disappearance curves are in reasonably good agreement with the experimental data, and that the best fit is given by assuming 50 percent saturation, relative to a pure oxygen atmosphere.

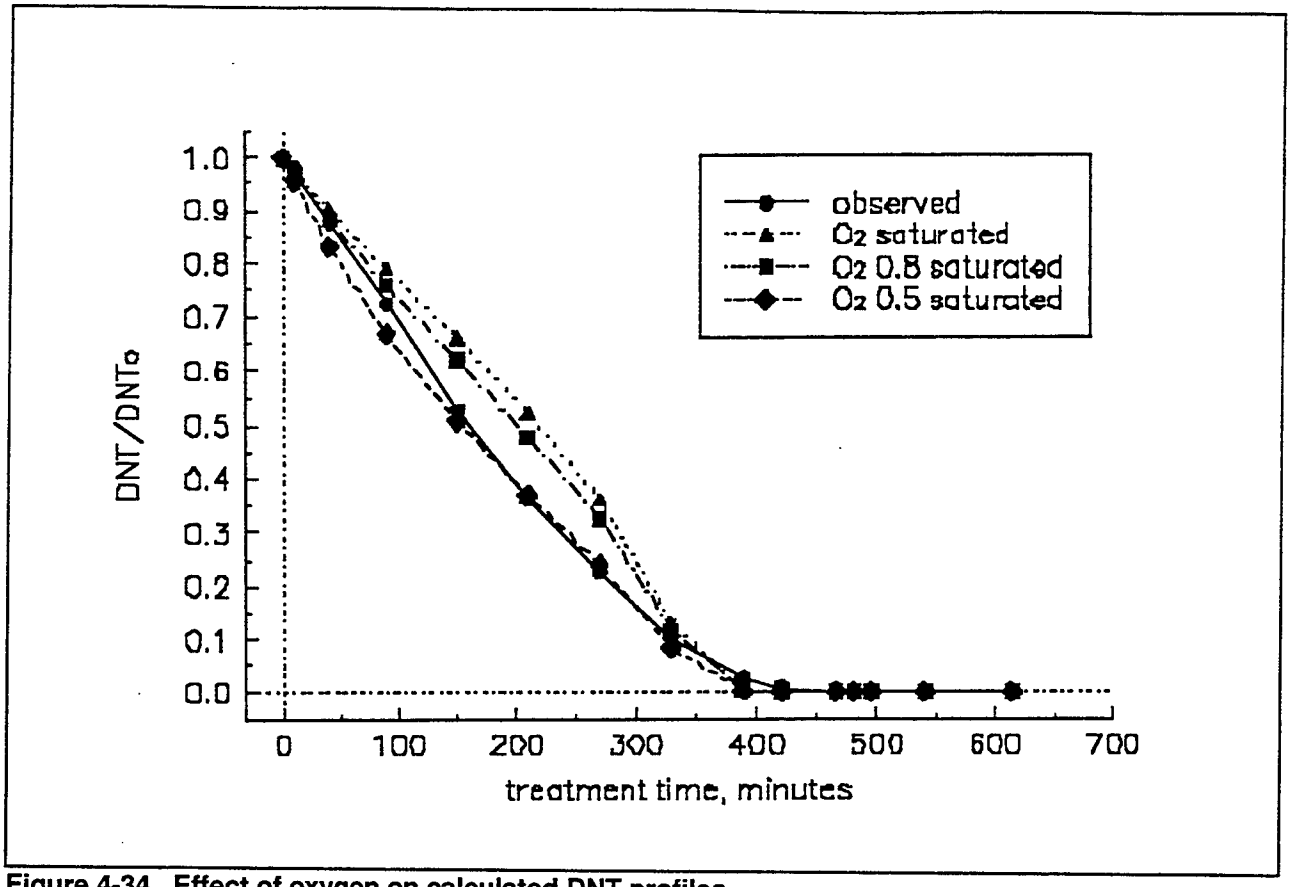

Figure 4-34. Effect of oxygen on calculated DNT profiles.

A similar simulation was done for the experiment A19 where DNT was treated with O_3/UV using a high power lamp (Solarchem 1-kw lamp, instead of 3.5 low-pressure lamps totaling 57 w of power consumed). In this case, the actual DNT removal was much faster than that predicted by the model (Figure 4-35).

The two most likely reasons for the inability of the model to describe treatment with the high powered lamps are: (1) the rate of direct DNT photolysis by a high power lamp is undoubtedly much higher than with 254 nm low pressure lamps used in Experiment A15, since the UV intensity is 50 times higher, and (2) higher intensity of the Solarchem lamp at shorter wavelength makes ozone photolysis followed by photolysis of the H_2O_2 that is formed a more important hydroxyl radical generation process relative to generation of OH radical by direct promotion, i.e., by electron transfer to ozone. The model was developed for the conditions of low UV power where DNT and hydrogen peroxide photolysis are slow compared to promotion, and therefore the rate equation does not contain terms representing these processes. Since the 18-fold increase in power consumption for UV generation results in an 18-fold increase in DNT disappearance, the higher-powered UV process is not necessarily more cost-effective. It is clear, however, that the model is not appropriate for high-powered lamps without the inclusion of additional terms in the rate equation.

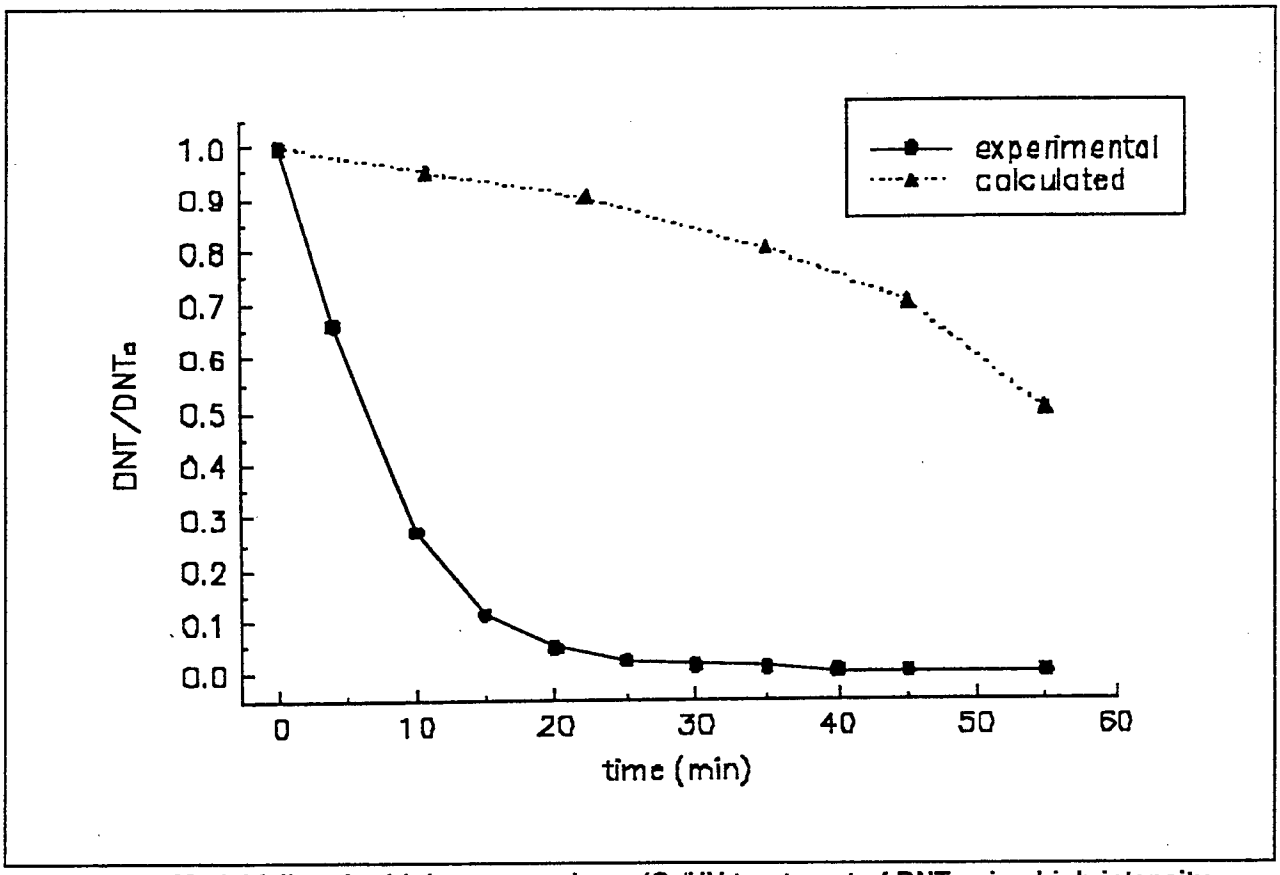

Figure 4-35. Model failure for high-pressure lamp (O_3/UV treatment of DNT using high-intensity lamp).

Experiments A-15 and A-19 were the only two experiments in the previous year's set of experiments in which both acetaldehyde and acetic acid were quantified throughout the experiment. These data are necessary for calculation of Σ_o in equation 4-42. Also, as stated previously, oxygen concentration data was not available for experiment A-15. More data were needed to confirm (or refute) the validity of the model for O_3/UV treatment using low-pressure lamps.

Experiment A-54 was an O_3/UV experiment in which the initial composition of the solution was close to the composition of the actual DNT wastewater. The oxygen concentration measurement method had been implemented by the time of Experiment A-54, and additional organic analytes (e.g., acetic acid and oxalic acid) were quantified as well, for inclusion in the scavenger sum (Σ_o in equation 4-39), since it was possible that they could become important scavengers in the later stages of treatment.

The experimental and calculated results are shown in Figure 4-36. Numerical integration of equation 4-42 involved input of pointwise data for six experimentally-measured quantities (DNT, ethanol, acetaldehyde, acetic acid, and oxalic acid concentrations and $\dot{D}_U$), thereby creating the possibility of accumulation of experimental error to a level that could seriously degrade the calculation (a well-known problem with numerical integration). Figure 4-36

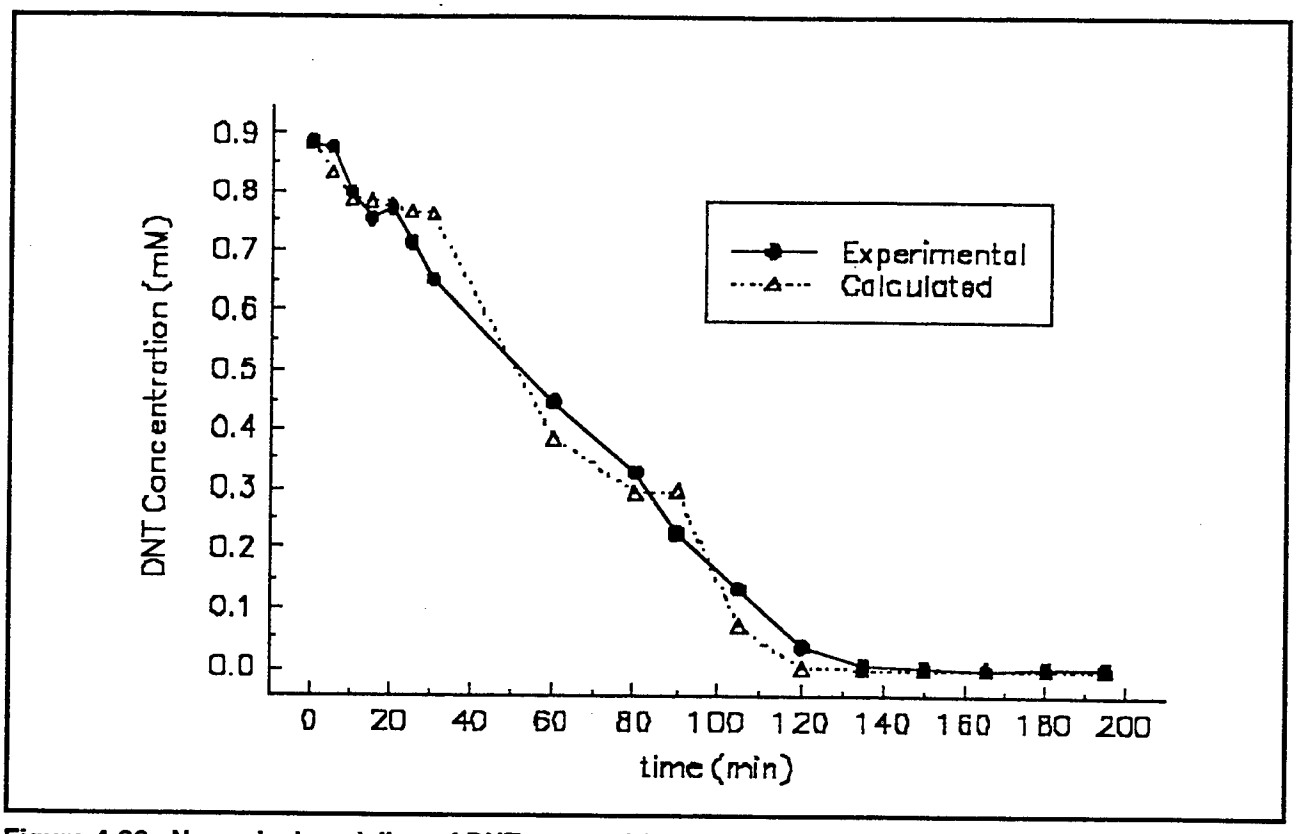

Figure 4-36. Numerical modeling of DNT removal (combined oxidative and reductive removal).

shows the calculation to be robust in this regard, in that the predicted result seems able to recover from irregularities that appear to be associated with the "roughness" of the DNT disappearance curve. This is a promising result, since, regardless of the irregularity of the calculated curve, the treatment time is predicted within about 10 percent. Inspection of the results of the numerical integration revealed that the reason that the calculated curve fell short during the 90- to 135-minute period is that some of the organic analytes fell below the detection limit during this time, and thus could not be included in the competition sum, resulting in overestimation of the DNT removal rate.

In Experiment A-15, the radical scavengers were at relatively high concentration (molar ratio of ethanol:DNT=83:1) so that DNT scavenged only a small fraction of OH radical. In A-54, sufficient DNT was present (ethanol:DNT=2:1) so that DNT was better able to compete for OH radical. The ratio of ethanol radical to hydroxyl radical removal of DNT ($2E/\alpha$ in equation 4-39) was calculated to vary between 1.1 and 3.8 (i.e., 52 to 79 percent removal by ethanol radical and 48 to 21 percent by hydroxyl radical) during the first 150 minutes (47 percent total DNT removal) of Experiment A-15, but only 0.02 to 0.08 (2 to 8 percent removal by ethanol radical, 92 to 98 percent removal by hydroxyl radical) during the first 60 minutes (50 percent total DNT removal) of Experiment A-54.

Oxygen concentration was high in both experiments (25.5 mg/L and 32 mg/L in A-15 and A-54, respectively), so that oxygen might be expected to scavenge most of the ethanol radical, leaving little for DNT removal. These calculations

demonstrate the necessity of a mechanism-based model, and illustrate that, in some cases, it is not absolute, but relative water quality parameters that are important in determining the most important mechanistic pathway.

Byproducts

During kinetic experiments on the reductive treatment of TNB (using H_2O_2/UV to generate OH radical) two byproducts were tracked and identified by their retention times. One of them was 3,5-dinitroaniline (DNA) and the other one was 3,5-dinitrophenol (DNP). Appearance of DNA was expected, because the mechanistic model predicts the formation of amino compounds as a result of reductive attack of ethanol radical on nitro compounds. Dinitrophenol was also identified as a byproduct of TNB photolysis in a previous study (Peyton et al. 1992). The analogous byproducts 3-nitroaniline and 3-nitrophenol were found in the present project when DNB was treated with H_2O_2/UV in the presence of ethanol. The phenolic products could result from photoinduced nucleophilic substitution (HO- for $-NO_2$), but can also arise from amines in the presence of nitrite in acidic solutions. This reaction produces diazonium ions that can react with other aromatic compounds (particularly phenols) to produce coupling products (e.g., "azo" dyes). Diazonium ions are stable at reduced temperature (0 °C), but decompose by loss of nitrogen at elevated temperatures (30 °C) to produce phenols:

$$ArNH_2+HNO_2+H^+ \rightarrow ArN{=}N^+ + 2H_2O \qquad \text{(4-43)}$$

$$ArN{=}N^+ + H_2O \rightarrow ArOH + N_2 + H^+$$

where Ar is the aromatic portion of the molecule.

This reaction occurs rapidly and in good yield, and is expected to occur in our system, where nitrite ion formation can occur, and in which the pH drifts more acidic as treatment proceeds. This reaction would account for the 3-nitrophenol that was observed. The phenol formed by decomposition of the diazonium ions may couple with another diazonium ion to form diazo compounds similar to, but different from, those found by previous investigators during TNT photolysis, where compounds such as substituted azobenzenes were reported to be formed by the reaction of nitro—and hydroxylamine—intermediates. Repeated coupling leads to polymers.

A similar reductive experiment (A-53) was performed using nitrobenzene (NB) as the parent compound, because the expected products were known from the literature, and were available as authentic standard compounds. During H_2O_2/UV treatment of NB in the nitrogen-sparged aqueous ethanol solution, the corresponding amino compound, aniline, appeared at early stages of treatment (the maximum concentration was at ~8 min). Nitrosobenzene was also found at low concentrations. Its formation is also to be expected from the proposed mechanism for the reductive pathway. Both were tentatively identified by their retention times. As the concentration of the parent nitrobenzene decreased, the

nitrosobenzene concentration also decreased, and was at all times less than 10 percent of the remaining parent compound concentration. This relationship allows prediction of the maximum nitrosobenzene concentration present following treatment of the nitro compound to low levels.

Importance of Dissolved Oxygen to AOP Performance for DNT Removal

Effect on Reductive Pathway

It has already been seen that the minimization of the dissolved oxygen (DO) concentration is crucial to promotion of the reductive pathway. The quantitative relationship describing the effect of DO on reduction process efficiency has already been established, being embedded in the ν_D term in equation 4-36, which describes the case of the reductive pathway for DNT removal:

$$\nu_D = \frac{1}{1 + \frac{k_{RX}[O_2]}{k_{RD}D}} \quad \textbf{(4-44)}$$

The ratio k_{RX}/k_{RD} was measured to be 46, so the effect of oxygen on process efficiency depends on the ratio of the oxygen to DNT concentrations. This effect is most easily seen by the results of calculating (using equation 4-44) the value for several different oxygen concentrations, shown in Table 4-7. For a solution that is saturated with oxygen or air, the fraction of ethanol radicals (R) that is captured by DNT drops proportionately with DNT concentration. This means that, at constant oxygen concentration, the relative (i.e., normalized to initial concentration) rate of destruction will be the same in all cases, i.e., the half lives are the same. It should be noted, however, that, other things being equal, the reductive pathway proceeds five times as fast in an air-saturated solution as in an oxygen-saturated one. It is also seen that the fractions are rather small, until the oxygen concentration is decreased considerably below the air-saturation level.

Even at relatively high DNT concentrations, the oxygen concentration must be below 1 percent of oxygen saturation before the majority of ethanol radicals are captured by DNT. The importance of this efficiency can be seen from the following example. It has been observed that, in the presence of ethanol, the conversion efficiency (η) of ozone into hydroxyl radical approaches unity (Peyton, et al. 1995). Under these conditions, the removal efficiency of DNT would be the product of the efficiency with which ethanol radical is scavenged by DNT (ν_D, the values listed in Table 4-7) and the escape efficiency (ν_e). The escape efficiency remains relatively constant between (1/4) and (1/3). If ν_D was unity, the initial DNT concentration is 18 mg/L (10^{-4} M), and ν_e=1/4, then the cost for electrical power consumed in ozone generation is:

$$\frac{10^{-4}\,moles}{L} \cdot \frac{4OH}{DNT} \cdot \frac{48gO_3}{mole} \cdot \frac{1lb}{454g} \cdot \frac{3.8\times10^3 L}{kgal} \cdot \frac{11kWh}{lbO_3} \cdot \frac{\$0.08}{kWh} = \$0.14/kgal$$

Table 4-7. Effect of oxygen concentration on the efficiency of the reductive pathway.

		Efficiency where DNT concentration is:		
Condition	Oxygen [O_2], mM	181 mg/L (1 mM)	18 mg/L (0.1 mM)	2 mg/L (0.01 mM)
Oxygen-saturated	1.	0.021	0.002	0.0002
Air-saturated	0.2	0.10	0.011	0.0011
1% of O_2 sat'n.	0.01	0.68	0.18	0.021
0.1% of O_2 sat'n.	0.001	0.96	0.68	0.18
0.01% of O_2 sat'n.	0.0001	0.99+	0.96	0.68

This is a reasonable operating cost, whereas 100 times that (i.e., operation at 1 percent efficiency or ν_D = 0.01) would probably not be cost-effective at $14/kgal. The figure of 11 kwh/lb of O_3 is from Langlais, B., D. A. Reckhow, and D. R. Brink (1991).

For lower DNT concentrations, the oxygen concentration must be reduced even further to capture more than half of the radicals. This would seem to imply that during ozone/UV treatment, generation of ozone from air might be more effective than generation of ozone from oxygen, even though the electrical efficiency is lower by a factor of two, because the efficiency of the reductive reaction would be larger by a factor of five. It turns out that other factors also play an important role in this question. These complications are discussed below.

Effect on Oxidative Pathway

OH-Radical Generation by H_2O_2/UV. The effect of DO in the OH-radical portion of the pathway is more subtle than its effect on the reductive pathway. The discussion of this topic is most conveniently split into ozonation-based AOPs (such as O_3/UV or O_3/H_2O_2) and AOPs that do not require ozone (such as H_2O_2/UV). In the H_2O_2/UV system, hydroxyl radical is produced by photolysis of hydrogen peroxide

$$H_2O_2 \xrightarrow{h\nu} 2 \bullet OH \qquad \textbf{(4-45)}$$

Oxygen is not produced directly from the photolysis of peroxide unless hydroxyl radical attacks H_2O_2:

$$H_2O_2 + OH \varnothing HO_2 + HOH \qquad \textbf{(4-46)}$$

$$2\,HO_2 \varnothing H_2O_2 + O_2$$

Therefore in highly scavenged systems, such as when a high concentration of ethanol is present, only a small fraction of OH radical finds H_2O_2 and therefore little oxygen is formed by this pathway. When OH radical attacks organics, a

carbon-centered radical is formed, which then reacts quickly ($k \sim 2 \times 10^9\ M^{-1}s^{-1}$) with oxygen to form a peroxyl radical (RO_2). This peroxyl radical primarily: (1) eliminates superoxide, which disproportionates to yield H_2O_2 and oxygen, or (2) dimerizes, to yield hydrogen peroxide and perhaps a small amount of oxygen, while incorporating half of the oxygen into the organic molecule. This step is the central theme in the oxidation of organics. The above mechanisms are responsible for the regeneration of hydrogen peroxide in H_2O_2/UV treatment systems, as well as the ultimate oxidation of the organics to carbon dioxide. As long as some oxygen is present, those reactions will occur. If oxygen was completely excluded from the system, the organic radicals would dimerize to form larger molecules:

$$2R\bullet \rightarrow R-R \qquad \textbf{(4-47)}$$

At very low oxygen concentrations, the system will reach some balance between these pathways. If no oxygen is input into the system, the oxygen initially present will be consumed by formation of peroxyl radicals and oxidation of the organics present. In batch treatment or in flow systems with sufficiently high OH generation, this consumption constitutes a method for oxygen removal, as oxygen is gradually incorporated into the organic molecules. For this to be an effective method, the amount of OH radical generated must be several times the initial oxygen concentration. Under oxygen-saturated conditions, that requires generation of more than a millimole/L of OH radical.

OH-Radical Generation From Ozone. For ozonation systems, it can be seen that during the hydroxyl radical generation sequence:

$$O_3 + electron\ donor \rightarrow O_3^- \qquad \textbf{(4-48)}$$

$$O_3^- + H^+ \Leftrightarrow HO_3 \rightarrow HO + O_2 \qquad \textbf{(4-49)}$$

an oxygen molecule is generated for every OH radical that is generated. The usual electron donors are superoxide (O_2^-) and hydrogen peroxide, termed an "initiator" by Staehelin and Hoigné (1985), and generated as described above from the peroxyl radical dimers (tetroxides). A given organic molecule will usually generate predominantly superoxide or hydrogen peroxide. The initiator serves as the donor molecule shown in equation (4-48), liberating another oxygen molecule in the process. For superoxide, the initiation step is:

$$O_2^- + O_3 \rightarrow O_2 + O_3^- \qquad \textbf{(4-50)}$$

followed by the protonation reaction in equation 4-49. The net reaction for initiation by superoxide is therefore:

$$O_3 + O_2^- + H^+ \rightarrow OH + 2\,O_2 \qquad \textbf{(4-51)}$$

When the initiator is hydrogen peroxide:

$$H_2O_2 \Leftrightarrow HO_2^- + H^+$$
$$HO_2^- + O_3 \rightarrow HO_2 + O_3^- \quad (4\text{-}52)$$
$$HO_2 \Leftrightarrow H^+ + O_2^-$$

followed by equation 4-49. The net reaction for initiation by H_2O_2 is then:

$$H_2O_2 + 2O_3 \rightarrow 2OH + 3O_2 \quad (4\text{-}53)$$

Of the two molecules of oxygen (4 oxygen atoms) that went into the two peroxyl radicals, one is incorporated into the organics while one is converted to hydrogen peroxide, the yields of which appear from experimental results to be somewhat less than 100 percent.

Thus, in the above sequences, oxygen is first liberated in the formation of OH radical, but consumed again when the OH radical reacts with an organic compound, then some of it is again liberated when the peroxyl radicals decompose. Four cases arise, corresponding to superoxide (I) or peroxide (II) initiation, followed by superoxide (A) or peroxide (B) liberation upon peroxyl radical decomposition. The net reactions for the four cases are given below. Detailed intermediate reactions are given in Appendix A.

I. Initiation by superoxide

A. Superoxide liberation:

$$O_3 + HPH \rightarrow O_2 + H_2O + P \quad (4\text{-}54)$$

B. Hydrogen peroxide liberation:

$$O_3 + O_2^- + H^+ + HPH \rightarrow O_2 + \frac{1}{2}H_2O_2 + H_2O + PO \quad (4\text{-}55)$$

II. Initiation by Hydrogen Peroxide

A. Superoxide liberation:

$$O_3 + \frac{1}{2}H_2O_2 + HPH \rightarrow \frac{1}{2}O_2 + O_2^- + H^+ + H_2O + P \quad (4\text{-}56)$$

B. Hydrogen peroxide liberation:

$$O_3 + HPH \rightarrow H_2O + PO + \eta_\xi O_2 \quad (4\text{-}57)$$

where $\eta_x \leq 1$ is the yield of oxygen from the tetroxide (usually low, i.e., less than 10 percent). Therefore, not only will net oxygen consumption not occur, but the ensuing chemistry will actually contribute oxygen at the rate of OH radical production if the reaction is superoxide initiated, and half the rate of OH production or less in the case of peroxide initiation. Thus, with very good mass transfer characteristics in the reactor, it may be possible to maintain the oxygen content almost as low as the equilibrium value with the feed gas, but no lower.

With only moderately efficient mass transfer (as is the case in most ozonation reactors), there may be little difference between oxygen and air as the ozone carrier. This is consistent with experimental results obtained during earlier phases of the project.

It is also not possible to remove oxygen by sparging during application of an ozone-based process (for example, in a separate reactor following the ozonation reactor), because the ozone will also be sparged from solution. Therefore, any advantage to be gained in ozonation systems must be obtained by using ozone generator feed gas that has been depleted of oxygen. This option was not explored, because of the diminishing efficiency of ozone production at lower oxygen concentration in the feed gas.

Methods for Controlling DO

Ozonation Systems. It was seen above that oxygen consumption in ozonation systems will not deplete the oxygen concentration in solution below the value in equilibrium with the feed gas to the ozone generator. Thus, the only option is lowering the oxygen content of the feed gas. Lowering it from 100 to 20 percent (air) gives a reduction in power efficiency of about a factor of two, but the efficiency vs. oxygen concentration curve must drop off more rapidly at lower oxygen concentrations since it must approach zero at an oxygen concentration of zero. The exact shape of that curve will determine the optimum feed gas composition. There are probably questions of materials compatibility, nitrogen oxide formation, and other questions that arise in the use of oxygen-depleted gas streams in ozone generators.

H_2O_2/UV Systems. As was seen from the earlier experimental results, sparging of the reaction mixture by an inert gas is an effective method for oxygen control during H_2O_2/UV treatment. The dependence of the reaction efficiency on the oxygen concentration was discussed above. In a flow system, the oxygen concentration will depend on the composition and flow rate of the sparge gas, mass transfer characteristics and residence time in the reactor, and rate of OH-radical generation. To derive a predictive equation for the DNT removal rate, it is necessary to integrate the oxygen mass-balance equation and substitute the resulting expression for the oxygen concentration into the DNT rate equation. Thus, to use that equation to model DNT disappearance in a particular application, the mass transfer characteristics of the reactor being used must be known.

Within the two-film model for gas-liquid mass transfer:

$$\dot{X} = k_l A\left[\frac{X_g}{Z} - X\right] - \sum_i k_{X_i} S_i X + \sum_{jl} k_{kl} S_j S_l \qquad \text{(4-58)}$$

where the symbol X is used for the oxygen concentration, and Xg is the oxygen concentration in the gas (same units as X, mole/L). The two sums represent reactions that consume and produce oxygen, respectively. In ethanol solutions of relatively high ethanol concentration:

$$\sum_i k_{xi} S_i X \approx k_{XR} R X \approx R_g \quad \text{(4-59)}$$

where R is the ethanol radical and R_g is the OH-radical generation rate.

The second equal sign arises from the fact that essentially all OH radical is consumed by reaction with ethanol to form ethanol radical. Since ethanol is an efficient superoxide producer, every two OH attacks on ethanol liberates one O_2 by superoxide disproportionation:

$$2O_2^- + 2H^+ \rightarrow H_2O_2 + O_2 \quad \text{(4-60)}$$

and thus:

$$\sum_{j,l} k_{jl} S_j S_l \approx 0.5 R_g \quad \text{(4-61)}$$

This disproportionation reaction is not important in ozonation systems because of the rapid reaction of superoxide with ozone. Therefore, at steady-state, equation 4-58 simplifies to:

$$X = \frac{X_g}{Z} - \frac{R_g}{2 k_l A} \quad \text{(4-62)}$$

Thus, for constant oxygen concentration in the feed gas (X_g) a plot of experimentally-determined aqueous oxygen concentrations (X) versus the radical generation rate (R_g) for a series of experiments performed at different radical generation rates should give a straight line with intercept X_g/Z and slope $-1/2k_lA$. This provides a way to evaluate both the partition coefficient Z and the mass transfer coefficient k_lA. After these constants are evaluated, the solution of equation 4-58 (equation 4-62 in the steady-state case) provides the required expression for the oxygen concentration for substitution into the DNT rate equation to give the dependence of the DNT destruction rate on the treatment parameters that affect the oxygen concentration in solution.

This method was used to evaluate k_lA and Z for the experimental system used for the H_2O_2/UV experiments. Several series of experiments were performed, in which an OH radical was generated by UV photolysis of 13.3 mM H_2O_2, and converted to an ethanol radical by the inclusion of 137 mM ethanol in the solution. Under these conditions, ethanol scavenges 99.9 percent of the OH radicals. The equilibrium O_2 concentrations were measured for 3 to 5 different UV intensities at the same gas flow rate, Q_g=1.2 std. L/min ($V_{reactor}$=8.5 L). A series of experiments was then performed in which the ethanol solution was saturated with oxygen or air, then gas flow discontinued, and the disappearance rate of oxygen was monitored upon H_2O_2 photolysis. No oxygen loss due to outgassing was observed in the dark, even though the reactor was stirred at 550 rpm. Under photolytic conditions with no gas flow, the oxygen rate equation (eq. 4-58) simplifies to:

$$\dot{X} = -\sum_i k_{x_i} S_i X + \sum_{j,l} k_{j,l} S_j S_l$$

$$= net\ rate\ of\ O_2\ consumption \equiv r_c \qquad \text{(4-63)}$$

and equation 4-62 becomes:

$$X = \frac{X_g}{Z} - \frac{r_c}{k_l A} \qquad \text{(4-64)}$$

Figures 4-37 and 4-38 show plots of $X_{equilibrium}$ versus r_c for oxygen and air sparging, respectively. Values of k_lA for the oxygen and air experiments were calculated from the slopes of those plots to be 1.7±0.8 and 1.1±0.1 min^{-1}, respectively. The partition coefficient for oxygen was calculated to be 43±2 and 37±1 from the oxygen and air experiments, respectively. The mass transfer coefficients are probably low because of the low $Q_g/V_{reactor}$ ratio employed in these experiments. Differences between k_lA and Z values determined for oxygen and air sparging are probably due to the simplicity of the model, as they should be the same in both cases. Nonetheless, the utility of this relatively simple procedure in reactor characterization for modeling and scale-up is apparent.

Treatment Efficiency

Ozone, hydrogen peroxide, and ultraviolet light are all relatively expensive treatment agents compared to many treatment processes currently in common use. It is of the utmost importance to maximize the efficiency of use of these agents, for the AOPs to be economically feasible. The "cumulative treatment efficiency" is defined as the amount of contaminant destroyed per amount of ozone used. It is called "cumulative" because it describes an integrated result for a period of time over which the instantaneous efficiency may not be constant. Because of the relationship to reaction stoichiometry, molar units must be used for ΔP and D_u. For the case where f_{OR} is constant:

$$\varepsilon = \frac{\Delta R}{D_U} = \overline{\eta}\, f_{OR} = \overline{\eta} \frac{k_{OR} R}{\sum_I k_{Oi} S_i} \qquad \text{(4-65)}$$

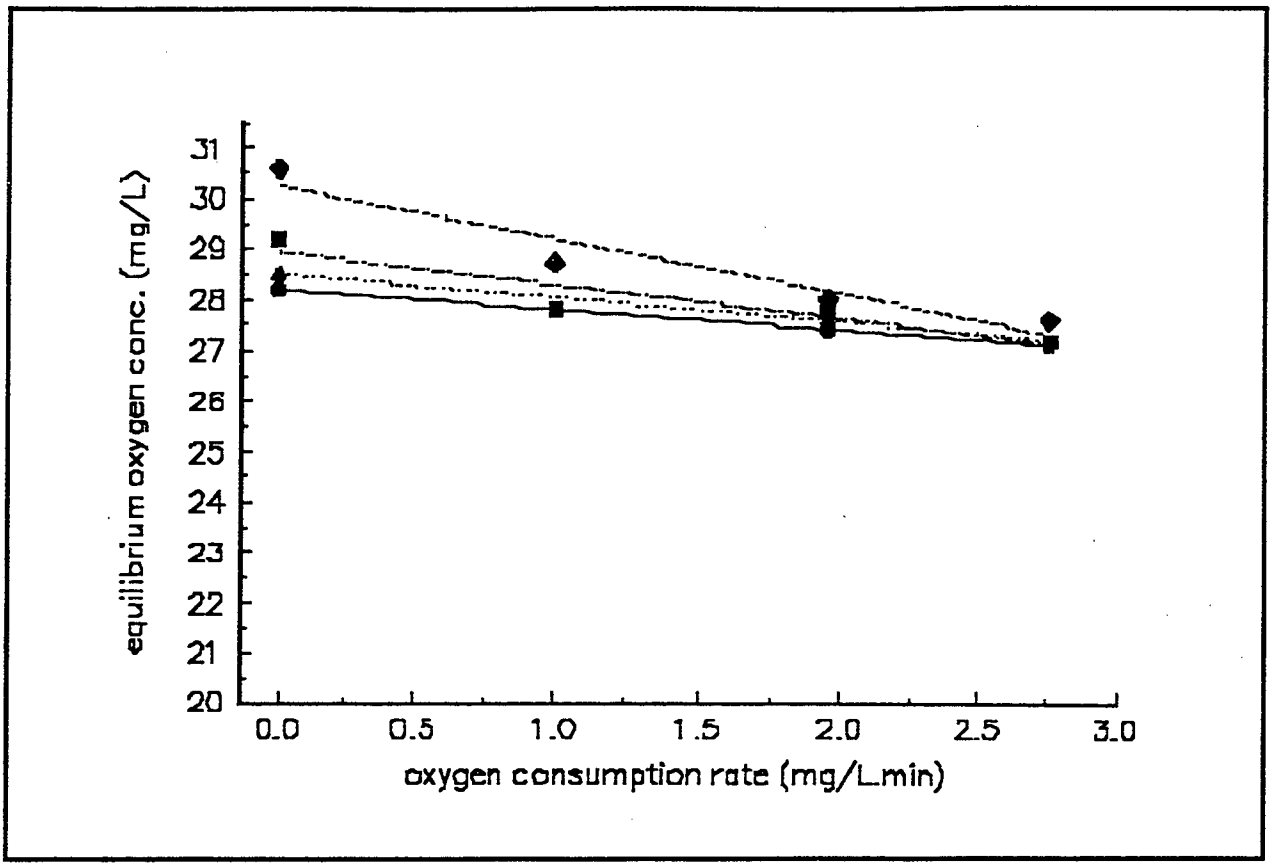

Figure 4-37. Equilibrium oxygen concentration (mg/L) as a function of oxygen consumption rate.

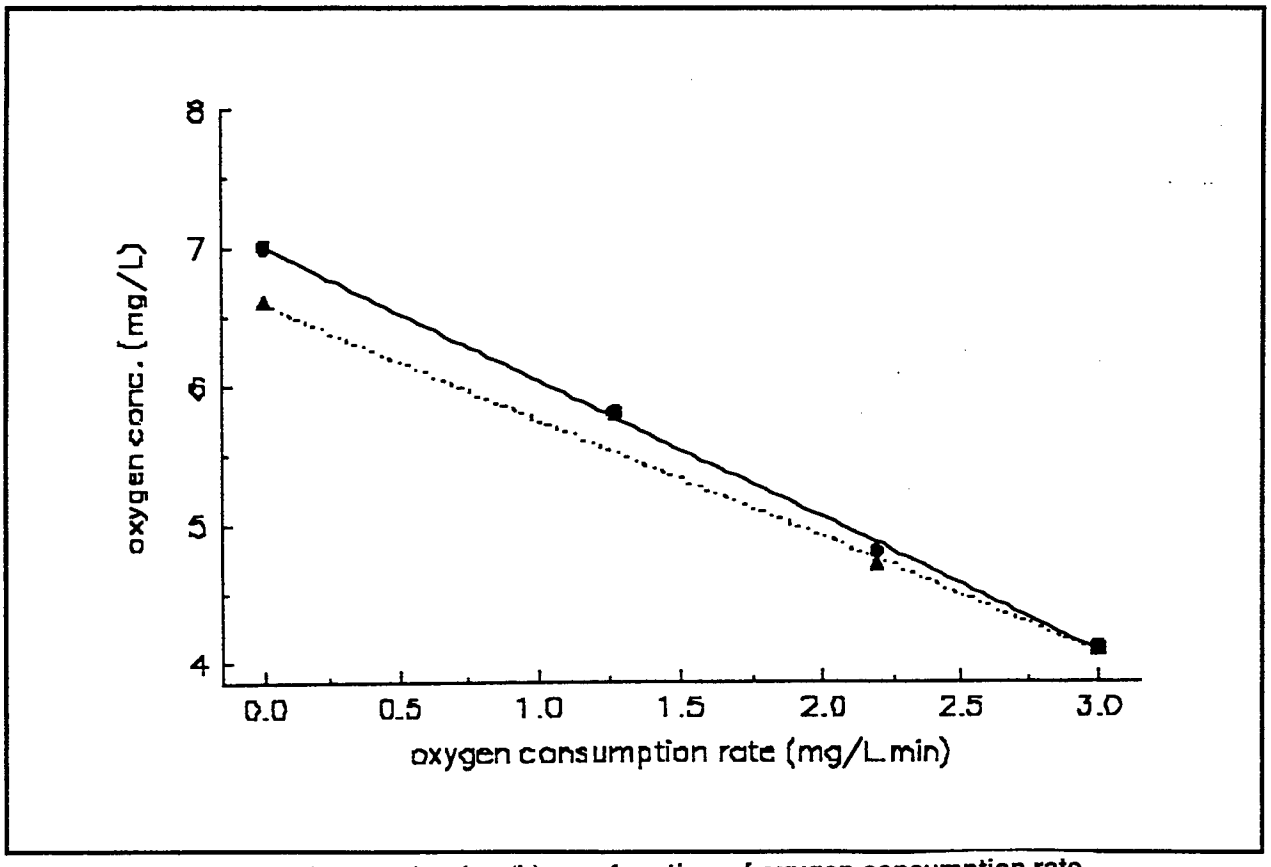

Figure 4-38. Oxygen concentration (mg/L) as a function of oxygen consumption rate.

where the second and third equal signs are the result of rearrangement of equation 4-36 and the substitution of equation 4-37, respectively. Since this equation describes behavior over a time period, in practice it is often necessary to assume that the concentrations R and S_i do not change over that period, or to pick a sufficiently short time period so that the assumption is valid. In the absence of that assumption, the expression becomes considerably more complicated. When the time period is infinitesimally small, $\Delta R/D_u$ approaches $dR/dD_u = \dot{R}/\dot{U}$, the efficiency defined is known as the "instantaneous" efficiency, and no constancy assumptions are required for h, R, and S_i.

Kinetic Model for Flow Treatment

In previous work on batch treatment systems (Peyton et al. 1995), conditions were optimized for verification of the model and measurement of kinetic parameters, rather than for cost-effectiveness of treatment. Ethanol and hydrogen peroxide concentrations were sufficiently high that all hydroxyl radical was scavenged by those solutes, so that virtually no hydroxyl radical reached the DNT. In addition, the peroxide concentration was high enough to absorb most of the photons, so that DNT photolysis was negligible. Thus, the situation was simplified in that DNT removal was solely due to reducing radical attack in those experiments.

At the DNT and ethanol concentrations present in the actual wastewater, DNT photolysis, OH attack, and reducing radical attack are all important modes of DNT removal, and so terms representing all three processes must be included in the rate equations. The photolytic process was represented by:

$$D_{phot} = \phi_D F_D I_o \qquad \textbf{(4-66)}$$

where I_o is the application rate of photons (the UV "dose rate") in einsteins/L/minute, F_D is the fraction of photons capture by DNT (subscript D), and ϕ_D is the quantum efficiency of DNT destruction upon absorbing a photon (i.e., fraction of absorptions that result in a DNT decomposition). For flow treatment, the feed and effluent terms are included, and $\dot{D}$ set to zero, since only steady-state operation is of interest:

$$0 = \dot{D} = \frac{Q}{V_R}(D_o - D) - \phi_D F_D I_o \qquad \textbf{(4-67)}$$

This equation was solved for ϕ_D, and experimentally-measured values of Q (flowrate), V_R (reactor volume), D_o (initial DNT concentration), D (effluent DNT concentration), and I_o (UV dose) were substituted into the equation to evaluate the quantum efficiency. The quantity F_D was calculated from:

$$F_D = f_D F_T = \frac{\in_D D\, l_{eff}}{A_t}(1-10^{A_t}) \quad \textbf{(4-68)}$$

where F_T is the total fraction of photons absorbed, f_D is the fraction of those that were absorbed by DNT, A_t is the (1-cm) absorbance of the solution times the effective path length l_{eff}, and $\in_D$ is the extinction coefficient of DNT. This value of the quantum efficiency was then used in the photolysis term in the complete DNT rate equation.

The complete rate equation was constructed by incorporating terms for hydroxyl radical and reducing radical attack on DNT. Preliminary calculations indicated that the system would be operated at a high extent of conversion of ethanol to acetaldehyde, so that the possibility of DNT attack by acetaldehyde radical could not be discounted. Since acetaldehyde is present in both the carbonyl and diol (hydrated carbonyl) forms, there are two branches to the acetyl radical pathway. The diol radical ($CH_3C[OH]_2$) is a reducing radical which can attack DNT or react with oxygen. The carbonyl form of the acetaldehyde radical (CH_3CO) forms a highly oxidizing peroxyl radical ($CH_3C[O]O_2$), with the net result that part of the acetaldehyde radicals could oxidize some species while the remainder reduced other species. At this point, the model only considers the reductive side, with respect to DNT reactions. The acetylperoxyl radical would not be expected to be as strong an oxidizing radical as OH radical, nor to be formed in as great a quantity as is OH, so for simplicity, the first version of the model does not take that reaction into consideration. The free-radical chemistry of acetaldehyde is discussed in more detail in *Modeling of Ethanol Oxidation* page 83 and by Schuchmann and von Sonntag (1988). The resulting DNT rate equation is:

$$0 = \dot{D} = \frac{Q}{V_R}(D_o - D) - \phi_D F_D I_o - f_{OD} R_g - f_{OE} f_\alpha \nu_e \nu_D R_g - f_{OA} f_r \nu_e \nu_{DA} R_g \quad \textbf{(4-69)}$$

where the f_{OE} and f_{OA} are the fractions of OH radical captured by ethanol and acetaldehyde, respectively, f_r is the fraction of acetaldehyde radicals that react through the diol radical, f_α is the fraction of OH radicals that attack ethanol in the α position, ν_D is the fraction of ethanol radicals that attack DNT, ν_{DA} is the fraction of acetaldehyde (diol) radicals that attack DNT, and ν_e is the fraction of DNT radical anions (formed by reducing radical attack on DNT) that escape to products. Except for the new acetaldehyde terms, these terms have the same meaning and symbols as earlier in this report. The DNT rate equation is not integrated as before, since the steady-state version ($\dot{D}$ =0) is no longer a differential equation, but is simply quadratic equation in D (since the form of a+bD appears in the denominators of the fractions ν_D), and is solved as such. The final solution of the DNT equation, written in terms of the quadratic formula, is:

$$\frac{D}{D_o} = \frac{b}{2a}\left[\sqrt{1-\frac{4ac}{b^2}} - 1\right] \quad \text{(4-70)}$$

where a=1:

$$b = \frac{\gamma X}{D_o} + \frac{\left[\frac{(f_a k_{OE} E + f_r k_{OA} A)}{\Sigma_o} \nu_e \frac{D_{OH}}{D_o} - 1\right]}{(1 + \alpha + \frac{k_{OD} D_{OH}}{\Sigma_o})} \quad \text{(4-71)}$$

and:

$$c = \frac{\gamma X}{D_0(1 + \alpha + \frac{k_{OD} D_{OH}}{\Sigma_0})} \quad \text{(4-72)}$$

with:

$$\gamma = \frac{k_{RX}}{k_{RD}} = \frac{k_{rX}}{k_{rD}} \quad \text{(4-73)}$$

where r=acetaldehyde radical, R=ethanol radical, and X=oxygen. The assumption in equation 4-73 is reasonable in view of the similarity of the ethanol (i.e., 1-hydroxyethyl) and hydrated acetaldehyde (i.e., 1,1-dihydroxyethyl) radicals. Rate constants for reaction of carbon-centered radicals with oxygen tend to be very similar for most radicals (von Sonntag 1987). D_{OH} is the average hydroxyl radical dose, given by the hydroxyl radical generation rate (R_g) times the average residence time ($t_R=V_R/Q$). The hydroxyl radical generation rate is given by:

$$R_\gamma = \phi_P \frac{\varepsilon_P P}{A_{1cm}} I_o \quad \text{(4-74)}$$

which is the product of the quantum yield for OH production by peroxide photolysis, the fraction of photons captured by hydrogen peroxide, and the applied photon dose rate. The quantity Σ_o is the "competition sum" for hydroxyl radical, given by:

$$\Sigma_o = \sum_i k_{Oi} S_i \quad \text{(4-75)}$$

which runs over all species with which OH radical reacts. In the present case, the major contributors to the sum are ethanol, acetaldehyde, and hydrogen peroxide. Although removal of DNT by OH attack is a significant DNT sink, comparison of the relative rates of the OH-DNT and OH-ethanol reactions shows that DNT is not a significant sink for OH:

$$\frac{k_{OD}OD}{k_{OE}OE} = \frac{k_{OD}D}{k_{OE}E} = \frac{2.4x10^{8}\ (1.7x10^{-4})}{1.9x10^{9}\ (4x10^{-3})} = 0.0054 \quad \textbf{(4-76)}$$

so that, when all OH scavengers are considered, DNT accounts for less than ½ percent of OH radical consumption, and need not be included in the sum. Similar arguments hold for DNT byproducts. With OH-radical rate constants of $8.5x10^{7}$ for acetate and $1.6x10^{7}$ for acetic acid, these substances need not be included unless the ethanol and acetaldehyde concentrations fall to very low values, which did not occur in the present study. Thus, terms for ethanol, acetaldehyde, and hydrogen peroxide in the competition sum are all that is needed.

Finally, α is the product of the DNT photolysis quantum yield, the fraction of photons absorbed by DNT, the photon dose rate, and the average residence time of the solution in the reactor:

$$\alpha = \phi_D \frac{\varepsilon_D}{A_{1cm}} I_o t_R \quad \textbf{(4-77)}$$

As before, $A_{1\,cm}$ is the 254 nm absorbance of the reactor charge in a 1-cm cell. No exponential term is required in the fraction of photons absorbed, since with 1-cm absorbances of 2 to 3 and a 3.27-cm pathlength in the reactor, virtually all photons are absorbed. Equations for ethanol and acetaldehyde are constructed similarly, but are simpler since there are only hydroxyl radical terms and the feed/washout term:

$$0 = \dot{E} = \frac{Q}{V_R}(E_o - E) - f_{OE}\ R_g \quad \textbf{(4-78)}$$

$$0 = \dot{A} = \frac{Q}{V_R}(A_o - A) + f_{OE} f_{\alpha} R_g - f_{OA} R_g \quad \textbf{(4-79)}$$

The presence of f_{α} in the acetaldehyde equation represents the fact that only attack of ethanol at the α position produces acetaldehyde.

The peroxide rate equation is somewhat more complicated, because, in addition to washout and disappearance terms, peroxide is also produced as a byproduct of free-radical reactions. In the rate equation:

$$0 = P = \frac{Q}{V_R}(P_0 - P) - \frac{1}{2}R_g - \frac{1}{2}f_{OP}R_g - \frac{\rho}{2}(1 - f_{OP})R_g \quad \textbf{(4-80)}$$

the order of the terms is feed/washout, peroxide photolysis, attack by hydroxyl radical, and peroxide regeneration as a byproduct of OH attack on all species other than peroxide. The ½ in the second (photolysis) term arises from the fact that two OH radicals are produced each time a peroxide molecule is photolyzed.

The factor of ½ in the third (OH-attack on peroxide) term comes from the fact that the product of OH attack on peroxide is superoxide, which disproportionates back to peroxide with 50 percent efficiency. The form of the fourth term comes from the fact that if fraction f_{OP} of the OH radicals react with peroxide, then $1-f_{OP}$ must react with something else. When peroxide is formed as a byproduct, it takes two OH reactions to reform one peroxide molecule (hence the factor of ½); however, this does not occur with all species that OH attacks. Thus, the fraction ρ of those reactions that leads to peroxide production must be included.

By considering the fact that the fractions:

$$f_{Oi} = \frac{k_{Oi}C_i}{\sum_j k_{Oj}C_j} \qquad \text{4-81}$$

that appear in the above equations all contain the concentrations of all solutes in the sum in the denominator, it can be seen that the rate equation for each species is at least a quadratic in that species. This makes an analytical solution of the set of four equations extremely difficult. The approach that was taken instead was to algebraically "solve" each species equation for its species concentration, treating the competition sum ($\Sigma k_{Oi}C_i$) as if it were a constant. The equation set was then solved iteratively, using initial estimates of the steady-state concentrations for each species to provide a calculated value of the competition sum for use in the equations. Substitution of this value for the competition sum into the equations resulted in new estimates for the species concentrations, which were then used to calculate a new competition sum to be used in the next iteration. The procedure was carried out using a very simple program written in QBASIC. The results converged very quickly, usually in three to 6 iterations, even using the feed concentrations as the initial estimates of the effluent concentrations. The convergence is quick and stable because the competition sum changes more slowly than do the individual species concentrations.

The calculated effluent DNT concentrations were found to be insensitive to the initial estimates of D, P, E, and A, as well as to ρ, f_r, and k_{OA}. Values of ρ =0.9 (peroxide regeneration efficiency) and f_r=1.0 (fraction of acetaldehyde that reacts through the diol form) were taken as the best estimates. Variation of these "parameters" over a wide range had very little effect on the calculated DNT removal. The value of ν_e has not been determined beyond confining it to the range ¼ to 1/3 (Peyton et al. 1995) Varying that constant between 0.3 and 0.33 only varied the calculated effluent DNT concentration between 37 and 35 µM when D_o=160 µM was used. Thus, $\Delta D/D_o$ varied from 0.77 to 0.78 under these conditions.

Results of Flow Through Studies

Organization of Experiments

A series of 29 flow experiments was performed using similar UV and H_2O_2 dose rates. This set is conveniently divided into six subsets, as follows:

DNT Photolysis Control	Experiment A-78
Ethanol Photolysis Control	Experiment A-81
Group A - "low" DNT concentration (0.14 to 0.17 mM, 25-31 mg/L)—before gas manifold was added to system.	Experiments A-79, 82-89, 92-95
Group B - "low" DNT concentration - After gas manifold added, with gas sparging during experiment.	Experiments A-96-100, 104-106
Group C - "low" DNT concentrations - After gas manifold added, but with no sparging of the reactor during the experiments.	Experiments A-101, 103, 107
Group D - "high" DNT concentration - (0.42-0.44 mM, 76-80 mg/L) - all performed before gas manifold added.	Experiments 80, 90, and 91

In addition, quality control actinometry experiments (A-102) were performed to ensure that there had not been a major change in the UV intensity during the series of experiments.

DNT Photolysis Control

The photolysis control was performed to allow determination of the portion of DNT removal in subsequent experiments that is due to photolysis rather than to free-radical processes. Approximately 10 percent of the DNT was removed by photolysis, using the same flow rate as was to be used in subsequent oxidation experiments. Since other substances compete for photons in free-radical experiments, the results of the photolysis control must be generalized by fitting to a photolysis rate equation, rather than simply assuming the same extent of DNT disappearance due to photolysis in subsequent free-radical experimentals. The photolysis rate equation is equation 4-68, discussed above. Experimental determination of the 254-nm extinction coefficient for DNT allowed calculation of the quantum efficiency for DNT disappearance due to photolysis, Φ_D=2.5x10-3 mole/einstein. This is in reasonable agreement with the value of 1x10-3 (in heptane) from Kamlet, Hoffsommer, and Adolph (1962), considering the difference in solvents.

Ethanol Photolysis Control

This experiment was performed because hydrogen peroxide formation was observed in the DNT photolysis control experiment (A-78). If formed as a result

of DNT photolysis, this can be taken as evidence for a free-radical pathway and the formation of a carbon-centered radical. This control experiment was performed to eliminate the possibility that the peroxide was formed from ethanol, oxygen, or water. Results were negative, indicating at least some free-radical involvement in the DNT photolysis pathway.

Group A Experiments

As discussed above, prior to the installation of the gas manifold, high and low values of the DO (dissolved oxygen concentration) could be attained by adjustment of the needle valves controlling gas flow, but the gas flow rates could apparently not be regulated well enough to obtain an intermediate range of DO concentrations (0.5 to 0.9 mg/L). The results from this group of experiments (Group A) are shown in Figure 4-39, along with the predictions of the model. Despite the absence of points in the region of the break in the curve, it is clear that agreement of the model with the flow experiment results was not particularly good.

Group B Experiments

After inclusion of the gas manifold in the experimental setup, another series of experiments (group B) was performed. Greater control over the gas flow rates allowed the collection of data in the previously unattainable region of DO=0.5 to 0.9 mg/L. However, it was still not possible to maintain the DO in this region by simply starting with the appropriately higher DO values prior to photolysis. Continual adjustment of the relative gas flow rates, gradually increasing the fraction of oxygen in the gas stream, was necessary to obtain points in this region.

These points are shown in Figure 4-40, along with the points from the Group A experiments. Although both the Group A and Group B sets appear to be fairly self consistent, they are not in agreement with each other, either in the DO region in which the break in the curve occurs, or in the asymptotic value of DNT removal at high oxygen concentration. Since the plot is shown on a logarithmic scale that "stretches" the scale at lower values, the accuracy of point placement in the horizontal direction is very poor at the lower DO concentrations (left-hand side of Figure 4-40) because the left-most point corresponds to the lowest readable DO concentration (0.1 mg/L) and the DO meter resolution was only ± 0.1 mg/L. The accuracy of the DO readings at these low values is not known.

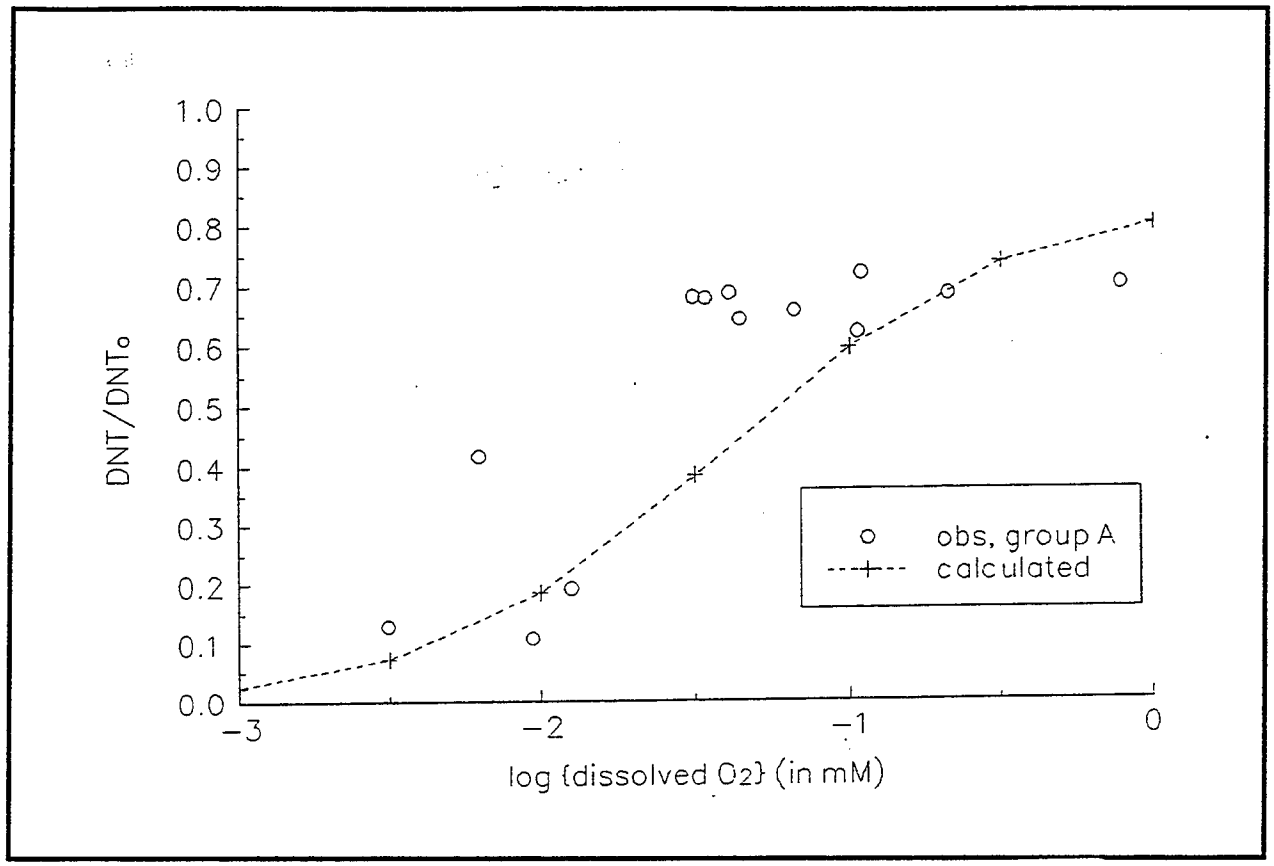

Figure 4-39. Effect of oxygen on DNT removal flow system, D_o = 147-172 µM, $EtOH_o$ = 4.9-7.6 mM (Group A).

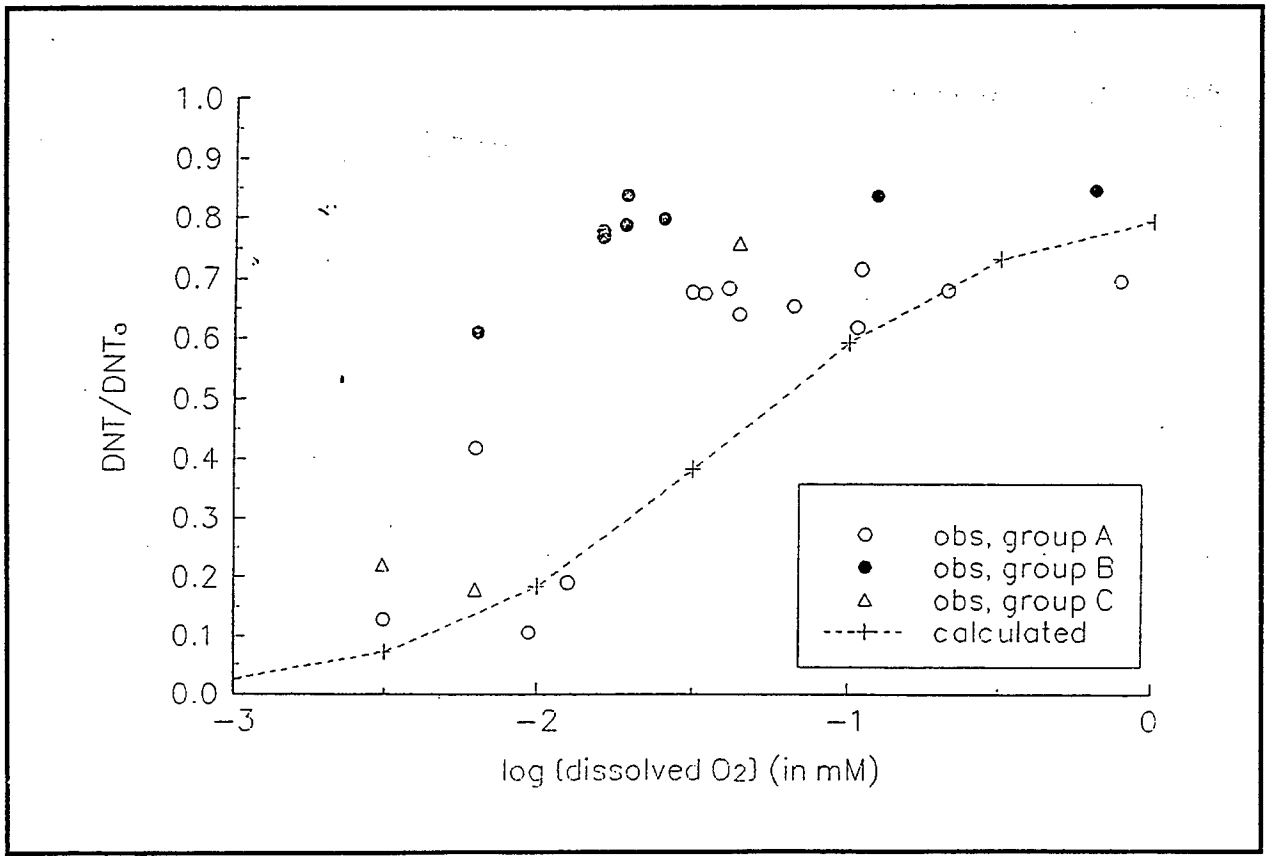

Figure 4-40. Effect of oxygen on DNT removal flow system, D_o = 147-172 µM, $EtOH_o$ = 4.9-7.6 mM (Groups A & B).

However, the accuracy at 1 mg/L (log DO{mM}=-1.5 in Figure 4-40) is probably acceptable. Manufacturers specifications are ±0.1 mg/L or 1 percent, whichever is larger. Despite these uncertainties at the lower end of the DO scale, a clear difference in oxygen dependence can be seen between Group A and Group B experiments.

Group C Experiments

A third group of experiments (Group C) was performed to demonstrate the enhancement of DNT removal without the need to sparge the reactor with inert gas. Removal of this requirement would represent a significant treatment cost savings, both in capital and operating costs, over treatment methods requiring gas sparging. Points from these four experiments are also shown in Figure 4-40, where they appear to fall between the Group A and Group B experiments. Group C results attained at the lowest DO concentration (at log DO=-2.5, or 0.1 mg/L) were from two experiments. In the first, oxygen was presparged down to about 0.6 mg/L (primarily to save time), then sparging was discontinued and 2 mM sulfite added to the reservoir, and the experiment started. The DO dropped to 0.2 mg/L by 60 minutes (one reactor volume passed) and 0.1 mg/L by 170 minutes. In the second sulfite experiment, no sparging of the synthetic waste water occurred, either in the reservoir or in the photochemical reactor. After addition of 4 mM sulfite, the DO dropped to 0.8 mg/L by the time the lamps were turned on, 0.2 mg/L by 60 minutes, and 0.1 by 210 minutes. Because of the coarseness of the DO measurements at this level, any differences in observed DO concentration/time profiles for these two experiments are probably insignificant.

A third experiment in Group C (Experiment A-107) proved that even sulfite addition is unnecessary. Synthetic wastewater is stirred overnight to dissolve DNT prior to use the next day in an experiment, and would therefore be expected to be at equilibrium with air with respect to oxygen concentration. Measurement of the DO in the photochemical reactor prior to turning the lamps on, however, gave 4 mg/L rather than the expected 8 mg/L. On observation for less than 0.5 hour, the DO dropped to 2 mg/L with no sparging or sulfite addition. During all of the group C experiments, the headspace of the photochemical reactor was flushed with nitrogen to avoid contact of the solution with air. This was necessary because the effluent pump runs faster than the influent pump (to maintain liquid level) and pulls air into the reactor if gas is not supplied to the headspace faster than that pumping rate. At this point, the gas flow rate of the CSTPR headspace sweep (one small bubble per second through the bubbler) and stir rate were turned down to the lowest possible values, and the feedwater reservoir was sparged continually with air to maintain equilibrium values. Even under these conditions, oxygen was still lost from the solution at a rate such that the DO was 0.9 by the time the experiment was started. Clearly, oxygen is still transferred at a significant rate through the calm surface of the water in the reactor. This situation is undoubtedly aggravated by the long residence times in the reactor.

Upon turning on the UV lamps to begin the experiment, the DO fell to 0.3 mg/L in 50 minutes and stabilized at 0.2 mg/L by 140 minutes (point plotted at log O_2 = -2.2), giving 84 percent DNT removal. To verify that oxygen mass transfer through the calm water surface was responsible for the previously observed DO behavior, the nitrogen headspace sweep was turned off after the effluent DNT concentration reached steady-state. The measured DO concentration rose steadily to level out at 1.0 mg/L over the next 2 hours, while DNT removal dropped to 24 percent, confirming that this difference in performance was due to the "leak rate" of oxygen into the reactor.

Group D Experiments

Another set of experiments was performed at DNT concentrations that were a factor of three higher than those described so far. The DNT concentrations used in the Group A, B, and C experiments were considerably lower than the average concentration in the actual wastewater, because the limitation to the photon dose rate in the available photoreactor would require such a long residence time as to make such experiments impractically long. Three experiments were performed in the 0.40 to 0.42 mM range (73 to 76 mg/L) to determine the ability of the model to correctly predict results at these concentrations. Other than the difference in initial DNT concentrations, these experiments were performed in the same manner as the Group A experiments.

The results are represented in Figure 4-41, where the observed and calculated removals are shown. The relationship of calculated to observed removals appears to be following the same trend as in Group A, Figure 4-39, where at high oxygen concentration the observed removal is better than predicted by the model, whereas at low DO values, observed removal is poorer than predicted by the calculation.

Discussion of Results From Flow-Through Experiments

It was anticipated from the beginning of the study that, because of the relative rate of oxygen introduction in the influent (0.016 L/minute x $2x10^{-4}$ moles/L in equilibrium with air = $3.2x10^{-6}$ moles/L/minute) compared to the radical generation rate (approximately $9x10^{-5}$ einsteins/L/minute x 0.5 moles OH generated/einstein absorbed = $4.5x10^{-5}$ moles/L/minute), virtually all oxygen that was carried in by the influent could be consumed by reaction with the organic radicals generated by OH reaction with ethanol. Therefore, the purpose of the series of experiments with oxygen/nitrogen sparging to maintain particular DO concentrations was to generate data to test the kinetic model, rather than the efficacy of the process itself.

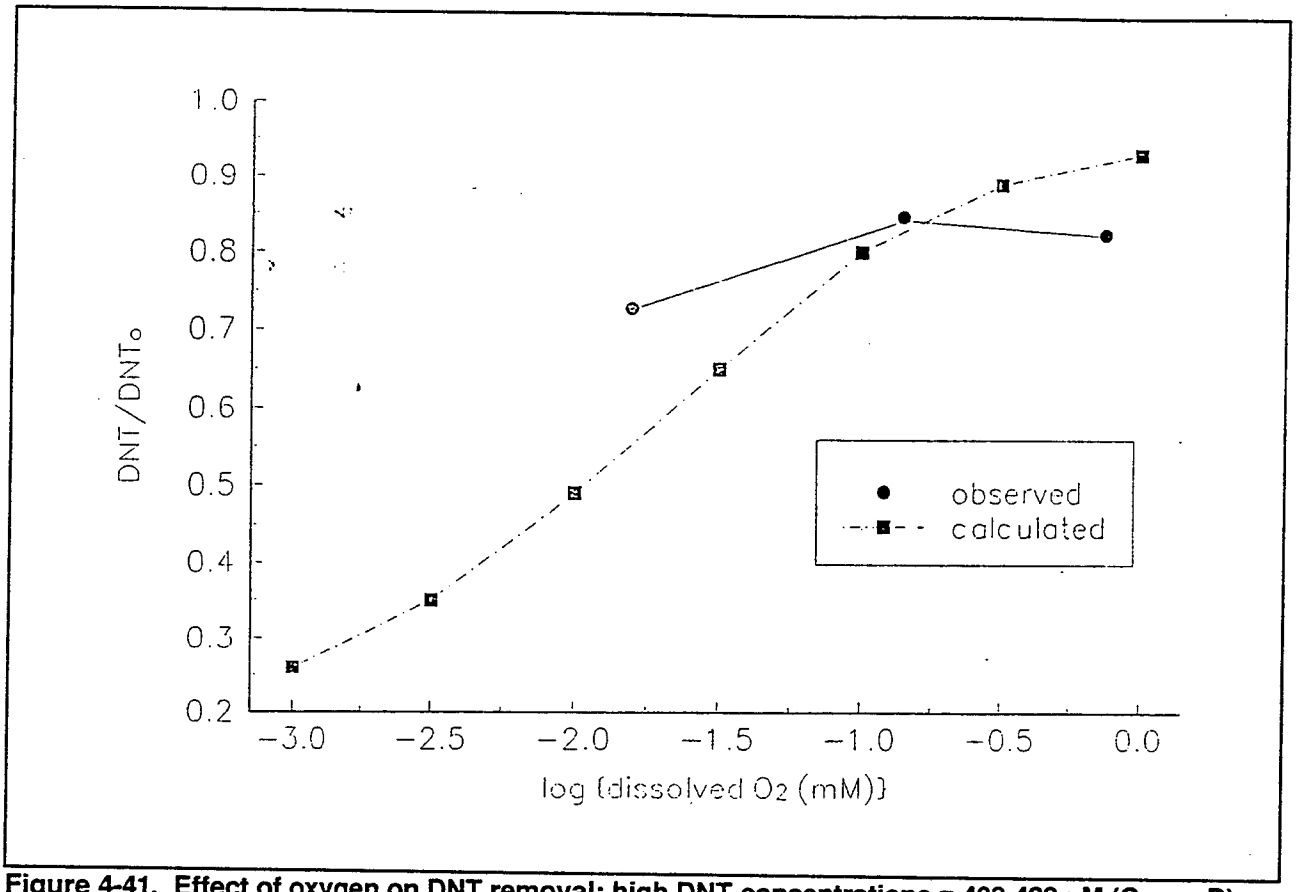

Figure 4-41. Effect of oxygen on DNT removal; high DNT concentrations = 402-422 µM (Group D).

It can be seen from the results of the last experiment (A-107, described above) that if access of oxygen to the photochemical reactor is excluded, the treatment process itself can easily deplete the oxygen content to the point that DNT removal is greatly enhanced. If there is even a slight leak rate of oxygen to the reactor headspace, process performance will be significantly degraded. In actual practice, this poses no special purging requirements on the reactor since on startup, feedstock can simply be recirculated until the oxygen in the reactor headspace is depleted and DNT removal becomes satisfactory. Therefore, Anoxic hydrogen Peroxide/UltraViolet (APUV) treatment has been demonstrated to be a viable treatment method for "water dry" and other DNT-containing wastewaters.

Important questions remain, however, about the chemistry of the processes occurring in the reactor. Whenever accurate knowledge of the gas composition allowed comparisons of the DO concentrations indicated by the meter with those expected from Henry's Law, they verified the correct operation of the DO meter, so that the differences in behavior of the Group A and Group B experiments with respect to oxygen concentration (Figure 4-40) indicate that the proposed mechanism (Peyton et al. 1995) is incomplete. Apparently, the importance of the additional reactions depends on how flow treatment is carried out; these effects are constant, are unimportant, or cancel during batch treatment. These

differences are clearly important to our understanding of free-radical nitroaromatic chemistry, since order-of-magnitude differences in oxygen effects shown in Figure 4-40 appear to depend on the way the treatment process is applied.

The major difference between the Group A, B, and C experiments appears to be the rate at which oxygen can be supplied to the system, rather than the initial oxygen concentration. For this to be consistent with mass action kinetics, there must be complex interdependencies between the various reactions in the system, which implies the possibility of multiple steady states. This is indeed consistent with the behavior observed under some conditions, where the DNT concentration would equilibrate at one value, only to suddenly change and re-equilibrate at a much different value. A preliminary analysis of the reaction system using the methods of reaction network structure analysis (e.g., Schlosser and Feinberg 1994) indicates the potential for multiple steady states to exist, a situation in which given treatment conditions can lead to one of several steady states. Such situations occasionally show up in flow studies, using CSTRs, which typically operate at steady-state, whereas they cannot be observed in batch oxidation studies, since in the latter, the only steady state is that attained after everything is destroyed. This point is of major importance to the understanding of these free-radical treatment processes, and may have some connection to why results of treatability studies vary so widely.

In the present case, the complexity most likely arises from the complex chemistry of the acetaldehyde radical, discussed above. A simplified version of this subsystem is shown schematically in Scheme II (Figure 4-18). Of the two main branches in this pathway, one ($CH_3C(O)O_2$, the acetylperoxyl radical) is oxidative, while the other ($CH_3C(OH)_2$, the diol radical) can be reductive (e.g., reaction with DNT, *not* shown in Scheme II. The reduction of DNT is in competition with reaction of the diol radical with oxygen (which *is* shown in Scheme II). In addition to oxidizing superoxide as shown in Scheme II, the acetylperoxyl radical can also oxidize acetaldehyde, probably DNT, and almost certainly oxidize the DNT radical anion back to DNT, although this reaction may be slow because of being a radical-radical reaction, i.e., a reaction between two species of very low concentration. Thus greater availability of oxygen not only favors formation of peroxyl radicals at the expense of the reductive pathways, but may actually produce a species that reverses the reductive pathway, as well. This question can only be answered through further investigation, but is clearly important to our knowledge of nitroaromatic chemistry, since many substances other than ethanol and acetaldehyde, that may be present in wastestreams of interest to the Army, can participate in this type of chemistry.

5 Conclusions and Recommendations

Conclusions

Conclusions From Literature Review

Although considerable work has been reported on the treatment of Army and related wastes using AOPs, much of it was done somewhat randomly with respect to treatment parameters such as ozone dose rate, peroxide concentration, and UV intensity, due to the emerging nature of the technology and a lack of knowledge of the fundamental principles underlying AOPs. Widely varying treatment efficiencies and apparently conflicting results between investigators reflect the state of disorganization of existing knowledge about the AOPs.

The analysis of existing information on AOP treatment of Army wastes from the standpoint of AOP chemistry revealed significant data gaps. One of them is a lack of comparison of various AOPs for a particular application. There are only a few studies where comparative analysis of various AOPs was done (primarily for explosive contaminated wastewaters). Another gap is a lack of oxidant data. AOP treatment efficiency and, therefore, treatment cost are strongly affected by the way oxidants are applied. As it can be seen from this literature review, the importance of thorough investigation of the oxidant behavior (initial concentrations, amount used, mass transfer, possible reactions, etc.) have not always been recognized. It is not surprising that, although the effectiveness of target compound removal was often high, treatment efficiency in terms of oxidant consumed appears to have been generally poor. Yet another gap is identification of oxidation byproducts, which is important in terms of their ability to promote the oxidation cycle. A few relatively extensive studies have been carried out for the explosive-contaminated wastes, but the byproducts formed in other Army wastewaters treated with AOPs have not received much study. The identification and even tracking of byproducts very often is not an easy task. However, the majority of studies was focused on the removal of target compounds and TOC was not monitored.

Identified information gaps in the literature can be summarized as:

- shortage of data on AOP application to treatment of wastes other than the explosive-contaminated wastewaters (Table 2-1, p 15)
- lack of identification of important types of wastewater components
- lack of the comparative analysis of various AOPs
- lack of oxidant data during treatability studies

- shortage of TOC and byproduct data
- lack of suitable models for analytical and predictive purposes.

The conclusion on which AOP is the best for Army wastewaters of interest in many cases cannot be made before the data gaps discussed above are filled. Even with all of the information available any statement on AOP selection should be qualified, since the majority of literature data was obtained under different experimental conditions. Nonetheless, these data indicate that O_3/UV is, in general, more effective for pinkwater treatment than H_2O_2/UV. Photolysis is very effective for the treatment of the wastewaters contaminated predominantly with nitramines. Ozone/UV seems to be the best in TOC removal.

Development and verification of a model for Army wastewaters that may contain such compounds as nitramines and other nitrated organics would fill a severe information gap in the application of AOPs and permit organization of AOP knowledge on a common basis.

Competition for radicals and photons is governed by particular solution components. Development of the model and identification of important types of solution components could lead to a standardized protocol for waste stream characterization during AOP treatability studies, ensuring that the required data was available for modeling.

From the literature review, the following general conclusions on process comparison/selection can be made:

1. Lower oxidant dose rates may be more efficient for the destruction of dilute contaminants than high dose rates, to avoid scavenging of hydroxyl radical by ozone and hydrogen peroxide. However, a longer retention time is then required.
2. Below pH 7, ozone/UV provides more rapid initiation than ozone/peroxide, and can therefore sustain a faster reaction rate when promoters are scarce.
3. The ozone/UV system is self-regulating, and thus can accommodate changes in the promoter content of the reaction mixture more efficiently than can ozone/peroxide. Therefore, ozone/UV may be more suitable than ozone/peroxide for streams that vary greatly in composition, or for batch treatment, in which the suite of byproducts may change during treatment.
4. In the absence of contaminant photolysis, ozone/peroxide may be more suitable than ozone/UV for treating streams of relatively constant composition because the former is a simpler system and requires less maintenance.
5. In the absence of promoters, peroxide/UV may be the most appropriate system, since both the ozone/UV and ozone/peroxide system chains would have to be sustained by initiation-type reactions throughout treatment. However, if the solution absorbance is high at the UV wavelength, a high UV intensity may be required because of the low absorbance of peroxide.

6. In the general case, there is no need to simultaneously use both UV and peroxide in combination with ozone. It might be advantageous to use different pairs in successive staged reactors. There may be specific cases where simultaneous application is advantageous.

7. Selection of an AOP for a particular cleanup task should be made on a case-by-case basis.

8. Mathematical modeling of the treatment chemistry can clarify complex interactions between reaction pathways and simplify the optimization process. Predictive modeling of AOPs can greatly aid process optimization, and therefore, cost-effectiveness. The ideal model would incorporate fundamental theoretical principles and the concept of process efficiency, into an easily-applied practical model capable of accommodating surrogate parameters to describe unknown matrix components.

Conclusions From Treatability Study

Important AOP Treatment Process Modification. The experimental results described suggest a useful treatment process modification that is novel because:

1. The contaminant is destroyed by reduction while the water is being treated with a highly oxidizing process (Figures 4-22 and 4-23, pp 94-95).

2. Treatment is improved by the introduction (or presence) of an additive that can successfully compete with contaminant for what is typically thought to be the primary active species (hydroxyl radical) (Figure 4-21, p 92).

3. Oxygen, the presence of which is usually beneficial to treatment by free-radical methods, must be removed or its concentration greatly reduced for the improvement to be most effectively realized.

Implications of Results. In addition to the novel aspects of this treatment modification, the results obtained in this study have several important implications with respect to water treatment using processes that generate free radicals:

1. Considerable improvement in the treatment of nitrated compounds with high electron affinity may be realized by eliminating or depleting oxygen and adding a substrate capable of producing reducing radicals. In the case of the DNT wastewater under study, the "additive" was already present. This may be the case for other wastewaters and natural waters as well. Additives other than alcohols may be more appropriate in other applications.

2. Reduction as described appears to provide a means to more easily eliminate DNB in the case of DNT treatment and make treatment cost more effective.

3. The same principle should be applicable to other contaminants with high electron affinity, such as halogenated solvents, PCBs, etc., and compounds

having aromatic rings substituted with other electron-withdrawing functional groups. The feasibility of this application was demonstrated in this laboratory for the destruction of carbon tetrachloride. It is likely that some past reports of carbon tetrachloride destruction using hydroxyl radical processes are actually attributable to reduction reactions such as those described above, involving other organic constituents in the formation of the reducing radicals.

4. Hydrogen peroxide photolysis used in this study to generate OH radicals may not be practical for actual treatment because of strong UV absorbance by DNT and its byproducts (H_2O_2 is a poor absorber at the wavelength 254 nm, which is commonly used in commercial units).

5. Significant improvement in DNT destruction efficiency may be attained by generating ozone from air rather than oxygen during ozone/UV or ozone/peroxide treatment, because of the lower saturation concentration of oxygen in the water. Even lower oxygen concentrations might give further improvements. These lower concentrations may be obtained, for example, by recycle of the air streams that are off-gas from the processes. However, preliminary data on the DNT treatment with O_3/UV using ozone generated from air (Experiment A40) did not show any improvement in the *rate* of DNT removal compared with that in a similar experiment (Experiment A14), in which ozone was generated from oxygen. There may be a variety of reasons for the observed effect, however, they have not yet been delineated. The possibility of using AOPs involving ozone generated from air or oxygen depleted air should be further addressed in future work.

6. Finally, the results suggest that, in addition to oxidants such as ozone and hydrogen peroxide, it is also important to measure the dissolved oxygen concentration during treatment experiments using free-radical processes.

Conclusions From Modeling Studies

A mechanistic/kinetic model was developed from information in the radiation chemistry literature, and calibrated from initial rate data obtained from "clean" kinetic experiments (i.e., conditions optimized to minimize interferences) using H_2O_2/UV to generate OH radical. This model gave predictions that were in excellent agreement with results from other experiments that were performed under quite different conditions, including different DNT concentration range, widely varying ethanol concentration, and different AOP (ozonation-based, rather than H_2O_2/UV), with little or no change in the parameters from the values predicted theoretically and from the initial calibration. Therefore the following conclusions, can be made that:

1. The hypothesized mechanism of electron transfer from α-hydroxyethyl radical to DNT is essentially correct.

2. Attack by both hydroxyl radical and α-hydroxyethyl radical may be important for the removal of DNT during AOP treatment. Under conditions where OH-radical attack on DNT was insignificant, the hypothesized

reduction mechanism was the only important removal mechanism throughout the lifetime of DNT.

3. The presence of byproducts in the latter part of treatment does affect the kinetics of DNT removal. This is indicated by the goodness of the model fit over the entire DNT life in Experiment A-39.
4. The model can be applied to ozonation-based AOPs as well as H_2O_2/UV.
5. The model can be used to determine optimized treatment conditions and to evaluate the effect of changes in process variables.
6. The values of the rate constants for reaction of DNT with α -hydroxyethyl radical and hydroxyl radical are $(3.5\pm0.5)\times10^8$ and 2.4×10^8 $M^{-1}s^{-1}$, respectively.

Conclusions From the RAAP DNT Wastewater Study System

A kinetic model was developed that successfully describes the combined reductive and oxidative removal of DNT during H_2O_2/UV and O_3/UV treatment. The comprehensive model was composed of a combination of the models developed for the separate OH and ethanol radical reactions, for the case where low-pressure UV lamps are used. The model developed for low-pressure lamps was unsuccessful in representing results obtained using a high-powered lamp.

The kinetic model predicts the effect of oxygen concentration on DNT removal and the relative amounts of DNT destruction due to OH and ethanol radicals, providing a tool for treatment process optimization.

The oxidant and UV requirements for reductive treatment vary inversely as a function of the oxygen concentration.

Oxygen concentration can be reduced in H_2O_2/UV systems, either by a pretreatment step or by the oxygen removal that occurs as the reaction proceeds. Oxygen is produced during application of AOPs that employ ozone, so that removal of oxygen below the concentration that is in equilibrium with the feed gas will not occur. Therefore, the reductive reactions are expected to be more important in H_2O_2/UV treatment than in O_3/treatment.

An equation was derived that represents the steady-state oxygen concentration during treatment, for substitution into the DNT removal equation of the kinetic model. The oxygen equation was used to evaluate the mass transfer coefficient of the reactor and the oxygen partition coefficient. During process design modeling, the appropriate values for the reactor being considered can be substituted into the DNT rate equation.

Byproducts observed for 1,3,5-trinitrobenzene and for nitrobenzene under reductive conditions were consistent with the proposed mechanism of reduction of the nitro compound to the nitroso compound, then to the amino compound, followed by replacement of an amino group by an hydroxyl group, possibly through a diazonium intermediate:

1. As was seen in the batch studies, DNT destruction by H_2O_2/UV treatment can be enhanced by removal of oxygen from the stream prior to H_2O_2/UV treatment. A greater extent of oxygen removal was necessary before the onset of enhancement than was required in the previous batch studies.

2. Removal of oxygen by pretreatment with sulfite allowed enhanced removal of DNT without gas sparging of the stream. The smallest amount tried, 2 mM or 240 mg/L as sodium bisulfite, was found to be adequate. Sulfite addition was later shown to also be unnecessary if the solution was protected from contact with air during treatment, since the rate of consumption of oxygen by the chemical reactions was sufficient to deplete the amount of oxygen contained in the incoming waste stream. However, treatment with bisulfite may prove to be more economical at lower oxidant doses than were used in the present experiment.

3. The system exhibited anomolous behavior with respect to oxygen concentration, indicating the importance of other complicating chemical reactions in the mechanism. Thus, the kinetic model developed from the batch kinetic data, appears to be based on an incomplete mechanism, and did not accurately predict the observed DNT removals under the conditions of many of the experiments. Further investigation into the mechanism is important to our understanding of the free-radical chemistry of nitroaromatic compounds, and will be required before a more complete model can be developed.

Recommendations

This study recommends that:

1. The reductive mechanism should be investigated in more detail for other compounds. This appears to be a general pathway common to the destruction of many ordnance compounds, and may be of considerable value to the Army in remediation as well as waste treatment.

2. In view of the process efficiency enhancement demonstrated during this project, the anoxic H_2O_2/UV (Anoxic Peroxide UV, APUV) system should be considered for application to DNT-containing wastewater streams at RAAP, as well as other streams containing nitroaromatic compounds.

3. Further investigation of the APUV system is warranted to determine the cause(s) of the anomolous behavior with respect to oxygen that was demonstrated in the present flow studies. There appears to be important, previously unknown chemistry occuring in this system, which deserves further study. This study should be carried out in a flow-kinetic reactor system designed specifically for this study, incorporating the lessons learned from the present study.

4. Further optimization of the APUV system is recommended. This should preferably be carried out after the flow kinetic study (above) has provided the basis for a kinetic model.

5. On-site pilot-scale testing should be carried out for the process that emerges from the above studies as most promising.

The following future work is also recommended:

1. Further verify the ability of the model to fit DNT-H_2O_2/UV treatability data, using parameters (rate constants,etc.) obtained in kinetic experiments.
2. Use the model to optimize the H_2O_2/UV process.
3. Develop and verify a kinetic model for the treatment involving OH radical generation by ozonation methods.
4. Determine whether any DNT treatability advantage may be gained by using ozone generated from air or oxygen-depleted air.
5. Investigate the synergetic removal of TNT and RDX by AOPs and UV photolysis in pinkwater including development of a mechanistic/kinetic model.
6. Determine to what extent (if any) diethyl ether also participates in the reduction pathways.

References

Adams, G.E., and R.L. Willson, "Pulse Radiolysis Studies on the Oxidation of Organic Radicals in Aqueous Solution," *Trans. Farad. Soc.*, vol 63 (1969), pp 2981-2987.

Andrews, C.C., and J.L. Osmon, *The Effects of UV Light on TNT and Other Explosives in Aqueous Solution*, Technical Report (TR) WQEC/C77-32 (Naval Weapons Support Center, IN, 1977).

Andrews, C.C., *Photooxidative Treatment of TNT Contaminated Waste Waters*, TR WQEC/C 80-137 (Naval Weapons Support Center, IN, 1980).

Arisman, R.K., R.C. Musick, J.D. Zeff, and T. Crase, *Experience in Operation of a UV-Ozone (ULTROX7) Pilot Plant for Destroying PCB's in Industrial Waste Effluent* (35th Annual Purdue Industrial Waste Conference, May 1980).

Asmus, K.D., G. Beck, A. Henglein, and A. Wigger, "Pulsradiolytische Untersuchung der Oxydation und Reduktion des Nitrosobenzols in wäBriger L'sung," *Ber. Bunsenges. Physik. Chem.*, vol 70 (1966), pp 869-874.

Bader, H., and J. Hoigné, "Determination of Ozone in Water by the Indigo Method: A Submitted Standard Method," *Ozone: Science and Engineering*, vol 4 (1982), pp 169-176.

Baxendale, J.H., and J.A. Wilson, "The Photolysis of Hydrogen Peroxide at High Light Intensities," *Trans. Farad. Soc.*, vol 53 (1957), pp 344-347.

Botcher, T.R., and C.A. Wight, "Explosive Thermal Decomposition Mechanism of RDX," *J. Phys. Chem.*, vol 98 (1994), pp 5441-5444.

Botcher, T.R., and C.A. Wight, "Transient Thin-Film Laser Photolysis of RDX," *J. Phys. Chem.*, vol 97 (1993), pp 9149-9153.

Bothe, E., M.N. Schuchmann, D. Schulte-Frohlinde, and C. von Sonntag, "Hydroxyl Radical-Induced Oxidation of Ethanol in Oxygenated Aqueous Solutions. A Pulse Radiolysis and Product Study," *Z. Naturforsch.*, vol 38b (1983), pp 212-219.

Brabets, R.I., and G.E. Marks, *Ozonolysis of Pink Water*, TR IITRI-C6275 (IIT Research Institute, Chicago, IL, September 1973).

Buhts, R.E., P.G. Malone, and P.W. Thompson, *Evaluation of Ultraviolet/Ozone Treatment of Rocky Mountain Arsenal (RMA) Groundwater (Treatability Study)*, Final Report (Environmental Effects Laboratory, U.S. Army Engineer Waterways Experiment Station [USAWES], 1978).

Burlinson, N.E., M.E. Sitzmann, D.J. Glover, and L.A. Kaplan, *Photochemistry of TNT and Related Nitroaromatics, Part III*, TR ADB045845 (Naval Surface Weapon Center, White Oak, MD, December 1979).

Burrows, W.D. *Tertiary Treatment of Effluent From Holston AAP Industrial Liquid Waste Treatment Facility. III. Ultraviolet Radiation and Ozone Studies: TNT, RDX, HMX, TAX, and SEX*, TR 8306, ADA137672 (U.S. Army Medical Bioengineering Research and Development Laboratory, Fort Detrick, Frederick, MD, 1983).

Burrows, W.D., and E.E. Brueggermann, *Tertiary Treatment of Effluent From Holston AAP Industrial Liquid Waste Treatment Facility, Degradation of Nitramines in Holston AAP*

Wastewaters by Ultraviolet Radiation, TR ADA176195 (U.S. Army Medical Research and Development Laboratory, Fort Detrick, Frederick, MD, September 1986).

Burrows, W.D., B. Jackson, and J.M. Lachowski, *Tertiary Treatment of Effluent From Holston Army Ammunition Plant Industrial Liquid Waste Treatment Facility C Ultraviolet Radiation and Ozone Studies*, TR ADB088905 (U.S. Army Medical Bioengineering Research and Development Laboratory, Fort Detrick, Frederick, MD, November 1984).

Burrows, W.D., R.H. Chyrek, C.I. Noss, M.J. Small, and E.A. Kobylinski, "Treatment for Removal of Munition Chemicals From Army Industrial Wastewaters," *Proceedings of the 16th Mid-Atlantic Industrial Waste Conference, Lancaster, PA* (Technomic Publishing Company, Inc., 1984), pp 331-342.

Buxton, G.V., C.L. Greenstock, W.P. Helman, and A.B. Ross, "A Critical Review of Rate Constants for Reactions of Hydrated Electrons, Hydrogen Atoms, and Hydroxyl Radicals in Aqueous Solution," *J. Phys. Chem. Ref. Data*, vol 17 (1988), pp 513-886.

Cowen, W.F., R.A. Sierka, and J. Zirrolli, "Identification of the Partial Oxidation Products From Ozonation of Hydrazine, Monomethyl Hydrazine and Unsymmetrical Dimethyl Hydrazine," *Chemistry in Water Reuse*, vol 2 (1981), pp 101-118.

DeBerry, D.W., A. Viehbeck, and D. Meldrum, *Literature Survey: Basic Mechanisms of Explosive Compounds in Wastewater*, TR ADA141703 (SumX Corp, Austin, TX, May 1984).

DeBerry, D.W., A. Viehbeck, and D.A. Meldrum, *Basic Mechanisms of Explosive Compounds in Wastewater*, DTIC Report No. DRXTH-TE-CR-84279 (Final report to USATHAMA, 1984).

DeBerry, D.W., and J.S. Payne, *Low Toxicity Chemical/Biological Agent Decontamination*, TR ADB094959 (SumX Corporation, Austin, TX, June 1985).

DeMore, W.B., and Rapper, O.F., "Deactivation of O(1D) in the Atmosphere," *Astrophys. J.*, vol 139 (1964), p 1381.

Farrell, F.C., J.D. Zeff, T.C. Crase, and D.T. Boylan, *Development Effort To Design and Describe Pink Water Abatement Processes*, TR ADA045126 (Westgate Research Corporation, Los Angeles, CA, August 1977).

Fischer, G., B. Jackson, Jr., and J.M. Lachowski, *Ultraviolet-Ozone Treatment of RDX (Cyclonite) Contaminated Wastewater*, Contract Report ARLCD-CR-82024 (ARRADCOM, Dover, NJ, 1982).

Fleming, E.C., M.E. Zappi, J. Miller, R Hernandez, and E. Toro, "Evaluation of Peroxide Oxidation Techniques for Removal of Explosives from Cornhusker Army Ammunition Plant Waters," TR SERDP-97-2 (U.S. Army Engineer Waterways Experiment Station [USAWES], Vicksburg, MS, April, 1997).

Fochtman, E.G., and J.E. Huff, "Ozone-Ultraviolet Light Treatment of TNT Wastewaters," *Proceedings of the Second International Symposium on Ozone Technology* (Montreal, Canada, May 1975), pp 211-223.

Glaze, W.H., "An Overview of Advanced Oxidation Processes: Current Status and Kinetic Models," *Proceedings of the Third International Symposium, Chemical Oxidation : Technology for the Nineties* (February 1993), pp 1-9.

Glaze, W.H., and J.W. Kang, "Chemical Models of Advanced Oxidation Processes," *Proceedings of a Symposium on Advanced Oxidation Processes for the Treatment of Contaminated Water and Air* (Toronto, Canada, June 4-5, 1990).

Glaze, W.H., G.R. Peyton, F.Y. Saleh, and F.Y. Huang, "Analysis of Disinfection By-Products in Waterand Wastewater," *Intern. J. Environ. Anal. Chem.*, vol 7 (1979), pp 143-160.

Glaze, W.H., J-W Kang, and D.H. Chapin, "The Chemistry of Water Treatment Processes Involving Ozone, Hydrogen Peroxide and Ultraviolet Radiation," *Ozone Sci. Eng.*, vol 9 (1987), pp 335-352.

Glover, D.J., and J.C. Hoffsommer, *Photolysis of RDX in Aqueous Solution, With and Without Ozone*, NSWC/WOL TR 78-175 (Naval Surface Weapons Center, Dahlgren, VA, 1979).

Gould, E.S., *Mechanism and Structure in Organic Chemistry* (Holt, Rinehart and Winston, New York, 1959), pp 220-224, 435-436.

Gran, G., "Determination of the Equivalence Point in Potentiometric Titrations, Part II," *Analyst* (London), vol 77 (1952), pp 661-671.

Grasshoff, K., *Methods of Seawater Analysis* (Weinheim, New York: Verlag Chemie, 1976), pp 127-133.

Griest, W.H., A.J. Stewart, R.L. Tyndall, C.-h Ho, and E. Tan, *Characterization of Explosives Processing Waste Decomposition Due to Composting* (ORNL, 1990).

Grühnbein, W., A. Fojtik, and A. Henglein, "Pulsradiolytische Bestimmung der Absorptionsspektren und Dissoziationskonstanten Kurzlebiger Halbreduzierter Aromatischer Nitroverbindungen," *Z. Naturforsch.*, vol 24b (1969), pp 1336-1338.

Grühnbein, W., A. Fojtik, and A. Henglein, "Pulsradiolytische Untersuchung Kurzlebiger Hydrate von Aromatischen Nitrosoverbindungen," *Monatshefte für Chemie*, vol 101 (1970), pp 1243-1252.

Gründmann, C., and A. Kreutzberger, "Triazines, IX: 1,3,5-Triazine and Its Formation from Hydrocyanic Acid," *J. Amer. Chem. Soc.*, vol 76 (1954), p 5646.

Gründmann, C., G. Weisse, and S. Seide, Ann., 577, p 77 (1952), reported in Grundmann, C., and A._Kreutzberger, "1,3,5-Triazine," *J. Am. Chem. Soc.*, vol 76 (1954), pp 632-633 (reference 9).

Hao, D.J., and K.K. Phull, *TNT Red Water Treatment by Wet Air Oxidation*, Contract DACA 88-90-M-1418 (University of Maryland, College Park, MD, February 1991).

Heffinger J., and C, Jake, *Removal of DNT From Wastewaters at Radford Army Ammunition Plant*, Report No. CETHA-TS-CR-91031 (U.S. Army Corps of Engineers, 1991).

Heffinger, J., and C. Jake, *Removal of DNT From Wastewaters at Radford Army Ammunition Plant*, Report CETHA-TS-CR-91031 (U.S. Army Corps of Engineers, 1991).

Herlacher, M.F., and F.R. McGregor, "Photoozone Destruction of Cyanide Waste at Tinker AFB, Oklahoma, Pilot Plant Results," Paper presented at the *SAE 23rd Annual Aerospace/Aeroline Plating and Metal Finishing Forum and Exposition* (Jacksonville, FL, 16-19 February 1987).

Ho, Patience C., "Photooxidation of 2,4-Dinitrotoluene in Aqueous Solution in the Presence of Hydrogen Peroxide," *Environ. Sci. Technol.*, vol 20, No. 3. (1986), pp 260-267.

Hoigné, J., and H. Bader, "Beeinflussung der Oxidationwirkung von Ozon und OH-Radikalen durch Carbonat," *Vom Wasser*, vol 48 (1977), pp 283-304.

Hoigné, J., and H. Bader, "Beeinflussung der Oxidationwirkung von Ozon und OH-Radikalen durch Carbonat," *Vom Wasser*, vol 48 (1977), pp 283-304.

Hoigné, J., and H. Bader, "Ozone-Initiated Oxidations of Solutes in Wastewater: A Reaction Kinetic Approach," Presented at the *International Association on Water Pollution Research*, 9th International Conference (Stockholm, June 1978); later published as *Progr. Water Technol.*, vol 10 (1978), pp 657-671.

Hoigné, J., and H. Bader, "Ozone-Initiated Oxidations of Solutes in Wastewater: A Reaction Kinetic Approach," Presented at the *International Association on Water Pollution Research*, 9th International Conference (Stockholm, June 1978); Published as *Progr. Water Technol.*, vol 10 (1978), pp 657-671.

Hoigné, J., and H. Bader, "Rate Constants of Reactions of Ozone With Organic and Inorganic Compounds in Water - I," *Water Res.*, vol 17 (1983), pp 173-183.

Hong, A. Zappi, M.E., Kuo, C.H. and Hill D., "A Modelling Kinetics of Illuminated and Dark Advanced Oxidation Processes," *J. Envrn. Engr.*, vol 122, No.1 (1996), pp 58-62.

Hong, A. Zappi, M.E., Kuo, C.H., "A Peroxone for Remediation of TNT-Contaminated Groundwater," *Proc. 67th Annual Conf. and Exposition* (Water Envir. Federation, Chicago, IL, 1994).

Hunter, B.A., L. Sotsky, and J.A. Carrazza, *Dimethylnitrosamine (DMN) Pollution Abatement Methods*, TR ADB074784 (ARRADCOM, Dover, NJ, April 1983).

Ilan, Y., J. Rabani, and A. Henglein, "Pulse Radiolytic Investigations of Peroxy Radicals Produced From 2-Propanol and Methanol," *J. Chem. Phys.*, vol 80 (1976), pp 1558-1562.

Jackson, B., and J.M. Lachowsky, *Alternative Treatment Methods for Pink Wastewater*, TR ADB073648 (ARRADCOM, LCWSL, Dover, NJ, May 1983).

Jagannadham, V., and S. Steenken, "One-Electron Reduction of Nitrobenzenes by α-Hydroxyalkyl Radicals via Addition/Elimination. An Example of Organic Inner-Sphere Electron Transfer Reaction," *J. Am. Chem. Soc.*, vol 106 (1984), pp 6542-6551.

Judeikis, H., and M. Hill, *Treatment of Organic Hazardous Wastes With Ozone and Ultraviolet Radiation*, TR GAD-A252 799 (The Aerospace Corporation, El Segundo, CA, July 1991).

Kamlet, M.J., J.C. Hoffsommer, and H.G. Adolph, *J. Am. Chem. Soc.*, No. 84 (1962), pp 3925.

Kearney, P.C., Q. Zeng, and J.M., "Ruth Oxidative Pretreatment Accelerates TNT Metabolism in Soils," *Chemosphere*, vol 12, No. 11/12 (1983), pp 1583-1597.

Kobylinski, E.A., and B.W. Peterman, *Evaluation of Ozone Oxidation and UV Degradation of Dimethylnitrosamine*, TR 7908, ADAA080016 (U.S. Army Medical Bioengineering Research and Development Laboratory, Fort Detrick, Frederick, MD, 1979).

Kubose, D.A., and J.C. Hoffsommer, *Photolysis of RDX in Aqueous Solution. Initial Studies*, NSWC/WOL TR 77-20 (February 1977).

Kubose, D.A., and J.C. Hoffsommer, *Photolysis of RDX in Aqueous Solution, Initial Studies*, NSWC/WOL TR 77-20 (February 1977).

Kuo, P.P.K., E.S.K. Chian, and B.J. Chang, "Identification of End Products Resulting From Ozonation and Chlorination of Organic Compounds Commonly Found in Water," *Environ. Sci. Technol.*, vol 11, No. 13 (1977), pp 1177-1181.

Langlais, B., D.A. Reckhow, and D.R. Brink, *Ozone in Water Treatment* (Lewis Publishers, Chelsea, MI, 1991).

Larson, R.A., and R.G. Zepp, "A Reactivity of the Carbonate Radical With Aniline Derivatives," *Environ. Toxicological. Chem.*, vol 7 (1988), pp 265-274.

Layne, W.S., R.A. Nicholson, R.M. Wahl, P.M. O'Brien, B. Jackson, Jr., and J.M. Lachowski, *Ultraviolet-Ozone Treatment of Pink Wastewater, A Pilot Scale Study*, Contract Report ARLCD-CR-82023 (ARRADCOM, Dover, NJ, 1982).

Leitis, E., *An Investigation into the Chemistry of the UV-Ozone Purification Process*, Final Report, National Science Foundation, Grant No. ENV 76-24652 (Westgate Research Corporation, West Los Angeles, CA, February 1980).

Leitis, E., J.D. Zeff, M.M. Smith, and D.G. Crosby, "The Chemistry of Ozone/UV Light for Water Reuse," *Proceedings of the 2nd Symposium on Water Reuse, Washington, DC*, vol 2 (1981), pp 1121-1144.

Lu, Miaoqin, Wang Xiangming, Gong Yuhua, Lin Wenjie, and He Fenzhu, "Photodegradation of a-TNT in Aqueous Solution," *Huanjing Kexue* (Chinese) (abstract in English), vol 8 (1987), pp 15-20.

Mallevialle, J. "Identified Reaction Products in Ozonation," *Ozonation Manual for Water and Wastewater Treatment*, W.J. Masscholein, ed. (John Wiley & Sons, New York, NY, 1982), pp 105-124.

Maloney, S.W., M.T. Suidan, and S.R. Berchtold, "Anaerobic Biodegradation of DNT in Fixed Film Reactors Applied to Industrial Wastewaters," *Proceedings of the Second International Specialized Conference on Biofilm Reactors* (IAWQ, Paris, France, September, 1993).

Masten, S.J., and J.N. Butler, "Ultraviolet-Enhanced Ozonation of Organic Compounds: 1,2-Dichoroethane and Trichloroethylene as Model Substrates," *Ozone Sci. Eng.*, vol 8 (1986), pp 339-353.

Mauk, C.E., H.W. Prengle, Jr., and J.E. Payne, *Oxidation of Pesticides by Ozone and Ultraviolet Light,* Report No. 7206 (U.S. Army Mobility Equipment Research and Development Command, Fort Belvoir, VA, 1976).

Mertens, R., C. von Sonntag, J. Linde and G. Merenyi, "A Kinetic Study of the Hydrolysis of Phosgene in Aqueous Solution by Pulse Radiolysis," *Angew. Chem. Int. Ed. Engl.*, vol 33 (1994), pp 1259-1261.

Mill, T., J. Epstein, and L.J. Schiff, *H_2O_2/UV for Disposal of Organophosphorous Wastes (Paper presented at the Seventh Annual Symposium on Environmental Research* (Edgewood Arsenal, MD, 14-16 September 1976).

Miller, J., E. Toro, and R. Hernandez, *A Pilot Scale Assessment of Peroxone Oxidation for Treatment of Contaminated Groundwater*, Draft TR (USAWES, November 1996).

Naval Weapons Support Center, Crane, IN, *Development of Design Parameters for an Explosive Contaminated Wastewater Treatment System*, TR WQEC/C 85-297/ADA159-416 (June 1985).

Noss, C. I., and R.H. Chyrek, *Tertiary Treatment of Effluent From Holston AAP Industrial Liquid Waste Treatment Facility; IV. Ultraviolet Radiation and Hydrogen Peroxide Studies: TNT, RDX, HMX, TAX, and SEX*, TR 8308, ADA141135 (U.S. Army Medical Bioengineering Research and Development Laboratory, Fort Detrick, Frederick, MD, 1984).

Oxley, J.C., A.B. Kooh, K. Szekeres, and W. Zheng, "Mechanism of Nitramine Thermolysis," *J. Phys. Chem.*, vol 98 (1994), pp 7004-7008.

Oxley, J.C., M.A. Hiskey, D. Naud, and R. Szekeres, "Thermal Decomposition of Nitramines: Dimethylnitramine, Diisopropylnitramine, and N-Nitropiperidine," *J. Phys. Chem.*, vol 96 (1992), pp 2505-2509.

Pacheco, J., M. Prairie, and L. Yellowhorse, *Photocatalytic Destruction of Chlorinated Solvents With Solar Energy* (International Solar Energy Conference, Reno, NV, March 1991).

Parker, G.A. *Colorimetric Determination of Nonmetals*, D.R. Boltz and J.A. Howell, eds. (Wiley, New York, 1928), p 301.

Patterson, J., N.I. Shapira, J. Brown, W. Duckert, and J. Polson, *State of the Art: Military Explosives and Propellants Production Industry. Vol_III._Wastewater Treatment*, PB 260918 (American Defense Preparedness Association, Washington, DC, 1976).

Peyton, G.R. "Oxidative Treatment Methods for the removal of Organic Compounds From Drinking Water," *Significance and Treatment of Volatile Organic Compounds in Water*

Supplies, N. Ram, L. Canter, and R. Christman, eds. (Lewis Publishers, Inc., Chelsea, MI, 1990).

Peyton, G.R., "Modeling Advanced Oxidation Processes for Water Treatment," *Emerging Technologies in Hazardous Waste Management*, Edited by D.W. Tedder and F.G. Pohland (ACS Symposium Series 422, Washington, DC, 1990), pp 100-118.

Peyton, G.R., and A. Law, *Initial Feasibility Report: Investigation of Photochemical Oxidative Techniques for Treatment of Contaminated Groundwaters*, NCEL Technical Memorandum No. TM-71-90-9 (Naval Civil Engineering Laboratory, Port Hueneme, CA, September 1990).

Peyton, G.R., and E. Girin, *Factors Affecting AOPs*, Final report to USACERL (March 1994).

Peyton, G.R., and M.A. Smith, *Solute Effects in Aquifer Cleanup/Hazardous Waste Treatment by Oxy-Radical Processes*, Final Report (Hazardous Waste Research and Information Center, Champaign, Illinois, submitted April 1994).

Peyton, G.R., and M.H. LeFaivre *Identificaation of Reaction By-Products From Oxidative and Photolytic Remediation if Groundwater Contaminated With TNT and RDX*, final report submitted to the U.S. Naval Civil Engineering Laboratory, Port Hueneme, CA (1993).

Peyton, G.R., and W.H. Glaze, "Destruction of Pollutants in Water With Ozone in Combination With Ultraviolet Radiation. 3. Photolysis of Aqueous Ozone," *Environ. Sci. Technol.*, vol 22 (1988), pp 761-767.

Peyton, G.R., C.-S. Gee, J. Bandy, and S.W. Maloney "By-Products From Ozonation and Photolytic Ozonation of Organic Pollutants in Water: Preliminary Observations," *Biohazards of Drinking Water Treatment*, R.A. Larson, ed. (Lewis Publishers, Inc., Chelsea, MI, 1989), pp 185-200.

Peyton, G.R., M.A. Smith, and B.M. Peyton, *Photolytic Ozonation for Protection and Rehabilitation of Ground Water Resources: A Mechanistic Study*, Research Report No. 206 (University of Illinois, Water Resources Center, 1987).

Peyton, G.R., M.H. LeFaivre, O.J. Bell, and Osia Smith, *Advanced Oxidation Treatability Study for Low-Level Ordnance Compounds in Ground Water*, Final Batch Testing Report to NCEL, Port Hueneme, CA (21 April 1992).

Peyton, G.R., M.J. Fleck, M.A. Smith, and J.E. Sanders, "Experimental Design for Accurate Delivery and Measurement of Gaseous Ozone in a Water Treatment System," to be submitted to *Ozone, Science and Engineering*.

Peyton, G.R., O.J. Bell, E.L. Girin, and M.H. LeFaivre, "Reductive Destruction of Water Contaminants During Treatment With Hydroxyl Radical Processes," *Environ. Sci. Technol.*, vol 29 (1995), pp 1710-1712.

Peyton, G.R., O.J. Bell, E.L. Girin, M.H. LeFaivre, and J.E. Sanders, *The Effect of Carbonate/Bicarbonate Alkalinity on the Advanced Oxidation Processes: Treatment Efficiency and Oxidation By-Products*, Final Report (AWWA Research Foundation, submitted in November, 1996).

Peyton, G.R., Unpublished data (1992).

Piesiak, A., M.N. Schuchmann, H. Zegota, and C. von Sonntag, "8-Hydroxyethylperoxyl Radicals: A Study of the (-Radiolysis and Pulse Radiolysis of Ethylene in Oxygenated Aqueous Solutions," *Z. Naturforsch.*, vol 39b (1985), pp 1262-1267.

Roth, M., and J.M. Murphy, Jr., *Evaluation of the Ultraviolet-Ozone and Oxidant Treatment of Pink Water*, NTIS Order #PB 300763 (EPA 600/2-79-129, July 1979).

Schuchmann, M.N., and C. von Sonntag, "Hydroxyl Radical-Induced Oxidation of Diethyl Ether in Oxygenated Aqueous Solutions: A Product and Pulse Radiolysis Study," *J. Am. Chem. Soc.*, vol 86 (1982), pp 1995-2000.

Schuchmann, M.N., and C. von Sonntag, "Hydroxyl Radical-Induced Oxidation of 2-Methyl-2-Propanol in Oxygenated Aqueous Solution: A Product and Pulse Radiolysis Study," *J. Phys. Chem.*, vol 83 (1979), pp 780-784.

Schuchmann, M.N., and C. von Sonntag, "The Rapid Hydration of the Acetyl Radical. A Pulse Radiolysis Study of Acetaldehyde in Aqueous Solution," *J. Am. Chem. Soc.*, vol 110 (1988), pp 5698-5701.

Schuchmann, M.N., H. Zegota, and C. von Sonntag, "Acetate Peroxyl Radicals, .O2CH2CO2-: A Study on the -Radiolysis and Pulse-Radiolysis of Acetate in Oxygenated Aqueous Solutions," *Z. Naturforsch.*, vol 40b (1985), pp 215-221.

Schultze, H., and D. Schulte-Frohlinde, "OH Radical Induced Oxidation of Ethanol in Oxygenated Aqueous Solutions, Part I," *J. Chem. Soc., Faraday Trans. 1*, vol 5, No. 9 (1975), pp 1099-1105.

Sierka, R.A., and W.F. Cowen, "The Catalytical Ozone Oxidation of Aqueous Solutions of Hydrazine, Monomethyl Hydrazine and Unsymmetrical Dimethylhydrazine," *Proceedings of the 35th Industrial Waste Conference, Purdue University, Lafayette, IN* (May 1980), pp 406-415.

Smetana, A.F., and S. Bulusu, *Photochemical Studies of Secondary Nitroamines. Part II, Ultraviolet Photolysis and Ozonolysis of RDX in Aqueous Solutions*, TR ARLCD-TR-77039 (U.S. Army Armament Research and Development Command, Dover, NJ, June 1979).

Spanggord, R.J., T. Mill, T. Chou, W. Mabey, J. Smith, and S. Lee, *Environmental Fate Studies on Certain Munition Wastewater Constituents—Laboratory Studies*, TR ADA099256 (SRI International, Menlo Park, CA, 1980).

Spanggord, R.J., W.R. Mabey, T.W. Chou, S. Lee, and P.L. Alferness, *Environmental Fate Studies of HMX. Phase 2 C Detailed Studies*, TR ADA145122 (SRI International, Menlo Park, CA, 1983).

Staehelin, J., and J. Hoigné, "Decomposition of Ozone in Water in the Presence of Organic Solutes Acting as Promoters and Inhibitors of Radical Chain Reactions," *Environ. Sci. Technol.*, vol 19 (1985), pp 1206-1213.

Staehelin, J., and J. Hoigné, "Decomposition of Ozone in Water: Rate of Initiation by Hydroxide Ions and Hydrogen Peroxide," *Environ. Sci. Technol.*, vol 16 (1982), pp 676-681.

Staehelin, J., and J. Hoigné, "Mechanism and Kinetics of Decomposition of Ozone in Water in the Presence of Organic Solutes," *Vom Wasser*, vol 61 (1983), pp 337-348.

Swallow, A.J., "Reactions of Free Radicals Produced From Organic Compounds in Aqueous Solution by Means of Radiation," *Progr. Reaction Kinetics*, vol 9 (1978), pp 195-366.

Syracuse Research Corporation, *Environmental Fate of RDX and TNT, Progress Report* (1 May 1977 to 31 May 1978) and proposed studies, Contract DAMD 17-77-3-7026 (July 1978).

Takahashi, N. "Ozonation of Several Organic Compounds Having Low Molecular Weight Under Ultraviolet Irradiation," *Ozone Sci. Eng.*, vol 12, No. 1 (1990), pp 1-18.

Taube, H., "Photochemical Reactions of Ozone in Solution," *Trans. Farad. Soc.*, vol 53 (1956), pp 656-665.

Thompson, D.W., Ash Khan, R.E. Buhts, and J.D. Zeff, "Ultraviolet/Ozone Oxidation of Diisopropylmethylphosphonate (DIMP) in Contaminated Ground Water," *International Ozone Association News*, vol 6, No. 4, pt 2 (1979), pp 1-8.

von Sonntag, C., *The Chemical Basis of Radiation Biology* (Taylor and Francis, Inc., Philadelphia, PA, 1987).

Wardman, P., and E.D.Clarke, "Oxygen Inhibition of Nitroreductase: Electron Transfer From Nitro Radical-Anions to Oxygen," *Biochem. Biophys. Res. Comm.*, vol 69 (1976), pp 942-949.

Wigger, A., A. Henglein, and K.D. Asmus, "Pulsradiolytische Untersuchung der Oxydation des Phenylhydroxylamins in wäßriger Losung," *Ber. Bunsenges. Physik. Chem.*, vol 71 (1967), pp 513-516.

Zappi, M.E., E.C. Fleming, T.Miller, F. Regan, R. Swindle, R. Morgan, and S. Harvey, *A Pilot Scale Assessment of Peroxone Oxidation for Potential Treatment of Three Contaminated Groundwaters at the Rocky Mountain Arsenal, Commerce City, Colorado,* TR SERDP-97 (USAWES, August, 1997).

Zappi, M.E., Fleming E.C., and Cullinane, M.J., "A Treatment of Contaminated Groundwater Using Chemical Oxidation," *Proc. Hydr. Engrg. Session at Water Forum, Baltimore, MD* (1992).

Zappi, M.E., Fleming E.C., Thompson, D.W., and Francingues, N.R., *A Treatability Study of Four Contaminated Waters at Rocky Mountain Arsenal, Commerce City, Colorado Using Chemical Oxidation With Ultraviolet Radiation Catalyzation* (1989).

Zappi, M.E., Hong, A. and Cerar, R., "A Treatment Of Groundwater Contaminated With High Levels of Explosives Using Traditional and Non-Traditional Advanced Oxidation Processes," *HMCRI Superfund Conf.* (Washington, DC, 1993).

Appendix: Details of Superoxide Liberation

The reaction of OH radical with an aliphatic organic compound to form carbon-centered radical can be represented as:

$$^{\bullet}OH + HRH \rightarrow H_2O + {}^{\bullet}RH \qquad \text{A-1}$$

The carbon-centered radicals that react with oxygen to form peroxyl radicals:

$$^{\bullet}RH + O_2 \rightarrow HR_2\cdot \qquad \text{A-2}$$

The decomposition of peroxyl radical to give superoxide is (some peroxyl radicals do this and some do not):

$$HRO_2\cdot \rightarrow H^+ + R + O_2^- \qquad \text{A-3}$$

where R is a stable (non-radical) organic compound.

Eq. A-4, the mutual reaction of two peroxyl radicals to form tetroxide, and then hydrogen peroxide (some peroxyl radicals do this rather than A-3; most peroxyl radicals do primarily one or the other) is:

$$2\,HRO_2\cdot \rightarrow \left[HRO_2\right]_2 \rightarrow 2\,RO + H_2O_2 \qquad \text{A-4}$$

Accompanying this reaction is usually a small percentage of eq. A-5:

$$2\,HRO_2\cdot \rightarrow \left[HRO_2\right]_2 \rightarrow 2HRO\cdot + O_2 \qquad \text{A-5}$$

which ends up contributing a small quantity of oxygen to the solution. So the net reactions 4-54 through 4-57 can be derived, using A-1 through A-5.

I.A. *Superoxide initiation and liberation.* Add reactions 4-51 , A-1, A-2, and A-3, canceling any species that appears on both sides. This process results in equation 4-54. Note that, although superoxide is liberated (eq. A-3), it is rapidly consumed by reaction with ozone (eq. 4-51) so there is no net superoxide production.

I.B. *Hydrogen peroxide liberation.* Add equations 4-51, A-1, A-3, and A-4. There is net superoxide consumption and net hydrogen peroxide production. The net equation has been divided by 2 (hence the 1/2 coefficient on H_2O_2) to put all equations on the same basis with respect to ozone stiochiometry.

II. A. *Initiation by H_2O_2, superoxide production.* Add equations 4-53, A-1, A-2, and A-3. The equation is written to emphasize net H_2O_2 consumption and net superoxide and oxygen production. Since the superoxide reacts quickly with ozone, one could add equations 4-51, A-1, A-2, and A-4 to get

$$2\,O_3 + 2\,HRH \rightarrow 3/2\,O_2 + 2\,H_2O + R + RO$$

or

$$O_3 + 2HRH \rightarrow 3/4\,O_2 + H_2O + 1/2\,R + 1/2\,RO$$

but this really obscures the point, which is to show oxygen production stoichiometry for the 4 individual pathway types. The $\eta_x O_2$ term is only shown in equation 4-57 where it is significant, since there is no other source of oxygen. In all the other three equations (4-54, 4-55, and 4-56), oxygen is produced in amounts comparable to ozone consumption (within a factor of 2).

USACERL DISTRIBUTION

Chief of Engineers
ATTN: CEMP
ATTN: CEMP-E
ATTN: CEMP-C
ATTN: CEMP-M
ATTN: CERD-C
ATTN: CERD-ZA
ATTN: CERD-L
ATTN: CERD-M (2)

ACS(IM) 22060
ATTN: DAIM-FDP

AMMRC
ATTN: DRXMR-WE 02172

US Army Engr District
ATTN: Library (42)

US Army Engr Division
ATTN: Library (8)

US Army Cold Regions Res & Engr Lab
ATTN: Library 03755

Production base Modernization Activity
ATTN: SMSMC-PBE-C 07806

Defense Distribution Region East
ATTN: ASCE-WI 17070-5001

HQ AMC
ATTN: Tech Library 22333

HQ AFCESA/RA
ATTN: Tyndall AFB 32403

HQDLA
ATTN: DLA-WI 22304

USA Natick RD&E Center 01760
ATTN: STRNC-DT
ATTN: AMSSC-S-IMI

Watervliet Arsenal
ATTN: SMCWV-EH 12189

Red River Army Depot
ATTN: SDSRR-G

Corpus Christi Army Depot
ATTN: SDCC-ECD Mail Stop 24 78419

Aberdeen Proving Ground
ATTN: STEAP-DEH 18466

Savanna Army Depot
ATTN: SDSLE-VAE

Restone Arsenal
ATTN: DESMI-KLF

Rock Island Arsenal
ATTN: SMCRI-EH
ATTN: SMCRL-TL
ATTN: Library
ATTN: US Army Indust Engr Activity 61299

Tobyhanna Army Depot
ATTN: SDSTO-EH 18466

Radford Army Ammunition Plant
ATTN: SMCRA-EN 24141

US Army Materials Tech Lab
ATTN: SLCMT-DPW 02172

NAVCIVENGRLAB
ATTN: Bldg 560
ATTN: Lib/Info Div 93043

Navy Public Wtorks Center
ATTN: Tech Lib CODE 123C

SHAPE 09705
ATTN: Infrastructure Branch LANDA

CEWES 39180
ATTN: Library

CECRL 03755
ATTN: Library

US Army Engr School
ATTN: ATSE-DAC-LB
ATTN: ATSE-DAC-LG
ATTN: ATSE-DAC-FL 65473

USACPW
ATTN: CECPW-E
ATTN: CECPW-FT
ATTN: CECPW-ZC

Engineer Strategic Studies Ctr
ATTN: Library 22060

AFESC Program Office
ATTN: British Army Staff 32403

US Army RD&Std Group UK

US Army Harry Diamond Labs
ATTN: SLCHD-SD-TL 20783

US Army Belvoir RD&E Ctr
ATTN: Strebe 22060

US Army ARDEC 07806-5000
ATTN: AMSTA-AR-IMC

Engr Societies Library
ATTN: Acquisitions 10017

US Army Environmental Center (2)
ATTN: SFIM-AEC-NR 21010

US Military Academy 10996
ATTN: Geography & Envr Engrg

Naval Facilities Engr Command
ATTN: Facilities Engr Command (8)
ATTN: Engrg Field Divisions (11)
ATTN: Public Works Center (8)
ATTN: Naval Constr Battalion Ctr 93043
ATTN: Naval Facil. Engr. Service Ctr 93043-4328

US Gov't Printing Office 20401
ATTN: Rec Sec/Deposit Sec (2)

Nat'l Institute of Standards & Tech
ATTN: Library 20899

Defense Tech Info Center 22060-6218
ATTN: DTIC-O (2)